



A National Center of Excellence in Advanced Technology Applications

ISSN 1520-295X

Nonlinear Structural Analysis Towards Collapse Simulation: A Dynamical Systems Approach

by

Mettupalayam V. Sivaselvan and Andrei M. Reinhorn

University at Buffalo, State University of New York

Department of Civil, Structural and Environmental Engineering

Ketter Hall

Buffalo, New York 14260

Technical Report MCEER-04-0005

June 16, 2004

This research was conducted at the University at Buffalo, State University of New York and was supported primarily by the Earthquake Engineering Research Centers Program of the National Science Foundation under award number EEC-9701471.

NOTICE

This report was prepared by the University at Buffalo, State University of New York as a result of research sponsored by the Multidisciplinary Center for Earthquake Engineering Research (MCEER) through a grant from the Earthquake Engineering Research Centers Program of the National Science Foundation under NSF award number EEC-9701471 and other sponsors. Neither MCEER, associates of MCEER, its sponsors, the University at Buffalo, State University of New York, nor any person acting on their behalf:

- a. makes any warranty, express or implied, with respect to the use of any information, apparatus, method, or process disclosed in this report or that such use may not infringe upon privately owned rights; or
- b. assumes any liabilities of whatsoever kind with respect to the use of, or the damage resulting from the use of, any information, apparatus, method, or process disclosed in this report.

Any opinions, findings, and conclusions or recommendations expressed in this publication are those of the author(s) and do not necessarily reflect the views of MCEER, the National Science Foundation, or other sponsors.



Nonlinear Structural Analysis Towards Collapse Simulation: A Dynamical Systems Approach

by

Mettupalayam V. Sivaselvan¹ and Andrei M. Reinhorn²

Publication Date: June 16, 2004

Submittal Date: October 1, 2003

Technical Report MCEER-04-0005

Task Number 04-2004

NSF Master Contract Number EEC 9701471

- 1 Senior Scientific Programmer and Ph.D Graduate, Department of Civil, Structural and Environmental Engineering, University at Buffalo, State University of New York
- 2 Professor, Department of Civil, Structural and Environmental Engineering, University at Buffalo, State University of New York

MULTIDISCIPLINARY CENTER FOR EARTHQUAKE ENGINEERING RESEARCH
University at Buffalo, State University of New York
Red Jacket Quadrangle, Buffalo, NY 14261

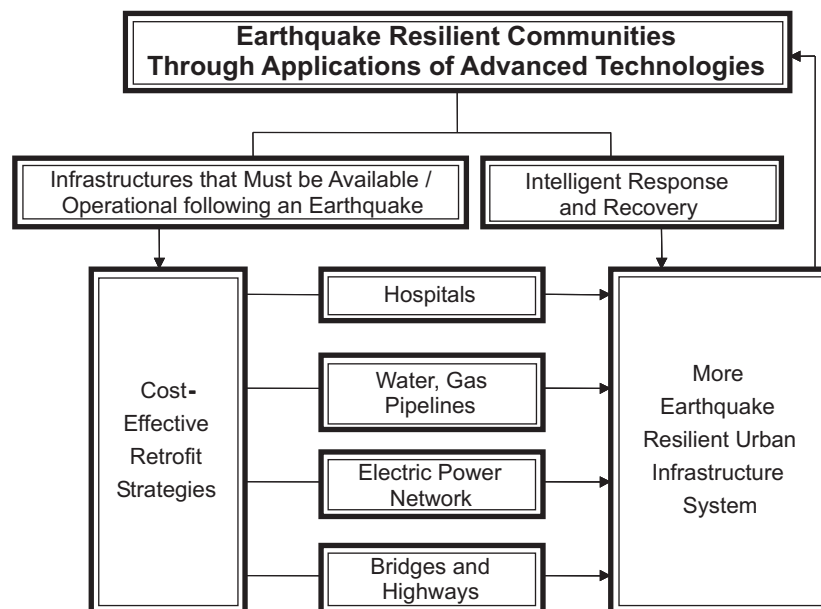
Preface

The Multidisciplinary Center for Earthquake Engineering Research (MCEER) is a national center of excellence in advanced technology applications that is dedicated to the reduction of earthquake losses nationwide. Headquartered at the University at Buffalo, State University of New York, the Center was originally established by the National Science Foundation in 1986, as the National Center for Earthquake Engineering Research (NCEER).

Comprising a consortium of researchers from numerous disciplines and institutions throughout the United States, the Center's mission is to reduce earthquake losses through research and the application of advanced technologies that improve engineering, pre-earthquake planning and post-earthquake recovery strategies. Toward this end, the Center coordinates a nationwide program of multidisciplinary team research, education and outreach activities.

MCEER's research is conducted under the sponsorship of two major federal agencies: the National Science Foundation (NSF) and the Federal Highway Administration (FHWA), and the State of New York. Significant support is derived from the Federal Emergency Management Agency (FEMA), other state governments, academic institutions, foreign governments and private industry.

MCEER's NSF-sponsored research objectives are twofold: to increase resilience by developing seismic evaluation and rehabilitation strategies for the post-disaster facilities and systems (hospitals, electrical and water lifelines, and bridges and highways) that society expects to be operational following an earthquake; and to further enhance resilience by developing improved emergency management capabilities to ensure an effective response and recovery following the earthquake (see the figure below).



A cross-program activity focuses on the establishment of an effective experimental and analytical network to facilitate the exchange of information between researchers located in various institutions across the country. These are complemented by, and integrated with, other MCEER activities in education, outreach, technology transfer, and industry partnerships.

The purpose of this study is to develop structural models and numerical techniques to perform analysis of structures in damage states up to collapse. These are needed for determining functional limit states required for performance and fragility based seismic design methodologies. The authors explored alternatives to the widely used displacement-based incremental iterative algorithms. They have developed a framework, termed a dynamical system, where displacements, internal forces and other state variables can be treated uniformly (i.e., modeling of components is clearly separated from the numerical solution). Two methods have been formulated: State Space and Lagrangian.

The State Space method considers the governing equations of motion and constitutive behavior of a structure as constituting a constrained dynamical system which is represented as a system of differential algebraic equations solved using numerical methods. The Lagrangian formulation is a new form that involves displacement and velocities as well as internal forces and their impulses. It leads to the concept of a generalized momentum for framed structures. It extends to continua with large deformations and can therefore also be used in geometric nonlinear analysis.

Both methods can potentially be used as alternatives to the conventional displacement-based incremental iterative method for the analysis of structures to collapse. Both clearly distinguish the modeling of components from the numerical solution. Thus, phenomenological models of components such as structural steel connections, reinforced concrete elements, semi-active devices, shock absorbers, etc. can be incorporated into the analysis without having to implement element-specific incremental state determination algorithms.

ABSTRACT

Nonlinear analysis of structures has become increasingly important in the study of structural response to hazardous loads. Such analyses should include (i) the effects of significant material and geometric nonlinearities (ii) various phenomenological models of structural components and (iii) the energy and momentum transfer to different parts of the structure when structural components fracture.

Computer analysis of structures has traditionally been carried out using the displacement method, wherein the displacements in the structure are treated as the primary unknowns, combined with an incremental iterative scheme for nonlinear problems. In this work, considering the structure as a dynamical system, two new approaches – (i) the state space approach and (ii) the Lagrangian approach are developed. These are mixed methods, where besides displacements, the stress-resultants and other variables of state are primary unknowns. These methods can potentially be used for the analysis of structures to collapse as demonstrated by numerical examples. Attention is focused on skeletal structures, although the extension of the methods to other systems is discussed.

In the state space approach, the governing equations of motion and constitutive behavior of a structure are considered as constituting a constrained dynamical system, which is represented as a system of differential algebraic equations (DAE) and solved using appropriate numerical methods. A large-deformation flexibility-based beam column element is formulated, for use with the state space approach.

In the Lagrangian approach, the evolution of the structural state in time is provided a weak formulation using Hamilton's principle. It is shown that a certain class

of structures, referred to in this work as reciprocal structures has a mixed Lagrangian formulation in terms of displacements and internal forces. The Lagrangian is invariant under finite displacements and can be used in geometric nonlinear analysis. For numerical solution, a discrete variational integrator is derived starting from the weak formulation. This integrator inherits the energy and momentum conservation characteristics for conservative systems and the contractivity of dissipative systems. The integration of each step is a constrained minimization problem and is solved using an Augmented Lagrangian algorithm.

In contrast to the displacement-based method, both the state space and the Lagrangian methods clearly separate the modeling of components from the numerical solution. Phenomenological models of components essential to simulate collapse can therefore be incorporated without having to implement model-specific incremental state determination algorithms. The state determination is performed at the global level by the DAE solver and by the optimization solver in the respective methods. The methods suggested herein can be coupled with suitable pre- and post- processors to develop a unified computational platform for analysis of collapsing structures.

TABLE OF CONTENTS

SECTION	TITLE	PAGE
1	INTRODUCTION	1
1.1	Background and Motivation	1
1.2	Challenges	2
1.3	Displacement-based Incremental Iterative Method	2
1.4	Mixed Methods	3
1.5	Dynamical Systems Approach	4
1.6	Scope and Outline	7
2	MATERIAL NONLINEARITY: CONSTITUTIVE RELATIONS OF PLASTICITY	11
2.1	Background	11
2.2	One Dimensional Plasticity	12
2.3	One Dimensional Plasticity - Rate Form	13
2.4	One Dimensional Plasticity – Dissipation Form	16
2.5	Kinematic Hardening – Series vs. Parallel Models	18
2.6	Multi-dimensional Plasticity	22
2.7	Yield Functions Φ	26
2.8	Summary	27
3	THE STATE SPACE APPROACH	29
3.1	Background	29
3.2	Overview of Previous Work	30
3.3	Section Outline	31
3.4	State Variables and Equations of a SDOF System	31
3.5	Differential-Algebraic Equations (DAE)	34
3.6	State Variables and Equations of a Multi-Degree-of-Freedom System	36
3.6.1	Global State Variables	36
3.6.2	Local State Variables	37
3.6.3	State Equations	37
3.7	Formulation of a Flexibility-Based Planar Beam Element	39
3.8	Numerical Solution	42
3.9	Numerical Example	42
3.10	Summary	44
4	LARGE DEFORMATION BEAM-COLUMN ELEMENT	49
4.1	Background	49
4.2	Overview of Previous Work	49
4.3	Element Formulation	51
4.4	Transformations of Displacements and Forces	54
4.5	Approximation of the Element Displacement Field	56
4.6	Constitutive Relations	58

TABLE OF CONTENTS

SECTION	TITLE	PAGE
4.7	Summary of State Equations	58
4.8	Numerical Example 1: Snap-through of a Deep Bent	59
4.9	Numerical Example 2: Collapse of a Single-story Structure	61
4.9.1	Constitutive Equation for S3x5.7 Cross Section	61
4.9.2	Nonlinear Static Analysis	62
4.9.3	Dynamic Analysis	62
5	THE LAGRANGIAN APPROACH – FORMULATION	67
5.1	Background	67
5.2	Outline	68
5.3	Variational Principles for Plasticity	68
5.4	Simple Phenomenological Models of Reciprocal Structures	71
5.4.1	Mass with Kelvin Type Resisting System	71
5.4.2	Mass with Maxwell Type Resisting System	73
5.4.3	Mass with Combined Kelvin and Maxwell Resisting Systems	75
5.4.4	Alternate Formulation for Combined Kelvin and Maxwell System	78
5.4.5	Elastic-Viscoplastic Dynamic System	80
5.4.6	Elastic-Ideal Plastic Dynamic System	81
5.4.7	Summary of Phenomenological Models	82
5.5	Reciprocal Structures	82
5.6	Compatibility Equations of a Frame Element	83
5.7	Governing Equations of Skeletal Structures	85
5.8	Effect of Geometric Nonlinearity on the Lagrangian Function	88
5.9	Extension to Continua	90
5.10	Summary of Lagrangian Formulation	91
6	THE LAGRANGIAN APPROACH – NUMERICAL SOLUTION	93
6.1	Background	93
6.2	Time Discretization - Discrete Calculus of Variations	93
6.2.1	Features of the Discrete Equation	97
6.3	Time-step Solution	98
6.3.1	Constrained Minimization by the Augmented Lagrangian Method	102
6.4	Numerical Example	106
6.4.1	Analysis without $P\Delta$ effect	106
6.4.2	Analysis with $P\Delta$ effect	107
6.5	Summary	108
7	SUMMARY AND CONCLUSIONS	115
7.1	Summary of Important Results	116

TABLE OF CONTENTS

SECTION	TITLE	PAGE
7.2	Extensions and Implementations	119
7.3	Recommendations for Further Work	120
7.4	Recommendations for New Directions	121
8	REFERENCES	123
APPENDIX I	REVIEW OF MATRIX STRUCTURAL ANALYSIS	135
APPENDIX II	PRINCIPLE OF VIRTUAL FORCES IN RATE FORM	143
APPENDIX III	ONE-DIMENSIONAL RECIPROCAL COMPONENTS	147
APPENDIX IV	LAGRANGIAN FORMULATION OF CONTINUA	149
AIV.1	Three Dimensional Continuum	149
AIV.1.1	Review of Continuum Kinematics	149
AIV.1.2	Continuum Plasticity	151
AIV.1.3	Lagrangian Formulation	152
AIV.1.4	Derivation of Euler-Lagrange Equations	153
AIV.2	Large Deformation Beam Element	157
AIV.2.1	Kinematics	157
AIV.2.2	Constitutive Relations	158
AIV.2.3	Lagrangian Formulation	158
AIV.2.4	Equilibrium Matrix	159
AIV.2.5	Derivation of Euler-Lagrange Equations	160

LIST OF FIGURES

FIGURE	TITLE	PAGE
1.1	Schematic of Development in this Work	6
2.1	1D Elastic-Ideal Plastic System	12
2.2	Visco-plastic Regularization	16
2.3	Kinematic Hardening	19
2.4	Kinematic Hardening - Series Model	20
2.5	Kinematic Hardening - Parallel Model	21
3.1	SDOF System	32
3.2	Example Frame	43
3.3	Node and Element Numbering and Active Displacement DOF	43
3.4	Quasi-Static Analysis: Shear Force vs Relative Horizontal Displacement of Left Beam Element	45
3.5	Dynamic Analysis: Shear Force vs Relative Horizontal Displacement of Left Beam Element	45
4.1	Euler-Bernoulli Beam Subjected to Large Deformation	52
4.2	Numerical Example 1: Force-Displacement Response	60
4.3	Numerical Example 2: Single Story Frame	64
4.4	Force-Strong Axis Bending Moment Interaction Diagram for S3x5.7 Section	64
4.5	Numerical Example 2: Response of One Column ($F^{axial}/F^{critical} = 0.2156$)	65
4.6	Convergence of Flexibility-based Element	65
4.7	Numerical Example 2: Dynamic Analysis to Collapse	66
5.1	Mass with Kelvin Type Resisting System and Force Input	71
5.2	Mass with Maxwell Type Resisting System and Displacement Input	73
5.3	Dual of System in Fig. 5.2	74
5.4	Mass with Combined Kelvin and Maxwell Resisting Systems	75
5.5	Electrical Circuit Analogous to Fig. 5.4	77
5.6	Elastic-visco-plastic Dynamic System	80
5.7	Elastic-ideal-plastic Dynamic System	81
5.8	Beam Element with Rigid-Plastic Hinges	85
6.1	No Axial Force: Horizontal Displacement Time History of Node 2	110
6.2	No Axial Force: Horizontal Displacement Time History of Node 2	110
6.3	No Axial Force: Rotation History of Node 2	111

LIST OF FIGURES

FIGURE	TITLE	PAGE
6.4	No Axial Force: Relative Displacement vs. Horizontal Reaction Column 1	111
6.5	Under Axial Force: Horizontal Displacement History of Node 2	112
6.6	Under Axial Force: Vertical Displacement History of Node 2	112
6.7	Under Axial Force: Rotation History of Node 2	113
6.8	No Axial Force: Relative Displacement vs. Horizontal Reaction Column 1	113

LIST OF TABLES

TABLE	TITLE	PAGE
1.1	Status of the State Space and Lagrangian Implementations	9
3.1	Local State Variables for Different Types of Element Formulation	46
3.2	Numerical Example - Model Properties	46
3.3	Quasi-Static Analysis - Global and Local State Variables	46
3.4	Dynamic Analysis - Global and Local State Variables	47
4.1	Numerical Example 1: Non-dimensional Structural Properties	60
5.1	Electrical Analogy	77

1. INTRODUCTION

1.1. Background and Motivation

In recent years, the requirements of structural analysis have become more challenging. Some of the reasons for this are that: (i) New approaches to the design of structures for earthquakes and other hazardous loads are based on structural *performance* and use *fragility functions* as measures of performance. Such fragility quantification is carried out with respect to predefined performance *limit states* describing the condition of the structure in relation to usability and safety. Often, the limit states used in seismic design are well beyond linear elastic behavior, in many cases approaching collapse conditions. (ii) *Structures in areas of low to moderate seismicity* have traditionally been designed for gravity loads. Evaluation of such structures under more stringent loads prescribed by modern codes requires estimation of their strength and ductility reserves at various levels of ground motion. (iii) To study the effectiveness of *structural protective devices and retrofit measures* at higher levels of ground shaking requires analysis of highly nonlinear systems. Hence analysis methods that cater to these requirements should be developed. The objective of this work is to create a basis for the development of a unified approach for such analysis methods. Attention is focused here on skeletal structures (framed structures comprising components with one prominent dimension – beams, columns, truss members, energy dissipation devices etc.), common in buildings and bridges. It is shown however that the formulations derived here can be extended to continua.

1.2. Challenges

A precise definition of collapse is not attempted, but it is recognized as a condition where the structure has lost the abilities to sustain gravity loads or to shakedown under repeated lateral loading. Such a condition is presumed to be caused by three factors – (i) plasticity (the fact that the load carrying capacities of structural components are limited) – (ii) damage (the fact that the strength, stiffness and energy dissipation characteristics of structural components deteriorate under increased and repeated loading) and (iii) geometric nonlinearity or P- Δ effects (under large displacements, the gravity loads cause significant additional stresses in structural components). Of these, only factors (i) and (iii) are considered in this work.

To accurately model the nonlinear response of the structure, detailed phenomenological models of parts of the structure such as members and connections are often necessary. For example, Mazzolani and Piluso (1996) present such models for structural steel connections and Hsu (1993) does so for reinforced concrete elements. It should be possible to seamlessly incorporate such models in the analysis.

Moreover, when a component fractures, i.e. loses strength instantaneously, there is transfer of energy and momentum between various parts of the structure, which must be accounted for.

1.3. Displacement-based Incremental Iterative Method

The response variables of the structure which, when known, determine future response of the structure are called state variables. These include displacements, internal forces, plastic strains etc. A more detailed discussion of state variables is presented in Section 3. Computer analysis of structures has traditionally been carried out using the

displacement method, wherein the displacements in the structure are treated as the primary unknowns, combined with an incremental iterative scheme for nonlinear problems. Stresses and other state variables that appear in the mathematical model of the structure in constitutive relations, in mixed variational formulations or in any other fashion are treated “locally”, i.e. at the level of a unit of spatial discretization – a finite element, a quadrature point etc. In linear analysis, these additional state variables are “condensed out” of the system of equations. In nonlinear analysis, however, every iteration of the solution process at an increment comprises of two stages: (i) a *global* stage where the primary unknowns, the displacements, are obtained using the “condensed” equation system (ii) and a *local* stage where all other state variables are updated. The local stage is referred to as the incremental state determination and requires element-specific algorithms (see for example, Neuenhofer and Filippou (1997), de Souza (2000) and Lowes and Altoontash (2002)). The widespread use of the displacement method is primarily because the techniques of nonlinear structural analysis have grown as extensions to those of linear analysis and have most often been implemented in general purpose computer programs originally designed for linear analysis. The displacement method also enables the automatic construction and efficient structuring of the stiffness matrix, which plays a central role in linear analysis.

1.4. Mixed Methods

More recently, however, mixed methods have been explored wherein the fields of displacements, stresses (or stress-resultants), strains, plastic multipliers etc. are all given separate spatially discretized representations (see for example, Washizu (1982), Simo et al. (1989) and Han and Reddy (1999)).

The advantage of the *flexibility formulation* of beam-column elements, resulting from force-interpolation functions being always exact even when the element is non-prismatic and undergoes inelastic behavior, has been well documented (see for example, Park et al. (1987) and Neuenhofer and Filippou (1997)). The *yield function* in plasticity theory that defines the elastic domain (see for example, Simo and Hughes (1998)), and the damage function in damage mechanics (see for example, De Sciarra (1997)) are most naturally expressed in terms of stresses and stress-like quantities (or stress-resultants) using the tools of convex analysis. Thus stress-resultants play an important role in nonlinear analysis.

The use of mixed methods alleviates *locking* effects at the element level due to deformation modes in linear elastic structures (see for example, Hughes (1987)) and yielding modes in elastic-plastic structures (see for example, Comi and Perego (1995)). Moreover, various state variables besides forces and displacements play important roles in modern structural protective systems such as active and semi-active devices.

These factors motivate an approach where besides displacements, stress-resultants and other variables of state play a fundamental role.

1.5. Dynamical Systems Approach

In this work a variant of the mixed formulation is adopted, where the structure is viewed as a *dynamical system*. A dynamical system is *a collection of states along with a means of specifying how these states evolve in time*. Two such means of specifying the evolution of the states are studied:

1. The State Space Approach: The evolution of states is characterized as the solution of a system of first order differential equations. However, not all states are independent

and free. Some states are constrained by (i) algebraic equations – *holonomic* constraints (e.g. the equilibrium equations that constrain stress-resultants, kinematic constraints on displacements such as in rigid floor diaphragms etc.), (ii) inequality constraints (e.g. yield condition on stress-resultants) and (iii) non-integrable constraints involving velocities – *nonholonomic* constraints (e.g. the inequality constraints on certain state variables can be expressed as nonholonomic constraints in the conjugate variables; for example, the yield condition on the stress-resultants leads to nonholonomic constraints in terms of strain rates as will be seen later). The first order differential equations of evolution along with the holonomic constraints (algebraic equations) and the nonholonomic (implicit differential equations) constraints form a system of *differential algebraic equations* (DAE).

2. The Lagrangian Approach: The evolution of the states is characterized by the stationarity of the time integral of a certain functional (Hamilton's Principle). The time integral depends on a system *Lagrangian function* and a system *Dissipation function*, both functions of the state variables and their rates of change with time. The various constraints are embodied in these functions.

The state space approach uses the strong form of the governing equations in time, while the Lagrangian formulation uses the weak form. This distinction is discussed in greater detail in Section 5. The two approaches reveal different properties of the structural system and lead to different numerical methods as shown in Fig. 1.1.

Both methods consider material and geometric nonlinearity. In contrast to the displacement-based method, both the state space and the Lagrangian methods clearly separate the modeling of components from the numerical solution. Phenomenological

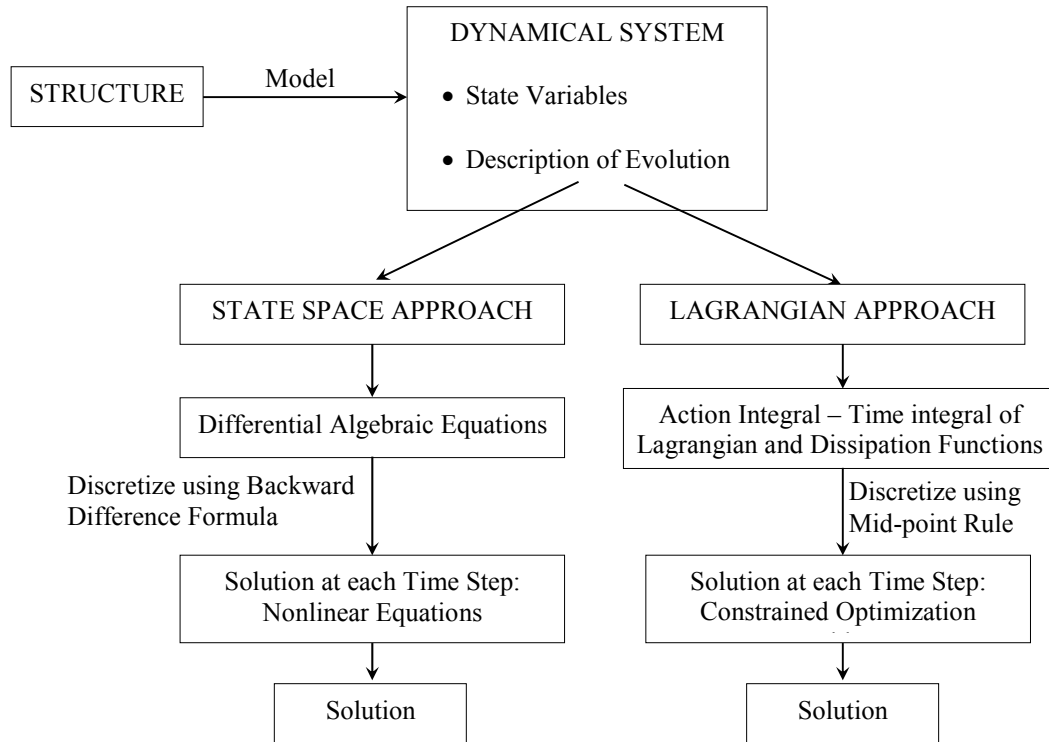


Fig. 1.1. Schematic of Development in this Work

models of components essential to simulate collapse can therefore be incorporated without having to implement model-specific incremental state determination algorithms. The state determination is performed at the global level by the DAE solver and by the optimization solver in the respective methods. The Lagrangian formulation results in the concept of the generalized momentum of the structure as shown in Section 5. This could provide insights into the momentum transfer that occur when there is component fracture.

It has been shown that for systems such as elasto-plastic structures where loading and unloading occur on different paths, the stiffness matrix (the tangent stiffness matrix, in the case of nonlinear analysis) which plays such a central role in linear systems, is no

more than an iteration matrix. The indefiniteness of the tangent matrix is not related to instability (see for example, Nguyen (2000)). The approach followed in this work eliminates the need for a global tangent stiffness matrix. The present formulations are likely to enable a broader notion of stability, although this is only briefly studied here.

The proposed methods follow a generalized approach which addresses modeling and solution through rigorous formulations which make very few assumptions to obtain the solution of complex non-linear problems. While traditional displacement methods address implicitly the model and the solution, the proposed methods distinguish the modeling of components from the numerical solution. The advantage of such formulations is indicated in this report.

The second formulation, the Lagrangian approach, implicitly addresses the equilibrium and the conservation of impulse, within a variational formulation. This approach allows addressing problems involving sudden collapse, or sudden degradation before collapse, which involves instantaneous lack of equilibrium and impulses. Moreover, the suggested formulation opens the way to addressing impulse driven processes such as blasts and impacts in complex structures without or with modern protective systems. As such this method pioneers a generalized approach to solving complex nonlinear dynamics problems.

1.6. Scope and Outline

In Section 2, constitutive relations of uni-axial and multi-axial ideal and kinematic hardening plasticity are established in two equivalent forms – the rate form and the dissipation form – for use in the State Space Approach and in the Lagrangian Approach respectively. In Section 3, the State Space Approach is developed. The governing

equations of motion and constitutive behavior of a structure are considered as constituting a constrained dynamical system, which is represented as a system of Differential Algebraic Equations (DAE). These equations are solved using appropriate numerical methods. An inelastic large deformation beam-column element is formulated in Section 4 for use with the state space approach, starting from the finite deformation compatibility equations and applying the principle of virtual forces in rate form. The element uses stress-resultant-strain constitutive equations and includes the effect of axial force-bending moment interaction. The element is utilized in structural analysis to collapse. In Section 5, the evolution of the structural state in time is provided a weak formulation using Hamilton's principle. It is shown that a certain class of structures, referred to here as *reciprocal structures*, has a *mixed Lagrangian formulation*. This class includes structures with a wide range of material behavior including hyperelasticity, rate-independent plasticity, viscoelasticity, viscoplasticity, tension- or compression-only resistance etc. The resulting Lagrangian has some special properties: (i) The generalized displacements that appear in the Lagrangian consist of both physical displacements at certain nodes and the impulses of the forces in certain members, leading to the idea of a *generalized momentum*; (ii) The Lagrangian is invariant under finite displacements and can be used in geometric nonlinear analysis. A *discrete variational integrator* is derived in section 6, starting from the variational statement of Hamilton's Principle to numerically integrate the Euler-Lagrange equations in time. This integrator inherits the energy and momentum conservation characteristics for conservative systems and the contractivity of dissipative systems. The integration of each step is a constrained minimization problem and is solved using an Augmented Lagrangian algorithm. Finally, the work is summarized and some

conclusions are drawn in Section 7. Since the State Space and Lagrangian Approaches were at first developed independently, their implementations are currently not on par with each other. The implementation status is shown in Table 1.1. While the state space formulation has been implemented for all four features of Table 1.1, the Lagrangian formulation is yet to be implemented for large deformations and post-yield hardening.

Table 1.1. Status of the State Space and Lagrangian Implementations

Feature	State Space Approach	Lagrangian Approach
Plasticity	Implemented	Implemented
Hardening	Implemented	Formulated
Large Displacements	Implemented	Implemented
Large Deformations	Implemented	Formulated

2. MATERIAL NONLINEARITY: CONSTITUTIVE RELATIONS OF PLASTICITY

2.1. Background

Structural materials and components have limits on strengths coupled with different loading and unloading paths, leading to nonlinear inelastic behavior. This section addresses formulations of hysteretic behavior with deterioration. The formulations are structural extensions of plasticity theory. The constitutive laws commonly used for analysis of structures with nonlinear inelastic material properties are based on classical plasticity theory. They are characterized by a yield surface, a flow rule and a hardening rule (see for example, Lubliner (1990) and Simo and Hughes (1998)). When working with macro-elements such as members of a frame, it is favorable to formulate constitutive equations in terms of stress resultants and their conjugate strain quantities rather than in terms of stresses and strains. For example, in a beam, the constitutive relationship is defined between the cross-sectional stress resultants – axial force and bending moment, and the strains – centroidal axial strain and curvature. Classical plasticity theory may be applied in this context by looking at the principle of maximum dissipation as holding in an integral sense (Lubliner (1990)). In its classical form, the maximum dissipation principle states that for a given strain rate, the stress is such that it maximizes the rate of energy dissipation. This statement can be approximated by stating instead that the integrals of the stresses over a cross-section (stress-resultants) are such that the total rate of energy dissipation over the cross-section is maximized for given plastic strain rates that satisfy compatibility (e.g. plane sections remain plane). The material in this section, although not original, is presented in order to establish the relations of plasticity in forms that are suitable for use in the following sections.

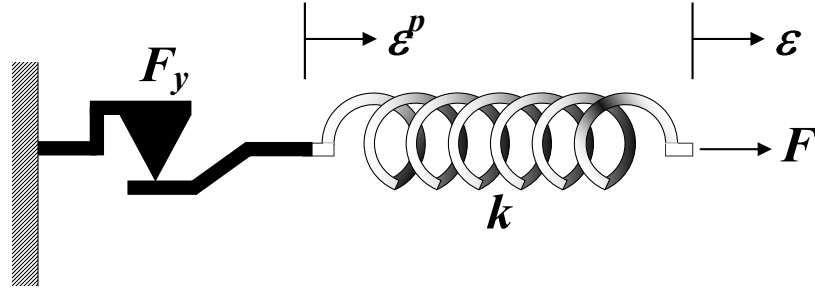


Fig. 2.1. 1D Elastic-Ideal Plastic System

2.2. One Dimensional Plasticity

Consider the one-dimensional elastic-ideal plastic system of Fig. 2.1. The total deformation can be decomposed as:

$$\varepsilon = \varepsilon^e + \varepsilon^p \quad (2.1)$$

where ε^e is the elastic deformation and ε^p is the plastic deformation. The stiffness of the spring is k and the force in the spring is given by:

$$F = k\varepsilon^e = k(\varepsilon - \varepsilon^p) \quad (2.2)$$

The slider shown in the figure is characterized by the convex yield condition:

$$\Phi(F) = |F| - F_y \leq 0 \quad (2.3)$$

When $\Phi = 0$, sliding occurs and plastic strain develops. Let the absolute value of the sliding rate, called the plastic multiplier, be λ ($\lambda > 0$, when sliding). Then,

$$\dot{\varepsilon}^p = \frac{\partial \varepsilon^p}{\partial t} = \lambda \operatorname{sgn}(F) \quad (2.4)$$

where $\text{sgn}(x) = 1$ if $x = 0$ and $x/|x|$ otherwise (the signum function). Or using equation (2.3):

$$\dot{\varepsilon}^p = \lambda \frac{\partial \Phi}{\partial F} \quad (2.5)$$

This is the *flow rule*. When $\Phi < 0$, no sliding occurs and $\lambda = 0$. Hence,

$$\begin{aligned} \lambda &= 0 & \text{when } \Phi < 0 \\ \lambda &> 0 & \text{when } \Phi = 0 \\ \Phi &> 0 & \text{cannot occur} \end{aligned} \quad (2.6)$$

These conditions can be summarized as follows:

$$\lambda \geq 0 \quad \Phi(F) \leq 0 \quad \lambda \Phi = 0 \quad (2.7)$$

Equations (2.7) can be recognized as the Kuhn-Tucker optimality conditions (see for example, Fletcher (2000)). It is also seen that when $\Phi(F) = 0$, i.e. when yielding has

occurred, $\dot{\Phi} = \frac{\partial \Phi}{\partial t} \leq 0$, for if $\dot{\Phi} > 0$, then $\Phi(t + \Delta t) = \Phi(t) + \dot{\Phi} \Delta t + O(\Delta t^2) > 0$ for

sufficiently small Δt . Hence when $\Phi(F) = 0$:

$$\lambda \dot{\Phi} = 0 \quad (2.8)$$

This is known as the consistency condition of classical plasticity.

2.3. One Dimensional Plasticity - Rate Form

Equation (2.2) can be written in rate form as:

$$\dot{F} = k(\dot{\varepsilon} - \dot{\varepsilon}^p) \quad (2.9)$$

Since $\dot{\Phi} = \frac{\partial \Phi}{\partial F} \dot{F}$, it can be concluded from equation (2.8) that when $\Phi(F) = 0$,

$\lambda \frac{\partial \Phi}{\partial F} \dot{F} = 0$. Substituting in equation (2.9), we have:

$$\lambda \frac{\partial \Phi}{\partial F} \dot{F} = \lambda \frac{\partial \Phi}{\partial F} k(\dot{\epsilon} - \dot{\epsilon}^p) = 0 \quad (2.10)$$

If $\lambda \neq 0$, then $\frac{\partial \Phi}{\partial F} k(\dot{\epsilon} - \dot{\epsilon}^p) = 0 \Rightarrow \frac{\partial \Phi}{\partial F} k\left(\dot{\epsilon} - \lambda \frac{\partial \Phi}{\partial F}\right) = 0 \Rightarrow$

$$\lambda = \frac{\frac{\partial \Phi}{\partial F} k \dot{\epsilon}}{k\left(\frac{\partial \Phi}{\partial F}\right)^2} = \dot{\epsilon} \operatorname{sgn}(F) \quad (2.11)$$

If $\lambda = 0$, then either $\Phi < 0$ (unyielded) or $\dot{\Phi} < 0$ with $\Phi = 0$ (unloading). Let $H(x)$ be the Heaviside step function: $H(x) = 1$ if $x \geq 0$, $H(x) = 0$ if $x < 0$. It is seen that $\lambda = 0$ if and only if $H(\Phi)H(\dot{\Phi}) = 0$. Combining this with equation (2.11), the following results are obtained:

$$\lambda = H(\Phi)H(\dot{\Phi})\dot{\epsilon} \operatorname{sgn}(F) \quad (2.12)$$

Noting that $\operatorname{sgn}(F)\operatorname{sgn}(F) = 1$, we have:

$$\dot{\epsilon}^p = \lambda \operatorname{sgn}(F) = H(\Phi)H(\dot{\Phi})\dot{\epsilon} \quad (2.13)$$

$$\dot{F} = k(\dot{\epsilon} - \dot{\epsilon}^p) = k(1 - H_1 H_2)\dot{\epsilon} \quad (2.14)$$

where $H_1 = H(\Phi)$, the step function signifying yielding and $H_2 = H(\dot{\Phi})$, that signifies unloading from the yield surface. This is the statement of ideal plasticity in rate form. Two further generalizations can be performed at this stage. First, the step function H_1 can be smoothed as follows:

$$H_1 = \left| \frac{F}{F_y} \right|^N \quad (2.15)$$

where N is a real number and ideal plasticity is recovered as $N \rightarrow \infty$. Second, H_2 can be modified as follows:

$$H_2 = H(\dot{\Phi}) = \frac{1 + \text{sgn}(\dot{\Phi})}{2} = \frac{1 + \text{sgn}(\dot{F} \text{sgn}(F))}{2} = \frac{1 + \text{sgn}(F) \text{sgn}(\dot{F})}{2} \quad (2.16)$$

Furthermore, since the directions of the rate of change of force and the rate of change of strain are presumably the same, $\text{sgn}(\dot{F}) = \text{sgn}(\dot{\epsilon})$. Hence:

$$H_2 = \frac{1 + \text{sgn}(F\dot{\epsilon})}{2} = \eta_1 + \eta_2 \text{sgn}(F\dot{\epsilon}) \quad (2.17)$$

where $\eta_1 = \eta_2 = 0.5$ for classical ideal plasticity. But The shape of the unloading curve can be varied by varying η_1 and η_2 . However, the sum $\eta_1 + \eta_2$ must be equal to one to satisfy the yield condition (Constantinou and Adane (1987)). Thus equation (2.14) may be written as:

$$\dot{F} = \left(1 - \left| \frac{F}{F_y} \right|^N (\eta_1 + \eta_2 \text{sgn}(F\dot{\epsilon})) \right) \dot{\epsilon} \quad (2.18)$$

This is identical to the Bouc-Wen model without hardening (Wen (1976)). Sivaselvan and Reinhorn (2000) derived such relationships between other one dimensional constitutive models and also extend the rate model to include various deterioration effects stiffness and strength degradation and pinching.

Notice that as mentioned in Section 1, the inequality constraint (2.3) has led to the nonholonomic constraint (implicit differential equation (2.18) connecting the rate of change of stress to the rate of change of strain.

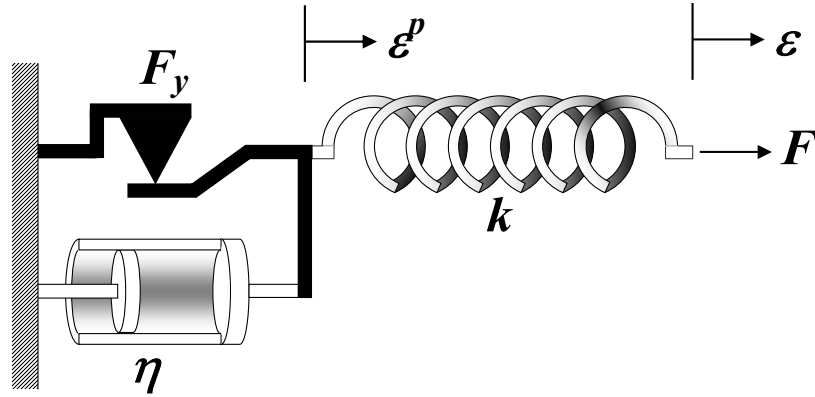


Fig. 2.2. Visco-plastic Regularization

2.4. One Dimensional Plasticity – Dissipation Form

Next, consider the elastic-visco-plastic system of Fig. 2.2. This is the visco-plastic regularization of the ideal plastic system of Fig. 2.1 (Duvaut and Lions (1976) and Simo and Hughes (1998)). If the force in the spring is F , then the force in the damper is:

$$F_{damper} = \begin{cases} 0 & \text{if } |F| \leq F_y \\ |F| - F_y & \text{if } |F| > F_y \end{cases} = \begin{cases} 0 & \text{if } |F| \leq F_y \\ (|F| - F_y) \text{sgn}(F) & \text{if } |F| > F_y \end{cases} = \langle |F| - F_y \rangle \text{sgn}(F) \quad (2.19)$$

Hence:

$$\dot{\varepsilon}^p = \frac{1}{\eta} F_{damper} = \frac{1}{\eta} \langle |F| - F_y \rangle \text{sgn}(F) \quad (2.20)$$

where η is the coefficient of the regularizing viscous damper and $\langle x \rangle = (x+|x|)/2$, the ramp function also known as the Mackaulay Bracket. The above constitutive equation can be derived from a convex dissipation function as follows:

Assume the function $\varphi(F)$ to be a penalty function that penalizes F 's that lie outside the elastic region:

$$\varphi(F) = \frac{1}{2\eta} \langle |F| - F_y \rangle^2 \quad (2.21)$$

Then:

$$\dot{\varepsilon}^p = \frac{\partial \varphi(F)}{\partial F} = \frac{1}{\eta} \langle |F| - F_y \rangle \text{sgn}(F) \quad (2.22)$$

In the limit of the viscous coefficient, η , going to zero, the dissipation function φ of equation (2.21) becomes:

$$\varphi(F) = \begin{cases} 0 & \text{if } |F_{slider}| \leq F_y \\ \infty & \text{if } |F_{slider}| > F_y \end{cases} \quad (2.23)$$

where F_{slider} is the force in the slider. In the language of Convex Analysis and Sub-differential Calculus, this function is referred to as the Indicator function of the elastic domain. The *Indicator Function* of a convex set C is defined as:

$$\mathbf{U}_C = \begin{cases} 0 & \text{if } x \in C \\ \infty & \text{if } x \notin C \end{cases} \quad (2.24)$$

Thus, if C is the elastic domain, $C = \{x: |x| < F_y\}$, then $\varphi(F) = \mathbf{U}_C(F)$. The plastic strain rate is such that:

$$\dot{\varepsilon}^p \in \partial \varphi(F) \quad (2.25)$$

where ∂ is the multi-valued sub-gradient operator. For a comprehensive treatment of this subject, the reader is referred to Hiriart-Urruty and Lemaréchal (1993) and for a discussion in the context of Plasticity Theory, to Han and Reddy (1999). However, since the tools of Sub-differential Calculus are not absolutely essential for the developments in this work and in order to keep the notation tractable, it is chosen to carry out all derivations involving the dissipation function using the well-behaved regularized form and impose the ideal-plastic limit as a final step.

2.5. Kinematic Hardening – Series vs. Parallel Models

The experimentally observed one-dimensional behavior of many materials and components can be idealized as follows: (i) after yielding, the slope of the force-deformation curve is positive, but smaller than that in the elastic region; (ii) under cyclic loading, the force lies between two parallel lines as shown in Fig. 2.3. This behavior is known as *kinematic hardening* and is closely related to the *Bauschinger Effect* in structural steel. Kinematic hardening can be modeled using the series model as shown in Fig. 2.4 or using the parallel model as shown in Fig. 2.5 (Nelson and Dorfmann (1995), Thyagarajan (1989) and Iwan (1966)).

In this work, we use the parallel model for kinematic hardening. The constitutive equations are as follows:

$$F = F^p + F^h \quad \text{and} \quad F^p = F - F^h = F - \alpha k \varepsilon \quad (2.26)$$

where F^p is the elastic-plastic force and F^h is the hardening force as shown in Fig. 2.5. The yield condition is given by:

$$\Phi(F^p) = |F^p| - (1 - \alpha) F_y \leq 0 \quad (2.27)$$

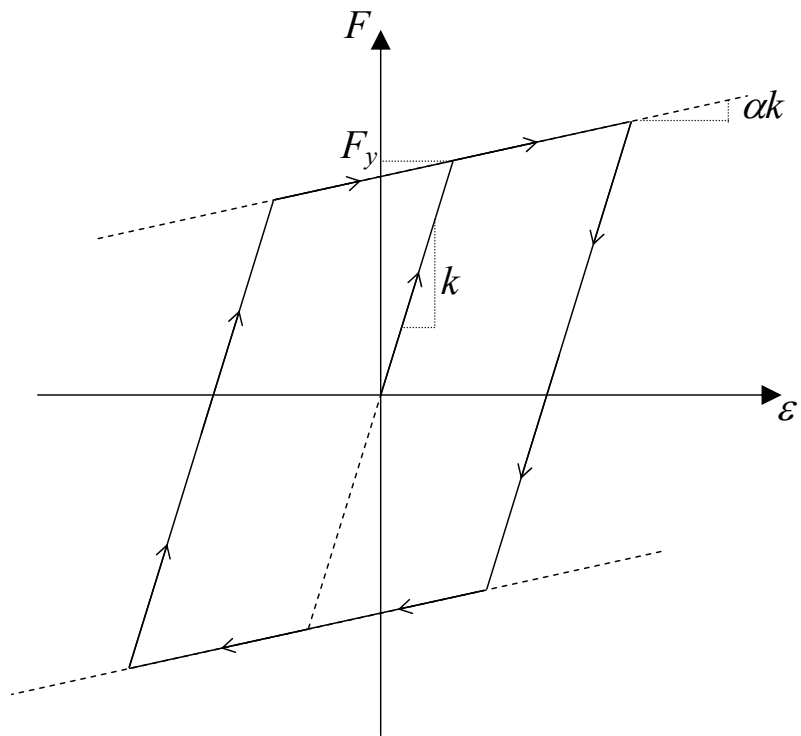


Fig. 2.3. Kinematic Hardening

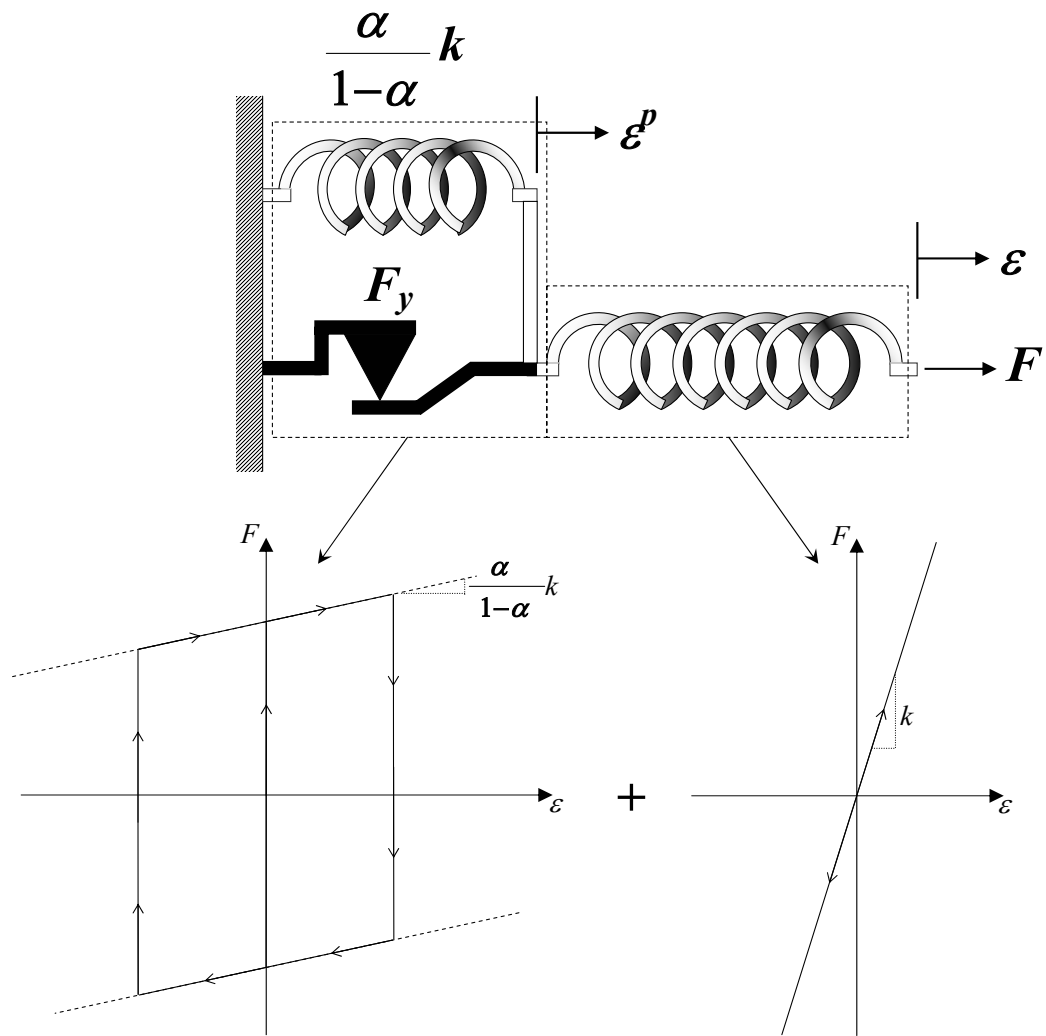


Fig. 2.4. Kinematic Hardening - Series Model

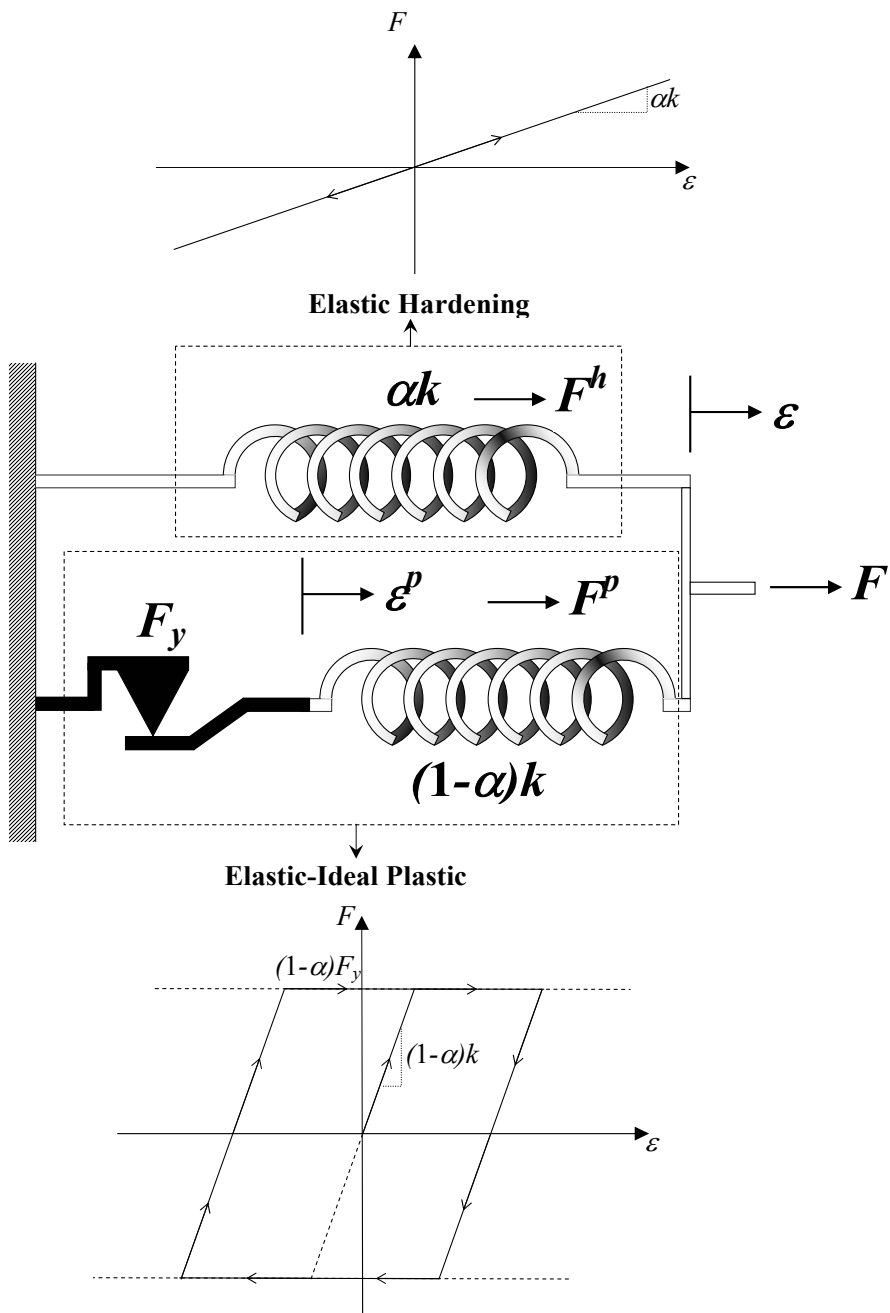


Fig. 2.5. Kinematic Hardening - Parallel Model

and the rate form of the plasticity relation by:

$$\dot{F} = \alpha k \dot{\varepsilon} + (1 - \alpha) k (1 - H_1 H_2) \dot{\varepsilon} \quad (2.28)$$

where H_1 and H_2 may be the modified functions:

$$H_1 = \left| \frac{F^p}{(1 - \alpha) F_y} \right|^N \quad \text{and} \quad H_2 = \eta_1 + \eta_2 \operatorname{sgn}(F^p \dot{\varepsilon}) \quad (2.29)$$

The elastic domain, $C = \{x : |x| < (1 - \alpha) F_y\}$. Then the dissipation function, regularized dissipation function and the dissipation form of the plasticity relation are given respectively by:

$$\varphi(F^p) = \mathbf{U}_C(F^p) \quad (2.30)$$

$$\varphi(F) = \frac{1}{2\eta} \left\langle |F^p| - (1 - \alpha) F_y \right\rangle^2 \quad (2.31)$$

$$\dot{\varepsilon}^p = \frac{\partial \varphi(F^p)}{\partial F^p} = \frac{1}{\eta} \left\langle |F^p| - (1 - \alpha) F_y \right\rangle \operatorname{sgn}(F) \quad (2.32)$$

The series formulation will be discussed briefly in Section 5. In the State Space Approach of Sections 3 and 4, the rate forms will be used, while in the Lagrangian Approach of Section 5, the dissipation form will be used.

2.6. Multi-dimensional Plasticity

The relations of plasticity can be derived for the multi-dimensional case, i.e., where there is interaction between the stress-resultants, along similar lines as the one dimensional case. Equations (2.1)-(2.4) have their multi-dimensional analogues:

$$\boldsymbol{\varepsilon} = \boldsymbol{\varepsilon}^e + \boldsymbol{\varepsilon}^p \quad (2.33)$$

$$\mathcal{F} = \mathbf{k}(\boldsymbol{\varepsilon} - \boldsymbol{\varepsilon}^p) \quad (2.34)$$

subject to the yield condition:

$$\Phi(\mathbf{F}) \leq 0 \quad (2.35)$$

and the flow rule:

$$\dot{\boldsymbol{\varepsilon}}^p = \lambda \frac{\partial \Phi}{\partial \mathcal{F}} \quad (2.36)$$

where \mathcal{F} is the stress-resultant vector, $\boldsymbol{\varepsilon}$ is the total deformation vector, $\boldsymbol{\varepsilon}^p$ is the plastic deformation vector, \mathbf{k} is the cross-section elastic rigidity matrix consisting of the axial rigidity (EA), the flexural rigidity (EI) etc. and λ is the plastic multiplier. The Kuhn-Tucker conditions:

$$\lambda \geq 0 \quad \Phi(\mathcal{F}) \leq 0 \quad \lambda \Phi = 0 \quad (2.37)$$

are identical to equations (2.7) except that the yield function Φ is now a function of \mathcal{F} , the stress-resultant vector. Using the consistency condition, $\lambda \dot{\Phi} = 0$, the plastic multiplier, λ , and the plastic strain rate, $\dot{\boldsymbol{\varepsilon}}^p$, are obtained in a fashion similar to equation (2.11) as:

$$\lambda = \frac{\left(\frac{\partial \Phi}{\partial \mathcal{F}}\right)^T \mathbf{k} \dot{\boldsymbol{\varepsilon}}}{\left(\frac{\partial \Phi}{\partial \mathcal{F}}\right)^T \mathbf{k} \left(\frac{\partial \Phi}{\partial \mathcal{F}}\right)} \quad (2.38)$$

$$\dot{\boldsymbol{\varepsilon}}^p = \frac{\left(\frac{\partial \Phi}{\partial \mathcal{F}}\right)^T \mathbf{k} \dot{\boldsymbol{\varepsilon}}}{\left(\frac{\partial \Phi}{\partial \mathcal{F}}\right)^T \mathbf{k} \left(\frac{\partial \Phi}{\partial \mathcal{F}}\right)} \frac{\partial \Phi}{\partial \mathcal{F}} \quad (2.39)$$

The following equation (2.14), the rate of change of the stress-resultant vector is:

$$\dot{\mathcal{F}} = \left[\mathbf{k}\dot{\boldsymbol{\varepsilon}} - H_1 H_2 \frac{\left(\frac{\partial\Phi}{\partial\mathcal{F}}\right)^T \mathbf{k}\dot{\boldsymbol{\varepsilon}}}{\left(\frac{\partial\Phi}{\partial\mathcal{F}}\right)^T \mathbf{k} \left(\frac{\partial\Phi}{\partial\mathcal{F}}\right)} \frac{\partial\Phi}{\partial\mathcal{F}} \right] \quad (2.40)$$

where, as before, where $H_1 = H(\Phi)$, the step function signifying yielding and $H_2 = H(\dot{\Phi})$, that signifies unloading from the yield surface. By non-dimensionalizing the stress-resultants, it can be arranged that $\Phi(\mathcal{F}) = \Phi'(\mathcal{F}) - 1$. Then again, these step functions may be generalized as follows:

$$H_1 = |\Phi(\mathcal{F}) + 1|^N \quad \text{and} \quad H_2 = \eta_1 + \eta_2 \operatorname{sgn}(\mathcal{F}^T \dot{\boldsymbol{\varepsilon}}) \quad (2.41)$$

Equation (2.40) can be attributed two geometric meanings:

1. Let $\hat{\mathbf{n}} = \frac{\mathbf{k} \left(\frac{\partial\Phi}{\partial\mathcal{F}}\right)}{\sqrt{\left(\frac{\partial\Phi}{\partial\mathcal{F}}\right)^T \mathbf{k} \left(\frac{\partial\Phi}{\partial\mathcal{F}}\right)}}$. $\hat{\mathbf{n}}$ is the unit normal to the yield surface in the \mathbf{k}^{-1} norm,

i.e., $\|\hat{\mathbf{n}}\|_{\mathbf{k}^{-1}}^2 = \hat{\mathbf{n}}^T \mathbf{k}^{-1} \hat{\mathbf{n}} = 1$. Then when $H_1 = H_2 = 1$, i.e., when on the yield

surface, $\dot{\mathcal{F}} = \left[\mathbf{k}\dot{\boldsymbol{\varepsilon}} - \left(\hat{\mathbf{n}}^T \mathbf{k}^{-1} \mathbf{k}\dot{\boldsymbol{\varepsilon}}\right) \hat{\mathbf{n}} \right]$. Thus $\dot{\mathcal{F}}$ is the projection in the \mathbf{k}^{-1} norm of $\mathbf{k}\dot{\boldsymbol{\varepsilon}}$ on

the tangent plane to the yield surface (Simo and Govindjee (1991)).

2. The interaction matrix

$$\mathbf{B} = \frac{\left(\frac{\partial\Phi}{\partial\mathcal{F}}\right) \left(\frac{\partial\Phi}{\partial\mathcal{F}}\right)^T \mathbf{k}}{\left(\frac{\partial\Phi}{\partial\mathcal{F}}\right)^T \mathbf{k} \left(\frac{\partial\Phi}{\partial\mathcal{F}}\right)} \quad (2.42)$$

is introduced. It can be verified from equation (2.39) that $\dot{\boldsymbol{\varepsilon}}^p = \mathbf{B}\dot{\boldsymbol{\varepsilon}}$. Also $\mathbf{B}\mathbf{B} = \mathbf{B}$.

Hence \mathbf{B} is a *projection matrix* (Trefethen and Bau (1997)). \mathbf{B} projects $\dot{\boldsymbol{\varepsilon}}$ onto the

normal $\frac{\partial\Phi}{\partial\mathcal{F}}$ to the yield surface. The rate form of plasticity is therefore:

$$\dot{\mathcal{F}} = \mathbf{k}[\mathbf{I} - H_1 H_2 \mathbf{B}]\dot{\boldsymbol{\varepsilon}} \quad (2.43)$$

where \mathbf{I} is the identity matrix. Observe the similarity between equations (2.43) and (2.14).

The elastic domain is given by $C = \{\mathcal{F} : \Phi(\mathcal{F}) < 0\}$. Hence, the dissipation function is $\varphi(\mathcal{F}) = U_c(\mathcal{F})$. In the multi-dimensional case, there are several possible regularizations. Two of these are (Simo and Hughes (1998)):

1. Duvaut-Lions Regularization:

$$\varphi(\mathcal{F}) = \frac{1}{2\eta} \|\mathcal{F} - \mathbb{P}_C \mathcal{F}\|^2 \quad (2.44)$$

where $\mathbb{P}_C \mathcal{F}$ is the orthogonal projection of \mathcal{F} on the set C and $\|\cdot\|$ is the vector 2-norm.

2. Perzyna Regularization:

$$\varphi(\mathcal{F}) = \frac{1}{2\eta} \langle \Phi(\mathcal{F}) \rangle^2 \quad (2.45)$$

where $\langle \cdot \rangle$ denote the Mackaulay brackets. The dissipation form of the plastic constitutive law is then:

$$\dot{\boldsymbol{\varepsilon}}^p = \frac{\partial \varphi(\mathcal{F})}{\partial \mathcal{F}} \quad (2.46)$$

Kinematic Hardening is again incorporated using the parallel model. The analogues of equations (2.27) and (2.28) are:

$$\Phi(\mathcal{F}^p) \leq 0 \quad (2.47)$$

$$\dot{\mathcal{F}} = \boldsymbol{\alpha} \mathbf{k} \dot{\boldsymbol{\varepsilon}} + (\mathbf{I} - \boldsymbol{\alpha}) \mathbf{k} (\mathbf{I} - H_1 H_2 \mathbf{B}) \dot{\boldsymbol{\varepsilon}} \quad (2.48)$$

where α is the diagonal matrix of post-yield slope ratios, and \mathcal{F}^p , the plastic component of the stress-resultant vector is $\mathcal{F}^p = \mathcal{F} - \alpha \mathbf{k} \epsilon$.

2.7. Yield Functions Φ

Two yield functions are used in this work to model the behavior of beam-column cross sections. In the following, p , m^y and m^z are the non-dimensional axial force, minor- and major-axis moments, $p = \frac{P}{P_y}$, $m^y = \frac{M^y}{M_y^y}$ and $m^z = \frac{M^z}{M_y^z}$. P is the axial force and M 's, the bending moments on the cross-section. Superscripts y and z on the bending moments denote the axis of bending and subscript y denotes the yielding value of the stress-resultant in the absence of the other stress-resultants. The stress-resultant vector, $\mathcal{F} = \{P \quad M^y \quad M^z\}^T$.

1. Yield Function 1: This is the function given by Simeonov (1999) for structural steel I-sections and is given by:

$$\Phi(\mathcal{F}) = \left(\frac{|m^y|}{1 - |p|^{b_1^y + b_2^y |p|}} \right)^{c_1^y + c_2^y |p|} + \left(\frac{|m^z|}{1 - |p|^{b_1^z + b_2^z |p|}} \right)^{c_1^z + c_2^z |p|} - 1 \quad (2.49)$$

where $b_1^y, b_2^y, c_1^y, c_2^y, b_1^z, b_2^z, c_1^z$ and c_2^z are coefficients that control the shape of the surface. The parameters of the surface are explained in detail by Simeonov (1999).

2. Yield Function 2: This is the yield function presented by McGuire et al. (2000) for wide-flanged structural steel I-sections and is given by:

$$\Phi(\mathcal{F}) = p^2 + (m^z)^2 + (m^y)^4 + 3.5p^2(m^z)^2 + 3p^6(m^y)^2 + 4.5(m^z)^2(m^y)^2 - 1 \quad (2.50)$$

When modeling kinematic hardening by the parallel model, the yield function has to be modified appropriately. In this case, the non-dimensional quantities used in equations

(2.49) and (2.50) are $p = \frac{P^p}{P_y^p}$, $m^y = \frac{M^{yp}}{M_y^{yp}}$ and $m^z = \frac{M^{zp}}{M_y^{zp}}$ where the plastic components,

$\mathcal{F}^p = \{P^p \quad M^{yp} \quad M^{zp}\}^T$, and P_y^p , M_y^{yp} and M_y^{zp} are the plastic components of the

respective yield values given by $P_y^p = (1-\alpha)P_y$, $M_y^{yp} = (1-\alpha)M_y^y$ and $M_y^{zp} = (1-\alpha)M_y^z$.

The biaxial hysteretic model used by Park et al. (1986) in random vibration, by Nagarajaiah et al. (1989) and Fenves et al. (1998) to model seismic isolation bearings and by Kunnath and Reinhorn (1990) to model the biaxial bending interaction in reinforced concrete cross-sections is in fact an application of equation (2.48) with a two dimensional circular or elliptic yield function.

2.8. Summary

The constitutive relations of classical plasticity theory have been established in forms suitable for use in following sections. In the state space approach of Sections 3 and 4, the rate forms (2.18) and (2.48) will be used as non-holonomic constraints, while in the Lagrangian Approach of Section 5, the Dissipation Form (2.46) will be used.

3. THE STATE SPACE APPROACH

3.1. Background

In this section, an alternate method is proposed for the static and dynamic analysis of structures with inelastic behavior. The solution is aimed at performing analysis beyond the onset of yielding near collapse and at considering strength changes as well as stability issues. The governing equations of motion and constitutive behavior of a structure are considered as constituting a constrained dynamical system. This leads to an alternative approach to the formulation and solution of initial-boundary-value problems involving nonlinear distributed-parameter structural systems by solving the equations of balance and the constitutive equations simultaneously.

For a dynamical system comprising lumped-parameter elements whose nodal force-displacement relationships are available directly (e.g. base isolation systems, various damping systems etc.), introducing nodal velocities and the forces in these elements as additional unknowns results in a set of explicit first-order Ordinary Differential Equations (ODE). Such dynamic system is *unconstrained* and can be solved using any appropriate numerical method. This approach has been extensively employed in the solution of dynamic linear and non-linear problems especially in structural control and non-deterministic analysis (see for example Nagarajaiah, Constantinou et al. (1989), Inaudi and de la Llera (1993), Casciati and Faravelli (1988) and Barroso et al. (1998)).

However, in the general case, the dynamic system has holonomic as well as non-holonomic constraints. When there are un-damped quasi-static degrees of freedom (i.e., the mass and/or damping matrix is singular) the equations of equilibrium in these degrees of freedom are holonomic constraints on the internal forces. When considering

distributed plasticity, the constitutive relations are non-holonomic constraints. The resulting system of equations not only consists of explicit ODE's but also contains implicit ODE's (arising from the non-holonomic constraints) and algebraic equations (arising from the holonomic constraints). The numerical solution of such systems of Differential-Algebraic Equations (DAE) is more complex than the solution of ODE's and reliable methods for this purpose have been developed more recently (Brenan et al. (1996))

The structure, which is spatially discretized following a weak formulation, is completely characterized by a set of state variables. These include global quantities such as nodal displacements and velocities and local quantities such as nodal forces and strains at integration points. The evolution of the global state variables is governed by physical principles such as momentum balance and that of the local variables by constitutive behavior. The response of the system is described by a set of equations involving the state variables and their rates.

3.2. Overview of Previous Work

The state-space approach (SSA) involving DAE's has been used extensively in multi-body dynamics of aerospace and mechanical assemblies (see for example, Bauchau et al. (1995) and Haug et al. (1997)). The first application of the state-space approach to finite-element solution of quasi-static distributed plasticity problems, is that of Richard and Blalock (1969), to solve plane-stress problems. Since this work considered only monotonic loading, the load factor (rather than time) served as the independent monotonically increasing variable. It is surprising, however, that no subsequent work in this direction has been reported until the beginning of the last decade. Hall et al. (1991),

used DAE's to solve large deformation plasticity problems arising in punch stretching in metal forming operations. Papadopoulos and Taylor (1994), presented a solution algorithm based on DAE for J_2 plasticity problems with infinitesimal strain. Papadopoulos and Lu (1998) subsequently extended this strategy to a generalized framework for solution of finite plasticity problems. Iura and Atluri (1995), used the DAE-based state-space approach for the dynamic analysis of planar flexible beams with finite rotations. The first formal description of the methodology of formulating initial-boundary-value problems in nonlinear structural analysis was provided by Fritzen and Wittekindt (1997) and by Shi and Babuska (1997). These works provide the motivation for the approach proposed here.

3.3. Section Outline

The work reported here consists of four parts. First, a general procedure is presented for identifying the state variables of a spatially-discretized structure. Second, the algorithm for constructing the system of state equations is introduced, accounting for element connectivity, boundary conditions, constitutive relationships, and different types of excitation. Third, a nonlinear beam element based on force-interpolation and a constitutive macro-model is developed in this framework. Fourth, the above development is implemented in a computer program and the quasi-static and dynamic responses of a typical frame structure are validated against benchmark solutions. The DAE solver DASSL (Brenan, Campbell et al. (1996)) has been used in this work.

3.4. State Variables and Equations of a SDOF System

A nonlinear single-degree-of-freedom (SDOF) system, subjected to dynamic and quasi-static forces, will be used to illustrate the state-space formulation. The constitutive

model of equation (2.28) will be used to represent the system. The model in Fig. 3.1 has three state variables and, therefore, three state equations.

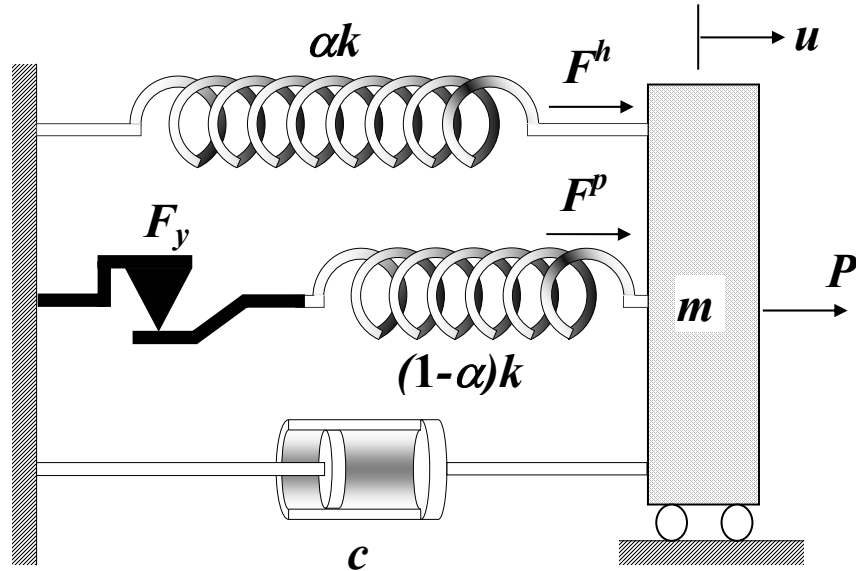


Fig. 3.1. SDOF System

Let,

$$y_1 = u \quad , \quad y_2 = \dot{u} \quad , \quad y_3 = F = F^p + F^h \quad (3.1)$$

Then, for the dynamic problem the response is described by,

$$m\dot{y}_2 + c\dot{y}_1 + y_3 - P = 0 \quad (3.2)$$

$$y_2 - \dot{y}_1 = 0 \quad (3.3)$$

$$\dot{y}_3 - [\alpha k + (1-\alpha)k(1-H_1H_2)]y_2 = 0 \quad (3.4)$$

For this system, y_1 and y_2 are the global state variables and y_3 is the local state variable. Correspondingly, (3.2) and (3.3) are the global state equations and (3.4) is the local state equation. In terms of the state variables H_1 and H_2 of equations (2.29) are as follows:

$$H_1 = \left| \frac{y_3 - \alpha k y_1}{(1 - \alpha) F_y} \right|^N \quad \text{and} \quad H_2 = \eta_1 \operatorname{sgn}[(y_3 - \alpha k y_1) y_2] + \eta_2 \quad (3.5)$$

Equations (3.5) are identical to equations (2.29) of Section 2 with the definitions of the state variables y_1 , y_2 and y_3 in equation (3.1). It should be noted that the choice of state variables for this system is not unique. For example, an alternative, and probably more natural, formulation of the same problem can be devised using the hysteretic component of the restoring force as a local state variable. Let,

$$y_1 = u, \quad y_2 = \dot{u}, \quad y_3 = F^p \quad (3.6)$$

Then, the response of the SDOF system is described by,

$$m\dot{y}_2 + c\dot{y}_1 + \alpha k y_1 + y_3 - P = 0 \quad (3.7)$$

$$y_2 - \dot{y}_1 = 0 \quad (3.8)$$

$$\dot{y}_3 - (1 - \alpha)k(1 - H_1 H_2) y_2 = 0 \quad (3.9)$$

H_1 and H_2 are then given by:

$$H_1 = \left| \frac{y_3}{(1 - \alpha) F_y} \right|^N \quad \text{and} \quad H_2 = \eta_1 \operatorname{sgn}(y_3 y_2) + \eta_2 \quad (3.10)$$

The first version, however, is preferred for reasons, which will become apparent later. In either case, we obtain a system of ODE.

In contrast to the dynamic system (3.2)-(3.4), a quasi-static system subjected to identical force history, has only two state variables, hence, two state equations. Let,

$$y_1 = u, \quad y_2 = F \quad (3.11)$$

Then, the response of the SDOF system is described by,

$$y_2 - P = 0 \quad (3.12)$$

$$\dot{y}_2 - [\alpha k + (1 - \alpha)k(1 - H_1 H_2)] \dot{y}_1 = 0 \quad (3.13)$$

In this case, the constitutive equation (3.13) is an implicit differential equation and the equation of equilibrium (3.12) is algebraic. Therefore, a set of DAE must be solved to obtain the quasi-static response of SDOF system with nonlinear restoring force.

3.5. Differential-Algebraic Equations (DAE)

A DAE system is a coupled system of N ordinary differential and algebraic equations, which can be written in the following form:

$$\Phi(t, \mathbf{y}, \dot{\mathbf{y}}) = \mathbf{0} \quad (3.14)$$

where Φ , \mathbf{y} and $\dot{\mathbf{y}}$ are N-dimensional vectors; t is the independent variable; \mathbf{y} and $\dot{\mathbf{y}}$ are the dependent variables and their derivatives with respect to t . Some of the equations in (3.14), however, may not have a component of $\dot{\mathbf{y}}$. Consequently, the matrix

$$\frac{\partial \Phi}{\partial \dot{\mathbf{y}}} = \begin{bmatrix} \frac{\partial \Phi_i}{\partial \dot{y}_j} \end{bmatrix} \quad (3.15)$$

may be singular. A measure of the singularity is the *index* (Brenan, Campbell et al. (1996)). This, in simple terms, is equal to the minimum number of times equation (3.14) must be differentiated with respect to t to determine $\dot{\mathbf{y}}$ explicitly as functions of \mathbf{y} and t . The explicit ODE system,

$$\dot{\mathbf{y}} = \mathbf{g}(t, \mathbf{y}) \quad (3.16)$$

therefore has index 0. The system composed of (3.2)-(3.4), for example, can be converted to the standard form without additional differentiation.

$$\dot{y}_1 = y_2 \quad (3.17)$$

$$\dot{y}_2 = \frac{P - cy_2 - y_3}{m} \quad (3.18)$$

$$\dot{y}_3 = \alpha ky_2 + (1 - \alpha)k \left\{ 1 - \left| \frac{y_3 - \alpha ky_1}{(1 - \alpha)F_y} \right|^n \left[\eta_1 \operatorname{sgn}((y_3 - \alpha ky_1)y_2) + \eta_2 \right] \right\} y_2 \quad (3.19)$$

Equations (3.12) and (3.13) modeling the quasi-static response of SDOF system, however, is index 1, because the algebraic equation (3.12) must be differentiated *once* before substitution in (3.13).

$$\dot{y}_2 = \dot{P} \quad (3.20)$$

$$\dot{y}_1 = \frac{\dot{P}}{\alpha k + (1 - \alpha)k \left\{ 1 - \left| \frac{y_3 - \alpha ky_1}{(1 - \alpha)F_y} \right|^n \left[\eta_1 \operatorname{sgn}((y_3 - \alpha ky_1)\dot{y}_1) + \eta_2 \right] \right\}} \quad (3.21)$$

Strictly speaking, this is not an explicit ODE because \dot{y}_1 appears on the right-hand side of (3.21). But since it appears only in the *signum* function, which is a constant function except for the singularity at $\dot{y}_1 = 0$, the index may be taken to be 1.

The numerical solution of DAE is more involved than the solution of ODE. A brief summary of the integration method in DASSL is provided for the sake of completeness. The derivative $\dot{\mathbf{y}}$ is approximated by a backward differentiation formula:

$$\dot{\mathbf{y}}_n = \frac{1}{h_n \beta_0} \left(\mathbf{y}_n - \sum_{i=1}^k \alpha_i \mathbf{y}_{n-i} \right) \quad (3.22)$$

where, \mathbf{y}_n , $\dot{\mathbf{y}}_n$ and \mathbf{y}_{n-1} are the approximations of the solution of (3.14) and its derivative at times t_n and t_{n-1} , respectively; $h_n = t_n - t_{n-1}$ is the time interval; k is the order of the backward differentiation formula relative to \mathbf{y}_n ; α_i and β_0 are the coefficients of the method. Substituting (3.22) in (3.14) results in a system of nonlinear algebraic equations:

$$\Phi \left[t_n, \mathbf{y}_n, \frac{1}{h_n \beta_0} \left(\mathbf{y}_n - \sum_{i=1}^k \alpha_i \mathbf{y}_{n-i} \right) \right] = \mathbf{0} \quad (3.23)$$

These are solved by the Newton-Raphson method using an iteration matrix of the form:

$$\mathbf{N}(t_n, \mathbf{y}_n, \dot{\mathbf{y}}_n) = \frac{\partial \Phi(t_n, \mathbf{y}_n, \dot{\mathbf{y}}_n)}{\partial \mathbf{y}} + \frac{1}{h_n \beta_0} \frac{\partial \Phi(t_n, \mathbf{y}_n, \dot{\mathbf{y}}_n)}{\partial \dot{\mathbf{y}}} \quad (3.24)$$

The process of advancing from time t_{n-1} to the current time t_n is summarized by the equation:

$$\mathbf{y}_n^{m+1} = \mathbf{y}_n^m - \mathbf{N}^{-1}(t_n, \mathbf{y}_n^m, \dot{\mathbf{y}}_n^m) \Phi(t_n, \mathbf{y}_n^m, \dot{\mathbf{y}}_n^m) \quad (3.25)$$

where the superscript m is the iteration counter. A detailed description of the numerical algorithm can be found in Brenan, Campbell et al. (1996).

3.6. State Variables and Equations of a Multi-Degree-of-Freedom System

The equation of motion of a multi-degree-of-freedom (MDOF) system is shown in equation (AI.15) of Appendix I.

3.6.1. Global State Variables

In the general case, the set of global state variables of the system consists of three parts:

1. Generalized displacements along all *free* nodal degrees of freedom: Displacements along constrained generalized coordinates are excluded by virtue of imposing boundary conditions.
2. Generalized displacements along degrees of freedom with imposed displacement histories: This occurs, for example, when support displacements due to settlement or earthquake motion are prescribed and in displacement-controlled laboratory testing.
3. Velocities along mass degrees of freedom: The number of velocity state variables may be less than the number of displacement variables because often, rotational and even some translational mass components, are ignored if their effect is presumed negligible.

3.6.2. Local State Variables

The local state variables describe the evolution of individual elements. These consist of,

1. Independent element internal end forces.
2. Constitutive variables, such as stresses or strains at the integration points, according to Table 3.1, which may be required to characterize inelasticity.
3. Any other internal variable that may govern the behavior of the element (e.g. yield stresses, back-stress, etc.)

3.6.3. State Equations

The three sets of global state equations can be summarized as follows:

$$N_{free} \begin{cases} N_{mass} \rightarrow \\ N_{damp} \rightarrow \\ N_{static} \rightarrow \end{cases} \begin{bmatrix} \mathbf{M} & \mathbf{0} & \mathbf{0} \\ \mathbf{0} & \mathbf{0} & \mathbf{0} \\ \mathbf{0} & \mathbf{0} & \mathbf{0} \end{bmatrix} \begin{Bmatrix} \dot{\mathbf{y}}_2^1 \\ \dot{\mathbf{y}}_2^2 \\ \dot{\mathbf{y}}_2^3 \end{Bmatrix} + \begin{bmatrix} \mathbf{C}_{11} & \mathbf{C}_{12} & \mathbf{0} \\ \mathbf{C}_{12}^T & \mathbf{C}_{22} & \mathbf{0} \\ \mathbf{0} & \mathbf{0} & \mathbf{0} \end{bmatrix} \begin{Bmatrix} \mathbf{y}_2^1 \\ \mathbf{y}_1^2 \\ \mathbf{y}_2^3 \end{Bmatrix} + \begin{bmatrix} \mathbf{B}_1^T \\ \mathbf{B}_2^T \\ \mathbf{B}_3^T \end{bmatrix}^T \mathbf{y}_3 - \begin{Bmatrix} \mathbf{P}^1 \\ \mathbf{P}^2 \\ \mathbf{P}^3 \end{Bmatrix} = \mathbf{0} \quad (3.26)$$

$$N_{spec} \left[\mathbf{y}_1^4 - \mathbf{d} = \mathbf{0} \right] \quad (3.27)$$

$$N_{mass} \left[\dot{\mathbf{y}}_1^1 - \mathbf{y}_2^1 = \mathbf{0} \right] \quad (3.28)$$

where, $\mathbf{y}_1 = \mathbf{u}(t)$, $\mathbf{y}_2 = \dot{\mathbf{u}}(t)$, $\mathbf{y}_3 = \mathbf{F} = \left\{ (\mathbf{Q}^1)^T \quad (\mathbf{Q}^2)^T \quad \dots \quad (\mathbf{Q}^{N_e})^T \right\}^T$, \mathbf{d} = prescribed displacement history vector and superscripts denote partitions described in Appendix I.

The state of each nonlinear element i is defined by evolution equations involving the end forces, displacements and the internal variables used in the formulation of the element model. These equations are of the form:

$$\mathbf{A}^{et}(\mathbf{u}^{e,i}, \mathbf{z}^i) \dot{\mathbf{Q}}^i = \mathbf{G}(\mathbf{Q}, \mathbf{u}^{e,i}, \dot{\mathbf{u}}^{e,i}, \mathbf{z}^i, \dot{\mathbf{z}}^i) \quad \dot{\mathbf{z}}^i = \mathbf{H}(\mathbf{z}^i, \mathbf{Q}^i, \dot{\mathbf{Q}}^i, \mathbf{u}^{e,i}, \dot{\mathbf{u}}^{e,i}) \quad (3.29)$$

where $\mathbf{A}^{et}(\mathbf{u}^{e,i}, \mathbf{z}^i)$ is the element tangent flexibility matrix; \mathbf{G} and \mathbf{H} are nonlinear functions; \mathbf{Q}^i and $\dot{\mathbf{Q}}^i$ are the independent element end forces and their rates; $\mathbf{u}^{e,i}$ and $\dot{\mathbf{u}}^{e,i}$ are the displacements of the element nodes and their rates; \mathbf{z}^i and $\dot{\mathbf{z}}^i$ are the internal variables and their rates. It must be noted that the first part of equation (3.29) would not be necessary in a displacement-based formulation. The formulation of these equations for a small deformation beam element is presented in the next subsection and that for a large deformation beam-column element in Section 4. The *state vector* of the structure is $\mathbf{y} = \left\{ \mathbf{y}_1^T \quad (\mathbf{y}_2^1)^T \quad \mathbf{y}_3^T \quad \mathbf{y}_4^T \right\}^T$, where $\mathbf{y}_4 = \left\{ (\mathbf{z}^1)^T \quad (\mathbf{z}^2)^T \quad \dots \quad (\mathbf{z}^{N_{elem}})^T \right\}^T$. The *state equations* (3.26)-(3.29) consist of explicit ordinary differential equations (the first two partitions of (3.26) and (3.28)), implicit ordinary differential equations (3.29), as well as algebraic equations (the third partition of (3.26) and (3.27)). They therefore constitute a system of DAE of the form (3.14).

3.7. Formulation of a Flexibility-Based Planar Beam Element

The beam element is internally statically determinate. Therefore, a flexibility formulation using force interpolation functions is utilized here. The displacement interpolation functions used in the usual stiffness-based formulations are exact only for elastic prismatic members. In contrast, the force interpolation functions, which are statements of equilibrium, are always exact. The state variables of the beam element are the *independent end forces* and the *strains and curvatures* of sections located at the *NG* quadrature points. Compatibility of deformation within the element may be expressed in weak form using the principle of virtual forces as:

$$\dot{\mathbf{q}} = \begin{Bmatrix} \dot{q}_1 \\ \dot{q}_5 \\ \dot{q}_6 \end{Bmatrix} = \int_0^L \mathbf{b}^T \begin{Bmatrix} \dot{\varepsilon} \\ \dot{\phi} \end{Bmatrix} dx = \int_0^L \mathbf{b}^T \dot{\boldsymbol{\varepsilon}} dx \quad (3.30)$$

where $\boldsymbol{\varepsilon} = \{\varepsilon \ \phi\}^T$, the vector of centroidal strain and curvature and \mathbf{b} is the force interpolation matrix:

$$\mathbf{b} = \begin{bmatrix} 1 & 0 & 0 \\ 0 & \frac{x}{L} - 1 & \frac{x}{L} \end{bmatrix} \quad (3.31)$$

where L is the length of the beam and x is the coordinate along the length of the beam. From the equilibrium of a segment, the stress resultant vector at any section can be obtained as:

$$\mathcal{F} = \begin{Bmatrix} N^x \\ M^z \end{Bmatrix} = \mathbf{b} \begin{Bmatrix} Q_1 \\ Q_5 \\ Q_6 \end{Bmatrix} = \mathbf{b}\mathbf{Q} \quad (3.32)$$

where N^x = axial force at any section, M^x = bending moment at any section, Q_1 = force component parallel to the element chord, Q_5 = bending moment at the left end and Q_6 = bending moment at the right end. From Appendix I, we have the following transformations:

$$\mathbf{P}^e = \mathbf{R}^T \mathbf{T}_R^T \mathbf{Q} = \mathbf{B}^e \mathbf{Q} \quad (3.33)$$

$$\dot{\mathbf{q}} = \mathbf{T}_R \mathbf{R} \dot{\mathbf{u}}^e = (\mathbf{B}^e)^T \dot{\mathbf{u}}^e \quad (3.34)$$

where \mathbf{R} = 6×6 rotation matrix (Weaver and Gere (1990)) and

$$\mathbf{T}_R = \begin{bmatrix} -1 & 0 & 0 & 1 & 0 & 0 \\ 0 & \frac{1}{L} & 1 & 0 & -\frac{1}{L} & 0 \\ 0 & \frac{1}{L} & 0 & 0 & -\frac{1}{L} & 1 \end{bmatrix} \quad (3.35)$$

The rate form of plasticity, (2.28), is used to represent this constitutive macro-model. In this section, the beam element is assumed to be axially elastic without any interaction between the axial force and the bending moment. Axial force-biaxial bending moment interaction and large deformations are treated in Section 4. Then the section constitutive equations can be written as:

$$\dot{\boldsymbol{\varepsilon}} = \mathbf{a}' \dot{\mathcal{F}} \quad \text{or} \quad \dot{\boldsymbol{\varepsilon}} = \mathbf{a}' \mathbf{b} \dot{\mathbf{Q}} \quad (3.36)$$

where \mathbf{a}' is the cross-section tangent flexibility matrix:

$$\mathbf{a}' = \begin{bmatrix} EA & 0 \\ 0 & [\alpha EI + (1-\alpha) EI (1-H_1 H_2)] \end{bmatrix}^{-1} \quad (3.37)$$

where EA and EI are the cross-section elastic axial and flexural rigidities and H_1 and H_2 are then given by:

$$H_1 = \left| \frac{M - \alpha EI \phi}{(1 - \alpha) M_y} \right|^N \quad \text{and} \quad H_2 = \eta_1 \operatorname{sgn} \left[(\dot{M} - \alpha EI \dot{\phi}) \dot{\phi} \right] + \eta_2 \quad (3.38)$$

and M_y is the yield moment of the cross-section. Substituting (3.36) in (3.30), we have:

$$\left[\int_0^L \mathbf{b}^T \mathbf{a}' \mathbf{b} dx \right] \dot{\mathbf{Q}} = \mathbf{T}_R \mathbf{R} \dot{\mathbf{u}}_e \quad (3.39)$$

The state equations of the beam element can be summarized as:

$$\left[\int_0^L \mathbf{b}^T \mathbf{a}' \mathbf{b} dx \right] \dot{\mathbf{Q}} = \mathbf{T}_R \mathbf{R} \dot{\mathbf{u}}_e \quad (3.39)$$

$$\dot{\boldsymbol{\varepsilon}}_i = \mathbf{a}'_i \mathbf{b}_i \dot{\mathbf{Q}} \quad i = 1, 2, \dots, NG \quad (3.40)$$

The section tangent flexibility matrix, \mathbf{a}' , which is 2x2 in the planar case and 3x3 in the three-dimensional case, can be inverted in closed form. It should be noted however, that the formulation does not require the explicit inversion of the element flexibility matrix, which is of sizes 3x3 and 6x6 respectively in the two and three-dimensional cases. In this work, the Gauss-Lobatto rule (Stroud and Secrest (1966)) is used for element quadrature. Though this rule has lower order of accuracy than the customary Gauss-Legendre rule, it has integration points at the ends of the element and hence performs better in detecting yielding. Comparing equations (3.39) and (3.40) with the generic equations (3.29), we have:

$$\mathbf{A}^{et} = \int_0^L \mathbf{b}^T \mathbf{a}' \mathbf{b} dx \quad \mathbf{z}_e = \{ \boldsymbol{\varepsilon}_1^T, \boldsymbol{\varepsilon}_2^T, \dots, \boldsymbol{\varepsilon}_{NG}^T \}^T \quad \mathbf{G} = \mathbf{T}_R \mathbf{R} \dot{\mathbf{u}}_e \quad (3.41)$$

$$\mathbf{H} = \left\{ \left[\mathbf{a}'_1 \mathbf{b}_1 \dot{\mathbf{Q}} \right]^T, \left[\mathbf{a}'_2 \mathbf{b}_2 \dot{\mathbf{Q}} \right]^T, \dots, \left[\mathbf{a}'_{NG} \mathbf{b}_{NG} \dot{\mathbf{Q}} \right]^T \right\}^T \quad (3.42)$$

3.8. Numerical Solution

Equations (3.26)-(3.28) and equations (3.39)-(3.40) written for every element in the structure constitute the state equations. They are solved by the numerical algorithm outlined in subsection 3.5 using the routine DASSL.

3.9. Numerical Example

To illustrate the method, the system of state equations of an example structure is assembled and solved for two different types of excitation: quasi-static and dynamic. The response of the state space model is then compared with finite-element solutions of ANSYS (1992) which uses a conventional incremental displacement method and stiffness-based beam elements.

The example structure is shown in Fig. 3.2. It is a portal frame consisting of three element. The connections are assumed rigid. The stress-strain curve of the material is assumed bilinear with the following properties: $E = 199955 \text{ kN/mm}^2$, $\sigma_y = 248.2 \text{ kN/mm}^2$, $E_T = 0.03E$. The section constitutive model of equation (3.36), requires definition of five parameters: (i) the elastic axial rigidity EA , (ii) the initial bending rigidity (iii) the post-yield bending rigidity aK_0 , (iv) the parameter n controlling the

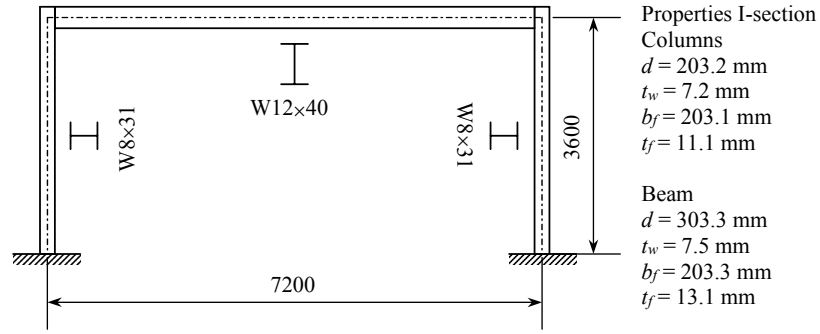


Fig. 3.2. Example Frame

smoothness of transition and (v) a discrete yield point M_y . These are obtained by analysis of the cross-section and are listed in Table 3.2. For dynamic analysis, lumped masses of 24.96 kN.s/m² each are assumed at the top two nodes in the horizontal direction, giving a structural period of 0.75s. A damping ratio 5% of critical damping is assumed.

The finite-element model in ANSYS was created using the thin-walled plastic beam element BEAM 24 (ANSYS (1992)). It belongs to the class of stiffness-based fiber element models. The cross sections of the frame members were divided into 10 layers. The number of elements was obtained by a convergence study. The macro-element model for the proposed state-space solution is shown in Fig. 3.3 and consists of three elements with 5 Gauss points each.

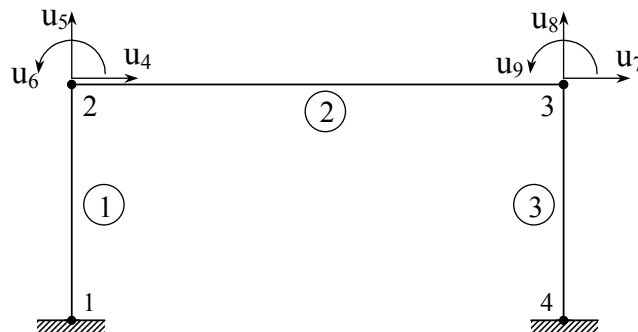


Fig. 3.3. Node and Element Numbering and Active Displacement DOF

The state variables for quasi-static analysis of this frame are summarized in Table 3.3. The result of a quasi-static analysis with cyclic displacement input of increasing amplitude is shown in Fig. 3.4. The state variables for a dynamic analysis are summarized in Table 3.4 and the results of a dynamic analysis using a ground acceleration record from the 1994 Northridge earthquake in Fig. 3.5. Also shown in the figures are results obtained using ANSYS, indicating good agreement.

3.10. Summary

A general formulation for state-space analysis of frame structures has been presented. The method has been applied to both quasi-static and dynamic problems. The global state equations of equilibrium and the local constitutive state equations are solved simultaneously as a system of differential-algebraic equations. The algorithms used for time-step selection in nonlinear dynamic analysis are to date largely heuristic based on such ideas as the number of iterations taken in a step for convergence. The state space approach provides a consistent algorithm based on the truncation error estimate for automatic time-stepping. A flexibility-based nonlinear bending element has also been developed in this framework. The accuracy of this macro-element can be refined by increasing the number of quadrature points, at which the constitutive equations are monitored, in contrast to increasing the number of elements in conventional finite element analysis. The feasibility of the state-space approach has been demonstrated by good correlation with results from a finite element program, which uses a conventional incremental solution algorithm with densely meshed displacement-based beam elements.

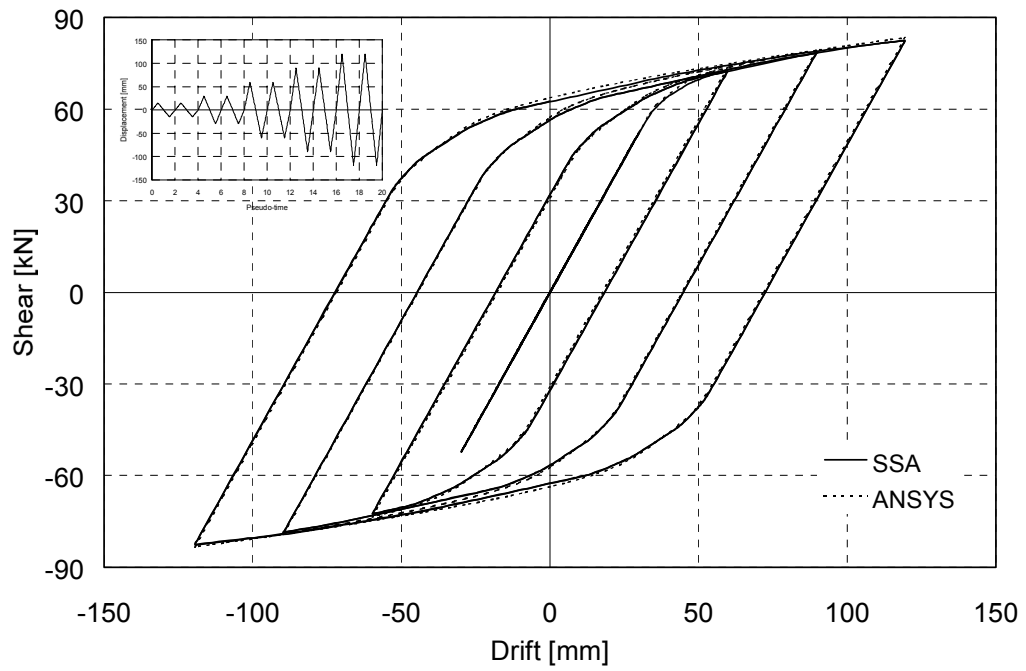


Fig. 3.4. Quasi-Static Analysis: Shear Force vs Relative Horizontal Displacement of Left Beam Element

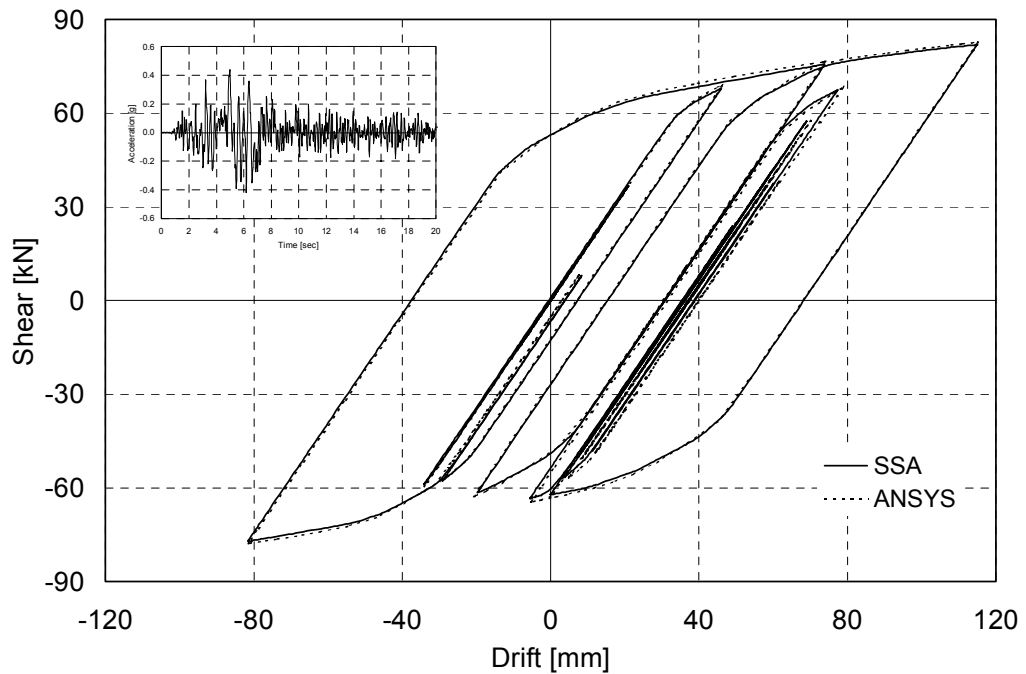


Fig. 3.5. Dynamic Analysis: Shear Force vs Relative Horizontal Displacement of Left Beam Element

Table 3.1. Local state variables for different types of element formulation

Type of Constitutive Model	Type of Element	
	Stiffness-based	Flexibility-based
Strain-decomposition	Total stresses	Plastic strains
Stress-decomposition	Hysteretic stresses	Total strains

Table 3.2. Numerical Example - Model Properties

Section	A (cm ²)	I (cm ⁴)	α (%)	N	M_y (kN-m)
Column	57.99	4504.98	3	8	117.05
Beam	73.96	12535.21	3	8	215.67

Table 3.3. Quasi-Static Analysis - Global and Local State Variables (y_{11} to y_{20} , y_{26} to y_{35} and y_{41} to y_{50} represent curvatures of quadrature sections)

Global	u_4	u_5	u_6	u_7	u_8	u_9
State Variable	y_1	y_2	y_3	y_4	y_5	y_6
Element 1	F_I	M_i	M_j	ϕ_1	...	ϕ_{12}
State Variable	y_7	y_8	y_9	y_{10}	...	y_{21}
Element 2	F_I	M_i	M_j	ϕ_1	...	ϕ_{12}
State Variable	y_{22}	y_{23}	y_{24}	y_{25}	...	y_{36}
Element 3	F_I	M_i	M_j	ϕ_1	...	ϕ_{12}
State Variable	y_{37}	y_{38}	y_{39}	y_{40}	...	y_{51}

Table 3.4. Dynamic Analysis - Global and Local State Variables

Global	u_4	u_5	u_6	u_7	u_8	u_9	\dot{u}_4	\dot{u}_7
State variable	y_1	y_2	y_3	y_4	y_5	y_6	y_7	y_8
Element state variables same as Table 3.3, but translated by the rule: $y_{n+2}^d = y_n^s$, for $n \geq 7$.								

4. LARGE DEFORMATION BEAM-COLUMN ELEMENT

4.1. Background

Besides inelastic behavior, due to large lateral forces and $P\Delta$ effects, structures undergo large displacements. In such cases, in order to capture the behavior accurately, the equilibrium of forces and the compatibility of deformations of the structure need to be considered in the displaced configuration as opposed to the original configuration. While the influence of large elastic deformations has been well studied, this section considered large inelastic deformations. An attempt is made herein to formulate a flexibility-based planar beam-column element, which can undergo large inelastic deformations. This element, in connection with the State Space Approach of Section 3, can be used to analyze structures until stability is lost and gravity loads cannot be sustained. The new element formulation has no restrictions on the size of rotations. It uses one co-rotational frame for the element to represent rigid-body motion, and a set of co-rotational frames attached to the integration points, used to represent the constitutive equations. The development in this section parallels that of subsection 3.7.

4.2. Overview of Previous Work

Reissner (1972) developed the governing equations of a plane geometric nonlinear Timoshenko beam starting from the equilibrium equations, and derived the nonlinear strain-deformation relationships that are compatible with the equilibrium equations in the sense of virtual work. Subsequently Reissner (1973) extended this formulation to three-dimensional beams. Huddleston (1979) independently developed nonlinear strain-deformation relationships for a geometric nonlinear Euler-Bernoulli

beam. These equations reduce to those of Reissner (1972), when shear deformations are neglected. Huddleston's approach forms the basis of the formulation presented herein.

Researchers have studied the computational solution of the nonlinear beam problem using the co-rotational, the total Lagrangian and the updated Lagrangian formulations. The treatment of large rotations using the co-rotational formulation was introduced by Belytschko and Hsieh (1973). In the co-rotational formulation, one or more coordinate systems called co-rotational frames are attached to material points and rotate along with them during deformation. Either a single co-rotational frame can be attached to the element chord or multiple co-rotational frames can be attached to one or more integration points along the length of the beam (Crisfield (1991)), Simo and Vu-quoi (1986) developed a general three-dimensional beam element with large rotations and shear deformation using the latter approach and using quaternion interpolation. Lo (1992) developed an element using a similar approach. Schulz and Filippou (2001) developed a total Lagrangian formulation using curvature-based rotation interpolation functions. They also describe the second order moments resulting from the use of the Green-Lagrange strain and the second Piola-Kirchoff stress. Yang and Kuo (1994), present an exhaustive discussion of frame elements using the updated Lagrangian formulation.

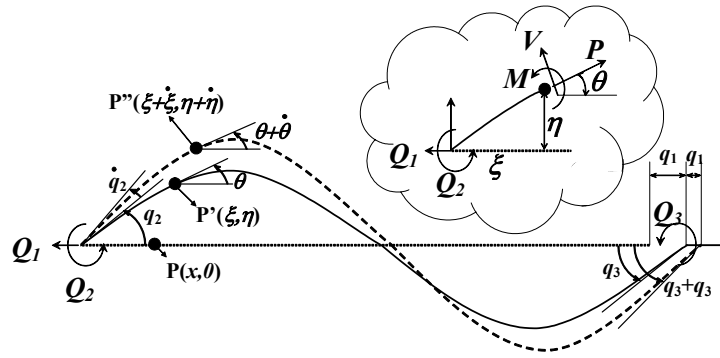
All of the above developments deal only with nonlinear elastic constitutive equations, although they can be extended in the incremental form to inelastic behavior. The formulations indicated above are based on the principle of virtual displacements. A flexibility-based approach (principle of virtual forces) for frame elements provides additional well-known benefits (Park, Reinhorn et al. (1987), Neuenhofer and Filippou (1997)). Backlund (1976) developed a flexibility-based element. However, large rotations

were restricted to only the co-rotational frame attached to the undeformed centerline, and moments and curvatures were assumed linearly distributed within the element. Carol and Murcia (1989) and Neuenhofer and Filippou (1998) approached the solution of geometric nonlinear flexibility formulations. The large rotations were restricted again to the element co-rotational frame. However, second order effects within the element were considered. Since the force-interpolation matrix is displacement-dependent, Carol and Murcia (1989) used conventional displacement interpolation functions, while Neuenhofer and Filippou (1998) used a curvature-based displacement interpolation procedure to approximate the displacement field within the element. Barsan and Chiorean (1999) used the geometric linear flexibility formulation and corrected the resulting stiffness matrix using stability functions. This formulation is also limited to small deformations within the element's co-rotational frame and to monotonic loading.

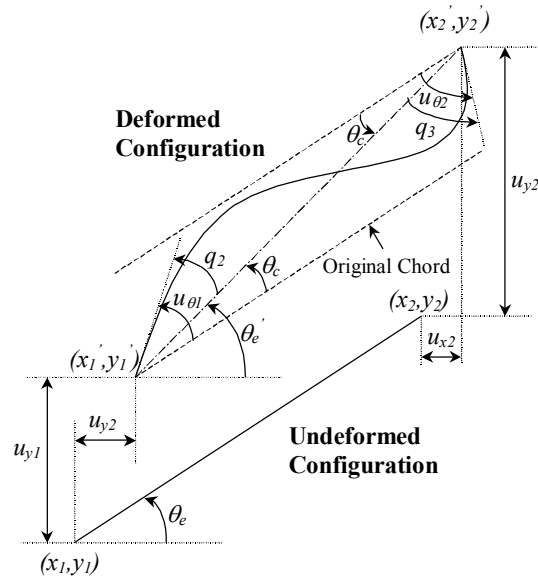
The development in this paper enhances existing modeling by including inelastic behavior, by introducing large rotations within the element co-rotational frame and by using the flexibility approach. The solution procedure associated with the proposed model allows the study of response up to complete flexural collapse.

4.3. Element Formulation

The formulation of the state equations of the flexibility-based large deformation beam-column element is developed herein. Fig. 4.1(a) shows the deformed shape of a beam, in co-rotational coordinates attached to the initially straight centerline of the beam, with the rigid body modes removed. The following assumptions are made: (1) The Euler-Bernoulli hypothesis holds, that is, plane sections perpendicular to the beam axis before



(a) Geometry and Segment Equilibrium



(b) Deformation and Transformations

Fig. 4.1. Euler-Bernoulli Beam subjected to Large Deformation

deformation, remain so after deformation and shear deformations are ignored in this formulation. (2) The cross-section has an axis of symmetry and in the planar case, bending is about this axis. (3) The only sources of inelasticity are axial and flexural.

There is no inelasticity in shear. The nonlinear strain displacement relationships are (Huddleston (1979)):

$$\frac{d\theta}{dx} = (1 + \varepsilon)\phi \quad \frac{d\xi}{dx} = (1 + \varepsilon)\cos\theta \quad \frac{d\eta}{dx} = (1 + \varepsilon)\sin\theta \quad (4.1)$$

where (ξ, η) is the coordinate of a point which was at $(x, 0)$ before deformation, θ is the angle made by the tangent to the center-line with the horizontal, ε is the axial strain of the centerline and ϕ is the curvature. Considering a small perturbation about this deformed position, the incremental compatibility conditions are given by:

$$\frac{d\dot{\theta}}{dx} = \dot{\varepsilon}\phi + (1 + \varepsilon)\dot{\phi} \quad (4.2)$$

$$\frac{d\dot{\xi}}{dx} = \dot{\varepsilon}\cos\theta - [(1 + \varepsilon)\sin\theta]\dot{\theta} \quad (4.3)$$

$$\frac{d\dot{\eta}}{dx} = \dot{\varepsilon}\sin\theta + [(1 + \varepsilon)\cos\theta]\dot{\theta} \quad (4.4)$$

Integrating these equations over the length of the element and performing a series of integrations by parts (see a detailed derivation in Appendix II), the following variational equation is obtained:

$$\dot{\mathbf{q}} = \begin{Bmatrix} \dot{q}_1 \\ \dot{q}_2 \\ \dot{q}_3 \end{Bmatrix} = \int_0^L \mathbf{b}^T \begin{Bmatrix} \dot{\varepsilon} \\ \dot{\phi} \end{Bmatrix} dx = \int_0^L \mathbf{b}^T \dot{\tilde{\varepsilon}} dx \quad (4.5)$$

where q_1 = the component along the element chord of the displacement of the right end of the element relative to the left end, q_2, q_3 = rotations at left and right ends relative to the chord as shown in Fig. 4.1(a). $\tilde{\varepsilon} = (1 + \varepsilon)\phi$, rather than ϕ , is found to be the work

conjugate of the co-rotational moment. This is in agreement with the formulation by Reissner (1972). $\boldsymbol{\varepsilon} = \{\varepsilon \quad \tilde{\phi}\}^T \mathbf{b}$ is the force interpolation matrix given by:

$$\mathbf{b} = \begin{bmatrix} \cos \theta & -\frac{\sin \theta}{\xi(L)} & -\frac{\sin \theta}{\xi(L)} \\ \eta & \frac{\xi}{\xi(L)} - 1 & \frac{\xi}{\xi(L)} \end{bmatrix} \quad (4.6)$$

It is observed that under small deformations, equation (4.6) reduces the result of Neuenhofer and Filippou (1998). From the equilibrium of a segment, as shown in Fig. 4.1(a), the stress resultant vector at any section is obtained as:

$$\mathcal{F} = \begin{Bmatrix} P \\ M \end{Bmatrix} = \mathbf{b} \begin{Bmatrix} Q_1 \\ Q_2 \\ Q_3 \end{Bmatrix} = \mathbf{b} \mathbf{Q} \quad (4.7)$$

where P = axial force at any section, M = bending moment at any section, Q_1 = force component parallel to the element chord, Q_2 = bending moment at the left end and Q_3 = bending moment at the right end. Note that the forces in the vector \mathbf{Q} are in element coordinates.

4.4. Transformations of Displacements and Forces

The global displacements and the rates of displacement have to be converted to local element coordinates and subsequently to deformations in the element co-rotational system by eliminating the rigid body modes. Fig. 4.1(b) shows the element in the undeformed and the deformed configurations. θ_e is the undeformed chord angle made with the horizontal in the undeformed configuration. θ_e' is the chord angle after rigid

body rotation in the deformed configuration. The reference chord rotation is (see Fig. 4.1(b)):

$$\theta_c = \theta'_e - \theta_e \quad (4.8)$$

Assuming that (x_1, y_1) and (x_2, y_2) are the coordinates of the element end nodes in the undeformed configuration and (x'_1, y'_1) and (x'_2, y'_2) , those in the deformed configuration, then,

$$x'_1 = x_1 + u_{x1} \quad y'_1 = y_1 + u_{y1} \quad x'_2 = x_2 + u_{x2} \quad y'_2 = y_2 + u_{y2} \quad (4.9)$$

where $(u_{x1}, u_{y1}, u_{\theta1})$ and $(u_{x2}, u_{y2}, u_{\theta2})$ are the beam generalized displacements at the respective nodes. The length of the chord in the deformed configuration is then:

$$\xi(L) = \sqrt{(x'_2 - x'_1)^2 + (y'_2 - y'_1)^2} \quad (4.10)$$

where L is the original chord length. The generalized deformations, q_i , in the co-rotational system (see Fig. 4.1), devoid of rigid body components, are:

$$q_1 = \xi(L) - L \quad q_2 = u_{\theta1} - \theta_c \quad q_3 = u_{\theta2} - \theta_c \quad (4.11)$$

The independent end forces in the co-rotational system have to be transformed into the global coordinate system so that they can participate in the global equations. Considering equilibrium in the deformed configuration leads to the following transformation for the forces:

$$\mathbf{F} = \mathbf{B}^e \mathbf{Q} \quad \text{or} \quad \mathbf{F} = \mathbf{R}^T \mathbf{T}_R^T \mathbf{Q} \quad (4.12)$$

where \mathbf{F} is the vector of end forces in the global coordinate system. \mathbf{R} is the rotation matrix from global to local coordinates, \mathbf{T}_R is the transformation from local to co-rotational coordinates and $\mathbf{B}^e = \mathbf{R}^T \mathbf{T}_R^T$ is the element equilibrium matrix.

$$\mathbf{R} = \left[\begin{array}{ccc|cc} \cos \theta'_e & -\sin \theta'_e & 0 & & \\ \sin \theta'_e & \cos \theta'_e & 0 & & 0 \\ 0 & 0 & 1 & & \\ \hline & & & \cos \theta'_e & -\sin \theta'_e & 0 \\ & & & \sin \theta'_e & \cos \theta'_e & 0 \\ & & & 0 & 0 & 1 \end{array} \right] \quad (4.13)$$

$$\mathbf{T}_R = \left[\begin{array}{cccccc} 1 & 0 & 0 & -1 & 0 & 0 \\ 0 & \frac{1}{\xi(L)} & 1 & 0 & -\frac{1}{\xi(L)} & 0 \\ 0 & \frac{1}{\xi(L)} & 0 & 0 & -\frac{1}{\xi(L)} & 1 \end{array} \right] \quad (4.14)$$

Since the displacement rates are work conjugate to the forces, they are transformed by:

$$\dot{\mathbf{q}} = \mathbf{T}_R \mathbf{R} \dot{\mathbf{u}}_e \quad (4.15)$$

where $\mathbf{u}_e = \{u_{x1} \quad u_{y1} \quad u_{\theta1} \quad u_{x2} \quad u_{y2} \quad u_{\theta2}\}^T$.

4.5. Approximation of the Element Displacement Field

As seen in Eq. (4.6), the instantaneous force-interpolation matrix, \mathbf{b} , depends on the displacement field in the element, relative to the element co-rotational frame. This field therefore needs to be approximated. The determination of the displacement field using the compatibility equations (4.1), is an over-specified two-point boundary value problem, since all the end displacements and the strains at the integration points are

known at a given instant. For small deformations, Neuenhofer and Filippou (1998) successfully used a *Curvature Based Displacement Interpolation* procedure to obtain the displacement field. However, when used with the large deformation compatibility equations, and with more integration points, this procedure is found to result in oscillatory displacement fields. Hence, the following procedure is used for this purpose:

(i) An implicit first order method is used to integrate Eqs. (4.1) as an initial value problem (IVP) starting from one end of the element as shown below:

$$\begin{aligned}\theta_{i+1}^1 &= \theta_i^1 + (x_{i+1} - x_i) \tilde{\phi}_{i+1} & \xi_{i+1}^1 &= \xi_i^1 + (x_{i+1} - x_i) \cos(\theta_{i+1}^1) \\ \eta_{i+1}^1 &= \eta_i^1 + (x_{i+1} - x_i) \sin(\theta_{i+1}^1) & i &= 1, 2, \dots, NG-1\end{aligned}\quad (4.16)$$

where NG = number of integration points and subscript i denotes the i^{th} integration point.

(ii) The equations are solved a second time as an IVP starting from the other end of the element.

$$\begin{aligned}\theta_{i-1}^2 &= \theta_i^2 + (x_{i-1} - x_i) \tilde{\phi}_{i-1} & \xi_{i-1}^2 &= \xi_i^2 + (x_{i-1} - x_i) \cos(\theta_{i-1}^2) \\ \eta_{i-1}^2 &= \eta_i^2 + (x_{i-1} - x_i) \sin(\theta_{i-1}^2) & i &= NG, NG-1, \dots, 2\end{aligned}\quad (4.17)$$

(iii) The displacements at the integration points are approximated as the weighted average of the two solutions: $\chi_i = \lambda \chi_i^1 + (1 - \lambda) \chi_i^2$ where χ denotes any of the components of the element displacement field, θ , ξ or η , and λ is a weighting factor. $\lambda = 0.5$ is used in this work. This approach is found to produce sufficiently accurate results, as shown in the numerical examples.

4.6. Constitutive Relations

The inelastic behavior of members is modeled in a macroscopic sense. The relationships between stress resultants (axial force, bending moment etc.) and generalized strains (centerline strain, curvature etc.) are used directly, instead of the material stress-strain relationships. The rate form of multi-axial plasticity (2.48) is used along with the cross-section yield function (2.49). The section constitutive equation is given by:

$$\dot{\boldsymbol{\varepsilon}} = \mathbf{a}' \mathcal{F} \quad \text{or} \quad \dot{\boldsymbol{\varepsilon}} = \mathbf{a}' (\mathbf{b}\dot{\mathbf{Q}} + \dot{\mathbf{b}}\mathbf{Q}) \quad (4.18)$$

where \mathbf{a}' is the section tangent flexibility matrix, $\mathbf{f} = \{\boldsymbol{\alpha}\mathbf{k} + (\mathbf{I} - \boldsymbol{\alpha})\mathbf{k}[\mathbf{I} - H_1 H_2 \mathbf{B}]\}^{-1}$, \mathbf{k} is the cross-section elastic rigidity matrix, $\boldsymbol{\alpha}$ is the diagonal matrix of post-yield rigidity ratios and \mathbf{I} is the identity matrix. \mathbf{B} is the matrix of the interaction between the stress resultants given by equation (2.42). Substituting equation (4.18) in equation (4.5), we have:

$$\left[\int_0^L \mathbf{b}^T \mathbf{a}' \mathbf{b} dx \right] \dot{\mathbf{Q}} = \mathbf{T}_R \mathbf{R} \dot{\mathbf{u}}_e - \left[\int_0^L \mathbf{b}^T \mathbf{a}' \dot{\mathbf{b}} dx \right] \mathbf{Q} \quad (4.19)$$

The second term on the right hand side is the *initial stress* term. The Gauss-Lobatto rule is again used for element quadrature.

4.7. Summary of State Equations

The element state equations of (3.29), for the large deformation element, take the form:

$$\left[\int_0^L \mathbf{b}^T \mathbf{a}' \mathbf{b} dx \right] \dot{\mathbf{Q}} = \mathbf{T}_R \mathbf{R} \dot{\mathbf{u}}_e - \left[\int_0^L \mathbf{b}^T \mathbf{a}' \dot{\mathbf{b}} dx \right] \mathbf{Q} \quad (4.19)$$

$$\dot{\boldsymbol{\varepsilon}}_i = \mathbf{a}_i (\mathbf{b}_i \dot{\mathbf{Q}} + \dot{\mathbf{b}}_i \mathbf{Q}) \quad i = 1, 2, \dots, NG \quad (4.20)$$

Comparing equations (4.19) and (4.20) with the generic equations (3.29), we have:

$$\mathbf{A}^{et} = \int_0^L \mathbf{b}^T \mathbf{a}^t \mathbf{b} dx, \text{ the element tangent flexibility matrix} \quad (4.21)$$

$$\mathbf{z}_e = \{\boldsymbol{\varepsilon}_1^T, \boldsymbol{\varepsilon}_2^T, \dots, \boldsymbol{\varepsilon}_{NG}^T\}^T, \text{ the element states} \quad (4.22)$$

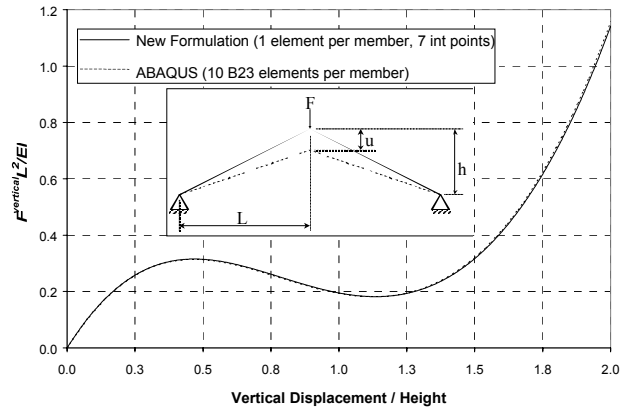
$$\mathbf{G} = \mathbf{T}_R \mathbf{R} \dot{\mathbf{u}}_e - \left[\int_0^L \mathbf{b}^T \mathbf{a} \mathbf{b} dx \right] \mathbf{Q} \quad (4.23)$$

$$\mathbf{H} = \left\{ \left[\mathbf{a}_1 (\mathbf{b}_1 \dot{\mathbf{Q}} + \dot{\mathbf{b}}_1 \mathbf{Q}) \right]^T, \left[\mathbf{a}_2 (\mathbf{b}_2 \dot{\mathbf{Q}} + \dot{\mathbf{b}}_2 \mathbf{Q}) \right]^T, \dots, \left[\mathbf{a}_{NG} (\mathbf{b}_{NG} \dot{\mathbf{Q}} + \dot{\mathbf{b}}_{NG} \mathbf{Q}) \right]^T \right\}^T \quad (4.24)$$

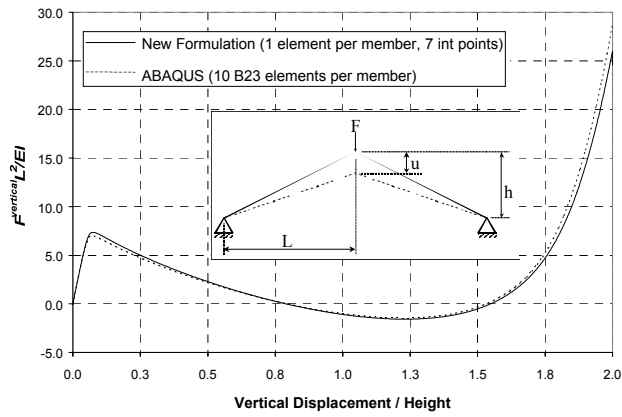
Equations (3.26)-(3.28) and equations (4.19)-(4.20) written for every element in the structure constitute the state equations. They are solved using DASSL.

4.8. Numerical Example 1: Snap-through of a deep bent

The elastic snap-through analysis of the bent structure (see for example, Crisfield (1991)) shown in Fig. 4.2 is carried out using two flexibility-based elements, one for each member and having seven integration points ($NG = 7$). The non-dimensional properties of the structure are shown in Table 4.1. Fig. 4.2(a) and (b) show the force-displacement behavior for two height/span ratios (0.05 – shallow bent and 0.25 – deep bent). The figures also show standard displacement-based solutions obtained using ABAQUS using 10 B23 type elements (ABAQUS, 2000). The results indicate discrepancies smaller than 5% at maximum and less than 1% on average.



(a) Case (1): Shallow Bent ($h/L = 0.05$)



(b) Case (2): Deep Bent ($h/L = 0.25$)

Fig. 4.2. Numerical Example 1: Force-Displacement Response

Table 4.1. Numerical Example 1: Non-dimensional Structural Properties

	Compressibility (Huddleston (1979))	Height / Span Ratio
	$\frac{I}{A(L^2 + h^2)}$	$\frac{h}{L}$
Case (1)	2×10^{-4}	0.05
Case (2)	1.88×10^{-4}	0.25

4.9. Numerical Example 2: Collapse of a single-story structure

Fig. 4.5 shows a single story frame. Each of the columns can be modeled as being fixed at the bottom and free to translate but fixed against rotation at the top. The columns have a standard AISC S3x5.7 cross-section. This choice is made because a series of experimental studies that have been planned using this configuration. The modulus of elasticity of the material is assumed as $E = 2 \times 10^5$ MPa (29000 ksi), the yield stress as $\sigma_y = 248.8$ MPa (36 ksi) and the hardening ratio as $a = 0.03$. The cross-section has axial rigidity, $EA = 2.11 \times 10^5$ kN (47362.8 kip), flexural rigidity, $EI = 2.08 \times 10^8$ kN-mm² (72210 kip-in²), axial force capacity, P_y , under no bending moment = 262.2 kN (58.8 kip), strong axis bending moment capacity, M_y , under no axial load = 7248.7 kN-mm (64 kip-in) and the ratio of post-yield to elastic rigidities, $a = 0.03$. One flexibility-based element with 10 integration points is used to represent each column.

4.9.1. Constitutive Equation for S3x5.7 cross section

The axial force-moment interaction diagram for the S3x5.7 cross-section, obtained by a fiber model analysis of the section is shown in Fig. 4.4. The parameters of the yield surface given by equation (2.49) are obtained as $b_1 = 1.5$ and $b_2 = -0.3$ to best fit the results from sectional analysis. The yield function the of the cross-section is therefore given by:

$$\Phi = |p|^{1.5-0.3|p|} + |m| - 1 = 0 \quad (4.25)$$

The constitutive equation of the section is then given by equation (2.48).

4.9.2. Nonlinear Static Analysis

The frame is subjected to a constant vertical load representing the weight and a lateral load applied in displacement control. Each column carries an axial force of 21% of the elastic critical buckling load, when vertical. The force deformation response of one of the columns is shown in Fig. 4.5. The figure also shows the standard displacement-based solution obtained using ABAQUS, with the material properties listed above and a kinematic hardening model. The slight difference in the two solutions stems from the fact that the flexibility formulation suggested in this paper uses the section-constitutive behavior, while the displacement-based solution in ABAQUS uses the material stress-strain relations directly. This results in the transition from elastic to inelastic behavior being represented differently in the two cases. Fig. 4.6 shows the convergence of the flexibility-based element with increasing number of integration points.

4.9.3. Dynamic Analysis

The above one-story structure is subjected to an earthquake excitation corresponding to the El Centro NS-1940 acceleration record with a peak ground acceleration of 2.55% of the acceleration due to gravity (g). The total mass on the structure = $4 \times 0.2156 F^{critical} / g$. The period of small amplitude elastic vibration of the structure is given by:

$$T = 2\pi \sqrt{\frac{L}{g}} \sqrt{\frac{\tan\left(\frac{\pi}{2} \sqrt{\frac{F^{axial}}{F^{critical}}}\right)}{\frac{\pi}{2} \sqrt{\frac{F^{axial}}{F^{critical}}}} - 1} \quad (4.26)$$

and equals 1.29 sec for $F^{axial}/F^{critical} = 0.2156$. The damping constant is taken to be $c = 1.304 \times 10^{-3}$ kN-sec/mm, which corresponds to a 5% damping ratio for small amplitude elastic vibration. The results of the dynamic analysis are shown in Fig. 4.7(a) to Fig. 4.7(c). The structure collapses after 2.5 sec as indicated by the large lateral and vertical displacements in Fig. 4.7(a) and (c) and by the loss of lateral strength capacity in Fig. 4.7(b). Additionally, the response of a similar structure tested to collapse was successfully simulated using the above procedure (see Vian et al. (2001)).

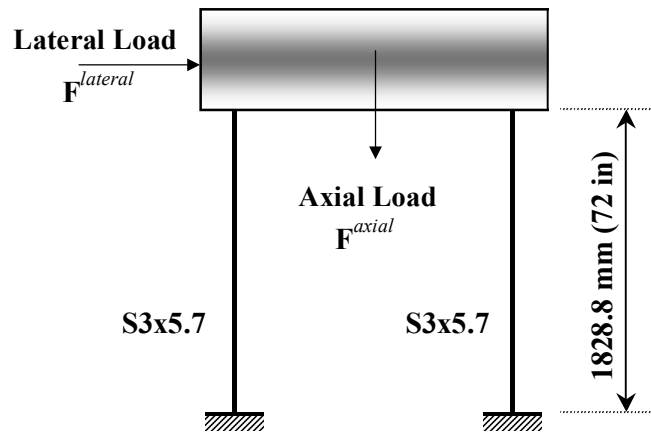


Fig. 4.3. Numerical Example 2: Single Story Frame

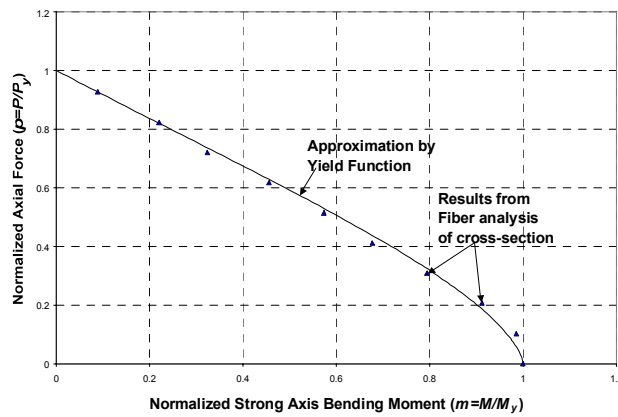


Fig. 4.4. Force-Strong Axis Bending Moment Interaction diagram for S3x5.7 section

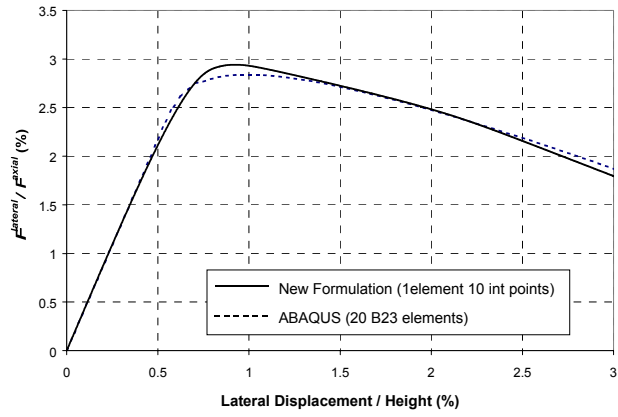


Fig. 4.5. Numerical Example 2: Response of one column ($F^{axial}/F^{critical} = 0.2156$)

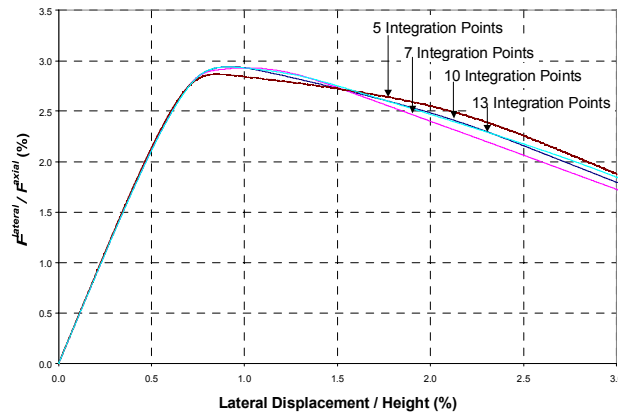
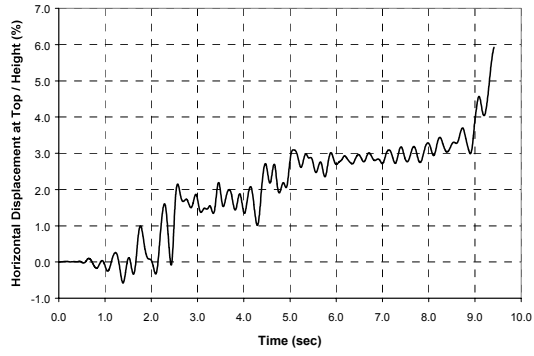
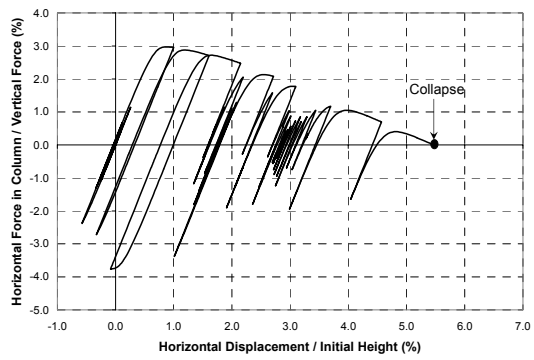


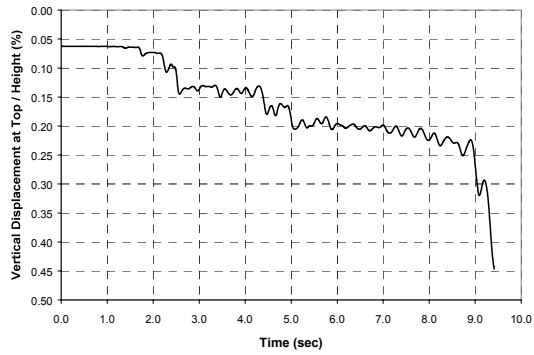
Fig. 4.6. Convergence of Flexibility-based Element



(a) Horizontal Displacement History



(b) Force-Displacement Response



(c) Vertical Displacement History

Fig. 4.7. Numerical Example 2: Dynamic Analysis to Collapse

5. THE LAGRANGIAN APPROACH – FORMULATION

5.1. Background

In this section, a second alternative method is proposed for the analysis of structures considering both material and geometric nonlinearities. The formulation attempts to solve problems using a force-based approach in which momentum appears explicitly and can be potentially used to deal with structures where deterioration and fracture occur before collapse. In Sections 3 and 4, the response of the structure was considered as the solution of a set of differential equations in time (DAE when there are constraints). Since the differential equations hold at a particular instant of time, they provide a temporally local description of the response and are often referred to as the *strong form*. In contrast, in this section, a time integral of functions of the response over the duration of the response is considered. Such an approach presents a temporally global picture of the response and is referred to as the *weak form*.

The kernel of the integral mentioned above consists of two functions – the *Lagrangian* and the *dissipation* functions – of the response variables that describe the configuration of the structure and their rates. The integral is called the *action integral*. A precise formulation of these functions is the subject of this section. In elastic systems, the configuration variables are typically displacements. It is shown here, however, that in considering elastic-plastic systems it is natural to also include the time integrals of internal forces in the structure as configuration variables. The Lagrangian function is energy-like and describes the conservative characteristics of the system, while the dissipation function is similar to a flow potential and describes the dissipative characteristics. In a conservative system, the action integral is rendered stationary

(maximum, minimum or saddle point) by the response. In analytical mechanics, this is called *Hamilton's principle* or more generally the *principle of least action*. For non-conservative systems such as elastic-plastic systems, such a variational statement is not possible, and only a weak form which is not a total integral is possible.

Such a weak formulation enables the construction of numerical integration schemes that have energy and momentum conservation characteristics. This construction and the numerical solution are presented in Section 6.

5.2. Outline

An overview of variational methods that have been developed for plasticity is first presented in order to place the present work in context. The concept of reciprocal structures and their Lagrangian formulation is then explained using simple systems with springs, masses, dashpots and sliders. The Lagrangian formulation for skeletal structures is subsequently developed and treatment of geometric nonlinearity is shown. Some remarks are then made about the uniqueness of the solution and the extension of the approach to continua. The numerical integration of the Lagrangian equations by *discrete variational integrators* is discussed in the next section.

5.3. Variational Principles for Plasticity

Variational formulations of plasticity are based on the principle of maximum dissipation and the consequent normality rule. The equivalence of maximum dissipation and normality is demonstrated for example by Simo, Kennedy et al. (1989). The local Gauss point level constitutive update has been ascribed a variational structure based on the concept of closest point projection (Simo and Hughes (1998) and Armero and Perez-Foguet (2002)). Various approaches have however been used for deriving global

variational formulations for plasticity, each of which when discretized in time, leads to a constrained minimization problem in every step. These are listed below:

1. Complementarity and Mathematical Programming Approach: Maier (1970) starting from the equivalence of the Kuhn-Tucker conditions and the linear complementarity problem for piecewise linear yield functions derived minimum theorems for holonomic elastic-plastic structures. Capurso and Maier (1970) extended this formulation to nonholonomic structures. They derived a primal minimum theorem for a function of displacement and plastic multiplier rates and a dual minimum theorem for a function of stress and back stress rates. When discretized in time using the Backward Euler method, these minimum principles lead to quadratic programming problems in displacement and stress increments respectively. For an extensive survey of this approach and its application by other authors, see Cohn et al. (1979). More recently, Tin-Loi (1997) has presented plasticity with nonlinear hardening as a nonlinear complementarity problem. For a discussion of the complementarity problem, the reader is referred to Isac (1992).
2. Variational Inequality Approach: Duvaut and Lions (1976) formulated static as well as dynamic plasticity problems as variational inequalities. Johnson (1977) and Han and Reddy (1999) formulated the static plasticity problem as a Variational inequality similar to that of Duvaut and Lions (1976). They used this formulation to show existence and uniqueness and to develop a finite element spatial discretization. For the solution of the minimization problem resulting in each increment, Johnson (1977) used Uzawa's iterative method (see for example, Ekeland et al. (1976)), while

Han and Reddy (1999) used a predictor corrector method. For a treatment of variational inequalities, see Kinderlehrer and Stampacchia (1980).

3. Convex Analysis and Monotone Operator Approach: Romano et al. (1993) used the variational theory of monotone multivalued operators to derive rate variational principles for plasticity. De Sciarra (1996) extended this approach to derive several variational principles involving stress rates, displacement rates, back stress rates, plastic multiplier rates etc. which are generalizations of the Hu-Washizu mixed variational principle (Washizu (1982)). These principles impose the yield conditions and flow rule in a variational sense, leading to the concept of a global yield function (Romano and Alfano (1995)). Cuomo and Contrafatto (2000) used an augmented Lagrangian approach to solve the nonlinear programming problem arising in each increment.

Panagiotopoulos (1985) and Stavroulakis (2001) discuss the relationship between these different approaches listed above. The most common procedure is to use the Backward Euler method to approximate the rate quantities in the variational statement leading to a constrained minimization problem in each time increment (see Simo, Kennedy et al. (1989) for a detailed presentation). Beyond the variational inequality formulation of Duvaut and Lions (1976), not much work has been done in the variational formulation of dynamic plasticity.

In this work, a *weak formulation for dynamic plasticity* is attempted using Hamilton's principle. It can be shown that the Backward Euler method used in the literature discussed above for quasi-static plasticity is unsuitable for dynamic analysis because of its excessive numerical damping. In the next section, a numerical integrator

well-suited for dynamic analysis is developed by discretizing the variational principle instead of the differential equations.

5.4. Simple Phenomenological Models of Reciprocal Structures

Reciprocal structures are those structures characterized by convex potential and dissipation functions. A more precise definition is provided in subsection 1.5. In this subsection, the concept of reciprocal structures is explained using simple spring-mass-damper-slider models. The mixed Lagrangian and Dissipation functions of such systems are derived and various structural components that such a formulation encompasses are listed.

5.4.1. Mass with Kelvin type Resisting System

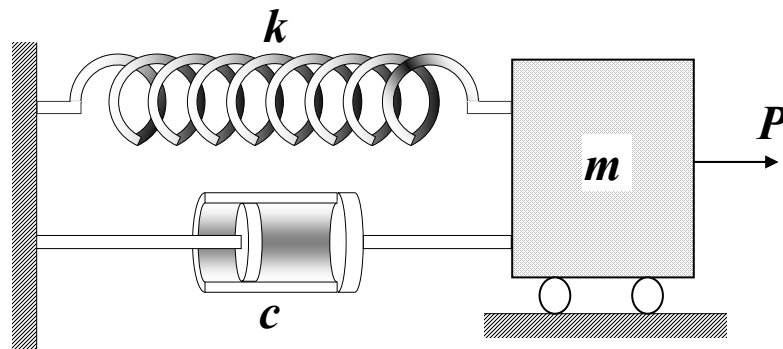


Fig. 5.1. Mass with Kelvin type Resisting System and Force Input

Consider a spring-mass-damper system where the spring and the damper are in parallel (Kelvin Model) as shown in Fig. 5.1 and subject to a time-varying force input $P(t)$. The well known equation of motion of this system is given by:

$$m\ddot{u} + c\dot{u} + ku = P \quad (5.1)$$

where m is the mass, k is the modulus of the spring, c is the damping constant, u is the displacement of the mass and a superscripted “.” denotes derivative with respect to time.

The well known approach in Analytical Mechanics is to multiply equation (5.1) by a virtual displacement function δu , integrate over the time interval $[0, T]$ by parts to obtain the action integral, \mathcal{Z} , in terms of the Lagrangian function, \mathcal{L} , and the dissipation function, φ , as shown below (see for example, José and Saletan (1998)):

$$\delta \mathcal{Z} = -\delta \int_0^T \mathcal{L}(u, \dot{u}) dt + \int_0^T \frac{\partial \varphi(\dot{u})}{\partial \dot{u}} \delta u dt - \int_0^T P \delta u dt = 0 \quad (5.2)$$

where δ denotes the variational operator, and the Lagrangian function, \mathcal{L} , and the dissipation function, φ , of this system are given by:

$$\mathcal{L}(u, \dot{u}) = \frac{1}{2} m \dot{u}^2 - \frac{1}{2} k u^2 \quad (5.3)$$

$$\varphi(\dot{u}) = \frac{1}{2} c \dot{u}^2 \quad (5.4)$$

Notice that due to the presence of the dissipation function and because the force $P(t)$ can in general be non-conservative, equation (5.2) defines $\delta \mathcal{Z}$ and not \mathcal{Z} itself. Conversely, starting from (5.2), equation (5.1) can be obtained as the Euler-Lagrange equations:

$$\frac{d}{dt} \left(\frac{\partial \mathcal{L}}{\partial \dot{u}} \right) - \left(\frac{\partial \mathcal{L}}{\partial u} \right) + \frac{\partial \varphi}{\partial \dot{u}} = P \Rightarrow m\ddot{u} + c\dot{u} + ku = P \quad (5.5)$$

Thus, the Lagrangian function, the dissipation function and the action integral determine the equation of motion.

5.4.2. Mass with Maxwell type Resisting System

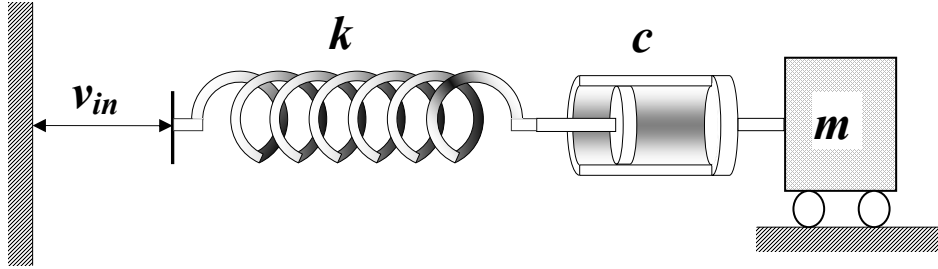


Fig. 5.2. Mass with Maxwell type Resisting System and Displacement Input

Consider on the other hand, a spring-mass-damper system where the spring and the damper are in series (Maxwell Model) as shown in Fig. 5.2 and subject to a time varying base-velocity input, $v_{in}(t)$. We wish to obtain a Lagrangian function and a dissipation function for this system that determine the equations of motion as above. Expressing the compatibility of deformations results in:

$$v_{in} + \frac{\dot{F}}{k} + \frac{F}{c} = \dot{u} \quad (5.6)$$

where F is the force in the spring and damper. Writing the equation of equilibrium of the mass, we have:

$$m\ddot{u} + F = 0 \quad (5.7)$$

Integrating equation (5.7) for \dot{u} and substituting in equation (5.6) gives:

$$\frac{1}{k}\dot{F} + \frac{1}{c}F + \frac{1}{m}\int_0^t F d\tau = -v_{in} - v_0 \quad (5.8)$$

where v_0 is the initial velocity of the mass. Letting $J = \int_0^t F d\tau$ (this idea has been used by El-Sayed et al. (1991)), the *impulse* of the force in the spring and damper, equation (5.8) can be written as:

$$\frac{1}{k} \ddot{J} + \frac{1}{c} \dot{J} + \frac{1}{m} J = -v_{in} - v_0 \quad (5.9)$$

From the correspondence between equations (5.9) and (5.1), we conclude that the Lagrangian function, \mathcal{L} , the dissipation function, φ and the action integral, \mathcal{I} of this system are given by:

$$\mathcal{L}(J, \dot{J}) = \frac{1}{2} \frac{1}{k} \dot{J}^2 - \frac{1}{2} \frac{1}{m} J^2 \quad (5.10)$$

$$\varphi(\dot{J}) = \frac{1}{2} \frac{1}{c} \dot{J}^2 \quad (5.11)$$

$$\delta \mathcal{I} = -\delta \int_0^T \mathcal{L}(J, \dot{J}) dt + \int_0^T \frac{\partial \varphi(\dot{J})}{\partial \dot{J}} \delta \dot{J} dt + \int_0^T [v_{in}(t) + v_0] \delta J dt \quad (5.12)$$

Equation (5.9) can also be thought of as the equation of motion of the *dual* system shown in Fig. 5.3.

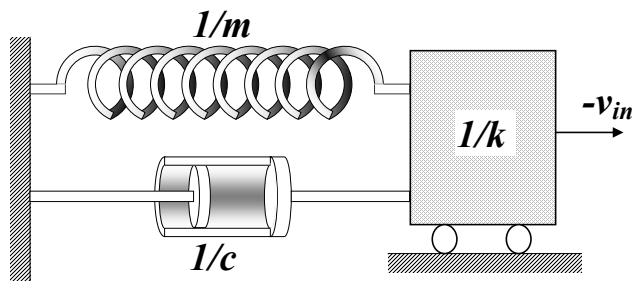


Fig. 5.3. Dual of System in Fig. 5.2

We observe that while the Lagrangian and Dissipation functions involve the displacement and the velocity for a parallel (Kelvin type) system, they involve the impulse and the force for a series (Maxwell type) system.

5.4.3. Mass with Combined Kelvin and Maxwell Resisting Systems

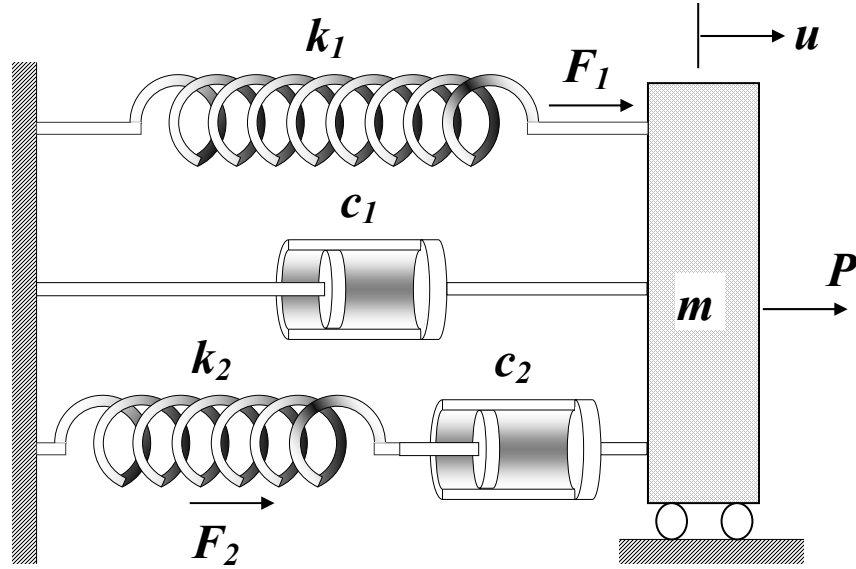


Fig. 5.4. Mass with Combined Kelvin and Maxwell Resisting Systems

Consider now the combined Kelvin-Maxwell system shown in Fig. 5.4 subject to a Force Input. (Note that the velocity input has been excluded for the sake of simplicity). The forces in the springs are denoted by F_1 and F_2 respectively and their impulses by J_1 and J_2 . If we define the flexibilities of the springs as $a_1 = 1/k_1$ and $a_2 = 1/k_2$, then the equations of equilibrium and compatibility become respectively:

$$m\ddot{u} + c\dot{u} + k_1u + \dot{J}_2 = P \quad (5.13)$$

$$a_2\ddot{J}_2 + \frac{1}{c_2}\dot{J}_2 - \dot{u} = 0 \quad (5.14)$$

It is found that elimination of either u or J_2 results in a differential equation that does not have a weak formulation (see introduction in subsection 5.1) that separates in to a Lagrangian part and a dissipation part. Such a formulation would therefore not lend itself to the derivation of the discrete variational integrators of the next section. Moreover, when considering plasticity, the dissipative term in equation (5.14) is not single valued and hence, elimination of J_2 would not be possible. It is therefore necessary to devise mixed Lagrangian and dissipation functions that contain u , J_2 and their time derivatives. Consider the following Lagrangian and dissipation functions and action integral:

$$\mathcal{L}(u, J_2, \dot{u}, \dot{J}_2) = \frac{1}{2} m \dot{u}^2 - \frac{1}{2} k_1 u^2 + \frac{1}{2} a_2 J_2^2 + J_2 \dot{u} \quad (5.15)$$

$$\varphi(\dot{u}, \dot{J}_2) = \frac{1}{2} c_1 \dot{u}^2 + \frac{1}{2} \frac{1}{c_2} \dot{J}_2^2 \quad (5.16)$$

$$\delta \mathcal{I} = -\delta \int_0^T \mathcal{L}(u, \dot{u}, J_2, \dot{J}_2) dt + \int_0^T \frac{\partial \varphi(\dot{u})}{\partial \dot{u}} \delta u dt + \int_0^T \frac{\partial \varphi(\dot{J}_2)}{\partial \dot{J}_2} \delta J_2 dt - \int_0^T P \delta u dt \quad (5.17)$$

It can be easily verified that the corresponding Euler-Lagrange equations are:

$$\frac{d}{dt} \left(\frac{\partial \mathcal{L}}{\partial \dot{u}} \right) - \left(\frac{\partial \mathcal{L}}{\partial u} \right) + \frac{\partial \varphi}{\partial \dot{u}} = P \Rightarrow m \ddot{u} + c_1 \dot{u} + k_1 u + \dot{J}_2 = P \quad (5.18)$$

$$\frac{d}{dt} \left(\frac{\partial \mathcal{L}}{\partial \dot{J}_2} \right) - \left(\frac{\partial \mathcal{L}}{\partial J_2} \right) + \frac{\partial \varphi}{\partial \dot{J}_2} = 0 \Rightarrow a_2 \ddot{J}_2 + \frac{1}{c_2} \dot{J}_2 - \dot{u} = 0 \quad (5.19)$$

which are respectively the equilibrium equation of the parallel subsystem and the compatibility equation of the series subsystem. Bryant (Bryant (1959)) and Stern (Stern (1965)) describe a method to determine a Lagrangian with a minimal set of variables for electrical networks. Fig. 5.5 shows the electrical circuit that is analogous to the

mechanical system of Fig. 5.4 (see Table 5.1). Equation (5.15) is indeed a minimal set Lagrangian.

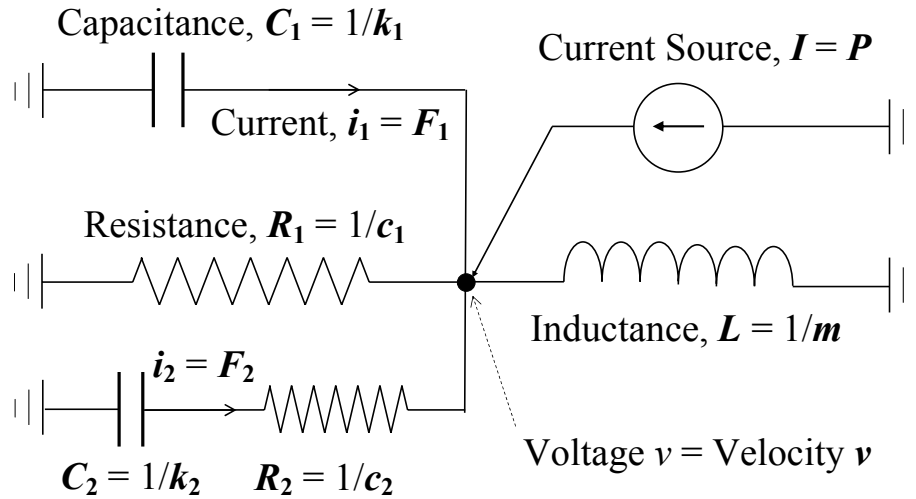


Fig. 5.5. Electrical Circuit Analogous to Fig. 5.4

Table 5.1. Electrical Analogy

Mechanical System	Electrical System
Force (F)	Current (i)
Velocity (v)	Voltage (v)
Impulse (J)	Charge (q)
Displacement (u)	Flux Linkage $\int_0^t v d\tau$
Spring Stiffness ($1/k$)	Capacitance (C)
Damping ($1/c$)	Resistance (R)
Mass ($1/m$)	Inductance (L)

5.4.4. Alternate formulation for Combined Kelvin and Maxwell System

It is found however, that it is more convenient for MDOF structural systems to use a Lagrangian function of all the spring forces as shown below, even though it is not minimal.

$$\mathcal{L}(J_2, \dot{u}, J_2) = \frac{1}{2} m \dot{u}^2 + \frac{1}{2} a_1 J_1^2 + \frac{1}{2} a_2 J_2^2 + (J_1 + J_2) \dot{u} \quad (5.20)$$

or in matrix notation:

$$\mathcal{L}(\mathbf{J}, \dot{u}, \mathbf{J}) = \frac{1}{2} m \dot{u}^2 + \frac{1}{2} \mathbf{J}^T \mathbf{A} \mathbf{J} + \mathbf{J}^T \mathbf{B}^T \dot{u} \quad (5.21)$$

where $\mathbf{J} = [J_1 \ J_2]^T$, $\mathbf{A} = \begin{bmatrix} a_1 & 0 \\ 0 & a_2 \end{bmatrix}$, the flexibility matrix and $\mathbf{B} = [1 \ 1]$, the *equilibrium matrix*.

The equilibrium matrix operates on the vector of internal forces to produce the vector of nodal forces. The *compatibility matrix* operates on the velocity vector to produce the rate of change of deformation. As a consequence of the Principle of Virtual Work, the transpose of the compatibility matrix is the equilibrium matrix. The dissipation function and the action integral are still given by equations (5.16) and (5.17). The Euler-Lagrange equations are:

$$\frac{d}{dt} \left(\frac{\partial \mathcal{L}}{\partial \dot{u}} \right) - \left(\frac{\partial \mathcal{L}}{\partial u} \right) + \frac{\partial \bar{\varphi}}{\partial \dot{u}} = P \Rightarrow m \ddot{u} + c \dot{u} + \mathbf{B} \mathbf{J} = P \quad (5.22)$$

$$\frac{d}{dt} \left(\frac{\partial \mathcal{L}}{\partial \dot{\mathbf{J}}} \right) - \left(\frac{\partial \mathcal{L}}{\partial \mathbf{J}} \right) + \frac{\partial \bar{\varphi}}{\partial \dot{\mathbf{J}}} = 0 \Rightarrow \mathbf{A} \ddot{\mathbf{J}} + \frac{\partial \bar{\varphi}}{\partial \dot{\mathbf{J}}} - \mathbf{B}^T \dot{u} = 0 \quad (5.23)$$

The mixed Lagrangian of equation (5.21) and the Dissipation function of equation (5.16) form the basis of further developments in this paper. Observe that the Lagrangian is not unique. For example, the Lagrangian:

$$\bar{\mathcal{L}}(u, \mathbf{J}, \dot{u}, \dot{\mathbf{J}}) = \frac{1}{2}m\dot{u}^2 + \frac{1}{2}\dot{\mathbf{J}}^T \mathbf{A} \dot{\mathbf{J}} - \dot{\mathbf{J}}^T \mathbf{B}^T u \quad (5.24)$$

would result in the same governing differential equations (5.22) and (5.23). In fact, any Lagrangian differing from that in (5.21) by only a *gauge transformation* of the form:

$$\bar{\mathcal{L}}(u, \mathbf{J}, \dot{u}, \dot{\mathbf{J}}) = \mathcal{L}(\mathbf{J}, \dot{u}, \dot{\mathbf{J}}) + \frac{d}{dt} \chi(u, \mathbf{J}) \quad (5.25)$$

where $\chi(u, \mathbf{J})$ is any scalar function would result in identical Euler-Lagrange equations (see for example, Scheck (1994)). The form (5.24) is obtained from a Legendre transformation of the potential energy in spring 2. However, we prefer the form (5.21) due to its following features:

1. It does not contain the displacement, u explicitly. Therefore the momentum, $\frac{\partial \mathcal{L}}{\partial u}$ is conserved (see for example, Scheck (1994)). This leads to the idea of the generalized momentum:

$$p_u = \frac{\partial \mathcal{L}}{\partial u} = m\dot{u} + J_1 + J_2 \quad (5.26)$$

2. It extends to geometric nonlinear problems where the equilibrium matrix \mathbf{B} is not constant, as shown in a later section.

Thus far, weak formulations have been derived for dynamic systems with viscous dissipative functions as illustrations. We now proceed towards the original goal of developing weak formulations for dynamic systems with plasticity.

5.4.5. Elastic-viscoplastic Dynamic System

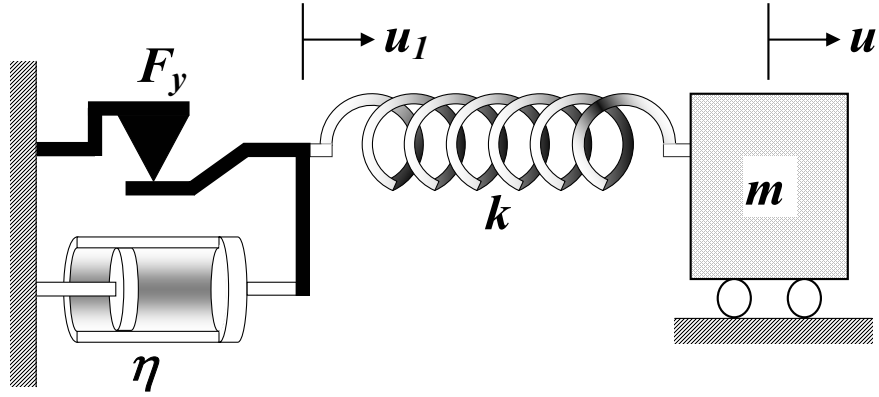


Fig. 5.6. Elastic-visco-plastic Dynamic System

Consider the elastic-visco-plastic dynamic system of Fig. 5.6. As shown in Section 2, this is in fact a visco-plastic regularization of the elastic-ideal-plastic system of Fig. 5.7. Let the yield force of the slider be F_y , so that that force F_{slider} in the slider is such that $|F_{\text{slider}}| \leq F_y$. If the force in the spring is F , then as in equation (2.20) of Section 2, the rate of deformation of the slider-dashpot combination is:

$$\dot{u}_1 = \frac{1}{\eta} \langle |F| - F_y \rangle \text{sgn}(F) = \frac{1}{\eta} \langle |J| - F_y \rangle \text{sgn}(\dot{J}) \quad (5.27)$$

where again, $J = \int_0^t F d\tau$, $\langle x \rangle$ is the Mackaulay Bracket and $\text{sgn}(x)$, the signum function.

Again, from equation (2.22) of Section 2, the above constitutive equation can be obtained as follows from a convex dissipation function:

$$\varphi(\dot{J}) = \frac{1}{2\eta} \langle |\dot{J}| - F_y \rangle^2 \Rightarrow \dot{u}_1 = \frac{\partial \varphi(\dot{J})}{\partial \dot{J}} = \frac{1}{\eta} \langle |\dot{J}| - F_y \rangle \text{sgn}(\dot{J}) \quad (5.28)$$

The equations of equilibrium and compatibility are therefore,

$$\begin{aligned} m\ddot{u} + \dot{J} &= P \\ a\ddot{J} + \frac{\partial \varphi(\dot{J})}{\partial \dot{J}} - \dot{u} &= 0 \end{aligned} \quad (5.29)$$

where $a = 1/k$, and it is verified without difficulty that the Lagrangian function, the dissipation function and the action integral are respectively:

$$\mathcal{L}(J, \dot{u}, \dot{J}) = \frac{1}{2} m \dot{u}^2 + \frac{1}{2} a \dot{J}^2 \quad (5.30)$$

$$\varphi(\dot{J}) = \frac{1}{2\eta} \langle |\dot{J}| - F_y \rangle^2 \quad (5.31)$$

$$\delta \mathcal{I} = -\delta \int_0^T \mathcal{L}(J, \dot{u}, \dot{J}) dt + \int_0^T \frac{\partial \varphi(\dot{J})}{\partial \dot{J}} \delta J dt - \int_0^T P \delta u dt \quad (5.32)$$

5.4.6. Elastic-Ideal plastic Dynamic System

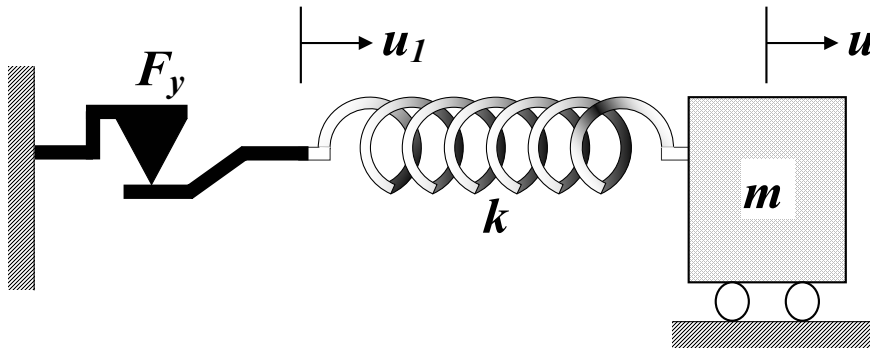


Fig. 5.7. Elastic-ideal-plastic Dynamic System

Fig. 5.7 shows an elastic-ideal plastic dynamic system. As noted above, this system is obtained from the viscoplastic one in the limit of the regularizing viscous coefficient, η , going to zero. The dissipation function φ of equation (5.28) then becomes:

$$\varphi(\dot{J}) = \begin{cases} 0 & \text{if } |\dot{J}| \leq F_y \\ \infty & \text{if } |\dot{J}| > F_y \end{cases} \quad (5.33)$$

i.e., $\varphi(\dot{J}) = \sqcup_C(\dot{J})$ where C is the elastic domain, $C = \{x : |x| < F_y\}$. The Lagrangian formulation of the elastic-ideal plastic system is then the same as that of the elastic viscoplastic system, i.e. equations (5.30)-(5.32), with the dissipation function of equation (5.31) suitably interpreted.

5.4.7. Summary of Phenomenological Models

It is observed from the preceding discussion that many types of phenomenological behavior can be modeled using a formulation consisting Lagrangian function, a dissipation function and an action integral. A new form of the Lagrangian function has been introduced which contains the impulse of the internal force. The specific forms of the dissipation function have been presented for viscous, visco-plastic and ideal plastic behaviors. The concepts are provided a formal terminology in subsection 5.5 and are extended to frame structures in the following subsections.

5.5. Reciprocal Structures

Materials whose constitutive behavior can be characterized by a potential function and a dissipation function are called *Generalized Standard Materials* (Nguyen (2000)). Components whose potential as well as dissipation functions are convex functions (Hiriart-Urruty and Lemaréchal (1993)) are called *reciprocal*. A structure composed

entirely of reciprocal components is called a *reciprocal structure* (analogous to the term *reciprocal network* of Stern (1965)). Such structures have a Lagrangian Formulation. The systems discussed in the previous sub-sections are of this type. This class also includes a wider variety of other behavior such as hyperelasticity, rate-independent plasticity, viscoelasticity, viscoplasticity and tension- or compression-only resistance. Appendix III shows the contributions of various one-dimensional reciprocal components to the Lagrangian and Dissipation functions. These can be expressed in their more general vector or tensor forms and used in the structural analysis methodology discussed below. However, for the sake of simplicity and concreteness, the derivations here are limited to *linear-elastic ideal-plastic* (non-hardening) components.

5.6. Compatibility Equations of a Frame Element

In order to obtain a Lagrangian formulation for a frame structure, the compatibility equations need to be expressed in a form similar to equation (5.23). The compatibility and constitutive equations of a frame element are now derived, which are then assembled to form the compatibility equation of the structure. Consider the beam element with rigid plastic hinges at the two ends. From Fig. 5.8(b), the compatibility of deformations in the element gives:

$$\begin{Bmatrix} \dot{\epsilon}_{hinge1} \\ 0 \\ -\dot{\theta}_{hinge1}^y \\ \dot{\theta}_{hinge1}^z \\ 0 \\ 0 \end{Bmatrix} + \begin{Bmatrix} \dot{q}_{beam}^1 \\ \dot{q}_{beam}^2 \\ \dot{q}_{beam}^3 \\ \dot{q}_{beam}^4 \\ \dot{q}_{beam}^5 \\ \dot{q}_{beam}^6 \end{Bmatrix} + \begin{Bmatrix} \dot{\epsilon}_{hinge2} \\ 0 \\ 0 \\ 0 \\ \dot{\theta}_{hinge2}^y \\ -\dot{\theta}_{hinge2}^z \end{Bmatrix} - \begin{Bmatrix} \dot{q}^1 \\ \dot{q}^2 \\ \dot{q}^3 \\ \dot{q}^4 \\ \dot{q}^5 \\ \dot{q}^6 \end{Bmatrix} = \mathbf{0} \quad (5.34)$$

Let \mathbf{A}^e be the elastic flexibility matrix of the element. Then:

$$\dot{\mathbf{q}}_{beam} = \mathbf{A}^e \dot{\mathbf{Q}} \quad (5.35)$$

where $\mathbf{q}_{beam} = \{q_{beam}^1 \ q_{beam}^2 \ q_{beam}^3 \ q_{beam}^4 \ q_{beam}^5 \ q_{beam}^6\}^T$ and \mathbf{Q} is the element independent end force vector. Let φ_{hinge1} and φ_{hinge2} be the dissipation functions of hinges 1 and 2 respectively. Then from equation (5.34) we have:

$$\begin{Bmatrix} \dot{\varepsilon}_{hinge1} \\ \dot{\theta}_{hinge1}^y \\ \dot{\theta}_{hinge1}^z \end{Bmatrix} = \frac{\partial \varphi_{hinge1}}{\mathcal{F}_{hinge1}} \quad \text{and} \quad \begin{Bmatrix} \dot{\varepsilon}_{hinge2} \\ \dot{\theta}_{hinge2}^y \\ \dot{\theta}_{hinge2}^z \end{Bmatrix} = \frac{\partial \varphi_{hinge2}}{\mathcal{F}_{hinge2}} \quad (5.36)$$

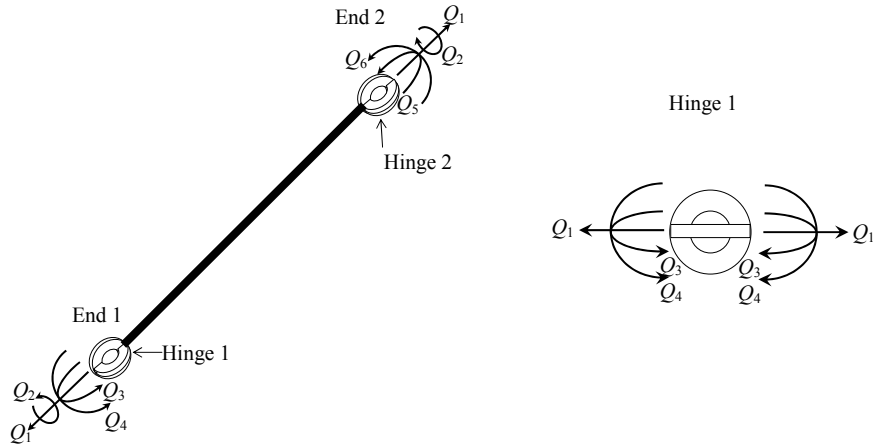
where \mathcal{F}_{hinge1} and \mathcal{F}_{hinge2} are the stress-resultants in hinges 1 and 2 respectively. But due to the sign conventions of the end forces and internal stress-resultants, $\mathcal{F}_{hinge1} = \{Q_1 \ -Q_3 \ Q_4\}^T$ and $\mathcal{F}_{hinge2} = \{Q_1 \ Q_5 \ -Q_6\}^T$. Define $\varphi^e = \varphi_{hinge1} + \varphi_{hinge2}$, the dissipation function of the element. Then we have:

$$\begin{Bmatrix} \dot{\varepsilon}_{hinge1} \\ 0 \\ -\dot{\theta}_{hinge1}^y \\ \dot{\theta}_{hinge1}^z \\ 0 \\ 0 \end{Bmatrix} + \begin{Bmatrix} \dot{\varepsilon}_{hinge2} \\ 0 \\ 0 \\ 0 \\ \dot{\theta}_{hinge2}^y \\ -\dot{\theta}_{hinge2}^z \end{Bmatrix} = \frac{\partial \varphi^e}{\partial \mathbf{Q}} \quad (5.37)$$

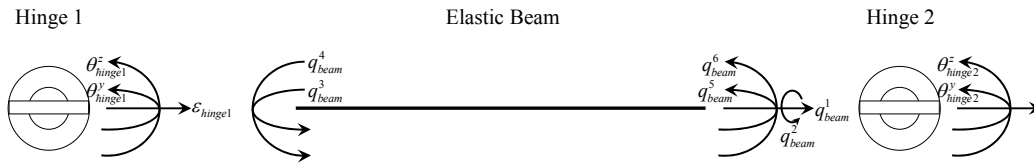
Substituting equations (5.35) and (5.37) in equation (5.34) gives the element equation:

$$\mathbf{A}^e \dot{\mathbf{Q}} + \frac{\partial \varphi^e}{\partial \mathbf{Q}} - \mathbf{B}^T \dot{\mathbf{u}}^e = \mathbf{0} \quad (5.38)$$

In the next subsection, the element compatibility equations are assembled to form the compatibility equation of the structure.



(a) Internal Forces



(b) Deformations

Fig. 5.8. Beam Element with Rigid-Plastic Hinges

5.7. Governing Equations of Skeletal Structures

The governing equations of the structure consist of the equilibrium equations, the compatibility equations and the constitutive equations. From Appendix I, the equilibrium equations are:

$$\mathbf{M}\ddot{\mathbf{u}} + \mathbf{C}\dot{\mathbf{u}} + \mathbf{B}\mathbf{J} - \mathbf{P} = \mathbf{0} \quad (5.39)$$

Define the elastic flexibility of the structure by:

$$\mathbf{A} = \begin{bmatrix} \mathbf{A}^{e,1} & & & \\ & \mathbf{A}^{e,2} & & \\ & & \ddots & \\ & & & \mathbf{A}^{e,N_{elem}} \end{bmatrix} \quad (5.40)$$

As in Appendix I, let $\mathbf{F} = \left\{ (\mathbf{Q}^1)^T \quad (\mathbf{Q}^2)^T \quad \dots \quad (\mathbf{Q}^{N_{elem}})^T \right\}^T$ and define $\mathbf{J} = \int_0^t \mathbf{F} d\tau$, the

impulse vector. Then the compatibility equation of the structure is given by:

$$\mathbf{A}\ddot{\mathbf{J}} + \frac{\partial \varphi(\dot{\mathbf{J}})}{\partial \dot{\mathbf{J}}} - \mathbf{B}^T \dot{\mathbf{u}} = \mathbf{0} \quad (5.41)$$

Internal imposed displacements within elements, such as resulting from pre-stressing or thermal loads have been neglected here for the sake of simplicity, resulting in there being no forcing term in equation (5.41). Pre-multiplying equation (5.39) by a kinematically admissible virtual displacement $\delta \mathbf{u}$ (satisfying compatibility), and equation (5.41) by a statically admissible virtual impulse $\delta \mathbf{J}$ (satisfying equilibrium), we have:

$$\begin{aligned} \delta \mathbf{u}^T \mathbf{M} \ddot{\mathbf{u}} + \delta \mathbf{u}^T \mathbf{C} \dot{\mathbf{u}} + \delta \mathbf{u}^T \mathbf{B} \dot{\mathbf{J}} - \delta \mathbf{u}^T \mathbf{P} &= \mathbf{0} \\ \delta \mathbf{J}^T \mathbf{A} \ddot{\mathbf{J}} + \delta \mathbf{J}^T \frac{\partial \varphi(\dot{\mathbf{J}})}{\partial \dot{\mathbf{J}}} - \delta \mathbf{J}^T \mathbf{B}^T \dot{\mathbf{u}} &= \mathbf{0} \end{aligned} \quad (5.42)$$

Adding equations (5.42) and integrating over the time interval $[0, T]$, we obtain:

$$\begin{aligned} \int_0^T \delta \mathbf{u}^T \mathbf{M} \ddot{\mathbf{u}} dt + \int_0^T \delta \mathbf{J}^T \mathbf{A} \ddot{\mathbf{J}} dt + \int_0^T \left[\mathbf{J}^T \mathbf{B}^T \delta \mathbf{u} - \delta \mathbf{J}^T \mathbf{B}^T \dot{\mathbf{u}} \right] dt \\ + \int_0^T \delta \mathbf{u}^T \mathbf{C} \dot{\mathbf{u}} dt + \int_0^T \delta \mathbf{J}^T \frac{\partial \varphi(\dot{\mathbf{J}})}{\partial \dot{\mathbf{J}}} dt - \int_0^T \delta \mathbf{u}^T \mathbf{P} dt &= \mathbf{0} \end{aligned} \quad (5.43)$$

Consider the first integral,

$$\int_0^T \delta \mathbf{u}^T \mathbf{M} \ddot{\mathbf{u}} dt = \delta \mathbf{u}^T \mathbf{M} \dot{\mathbf{u}} \Big|_0^T - \int_0^T \delta \dot{\mathbf{u}}^T \mathbf{M} \dot{\mathbf{u}} dt = -\delta \int_0^T \frac{1}{2} \dot{\mathbf{u}}^T \mathbf{M} \dot{\mathbf{u}} dt \quad (5.44)$$

Similarly the second integral,

$$\int_0^T \delta \mathbf{J}^T \mathbf{A} \ddot{\mathbf{J}} dt = -\delta \int_0^T \frac{1}{2} \dot{\mathbf{J}}^T \mathbf{A} \dot{\mathbf{J}} dt \quad (5.45)$$

Equilibrium is considered in the undeformed configuration, so that the equilibrium matrix \mathbf{B} is a constant. Geometric nonlinearity, where \mathbf{B} is a function of \mathbf{u} , is considered in the next subsection. The third integral of equation (5.43) is then,

$$\int_0^T \dot{\mathbf{J}}^T \mathbf{B}^T \delta \mathbf{u} dt - \int_0^T \delta \mathbf{J}^T \mathbf{B}^T \dot{\mathbf{u}} dt = \dot{\mathbf{J}}^T \mathbf{B}^T \delta \mathbf{u} \Big|_0^T - \int_0^T \mathbf{J}^T \mathbf{B}^T \delta \dot{\mathbf{u}} dt - \int_0^T \delta \mathbf{J}^T \mathbf{B}^T \dot{\mathbf{u}} dt = -\delta \int_0^T \mathbf{J}^T \mathbf{B} \dot{\mathbf{u}} dt \quad (5.46)$$

Substituting equations (5.44), (5.45) and (5.46) in equation (5.43), we have:

$$\begin{aligned} \delta \mathcal{L} = & -\delta \int_0^T \left[\frac{1}{2} \dot{\mathbf{u}}^T \mathbf{M} \dot{\mathbf{u}} + \frac{1}{2} \dot{\mathbf{J}}^T \mathbf{A} \dot{\mathbf{J}} + \mathbf{J}^T \mathbf{B}^T \dot{\mathbf{u}} \right] dt \\ & + \int_0^T \delta \mathbf{u}^T \mathbf{C} \dot{\mathbf{u}} dt + \int_0^T \delta \mathbf{J}^T \frac{\partial \varphi(\mathbf{J})}{\partial \dot{\mathbf{J}}} dt - \int_0^T \delta \mathbf{u}^T \mathbf{P} dt = \mathbf{0} \end{aligned} \quad (5.47)$$

The Lagrangian and the dissipation function are then given by:

$$\mathcal{L}(\mathbf{J}, \dot{\mathbf{u}}, \dot{\mathbf{J}}) = \frac{1}{2} \dot{\mathbf{u}}^T \mathbf{M} \dot{\mathbf{u}} + \frac{1}{2} \dot{\mathbf{J}}^T \mathbf{A} \dot{\mathbf{J}} + \mathbf{J}^T \mathbf{B}^T \dot{\mathbf{u}} \quad (5.48)$$

$$\bar{\varphi}(\dot{\mathbf{u}}, \dot{\mathbf{J}}) = \frac{1}{2} \dot{\mathbf{u}}^T \mathbf{C} \dot{\mathbf{u}} + \varphi(\mathbf{J}) \quad (5.49)$$

Conversely equations (5.39) and (5.41) can be obtained from the relation (5.47) as Euler-Lagrange equations.

5.8. Effect of Geometric Nonlinearity on the Lagrangian Function

Having examined the structural dynamic problem under small deformations, it is now desired to consider equilibrium in the deformed configuration. The effect of large structural displacements is considered, while that of large deformations within the corotational frames of elements is ignored. This seems to be justified for elastic-plastic frame elements where significant displacements occur after yielding when hinges form, thus not accompanied by large deformations within the element corotational frame. The effect of the change of length on the flexibility coefficients of beam-column members is also neglected since this is a higher order effect. Large deformations may be included by proceeding from the Lagrangian density and performing spatial discretization such as by the Finite Element Method. Some remarks on this are made in a later section.

The added ingredient is only the fact that the equilibrium matrix, \mathbf{B} , is a function of displacement, $\mathbf{B}(\mathbf{u})$, as seen for example from equation (4.12) of Section 4. However, the equilibrium equations (5.39) being in global coordinates and the compatibility equations (5.41) being incremental (compatibility of deformation and displacement rates) must both remain unchanged by this additional consideration. It is now demonstrated that the spatially pre-discretized Lagrangian of equation (5.48) holds in the deformed configuration as well. The Lagrangian is now:

$$\mathcal{L}(\mathbf{u}, \mathbf{J}, \dot{\mathbf{u}}, \dot{\mathbf{J}}) = \frac{1}{2} \dot{\mathbf{u}}^T \mathbf{M} \dot{\mathbf{u}} + \frac{1}{2} \dot{\mathbf{J}}^T \mathbf{A} \dot{\mathbf{J}} + \mathbf{J}^T [\mathbf{B}(\mathbf{u})]^T \dot{\mathbf{u}} \quad (5.50)$$

The dissipation terms and the external forcing function remain the same. Moreover, since only an additional function of \mathbf{u} is introduced, the term $\frac{d}{dt}\left(\frac{\partial \mathcal{L}}{\partial \dot{\mathbf{J}}}\right) - \left(\frac{\partial \mathcal{L}}{\partial \mathbf{J}}\right)$ also remains unchanged. Therefore, it is sufficient to examine the term $\frac{d}{dt}\left(\frac{\partial \mathcal{L}}{\partial \dot{\mathbf{u}}}\right) - \left(\frac{\partial \mathcal{L}}{\partial \mathbf{u}}\right)$.

$$\begin{aligned} \frac{d}{dt}\left(\frac{\partial \mathcal{L}}{\partial \dot{\mathbf{u}}}\right) - \left(\frac{\partial \mathcal{L}}{\partial \mathbf{u}}\right) &= \mathbf{M}\ddot{\mathbf{u}} + \frac{d}{dt}(\mathbf{B}^T \mathbf{J}) - \frac{\partial}{\partial \mathbf{u}}(\dot{\mathbf{u}}^T \mathbf{B}^T \mathbf{J}) \\ &= \mathbf{M}\ddot{\mathbf{u}} + \mathbf{B}^T \dot{\mathbf{J}} + \left[\left(\frac{d\mathbf{B}^T}{dt}\right) - \frac{\partial}{\partial \mathbf{u}}(\dot{\mathbf{u}}^T \mathbf{B}^T) \right] \mathbf{J} \end{aligned} \quad (5.51)$$

Let the structure have a total of N_ε deformations (and hence N_ε internal forces). The matrix \mathbf{B} therefore has N_ε columns. Let \mathbf{B}_i represent the i^{th} column of \mathbf{B} (Notice that the meaning of \mathbf{B}_i here is different from that in the last section, where it denoted the i^{th} column-wise partition of \mathbf{B}). Consider the i^{th} column of the term $\left(\frac{d\mathbf{B}}{dt}\right) - \frac{\partial}{\partial \mathbf{u}}(\dot{\mathbf{u}}^T \mathbf{B})$.

$$\frac{d\mathbf{B}_i}{dt} = \frac{d}{dt} \begin{bmatrix} B_{1i} \\ B_{2i} \\ \vdots \\ B_{N_u i} \end{bmatrix} = \begin{bmatrix} \frac{\partial B_{1i}}{\partial u_1} & \frac{\partial B_{1i}}{\partial u_2} & \cdots & \frac{\partial B_{1i}}{\partial u_{N_u}} \\ \frac{\partial B_{2i}}{\partial u_1} & \frac{\partial B_{2i}}{\partial u_2} & \cdots & \frac{\partial B_{2i}}{\partial u_{N_u}} \\ \vdots & \vdots & \ddots & \vdots \\ \frac{\partial B_{N_u i}}{\partial u_1} & \frac{\partial B_{N_u i}}{\partial u_2} & \cdots & \frac{\partial B_{N_u i}}{\partial u_{N_u}} \end{bmatrix} \dot{\mathbf{u}} \quad (5.52)$$

$$\begin{aligned} \dot{\mathbf{u}}^T \mathbf{B}^T &= \dot{\mathbf{u}}^T \begin{bmatrix} \mathbf{B}_1^T & \mathbf{B}_2^T & \cdots & \mathbf{B}_i^T & \cdots & \mathbf{B}_{N_u}^T \end{bmatrix} \\ &= \begin{bmatrix} \mathbf{B}_1^T \dot{\mathbf{u}} & \mathbf{B}_2^T \dot{\mathbf{u}} & \cdots & \mathbf{B}_i^T \dot{\mathbf{u}} & \cdots & \mathbf{B}_{N_u}^T \dot{\mathbf{u}} \end{bmatrix}, \text{ a row vector} \end{aligned} \quad (5.53)$$

Therefore,

$$\left[\frac{\partial}{\partial \mathbf{u}} (\dot{\mathbf{u}}^T \mathbf{B}) \right]_{i^{\text{th}} \text{ column}} = \frac{\partial}{\partial \mathbf{u}} (\mathbf{B}_i^T \dot{\mathbf{u}}) = \begin{bmatrix} \frac{\partial B_{1i}}{\partial u_1} & \frac{\partial B_{2i}}{\partial u_1} & \dots & \frac{\partial B_{N_u i}}{\partial u_1} \\ \frac{\partial B_{1i}}{\partial u_2} & \frac{\partial B_{2i}}{\partial u_2} & \dots & \frac{\partial B_{N_u i}}{\partial u_2} \\ \vdots & \vdots & & \vdots \\ \frac{\partial B_{1i}}{\partial u_{N_u}} & \frac{\partial B_{2i}}{\partial u_{N_u}} & \dots & \frac{\partial B_{N_u i}}{\partial u_{N_u}} \end{bmatrix} \dot{\mathbf{u}} \quad (5.54)$$

It is postulated that the i^{th} deformation component, $\varepsilon_i(\mathbf{u})$, is a twice continuously differentiable function of the deformed configuration. Then $\mathbf{B}_i = \left(\frac{\partial \varepsilon_i}{\partial \mathbf{u}} \right)^T$ is the Jacobian

of the deformation function, and $\frac{\partial \mathbf{B}_i}{\partial \mathbf{u}} = \left(\frac{\partial \mathbf{B}_i}{\partial \mathbf{u}} \right)^T = \frac{\partial^2 \varepsilon_i}{\partial \mathbf{u}^2}$, the Hessian is symmetric. Hence

the right hand sides of equations (5.52) and (5.54) are equal, implying that

$\left(\frac{d\mathbf{B}}{dt} \right) - \frac{\partial}{\partial \mathbf{u}} (\dot{\mathbf{u}}^T \mathbf{B}) = \mathbf{0}$. Having recognized the symmetry in \mathbf{B} , the above result may also

be proved using index notation as follows:

$$\left(\frac{d\mathbf{B}}{dt} \right) - \frac{\partial}{\partial \mathbf{u}} (\dot{\mathbf{u}}^T \mathbf{B}) = \dot{B}_{ij} - B_{ij,p} \dot{u}_p = B_{ij,p} \dot{u}_p - B_{ij,p} \dot{u}_i = B_{pj,i} \dot{u}_p - B_{ij,p} \dot{u}_i = \mathbf{0} \quad (5.55)$$

Thus the formulation remains unchanged when geometric nonlinearity is included.

5.9. Extension to Continua

It is shown in Appendix IV that weak formulations analogous to equations (5.47) through (5.49) can be obtained for continua. The final results are presented here. For a three dimensional continuum, the Lagrangian formulation is given by:

$$\mathcal{L} = \frac{1}{2} \dot{u}_k \dot{u}_k + \frac{1}{2} A_{ijkl} \mathbf{J}_{ij} \mathbf{J}_{kl} + \frac{1}{\rho_0} J_{ij} B_{ijk}^* \dot{u}_k \quad (5.56)$$

$$\varphi(\mathbf{J}, \dot{\mathbf{u}}) = U_C(\mathbf{J}) + \frac{1}{2} c_{ij} \dot{u}_i \dot{u}_j \quad (5.57)$$

$$\begin{aligned}
\delta \mathcal{Z} = & -\delta \int_0^T \int_{\Omega} \rho_0 \mathcal{L} d\Omega dt \\
& + \int_0^T \int_{\Omega} \rho_0 \frac{\partial \varphi}{\partial \dot{u}_k} \delta u_k d\Omega dt + \int_0^T \int_{\Omega} \rho_0 \frac{\partial \varphi}{\partial \dot{J}_{ij}} \delta J_{ij} d\Omega dt \\
& - \int_0^T \int_{\Omega} \rho_0 f_k \delta u_k d\Omega dt - \int_0^T \int_{\Gamma} \tau_k \delta u_k d\Gamma dt
\end{aligned} \tag{5.58}$$

and for a beam-column with finite deformation, by:

$$\mathcal{L} = \frac{1}{2} \rho_0 \dot{\mathbf{u}}^T \dot{\mathbf{u}} + \frac{1}{2} \mathbf{J}^T \mathbf{a} \mathbf{J} + \mathbf{J}^T \mathbf{B}^* \dot{\mathbf{u}} \tag{5.59}$$

$$\varphi(\mathbf{J}, \dot{\mathbf{u}}) = \mathbf{U}_C(\mathbf{J}) + \frac{1}{2} \dot{\mathbf{u}}^T \mathbf{c} \dot{\mathbf{u}} \tag{5.60}$$

$$\begin{aligned}
\delta \mathcal{Z} = & -\delta \int_0^T \int_0^L \mathcal{L} dx dt + \int_0^T \int_0^L \frac{\partial \varphi}{\partial \dot{\mathbf{u}}} \delta \mathbf{u} dx dt + \int_0^T \int_0^L \frac{\partial \varphi}{\partial \dot{\mathbf{J}}} \delta \mathbf{J} dx dt \\
& - \int_0^T \int_0^L \mathbf{f}^T \delta \mathbf{u} dx dt - \int_0^T \mathbf{Q}^T \delta \mathbf{q} dt
\end{aligned} \tag{5.61}$$

The analogy with equations (5.47) through (5.49) is seen easily. The integral over time can be discretized to obtain action sums from which discrete variational integrators can be obtained as shown in the next section. These can then be discretized in space using, for example, the finite element method. This is a subject of further work.

5.10. Summary of Lagrangian Formulation

Reciprocal structures and their Lagrangian formulation have been illustrated using simple systems with springs, masses, dashpots and sliders. The concept of generalized momentum has been demonstrated. The Lagrangian formulation for skeletal structures has been developed. It has been shown that the Lagrangian remains unchanged when geometric nonlinearity is included. The extension of the approach to continua has been

briefly discussed. The numerical integration of the Lagrangian equations by *discrete variational integrators* is discussed in the next section.

6. THE LAGRANGIAN APPROACH – NUMERICAL SOLUTION

6.1. Background

In this section, a numerical method is developed for the time integration of the governing equations (5.39) and (5.41) of the structure. This development consists of two stages:

1. Following Kane et al. (2000), the action integral of equation (5.47) is discretized in time to obtain an action sum. Using discrete calculus of variations, finite difference equations are obtained, which are the discrete counterparts of the Euler-Lagrange equations. It is seen that the numerical method obtained in this fashion conserves energy and momentum for a Lagrangian system and inherits the contractivity (stability in the energy norm) of dissipative systems.
2. The task in each time step is shown to be the solution of a constrained minimization problem for which an Augmented Lagrangian algorithm is developed.

A numerical example is presented to illustrate the feasibility of the method.

6.2. Time Discretization - Discrete Calculus of Variations

The action integral of equation (5.47) is discretized using the midpoint rule and a time step h , approximating derivatives using central differences. It is assumed in this process, that the \mathbf{J} and \mathbf{u} are twice continuously differentiable functions and \mathbf{P} is a once continuously differentiable function of time, and that the dissipation function is continuously differentiable with respect to $\dot{\mathbf{J}}$. It is shown by Simo and Govindjee (1991) using geometric arguments that the $O(h^2)$ accuracy holds in the limiting case of rate-

independent plasticity when the viscous coefficient $\eta \rightarrow 0$ as well. The resulting action sum is given by:

$$\begin{aligned}
& -\delta \sum_{k=0}^{n-1} h \left\{ \frac{1}{2} \left(\frac{\mathbf{u}_{k+1} - \mathbf{u}_k}{h} \right)^T \mathbf{M} \left(\frac{\mathbf{u}_{k+1} - \mathbf{u}_k}{h} \right) + \frac{1}{2} \left(\frac{\mathbf{J}_{k+1} - \mathbf{J}_k}{h} \right)^T \mathbf{A} \left(\frac{\mathbf{J}_{k+1} - \mathbf{J}_k}{h} \right) \right. \\
& \quad \left. + \left(\frac{\mathbf{J}_{k+1} + \mathbf{J}_k}{2} \right)^T \mathbf{B}^T \left(\frac{\mathbf{u}_{k+1} - \mathbf{u}_k}{h} \right) \right\} \\
& + \sum_{k=0}^{n-1} h \left\{ \left(\frac{\delta \mathbf{u}_{k+1} + \delta \mathbf{u}_k}{2} \right)^T \mathbf{C} \left(\frac{\mathbf{u}_{k+1} - \mathbf{u}_k}{h} \right) \right\} \\
& + \sum_{k=0}^{n-1} h \left\{ \left(\frac{\delta \mathbf{J}_{k+1} + \delta \mathbf{J}_k}{2} \right)^T \frac{\partial \varphi}{\partial \dot{\mathbf{J}}} \Big|_{k+\frac{1}{2}} \right\} \\
& + \sum_{k=0}^{n-1} h \left\{ \left(\frac{\delta \mathbf{u}_{k+1} + \delta \mathbf{u}_k}{2} \right)^T \mathbf{P}_{k+\frac{1}{2}} \right\} + O(h^2)
\end{aligned} \tag{6.1}$$

where $nh = T$ and subscript k denotes the approximation at time $t = kh$. The time integration problem may now be stated as: *Given $\{\mathbf{u}_0, \mathbf{u}_n\}$ and $\{\mathbf{J}_0, \mathbf{J}_n\}$, find the sequences $\{\mathbf{u}_1, \mathbf{u}_2, \dots, \mathbf{u}_{n-1}\}$ and $\{\mathbf{J}_1, \mathbf{J}_2, \dots, \mathbf{J}_{n-1}\}$ that make the action sum of equation (6.1) stationary.* This is the *discrete variational problem* (Shaflucas (1969), Cadzow (1970), Cybenko (1997), Kane, Marsden et al. (2000), and Marsden and West (2001)). Consider the first sum:

$$\delta \sum_{k=0}^{n-1} h \left\{ \frac{1}{2} \left(\frac{\mathbf{u}_{k+1} - \mathbf{u}_k}{h} \right)^T \mathbf{M} \left(\frac{\mathbf{u}_{k+1} - \mathbf{u}_k}{h} \right) \right\} = \sum_{k=0}^{n-1} h \left\{ \left(\frac{\delta \mathbf{u}_{k+1} - \delta \mathbf{u}_k}{h} \right)^T \mathbf{M} \left(\frac{\mathbf{u}_{k+1} - \mathbf{u}_k}{h} \right) \right\}$$

For a justification of using the δ operator as done here, see Cadzow (1970). Collecting the terms in $\delta \mathbf{u}_{k+1}$ and $\delta \mathbf{u}_k$, we have:

$$\sum_{k=0}^{n-1} \delta \mathbf{u}_{k+1}^T \mathbf{M} \left(\frac{\mathbf{u}_{k+1} - \mathbf{u}_k}{h} \right) - \sum_{k=0}^{n-1} \delta \mathbf{u}_k^T \mathbf{M} \left(\frac{\mathbf{u}_{k+1} - \mathbf{u}_k}{h} \right)$$

Pulling terms involving the boundaries of the time interval out of the sum gives:

$$\delta \mathbf{u}_n^T \mathbf{M} \left(\frac{\mathbf{u}_n - \mathbf{u}_{n-1}}{h} \right) + \sum_{k=0}^{n-2} \delta \mathbf{u}_{k+1}^T \mathbf{M} \left(\frac{\mathbf{u}_{k+1} - \mathbf{u}_k}{h} \right) - \delta \mathbf{u}_0^T \mathbf{M} \left(\frac{\mathbf{u}_1 - \mathbf{u}_0}{h} \right) - \sum_{k=1}^{n-1} \delta \mathbf{u}_k^T \mathbf{M} \left(\frac{\mathbf{u}_{k+1} - \mathbf{u}_k}{h} \right)$$

Changing the indexing in the first sum replacing the index k with $k+1$ and collecting terms results in:

$$\delta \mathbf{u}_n^T \mathbf{M} \left(\frac{\mathbf{u}_n - \mathbf{u}_{n-1}}{h} \right) - \delta \mathbf{u}_0^T \mathbf{M} \left(\frac{\mathbf{u}_1 - \mathbf{u}_0}{h} \right) - \sum_{k=1}^{n-1} h \delta \mathbf{u}_k^T \mathbf{M} \left(\frac{\mathbf{u}_{k+1} - 2\mathbf{u}_k + \mathbf{u}_{k-1}}{h^2} \right)$$

This procedure is called discrete integration by parts or summation by parts. The similarity with integration by parts in the continuous case can be clearly seen. Since $\delta \mathbf{u}_0 = \delta \mathbf{u}_n = 0$ in Hamilton's principle, we have:

$$\delta \sum_{k=0}^{n-1} h \left\{ \frac{1}{2} \left(\frac{\mathbf{u}_{k+1} - \mathbf{u}_k}{h} \right)^T \mathbf{M} \left(\frac{\mathbf{u}_{k+1} - \mathbf{u}_k}{h} \right) \right\} = - \sum_{k=1}^{n-1} h \delta \mathbf{u}_k^T \mathbf{M} \left(\frac{\mathbf{u}_{k+1} - 2\mathbf{u}_k + \mathbf{u}_{k-1}}{h^2} \right) \quad (6.2)$$

Proceeding in a similar fashion using Discrete Integration by Parts, the following equations are obtained:

$$\delta \sum_{k=0}^{n-1} h \left\{ \frac{1}{2} \left(\frac{\mathbf{J}_{k+1} - \mathbf{J}_k}{h} \right)^T \mathbf{A} \left(\frac{\mathbf{J}_{k+1} - \mathbf{J}_k}{h} \right) \right\} = - \sum_{k=1}^{n-1} h \delta \mathbf{J}_k^T \mathbf{A} \left(\frac{\mathbf{J}_{k+1} - 2\mathbf{J}_k + \mathbf{J}_{k-1}}{h^2} \right) \quad (6.3)$$

$$\begin{aligned} \delta \sum_{k=0}^{n-1} h \left\{ \frac{1}{2} \left(\frac{\mathbf{J}_{k+1} + \mathbf{J}_k}{2} \right)^T \mathbf{B}^T \left(\frac{\mathbf{u}_{k+1} - \mathbf{u}_k}{h} \right) \right\} \\ = \sum_{k=1}^{n-1} h \left\{ \delta \mathbf{J}_k^T \mathbf{B}^T \left(\frac{\mathbf{u}_{k+1} - \mathbf{u}_{k-1}}{2h} \right) - \delta \mathbf{u}_k^T \mathbf{B} \left(\frac{\mathbf{J}_{k+1} - \mathbf{J}_k}{2h} \right) \right\} \end{aligned} \quad (6.4)$$

$$\sum_{k=0}^{n-1} h \left\{ \left(\frac{\delta \mathbf{u}_{k+1} + \delta \mathbf{u}_k}{2} \right)^T \mathbf{C} \left(\frac{\mathbf{u}_{k+1} - \mathbf{u}_k}{h} \right) \right\} = \sum_{k=1}^{n-1} h \delta \mathbf{u}_k^T \mathbf{C} \left(\frac{\mathbf{u}_{k+1} - \mathbf{u}_{k-1}}{2h} \right) \quad (6.5)$$

$$\sum_{k=0}^{n-1} h \left\{ \left(\frac{\delta \mathbf{J}_{k+1} + \delta \mathbf{J}_k}{2} \right)^T \frac{\partial \varphi}{\partial \dot{\mathbf{J}}}_{k+\frac{1}{2}} \right\} = \sum_{k=1}^{n-1} \frac{h}{2} \delta \mathbf{J}_k^T \left(\frac{\partial \varphi}{\partial \dot{\mathbf{J}}}_{k+\frac{1}{2}} + \frac{\partial \varphi}{\partial \dot{\mathbf{J}}}_{k-\frac{1}{2}} \right) \quad (6.6)$$

$$\sum_{k=0}^{n-1} h \left\{ \left(\frac{\delta \mathbf{u}_{k+1} + \delta \mathbf{u}_k}{2} \right)^T \mathbf{P}_{k+\frac{1}{2}} \right\} = \sum_{k=1}^{n-1} \frac{h}{2} \delta \mathbf{u}_k^T (\mathbf{P}_{k+\frac{1}{2}} + \mathbf{P}_{k-\frac{1}{2}}) \quad (6.7)$$

Substituting equations (6.2) through (6.7) in equation (6.1) results in:

$$\begin{aligned} & \sum_{k=1}^{n-1} \delta \mathbf{u}_k^T \left[\mathbf{M} \left(\frac{\mathbf{u}_{k+1} - 2\mathbf{u}_k + \mathbf{u}_{k-1}}{h^2} \right) + \mathbf{C} \left(\frac{\mathbf{u}_{k+1} - \mathbf{u}_{k-1}}{2h} \right) + \mathbf{B} \left(\frac{\mathbf{J}_{k+1} - \mathbf{J}_k}{2h} \right) - \left(\frac{\mathbf{P}_{k+\frac{1}{2}} + \mathbf{P}_{k-\frac{1}{2}}}{2} \right) \right] \\ & + \sum_{k=1}^{n-1} \delta \mathbf{J}_k^T \left[\mathbf{A} \left(\frac{\mathbf{J}_{k+1} - 2\mathbf{J}_k + \mathbf{J}_{k-1}}{h^2} \right) + \frac{1}{2} \left(\frac{\partial \varphi}{\partial \dot{\mathbf{J}}}_{k+\frac{1}{2}} + \frac{\partial \varphi}{\partial \dot{\mathbf{J}}}_{k-\frac{1}{2}} \right) - \mathbf{B}^T \left(\frac{\mathbf{u}_{k+1} - \mathbf{u}_{k-1}}{2h} \right) \right] \\ & = 0 \end{aligned} \quad (6.8)$$

Since $\delta \mathbf{u}_k$ and $\delta \mathbf{J}_k$ are arbitrary variations, the discrete equations of motion are:

$$\begin{aligned} & \mathbf{M} \left(\frac{\mathbf{u}_{k+1} - 2\mathbf{u}_k + \mathbf{u}_{k-1}}{h^2} \right) + \mathbf{C} \left(\frac{\mathbf{u}_{k+1} - \mathbf{u}_{k-1}}{2h} \right) + \mathbf{B} \left(\frac{\mathbf{J}_{k+1} - \mathbf{J}_k}{2h} \right) = \left(\frac{\mathbf{P}_{k+\frac{1}{2}} + \mathbf{P}_{k-\frac{1}{2}}}{2} \right) \\ & \mathbf{A} \left(\frac{\mathbf{J}_{k+1} - 2\mathbf{J}_k + \mathbf{J}_{k-1}}{h^2} \right) + \frac{1}{2} \left(\frac{\partial \varphi}{\partial \dot{\mathbf{J}}}_{k+\frac{1}{2}} + \frac{\partial \varphi}{\partial \dot{\mathbf{J}}}_{k-\frac{1}{2}} \right) - \mathbf{B}^T \left(\frac{\mathbf{u}_{k+1} - \mathbf{u}_{k-1}}{2h} \right) = \mathbf{0} \end{aligned} \quad (6.9)$$

Notice that these equations could have been obtained directly from equations (5.39) and (5.41) by using the Central Difference approximation. But deriving them using Discrete Variational Calculus ensures that the resulting time-integration scheme possesses energy and momentum conserving properties. This is demonstrated below. This also provides a framework for consistently developing higher order methods and error estimation methods that preserve conservation.

6.2.1. Features of the Discrete Equation

It can be shown that the finite difference equations (6.9) inherit the energy and momentum characteristics of the differential equations (5.47). Consider first the momentum in the absence of dissipation and external forces. The equations (6.9) then become:

$$\mathbf{M} \left(\frac{\mathbf{u}_{k+1} - 2\mathbf{u}_k + \mathbf{u}_{k-1}}{h^2} \right) + \mathbf{B} \left(\frac{\mathbf{J}_{k+1} - \mathbf{J}_k}{2h} \right) = \mathbf{0} \quad (6.10)$$

$$\mathbf{A} \left(\frac{\mathbf{J}_{k+1} - 2\mathbf{J}_k + \mathbf{J}_{k-1}}{h^2} \right) - \mathbf{B}^T \left(\frac{\mathbf{u}_{k+1} - \mathbf{u}_{k-1}}{2h} \right) = \mathbf{0} \quad (6.11)$$

The difference in the generalized momentum between times $k+1/2$ and $k-1/2$ is given by:

$$\begin{aligned} & \left[\mathbf{M} \left(\frac{\mathbf{u}_{k+1} - \mathbf{u}_k}{h} \right) + \mathbf{B} \left(\frac{\mathbf{J}_{k+1} + \mathbf{J}_k}{2} \right) \right] - \left[\mathbf{M} \left(\frac{\mathbf{u}_k - \mathbf{u}_{k-1}}{h} \right) + \mathbf{B} \left(\frac{\mathbf{J}_k + \mathbf{J}_{k-1}}{2} \right) \right] \\ &= h \left[\mathbf{M} \left(\frac{\mathbf{u}_{k+1} - 2\mathbf{u}_k + \mathbf{u}_{k-1}}{h^2} \right) + \mathbf{B} \left(\frac{\mathbf{J}_{k+1} - \mathbf{J}_{k-1}}{2h} \right) \right] \\ &= \mathbf{0} \end{aligned} \quad (6.12)$$

from equation (6.10). Hence the generalized momentum is conserved. Consider now the difference in the energy between times $k+1/2$ and $k-1/2$:

$$\begin{aligned} & \left[\frac{1}{2} \left(\frac{\mathbf{u}_{k+1} - \mathbf{u}_k}{h} \right)^T \mathbf{M} \left(\frac{\mathbf{u}_{k+1} - \mathbf{u}_k}{h} \right) + \frac{1}{2} \left(\frac{\mathbf{J}_{k+1} - \mathbf{J}_k}{h} \right)^T \mathbf{A} \left(\frac{\mathbf{J}_{k+1} - \mathbf{J}_k}{h} \right) \right] \\ & - \left[\frac{1}{2} \left(\frac{\mathbf{u}_k - \mathbf{u}_{k-1}}{h} \right)^T \mathbf{M} \left(\frac{\mathbf{u}_k - \mathbf{u}_{k-1}}{h} \right) + \frac{1}{2} \left(\frac{\mathbf{J}_k - \mathbf{J}_{k-1}}{h} \right)^T \mathbf{A} \left(\frac{\mathbf{J}_k - \mathbf{J}_{k-1}}{h} \right) \right] \\ &= h \left[\left(\frac{\mathbf{u}_{k+1} - \mathbf{u}_{k-1}}{2h} \right)^T \mathbf{M} \left(\frac{\mathbf{u}_{k+1} - 2\mathbf{u}_k + \mathbf{u}_{k-1}}{h} \right) + \left(\frac{\mathbf{J}_{k+1} - \mathbf{J}_{k-1}}{2h} \right)^T \mathbf{A} \left(\frac{\mathbf{J}_{k+1} - 2\mathbf{J}_k + \mathbf{J}_{k-1}}{h} \right) \right] \\ &= h \left(\frac{\mathbf{u}_{k+1} - \mathbf{u}_{k-1}}{2h} \right)^T \left[\mathbf{M} \left(\frac{\mathbf{u}_{k+1} - 2\mathbf{u}_k + \mathbf{u}_{k-1}}{h} \right) + \mathbf{B} \left(\frac{\mathbf{J}_{k+1} - \mathbf{J}_{k-1}}{2h} \right) \right] \\ & + h \left(\frac{\mathbf{J}_{k+1} - \mathbf{J}_{k-1}}{2h} \right)^T \left[\mathbf{A} \left(\frac{\mathbf{J}_{k+1} - 2\mathbf{J}_k + \mathbf{J}_{k-1}}{h} \right) - \mathbf{B}^T \left(\frac{\mathbf{u}_{k+1} - \mathbf{u}_{k-1}}{2h} \right) \right] \\ &= \mathbf{0} \end{aligned} \quad (6.13)$$

from equations (6.10) and (6.11). Hence energy is conserved. Notice that the energy in equation (6.13) is $\frac{1}{2}\dot{\mathbf{u}}^T\mathbf{M}\dot{\mathbf{u}} + \frac{1}{2}\mathbf{J}^T\mathbf{A}\mathbf{J}$ because the strain energy function is assumed to be quadratic and so is equal to the complementary strain energy. Equations (6.12) and (6.13) are heuristic proofs of conservation. Kane, Marsden et al. (2000) present a discrete version of Noether's theorem (see for example, José and Saletan (1998)) by which it can be shown that any numerical integrator derived using the discrete calculus of variations approach inherits these conservation characteristics. Moreover, it is shown by Simo and Govindjee (1991) that the midpoint rule inherits the contractivity or B-stability of the dissipative system, i.e., systems with neighboring initial conditions converge in the energy norm.

6.3. Time-step Solution

The notation $n = k - 1/2$, $\mathbf{v}_n = \left(\frac{\mathbf{u}_{n+1/2} - \mathbf{u}_{n-1/2}}{h}\right)$ and $\mathbf{F}_n = \left(\frac{\mathbf{J}_{n+1/2} - \mathbf{J}_{n-1/2}}{h}\right)$ is introduced.

\mathbf{v}_n and \mathbf{F}_n are the Central Difference approximations of the velocity and the internal force respectively. Equation (6.9) then becomes:

$$\mathbf{M}\left(\frac{\mathbf{v}_{n+1} - \mathbf{v}_n}{h}\right) + \mathbf{C}\left(\frac{\mathbf{v}_{n+1} + \mathbf{v}_n}{2}\right) + \mathbf{B}\left(\frac{\mathbf{F}_{n+1} + \mathbf{F}_n}{2}\right) = \left(\frac{\mathbf{P}_{n+1} + \mathbf{P}_n}{2}\right) \quad (6.14)$$

$$\mathbf{A}\left(\frac{\mathbf{F}_{n+1} - \mathbf{F}_n}{h}\right) + \frac{1}{2}\left(\left.\frac{\partial\varphi}{\partial\mathbf{F}}\right|_{n+1} + \left.\frac{\partial\varphi}{\partial\mathbf{F}}\right|_n\right) - \mathbf{B}^T\left(\frac{\mathbf{v}_{n+1} + \mathbf{v}_n}{2}\right) = 0 \quad (6.15)$$

It is common in modeling frame structures for dynamic analyses to use a lumped mass matrix and to ignore rotational inertia. Hence the mass matrix could in general be singular. Similarly, the damping matrix could also be singular, for example when using

mass proportional damping. Thus, consistent with the convexity assumptions and without loss of generality, equation (6.14) can be rearranged and partitioned as follows:

$$\frac{2}{h} \begin{bmatrix} \mathbf{M} & \mathbf{0} & \mathbf{0} & \mathbf{0} \\ \mathbf{0} & \mathbf{0} & \mathbf{0} & \mathbf{0} \\ \mathbf{0} & \mathbf{0} & \mathbf{0} & \mathbf{0} \\ \mathbf{0} & \mathbf{0} & \mathbf{0} & \mathbf{0} \end{bmatrix} \begin{Bmatrix} \mathbf{v}^1 \\ \mathbf{v}^2 \\ \mathbf{v}^3 \\ \mathbf{v}^4 \end{Bmatrix} + \begin{bmatrix} \mathbf{C}_{11} & \mathbf{C}_{12} & \mathbf{0} & \mathbf{0} \\ \mathbf{C}_{12}^T & \mathbf{C}_{22} & \mathbf{0} & \mathbf{0} \\ \mathbf{0} & \mathbf{0} & \mathbf{0} & \mathbf{0} \\ \mathbf{0} & \mathbf{0} & \mathbf{0} & \mathbf{0} \end{bmatrix} \begin{Bmatrix} \mathbf{v}^1 \\ \mathbf{v}^2 \\ \mathbf{v}^3 \\ \mathbf{v}^4 \end{Bmatrix} + \begin{bmatrix} \mathbf{B}_1^T \\ \mathbf{B}_2^T \\ \mathbf{B}_3^T \\ \mathbf{B}_4^T \end{bmatrix}^T \mathbf{F} = \begin{Bmatrix} \mathbf{P}^1 \\ \mathbf{P}^2 \\ \mathbf{P}^3 \\ \mathbf{P}^4 \end{Bmatrix} + \frac{2}{h} \begin{Bmatrix} \mathbf{M}\mathbf{v}_n^1 \\ \mathbf{0} \\ \mathbf{0} \\ \mathbf{0} \end{Bmatrix} \quad (6.16)$$

where the partitions 1 through 4 represent respectively (i) degrees of freedom with mass, (ii) those with damping but no mass, (iii) those with prescribed forces and (iv) those with prescribed displacements (or velocities). The symbols \mathbf{F} , \mathbf{v}^i and \mathbf{P}^i denote respectively $\left(\frac{\mathbf{F}_{n+1} + \mathbf{F}_n}{2}\right)$, $\left(\frac{\mathbf{v}_{n+1}^i + \mathbf{v}_n^i}{2}\right)$ and $\left(\frac{\mathbf{P}_{n+1}^i + \mathbf{P}_n^i}{2}\right)$. The first two parts of equation (6.16) are:

$$\begin{aligned} \frac{2}{h} \mathbf{M}\mathbf{v}^1 + \mathbf{C}_{11}\mathbf{v}^1 + \mathbf{C}_{12}\mathbf{v}^2 + \mathbf{B}_1\mathbf{F} &= \mathbf{P}^1 + \frac{2}{h} \mathbf{M}\mathbf{v}_n^1 \\ \mathbf{C}_{12}^T\mathbf{v}^1 + \mathbf{C}_{22}\mathbf{v}^2 + \mathbf{B}_2\mathbf{F} &= \mathbf{P}^2 \end{aligned} \quad (6.17)$$

Eliminating \mathbf{v}^2 , we obtain:

$$\mathbf{v}^1 = -\frac{h}{2} \bar{\mathbf{M}}^{-1} \bar{\mathbf{B}}_1 \mathbf{F} + \frac{h}{2} \bar{\mathbf{M}}^{-1} \bar{\mathbf{P}}^1 + \bar{\mathbf{M}}^{-1} \mathbf{M}\mathbf{v}_n^1 \quad (6.18)$$

Then

$$\mathbf{v}^2 = \mathbf{C}_{22}^{-1} (\mathbf{P}^2 - \mathbf{B}_2\mathbf{F} - \mathbf{C}_{12}^T\mathbf{v}^1) \quad (6.19)$$

and

* The superscripts on \mathbf{v} and \mathbf{P} are to be interpreted as the index of the vector partition rather than as exponents. The other superscripts -1 and \mathbf{T} have their usual meanings of matrix inverse and transpose respectively.

$$\mathbf{B}_1^T \mathbf{v}^1 + \mathbf{B}_2^T \mathbf{v}^2 = \bar{\mathbf{B}}_1^T \mathbf{v}^1 - \mathbf{B}_2^T \mathbf{C}_{22}^{-1} \mathbf{B}_2 \mathbf{F} + \mathbf{B}_2^T \mathbf{C}_{22}^{-1} \mathbf{P}^2 \quad (6.20)$$

where $\bar{\mathbf{M}} = \mathbf{M} + \frac{h}{2} \bar{\mathbf{C}}_{11}$, $\bar{\mathbf{C}}_{11} = \mathbf{C}_{11} - \mathbf{C}_{12} \mathbf{C}_{22}^{-1} \mathbf{C}_{12}^T$, the Schur's complement of \mathbf{C}_{11} (Golub and Van Loan (1996)), $\bar{\mathbf{B}}_1 = \mathbf{B}_1 - \mathbf{C}_{12} \mathbf{C}_{22}^{-1} \mathbf{B}_2$ and $\bar{\mathbf{P}}^1 = \mathbf{P}^1 - \mathbf{C}_{12} \mathbf{C}_{22}^{-1} \mathbf{P}^2$. Equation (6.15) can similarly be partitioned as follows:

$$\mathbf{A} \left(\frac{\mathbf{F}_{n+1} - \mathbf{F}_n}{h} \right) + \frac{1}{2} \left(\left. \frac{\partial \varphi}{\partial \mathbf{F}} \right|_{n+1} + \left. \frac{\partial \varphi}{\partial \mathbf{F}} \right|_n \right) - \mathbf{B}_1^T \mathbf{v}^1 - \mathbf{B}_2^T \mathbf{v}^2 - \mathbf{B}_3^T \mathbf{v}^3 - \mathbf{B}_4^T \mathbf{v}^4 = 0 \quad (6.21)$$

Substituting equations (6.18) and (6.20) in equation (6.21) and rearranging terms, we obtain:

$$\bar{\mathbf{A}} \mathbf{F}_{n+1} + \frac{h}{2} \left(\left. \frac{\partial \varphi}{\partial \mathbf{F}} \right|_{n+1} \right) - \bar{\mathbf{b}} - h \mathbf{B}_3^T \mathbf{v}^3 = 0 \quad (6.22)$$

where

$$\bar{\mathbf{A}} = \mathbf{A} + \frac{h}{2} \mathbf{B}_2^T \mathbf{C}_{22}^{-1} \mathbf{B}_2 + \frac{h^2}{4} \bar{\mathbf{B}}_1^T \bar{\mathbf{M}}^{-1} \bar{\mathbf{B}}_1 \quad (6.23)$$

$$\bar{\mathbf{b}} = \left[\begin{array}{l} \left(\mathbf{A} - \frac{h}{2} \mathbf{B}_2^T \mathbf{C}_{22}^{-1} \mathbf{B}_2 - \frac{h^2}{4} \bar{\mathbf{B}}_1^T \bar{\mathbf{M}}^{-1} \bar{\mathbf{B}}_1 \right) \mathbf{F}_n \\ + \frac{h^2}{2} \bar{\mathbf{B}}_1^T \bar{\mathbf{M}}^{-1} \bar{\mathbf{P}}^1 + h \mathbf{B}_2^T \mathbf{C}_{22}^{-1} \mathbf{P}^2 + h \bar{\mathbf{B}}_1^T \bar{\mathbf{M}}^{-1} \mathbf{M} \mathbf{v}_n^1 + \frac{h}{2} \left. \frac{\partial \varphi}{\partial \mathbf{F}} \right|_n \end{array} \right] \quad (6.24)$$

Observe that the structure of $\bar{\mathbf{A}}$, the equivalent dynamic flexibility matrix, is *dual* to that of the equivalent dynamic stiffness matrix of Newmark's method with $\gamma = 1/2$. The roles of

the flexibility and mass matrices are interchanged. Pre-multiplying equation (6.22) by $\delta \mathbf{F}_{n+1}$ and integrating gives*:

$$\delta \left[\frac{1}{2} \mathbf{F}_{n+1}^T \bar{\mathbf{A}} \mathbf{F}_{n+1} - \mathbf{F}_{n+1}^T \bar{\mathbf{b}} + \frac{h}{2} \varphi(\mathbf{F}_{n+1}) \right] = 0 \quad (6.25)$$

In obtaining equation (6.25), it has been noted that $\mathbf{B}_3 \delta \mathbf{F}_{n+1} = \delta \mathbf{P}^3 = \mathbf{0}$, since \mathbf{P}^3 is prescribed. Since \mathbf{A} , \mathbf{C}_{22} and \mathbf{M} are positive definite, from equation (6.23) we have $\bar{\mathbf{A}}$ is positive definite. Hence the quantity in brackets in equation (6.25) is minimized. If dissipation is limited to plasticity, then the function φ is the regularized indicator function of the elastic domain. Hence, in the limit of rate-independent plasticity, the problem of obtaining \mathbf{F}_{n+1} at each step may be stated as follows:

$$\begin{aligned} \text{Minimize } \Pi(\mathbf{F}_{n+1}) &= \frac{1}{2} \mathbf{F}_{n+1}^T \bar{\mathbf{A}} \mathbf{F}_{n+1} - \mathbf{F}_{n+1}^T \bar{\mathbf{b}} \\ \text{Subject to (i) } \mathbf{B}_3 \mathbf{F}_{n+1} &= \mathbf{P}^3 \\ \text{and (ii) } \frac{h}{2} \phi_i(\mathbf{F}_{n+1}) &\leq 0 \quad i = 1, 2, \dots, N_y \end{aligned} \quad (6.26)$$

This then is the **Principle of Minimum Incremental Complementary Potential Energy** which can be stated as: *Of all the \mathbf{F}_{n+1} satisfying equilibrium with prescribed external forces at the un-damped quasi-static degrees of freedom and satisfying the yield conditions, the one that minimizes the incremental complementary potential energy Π is the one that satisfies equilibrium in the other degrees of freedom and compatibility.*

* Notice that δ here denotes spatial variation as opposed to temporal variation as in Section 5. In Appendix IV on continua, the same δ represents both spatial and temporal variations.

It is to be noted that due to the nature of the velocity-dependent Lagrangian and dissipation functions, it was possible to eliminate the velocities, leading to a minimum principle in forces only. In general, however, the incremental potential would be a function of \mathbf{F}_{n+1} and \mathbf{v}_{n+1} and would result in a saddle-point problem at each time step. Equation (6.26) is similar to the rate variational principles of plasticity in the references of Section 5.

6.3.1. Constrained Minimization by the Augmented Lagrangian Method

In this section, an Augmented Lagrangian algorithm for the solution of the minimization problem (6.26) and a dense matrix implementation of the algorithm are presented. For a detailed treatment of the Augmented Lagrangian formulation, the reader is referred to Bertsekas (1982), Glowinski and Le Tallec (1989) and Nocedal and Wright (1999). The problem (6.26) is reduced to a sequence of linearly constrained sub-problems using the Augmented Lagrangian regularization:

$$\Pi_{AL}(\mathbf{F}_{n+1}, \boldsymbol{\lambda}) = \frac{1}{2} \mathbf{F}_{n+1}^T \bar{\mathbf{A}} \mathbf{F}_{n+1} - \mathbf{F}_{n+1}^T \bar{\mathbf{b}} + \frac{h}{2} \sum_{i=1}^{N_p} \left[\lambda_i \phi_i(\mathbf{F}_{n+1}) + \frac{\nu}{2} \langle \phi_i(\mathbf{F}_{n+1}) \rangle^2 \right] \quad (6.27)$$

where $\boldsymbol{\lambda} = \{\lambda_1, \lambda_2, \dots, \lambda_{N_p}\}^T$ is the vector of plastic multipliers, ν is a penalty parameter and $\langle \cdot \rangle$ denotes the Mackaulay Brackets. The Augmented Lagrangian regularization is a combination of the usual Lagrangian term, $\lambda_i \phi_i(\mathbf{F}_{n+1})$ and the penalty function $\nu/2 \langle \phi_i(\mathbf{F}_{n+1}) \rangle^2$. The latter helps accelerate convergence while the former eliminates the need for the penalty parameter to be large, which leads to numerical ill-conditioning. Both terms vanish at a feasible point.

The solution is obtained in two nested stages. In the inner stage, the dual variables, i.e. the plastic multipliers λ are held fixed and the primal variables, i.e. the forces \mathbf{F}_{n+1} are obtained by solving the equality constrained sub-problem:

$$\begin{aligned} \text{Minimize}_{\mathbf{F}_{n+1}} \Pi_{AL}(\mathbf{F}_{n+1}, \lambda) &= \frac{1}{2} \mathbf{F}_{n+1}^T \bar{\mathbf{A}} \mathbf{F}_{n+1} - \mathbf{F}_{n+1}^T \bar{\mathbf{b}} + \frac{h}{2} \sum_{i=1}^{N_y} \left[\lambda_i \phi_i(\mathbf{F}_{n+1}) + \frac{\nu}{2} \langle \phi_i(\mathbf{F}_{n+1}) \rangle^2 \right] \\ \text{Subject to } \mathbf{B}_3 \mathbf{F}_{n+1} &= \mathbf{P}^3 \end{aligned} \quad (6.28)$$

This is called the inner or *primal stage*. In the outer or *dual stage*, the forces are held fixed and the plastic multipliers are updated using the formula:

$$\lambda_i^{new} = \langle \lambda_i^{new} + \nu \phi(\mathbf{F}_{n+1}) \rangle \quad (6.29)$$

The superscripts *new* and *old* have been used, rather than iteration indices, to denote values at the beginning and at the end of an iteration, to avoid the proliferation of subscripts and superscripts. Due to the Central Difference approximation, $\frac{h}{2} \lambda_i \frac{\partial \phi_i(\mathbf{F}_{n+1})}{\partial \mathbf{F}_{n+1}}$ is the plastic strain increment. In physically terms, therefore, the Augmented Lagrangian process is equivalent to relaxing the regularizing dashpot and allowing the frictional slider to incrementally develop plastic strain in each iteration.

A dense matrix algorithm for the solution of (6.28) is now presented. Consider the Lagrangian function:

$$L(\mathbf{F}_{n+1}, \boldsymbol{\mu}) = \frac{1}{2} \mathbf{F}_{n+1}^T \bar{\mathbf{A}} \mathbf{F}_{n+1} - \mathbf{F}_{n+1}^T \bar{\mathbf{b}} + \frac{h}{2} \sum_{i=1}^{N_y} \left[\lambda_i \phi_i(\mathbf{F}_{n+1}) + \frac{\nu}{2} \langle \phi_i(\mathbf{F}_{n+1}) \rangle^2 \right] - \boldsymbol{\mu}^T (\mathbf{B}_3 \mathbf{F}_{n+1} - \mathbf{P}^3) \quad (6.30)$$

where $\boldsymbol{\mu}$ is the vector of Lagrange multipliers corresponding to the equality constraints of equilibrium. The optimality conditions are:

$$\frac{\partial L}{\partial \mathbf{F}_{n+1}} = \mathbf{0} \Rightarrow \bar{\mathbf{A}}\mathbf{F}_{n+1} + \frac{h}{2} \sum_{i=1}^{N_y} \left[\lambda_i + \nu \langle \phi_i(\mathbf{F}_{n+1}) \rangle \right] \frac{\partial \phi_i}{\partial \mathbf{F}_{n+1}} - \mathbf{B}_3^T \boldsymbol{\mu} - \bar{\mathbf{b}} = \mathbf{0} \quad (6.31)$$

$$\frac{\partial L}{\partial \boldsymbol{\mu}} = \mathbf{0} \Rightarrow -\mathbf{B}_3 \mathbf{F}_{n+1} + \mathbf{P}^3 = \mathbf{0} \quad (6.32)$$

Equations (6.31) and (6.32) are solved using the Newton-Raphson method:

$$\begin{pmatrix} \mathbf{F}_{n+1} \\ \boldsymbol{\mu} \end{pmatrix}^{new} = \begin{pmatrix} \mathbf{F}_{n+1} \\ \boldsymbol{\mu} \end{pmatrix}^{old} - \mathbf{H}^{-1} \begin{pmatrix} \mathbf{p} \\ \mathbf{q} \end{pmatrix} \quad (6.33)$$

where \mathbf{H} , the Hessian of the Lagrangian L , is the iteration matrix.

$$\mathbf{H} = \begin{bmatrix} \bar{\mathbf{A}} & -\mathbf{B}^T \\ -\mathbf{B} & \mathbf{0} \end{bmatrix} \quad \mathbf{p} = \frac{\partial L}{\partial \mathbf{F}_{n+1}} \Big|_{(\mathbf{F}_{n+1}^{old}, \boldsymbol{\mu}^{old})} \quad \mathbf{q} = \frac{\partial L}{\partial \boldsymbol{\mu}} \Big|_{(\mathbf{F}_{n+1}^{old}, \boldsymbol{\mu}^{old})} \quad (6.34)$$

$$\bar{\bar{\mathbf{A}}} = \bar{\mathbf{A}} + \frac{h}{2} \sum_{i=1}^{N_y} \left\{ \left[\lambda_i + \nu \langle \phi_i(\mathbf{F}_{n+1}) \rangle \right] \frac{\partial^2 \phi_i}{\partial \mathbf{F}_{n+1}^2} + \nu H(\phi_i(\mathbf{F}_{n+1})) \left(\frac{\partial \phi_i}{\partial \mathbf{F}_{n+1}} \right) \left(\frac{\partial \phi_i}{\partial \mathbf{F}_{n+1}} \right)^T \right\} \quad (6.35)$$

The Newton-Raphson iteration, (6.33), involves solving the linear system:

$$\begin{bmatrix} \bar{\bar{\mathbf{A}}} & -\mathbf{B}^T \\ -\mathbf{B} & \mathbf{0} \end{bmatrix} \begin{pmatrix} \mathbf{x} \\ \mathbf{y} \end{pmatrix} = - \begin{pmatrix} \mathbf{p} \\ \mathbf{q} \end{pmatrix} \quad (6.36)$$

The *Range Space Method* of Fletcher (2000) is used for this purpose and is summarized below:

$\bar{\bar{\mathbf{A}}} = \mathbf{L}_{\bar{\mathbf{A}}} \mathbf{L}_{\bar{\mathbf{A}}}^T \rightarrow$ the Cholesky decomposition of $\bar{\bar{\mathbf{A}}}$

$\mathbf{L}_{\bar{\mathbf{A}}}^{-1} \mathbf{B}_3 = [\mathbf{Q}_1 \quad \mathbf{Q}_2] \begin{bmatrix} \mathbf{R} \\ \mathbf{0} \end{bmatrix} = \mathbf{Q}_1 \mathbf{R} \rightarrow$ QR decomposition

$\mathbf{S} = \mathbf{L}_{\bar{\mathbf{A}}}^{-T} (\mathbf{I} - \mathbf{Q}_1 \mathbf{Q}_1^T) \mathbf{L}_{\bar{\mathbf{A}}}^{-1}$

$\mathbf{T} = \mathbf{L}_{\bar{\mathbf{A}}}^{-T} \mathbf{Q}_1 \mathbf{R}^{-T} \tag{6.37}$

$\mathbf{U} = -\mathbf{R}^{-1} \mathbf{R}^{-T}$

$\mathbf{x} = -\mathbf{S} \mathbf{p} + \mathbf{T} \mathbf{q}$

$\mathbf{y} = \mathbf{T}^T \mathbf{p} - \mathbf{U} \mathbf{q}$

Steps are taken in the implementation to minimize computation and storage, for instance by using *rank k updates* to form $\bar{\bar{\mathbf{A}}}$, replacing \mathbf{B}_1 with $\mathbf{L}_{\bar{\mathbf{M}}}^{-1} \bar{\mathbf{B}}_1$, \mathbf{B}_2 with $\mathbf{L}_{\bar{\mathbf{C}}_{22}}^{-1} \bar{\mathbf{B}}_2$ etc. (where \mathbf{L}_X denotes the Cholesky factor of the matrix \mathbf{X}) and storing factored matrices wherever possible.

Having solved for \mathbf{F}_{n+1} , \mathbf{v}_{n+1}^1 and \mathbf{v}_{n+1}^2 are obtained using equations (6.18) and (6.19) respectively and \mathbf{u}_{n+1} by:

$$\mathbf{u}_{n+1}^1 = \mathbf{u}_n^1 + \left(\frac{\mathbf{v}_{n+1}^1 + \mathbf{v}_n^1}{2} \right) h \tag{6.38}$$

$$\mathbf{u}_{n+1}^2 = \mathbf{u}_n^2 + \left(\frac{\mathbf{v}_{n+1}^2 + \mathbf{v}_n^2}{2} \right) h \tag{6.39}$$

$$\mathbf{u}_{n+1}^3 = \mathbf{u}_n^3 + \boldsymbol{\mu} \tag{6.40}$$

Observe that the Lagrange multipliers corresponding to the equilibrium constraints are the displacement increments in those degrees of freedom. This can be seen from virtual work considerations. When performing a geometric nonlinear analysis the equilibrium matrix \mathbf{B} must be updated at every step. Strictly this requires an iterative procedure

because the matrix \mathbf{B} has to be evaluated at time $k+1/2$. But in order to save computational effort, this step is skipped and the equilibrium matrix at time k is used instead.

6.4. Numerical Example

The portal frame structure and the Northridge earthquake record of Section 3 (Fig 3.3) are used here as a numerical example. The dimensions and properties are as shown in Table 3.2, but it is assumed here, that there is no hardening in the stress-resultant strain behavior. In order to verify the results obtained the program DRAIN-2DX (Allahabadi and Powell (1988)) is used here. This choice is made here in contrast to the general purpose finite element programs used for verification in Sections 3 and 4 because the lumped plasticity and large-displacements-small deformations assumptions used by DRAIN-2DX are closer to the assumptions made in this section. For the sake of objectivity, it was also the intention not to use programs such as IDARC2D (Park, Reinhorn et al. (1987)), in the development of which the author has been involved. Two analyses, one with and one without $P\Delta$ effect, are performed and are discussed below.

6.4.1. Analysis without $P\Delta$ effect

First, a dynamic analysis is performed with no external axial load on the columns and hence no significant geometric nonlinearity and $P\Delta$ effects. Fig. 6.1 shows the horizontal displacement history of node 2 (Fig. 3.4). The permanent displacement resulting from plastic deformation can be observed as well as close agreement between the results from the Lagrangian Approach and from DRAIN-2DX. Fig. 6.2 shows that there is significant difference between the Lagrangian approach and DRAIN-2DX in

predicting the vertical displacements. This is because, while the plastic material model in DRAIN-2DX accounts for the reduction of bending moment capacity resulting from the axial force interaction, it does not consider the fact that centroidal axial plastic strain develops from plastification caused by bending because of the normality rule. It is important to consider this effect when relying on tension stiffening in beams for collapse prevention. Fig. 6.3 shows the time history of the rotation of node 2. The regions where the curve is flat correspond to the development of plastic rotations in the columns at constant joint rotation. The differences between results from the Lagrangian approach and from DRAIN-2DX stem from the fact that additional joint rotations are caused by differential settlements of the columns resulting from permanent axial deformation in the Lagrangian approach. Fig. 6.4 shows a plot of the horizontal reaction at node 1 versus the horizontal displacement at node 2, also showing good agreement between the two approaches.

6.4.2. Analysis with $P\Delta$ effect

Next, a dynamic analysis is performed with an axial force of 731.05 kN on each column, corresponding 50% of the yield force. In this case there is significant geometric nonlinearity. Fig. 6.5 and Fig. 6.6 show that the horizontal and vertical displacements continue to grow. The point marked “collapse” in Fig. 6.8 is the point beyond which an external horizontal force is required to pull the structure back to keep displacements from growing autonomously under the vertical loads acting on it. During a dynamic analysis, when this point is crossed, displacements continue to grow without reversal even when the input reverses; the analysis is terminated at this point. It is also noticed that under

load reversal, the yield force in the opposite direction is higher than the original yield force since the moments resulting from $P\Delta$ effects need to be overcome in addition.

6.5. Summary

A numerical method has been developed for the time integration of the governing equations (5.39) and (5.41) of the structure. Using discrete calculus of variations the action integral is discretized in time to obtain finite difference equations which are the discrete counterparts of the Euler-Lagrange equations. These equations have been shown to preserve the energy and momentum characteristics of the continuous time structure. It has been shown that at each time step the problem becomes one of constrained minimization in forces. This is the principle of minimum incremental complementary potential energy. An augmented Lagrangian method and a dense matrix solution algorithm have been developed for the solution of this minimization problem. Since the matrix $\bar{\mathbf{A}}$ of the minimization problem (6.26) is positive definite, the solution is globally convergent, allowing for larger time steps for computation. This is however not the case in the conventional incremental iterative approach where the tangent matrix may not be positive definite and the Newton iterations may not be globally convergent, limiting the time step. In the continuum case discussed in Section 1.10, the minimization problem (6.26) would be over the function space of stresses rather than over the vector space of internal forces as shown here. This minimization problem can then be discretized for example using a mixed finite element method (see for example, Pian and Sumihara (1984) and Cuomo and Contrafatto (2000)). A numerical example has been presented to demonstrate the feasibility of the method. The example has been chosen to be simple to enable comparing the results with other computational tools that have different modeling

assumptions. The formulation presented here can be used in three-dimensional problems with no changes.

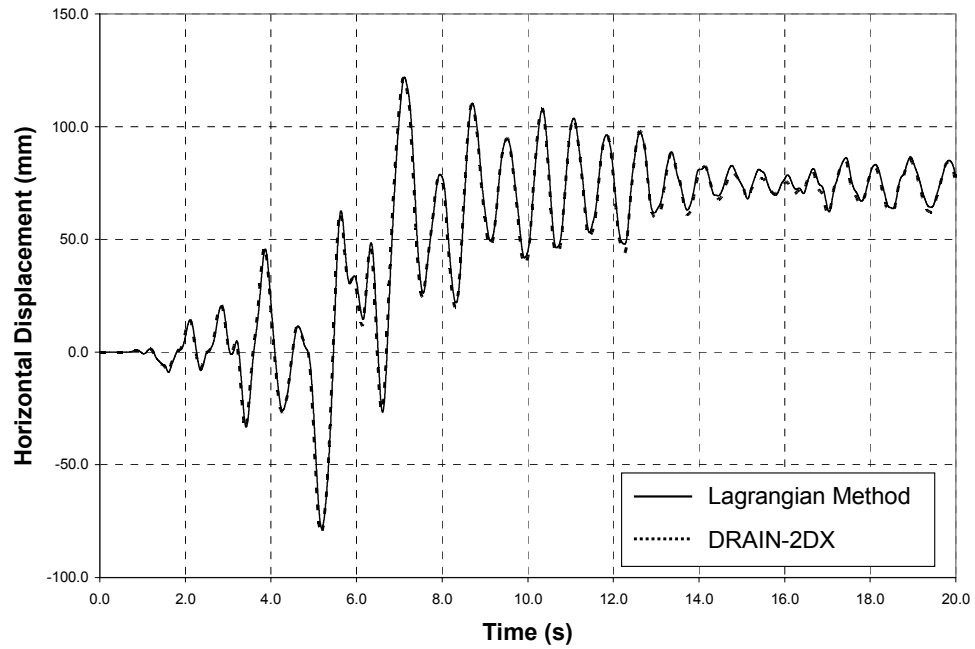


Fig. 6.1. No Axial Force: Horizontal Displacement Time History of Node 2

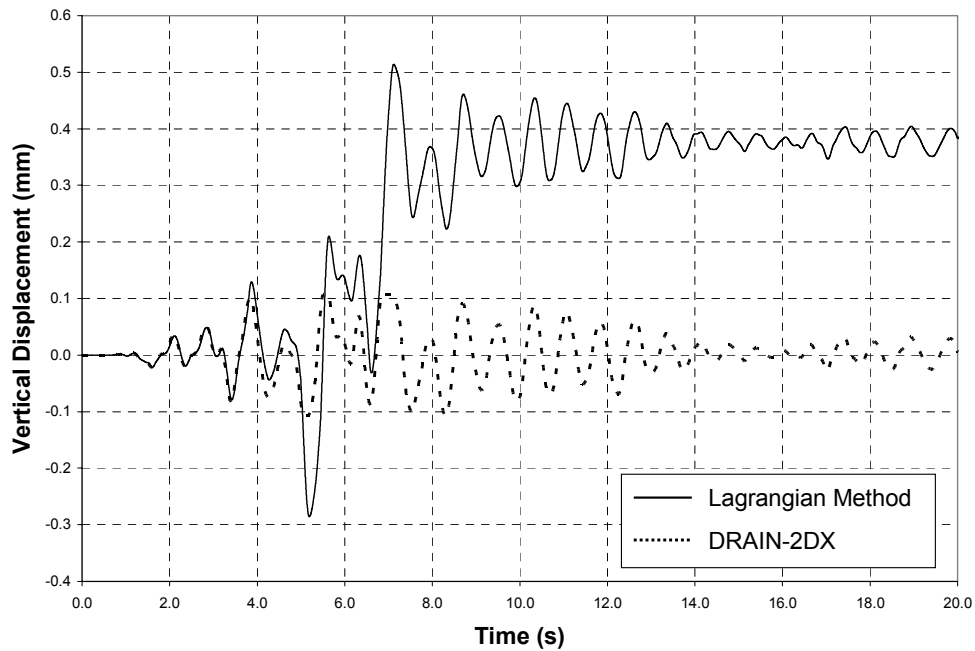


Fig. 6.2. No Axial Force: Horizontal Displacement Time History of Node 2

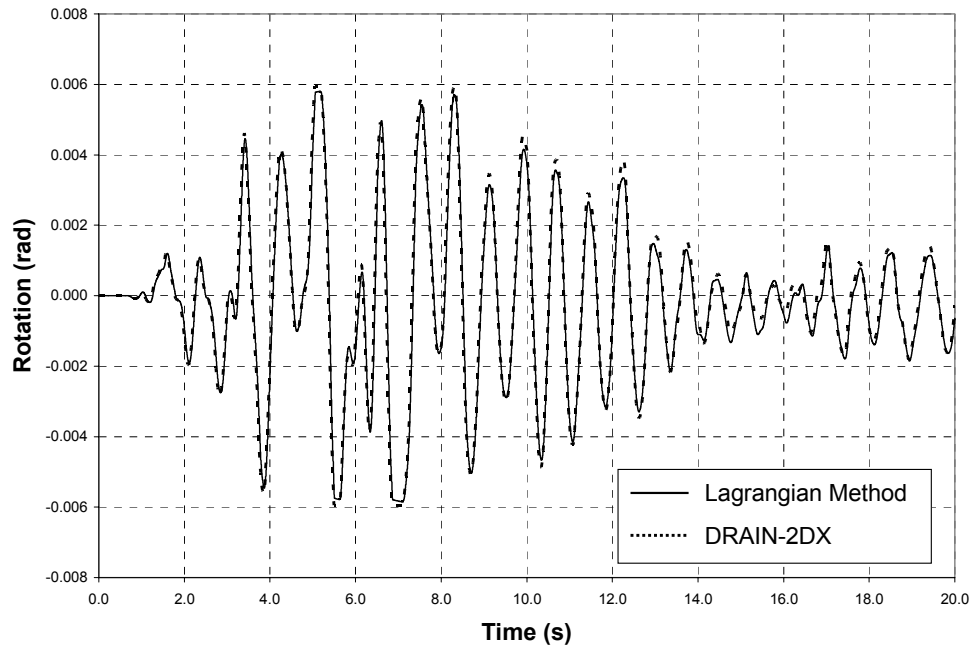


Fig. 6.3. No Axial Force: Rotation History of Node 2

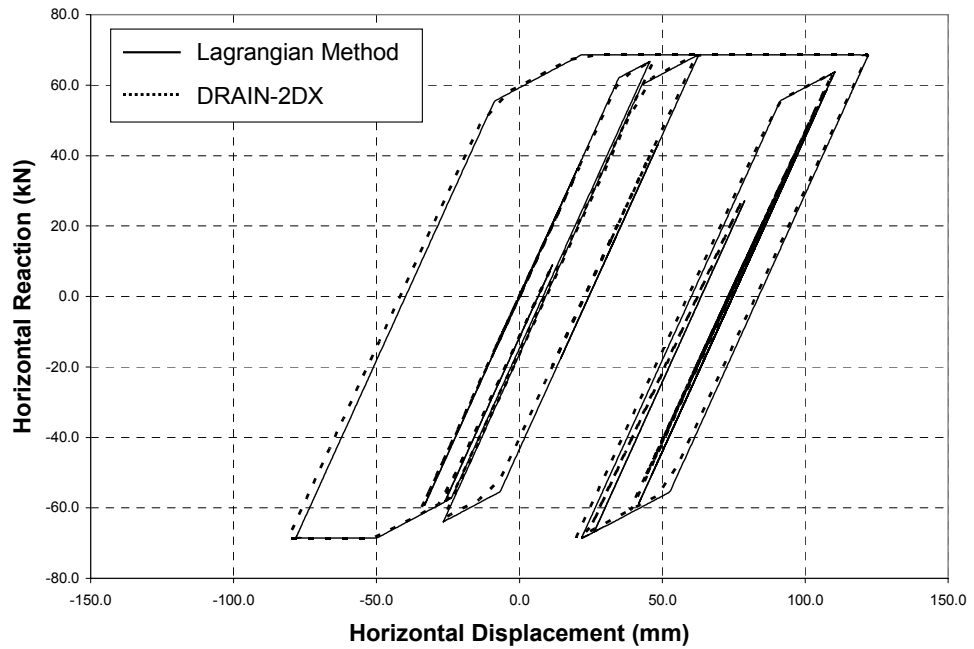


Fig. 6.4. No Axial Force: Relative Displacement vs. Horizontal Reaction Column 1

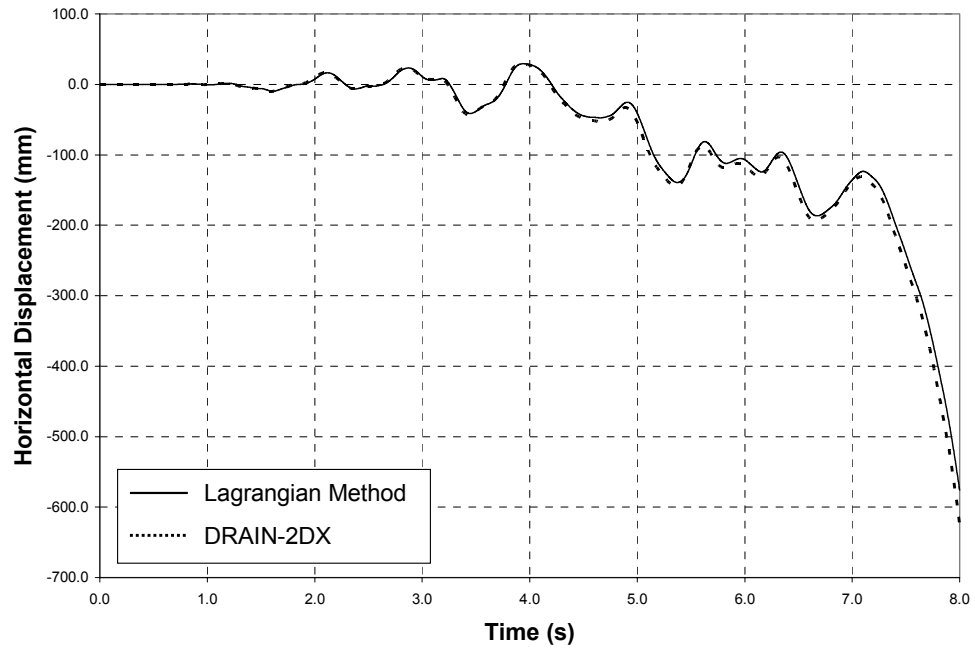


Fig. 6.5. Under Axial Force: Horizontal Displacement History of Node 2

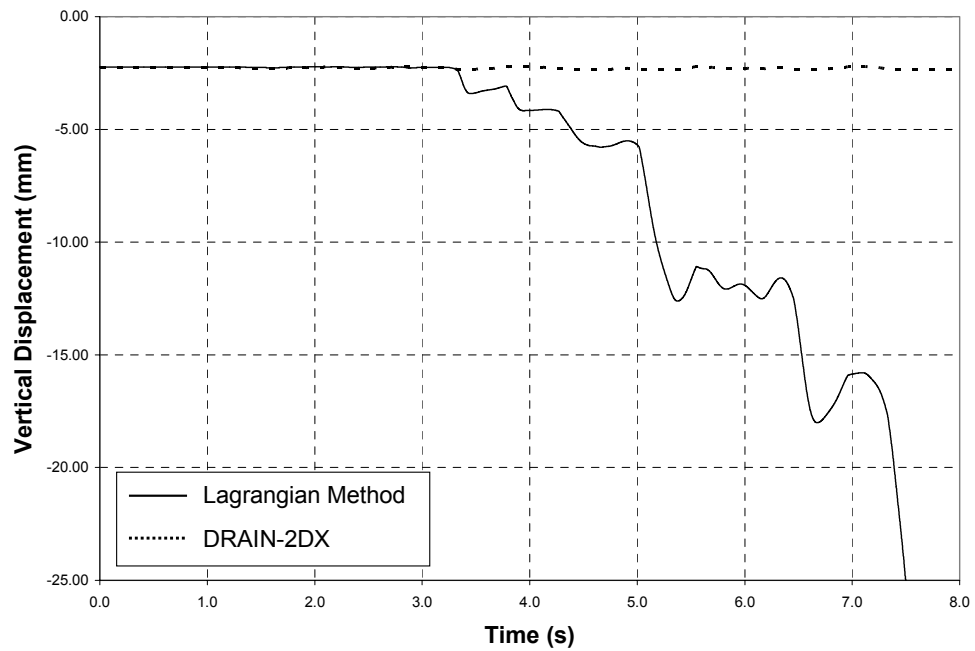


Fig. 6.6. Under Axial Force: Vertical Displacement History of Node 2

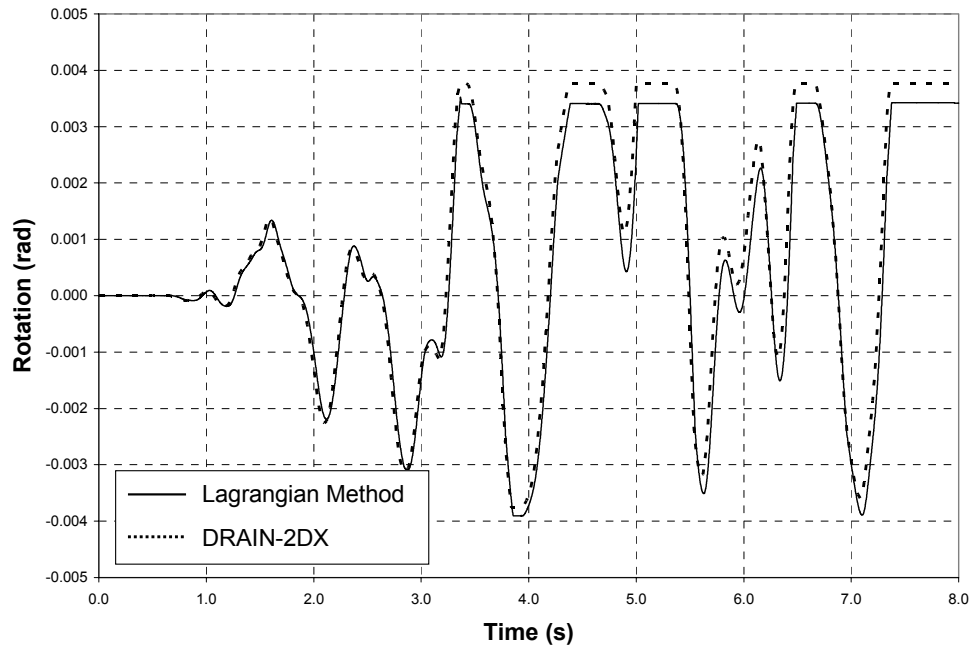


Fig. 6.7. Under Axial Force: Rotation History of Node 2

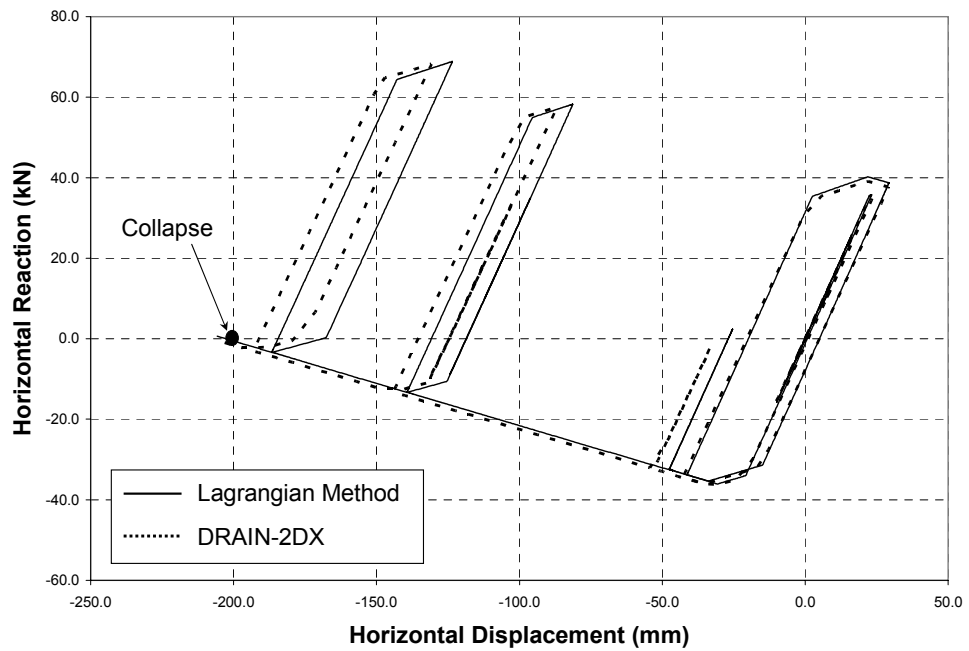


Fig. 6.8. No Axial Force: Relative Displacement vs. Horizontal Reaction Column 1

7. SUMMARY AND CONCLUSIONS

Motivated by the need of performance and fragility based seismic design methodologies for the analysis of structures near collapse with significant material and geometric nonlinearities, it was sought to develop structural models and numerical methods for such analyses.

Rather than extending the widely used displacement-based incremental iterative algorithms, it was desired to explore alternative methods that could offer potential benefits. In considering skeletal structures, the following facts were noted: (i) The advantage of the flexibility formulation for beam-column elements, resulting from force-interpolation functions being always exact even when the element is non-prismatic and undergoes inelastic behavior is well known. (ii) The yield-function in plasticity theory that defines the elastic domain and the damage domain in damage mechanics are most naturally expressed in terms of stresses and stress-like quantities (or stress-resultants). Thus stress-resultants play an important role in nonlinear analysis. Hence it was desired that internal forces are principal unknowns as well in the solution. Also, it has been shown in the literature that mixed methods alleviate locking in plasticity models. Moreover, various state variables besides forces and displacements play important roles in modern structural protective devices such as semi-active components.

The dynamical systems approach, wherein the structural model is perceived as a collection of states along with a means of specifying how these states evolve in time, provides a framework where displacements, internal forces and other state variables can be treated uniformly. The modeling of components is clearly separated from the numerical solution. Dynamical systems theory can be applied to the models and

numerical solutions to define broader notions of stability that are important in collapse analysis. A study with these factors in consideration showed potential and led to the following results:

7.1. Summary of Important Results

1. By considering the structure as a dynamical system, two new approaches – (i) the state space approach and (ii) the Lagrangian approach have been developed. These are mixed methods, where besides displacements, the stress-resultants and other variables of state are primary unknowns.
2. In Section 2, the constitutive relations of plasticity with hardening have been established in two equivalent forms – (i) the rate form and (ii) the dissipation form. The former is used as a nonholonomic constraint in the state space approach, while the latter is used in the Lagrangian approach.
3. In the state space approach, the subject of Section 3, the governing equations of motion and constitutive behavior of a structure are considered as constituting a constrained dynamical system which is represented as a system of differential algebraic equations (DAE) and solved using appropriate numerical methods. In this work, the DASSL solver which uses backward difference formulas to approximate the DAE is used.
4. Even very advanced displacement-based finite element packages do not have robust time-stepping algorithms. For instance, the elastic-plastic dynamic analysis of a simple three dimensional portal frame Simeonov (1999) was impossible to perform using ABAQUS ABAQUS (2000). However, the same problem formulated and solved using the proposed state-space approach. The only way of verifying the result

obtained from such new analysis was the agreement with the response envelopes obtained using static analyses.

5. A flexibility-based inelastic large deformation planar beam-column element has been formulated in Section 4 for use with the state space approach, starting from the finite deformation compatibility equations and applying the principle of virtual forces in rate form. The element uses stress-resultant-strain constitutive equations and includes the effect of axial force-bending moment interaction. The element is utilized for structural analysis to collapse as shown in a numerical example.
6. In Section 5, the evolution of the elastic-plastic structural state in time is provided a weak formulation using Hamilton's principle. It is shown that a certain class of structures called reciprocal structures has a mixed weak formulation in time involving Lagrangian and dissipation functions. The new form of the Lagrangian developed in this work involves not only displacements and velocities but also internal forces and their impulses leading to the concept of the generalized momentum for framed structures. This Lagrangian has been shown to extend to continua. The derivative of the compatibility operator with respect to displacements possesses a symmetry that renders the Lagrangian invariant under finite displacements. The formulation can therefore be used in geometric nonlinear analysis.
7. In Section 6, a discrete variational integrator has been derived starting from the weak formulation of Section 5. This integrator inherits the energy and momentum conservation characteristics for Lagrangian systems and the contractivity in the energy norm of dissipative systems. The integration of each step has been shown to

be a constrained minimization problem – the principle of incremental minimum complementary potential energy. An Augmented Lagrangian algorithm and a dense matrix implementation have been derived for the solution of this problem.

The two methods proposed in this work can potentially be used as alternatives to the conventional displacement-based incremental iterative method for the analysis of structures to collapse as has been demonstrated by numerical examples. In contrast to the displacement method, however, both proposed methods clearly distinguish the modeling of components from the numerical solution. The state space approach requires just the specification of the state equations in the form of DAE, while the Lagrangian approach requires the specification of the Lagrangian and dissipation functions. Thus phenomenological models of components such as structural steel connections, reinforced concrete elements, semi-active devices etc. can be incorporated in the analysis without having to implement element-specific incremental state determination algorithms. The state determination is performed at the global level by the DAE solver and by the optimization solver in the respective methods.

The proposed methods follow a generalized approach which addresses modeling and solution through rigorous formulations which make very few assumptions to obtain the solution of complex non-linear problems. While traditional displacement methods address implicitly the model and the solution, the proposed methods distinguish the modeling of components from the numerical solution. The advantage of such formulations is indicated in this report.

The second formulation, the Lagrangian approach, implicitly addresses the equilibrium and the conservation of impulse, within a variational formulation. This

approach allows addressing problems involving sudden collapse, or sudden degradation before collapse, which involves instantaneous lack of equilibrium and impulses. Moreover, the suggested formulation opens the way to addressing impulse driven processes such as blasts and impacts in complex structures without or with modern protective systems. As such this method pioneers a generalized approach to solving complex nonlinear dynamics problems.

7.2. Extensions and Implementations

Parts of the work reported here have been extended and implemented in computational platforms and have been published in peer-reviewed journals.

1. The rate form of the one-dimensional plasticity model of Section 2 has been extended by the author to include the effects of hysteretic degradation effects (Sivaselvan and Reinhorn (2000)).
2. The above hysteretic degrading model has been implemented in the nonlinear analysis computer programs (i) IDARC2D at the University at Buffalo (Park, Reinhorn et al. (1987)), (ii) NONLIN available from the Federal Emergency Management Agency (<http://training.fema.gov/EMIWeb/nonlin.htm>) and (iii) LARSA (LARSA (2002)), a commercial software.
3. The large deformation beam column element of Section 3, suitably modified to work in a displacement-based framework, has also been implemented in the programs IDARC3D and LARSA.
4. An elaborate discussion of the State Space Approach of Section 3 was published by the author and others (Simeonov, Sivaselvan and Reinhorn (2002)).

5. An abridged discussion of the large deformation beam-column formulation in Sections 4 has also been published by the author (Sivaselvan and Reinhorn (2002)).

7.3. Recommendations for Further Work

1. The DAE solution of Section 3 uses general purpose dense matrix algorithms. Incorporation of efficient numerical methods that utilize the particular form of the structural analysis problem could result in significant performance improvement. For example, Hall, Rheinboldt et al. (1991) have shown in finite strain plasticity problems in metal forming that the DAE solution can be up to 26 times faster than the conventional displacement-based approach.
2. The development of Section 3 can be extended to three dimensions. Such a formulation has recently been proposed by de Souza (2000). It will be fruitful to study its implementation.
3. The continuum extensions of Section 5 need to be discretized using for example the finite element method and to be implemented. The characteristics of the resulting methods need to be investigated relative to displacement-based methods.
4. Recently, libraries have become available to develop and implement algorithms for large scale optimization exploiting problem structure (see for example, Gertz and Wright (2001)). Exploration of such algorithms for the solution of the incremental constrained optimization problem of Section 6 would help evolve the method for general purpose.
5. When using the variable step variable order backward difference formula algorithm of DASSL in the state space approach, it was observed that the method has to restart often with a one step first order method due to plastic yielding and unloading. Thus it

may be advantageous to use higher order one-step methods. The discrete calculus of variations approach can be used to systematically construct such methods. Even very advanced displacement-based finite element packages do not have robust time-stepping algorithms. For instance, the elastic-plastic dynamic analysis of a simple three dimensional portal frame Simeonov (1999) was impossible to perform using ABAQUS ABAQUS (2000). However, the same problem formulated and solved using the proposed state-space approach. The only way of verifying the result obtained from such new analysis was the agreement with the response envelopes obtained using static analyses.

6. Damage Mechanics: De Sciarra (1997), for example, has shown that the constitutive equations of damage mechanics, in a manner analogous to plasticity, can be characterized by a dissipation function involving a stress-like quantity that is conjugate to the damage variable. The weak formulation developed in this work can therefore be extended to damage mechanics, thus permitting the modeling of material degradation in collapse simulation.

7.4. Recommendations for New Directions

1. The formulations of this work could be used to develop a qualitative theory for structures which can be used to bound structural response. Such a bounding method could be used as an alternative to the “pushover analysis” currently used in seismic design.
2. The stability theory of dynamic systems can be used to *define* collapse at the scale of the whole structure and study dynamic shakedown.

3. As mentioned above, the methods presented in this work allow a separation of modeling and numerical solution, especially time discretization. This may help at least a partial automation of the development of numerical code from an abstract model definition.

8. REFERENCES

- ABAQUS (2000). ABAQUS. Houston, Hibbitt, Karlsson & Sorensen, Inc.
- Allahabadi, R. and G. H. Powell (1988). Drain-2DX user guide. Report / Earthquake Engineering Research Center ;; no. UCB/EERC-88/06; Variation: Report (University of California, Berkeley. Earthquake Engineering Research Center) ;; no. . Berkeley, Calif., University of California at Berkeley.
- ANSYS (1992). ANSYS. Houston, Swanson Analysis Systems.
- Armero, F. and A. Perez-Foguet (2002). "On the formulation of closest-point projection algorithms in elastoplasticity - Part I: The variational structure." *International Journal for Numerical Methods in Engineering* **53**(2): 297-329.
- Backlund, J. (1976). "Large Deflection Analysis of Eleasto-plastic Beams and Frames." *International Journal of Mechanical Sciences* **18**(1): 269-277.
- Barroso, L. R., S. E. Breneman and H. A. Smith (1998). Evaluating the effectiveness of structural control within the context of performance-based engineering. Proceedings of the Sixth US National Conference on Earthquake Engineering, Seattle, Washington, Earthquake Engineering Research Institute.
- Barsan, G. M. and C. G. Chiorean (1999). "Computer program for large deflection elastoplastic analysis of semi-rigid steel frameworks." *Computers & Structures* **72**(6): 699-711.
- Bauchau, O. A., G. Damilano and N. J. Theron (1995). "Numerical Integration of Non-Linear Elastic Multi-Body Systems." *International Journal for Numerical Methods in Engineering* **38**(16): 2727-2751.

- Belytschko, T. and B. J. Hsieh (1973). "Nonlinear transient finite element analysis with convected coordinates." *International Journal for Numerical Methods in Engineering* **119**: 1-15.
- Belytschko, T., W. K. Liu and B. Moran (2000). *Nonlinear finite elements for continua and structures*. New York, Chichester.
- Bertsekas, D. P. (1982). *Constrained optimization and Lagrange multiplier methods*. Academic Press, New York.
- Brenan, K. E., S. L. Campbell and L. R. Petzold (1996). *Numerical solution of initial-value problems in differential-algebraic equations*. Society for Industrial and Applied Mathematics, Philadelphia.
- Bryant, P. R. (1959). "The order of complexity of electrical networks." *The Institution of Electrical Engineers*(Monograph No. 335E): 174-188.
- Cadzow, J. A. (1970). "Discrete Calculus of Variations." *International Journal of Control* **11**(3): 393-407.
- Capurso, M. and G. Maier (1970). "Incremental Elastoplastic Analysis and Quadratic Optimization." *Meccanica* **5**(2): 107-116.
- Carol, I. and J. Murcia (1989). "Nonlinear Time-Dependent Analysis of Planar Frames using an 'Exact' Formulation - I. Theory and II. Computer Implementation for R.C. Structures and Examples." *Computers and Structures* **33**(1): 79-102.
- Casciati, F. and L. Faravelli (1988). "Stochastic Equivalent Linearization for 3-D Frames." *Journal of Engineering Mechanics-ASCE* **114**(10): 1760-1771.

- Cohn, M. Z., G. Maier and D. E. Grierson (1979). *Engineering plasticity by mathematical programming : proceedings of the NATO Advanced Study Institute, University of Waterloo, Waterloo, Canada, August 2-12, 1977*. Pergamon Press, New York.
- Comi, C. and U. Perego (1995). "A Unified Approach for Variationally Consistent Finite-Elements in Elastoplasticity." *Computer Methods in Applied Mechanics and Engineering* **121**(1-4): 323-344.
- Constantinou, M. C. and M. A. Adane (1987). Dynamics of Soil-base-isolated-structure systems, NSF.
- Crisfield, M. A. (1991). *Non-linear finite element analysis of solids and structures*. Wiley, Chichester ; New York.
- Cuomo, M. and L. Contrafatto (2000). "Stress rate formulation for elastoplastic models with internal variables based on augmented Lagrangian regularization." *International Journal of Solids & Structures* **37**(29): 3935-3964.
- Cybenko, G. (1997). "Dynamic programming: A discrete calculus of variations." *Ieee Computational Science & Engineering* **4**(1): 92-97.
- De Sciarra, F. M. (1996). "A consistent approach to continuum and discrete rate elastoplastic structural problems." *Computer Methods in Applied Mechanics and Engineering* **137**(3-4): 207-238.
- De Sciarra, F. M. (1997). "General Theory of Damage Elastoplastic Models." *Journal of Engineering Mechanics* **123**(10): 1003-1011.
- de Souza, R. M. (2000). Force-based Finite Element for Large Displacement Inelastic Analysis of Frames, PhD, University of California, Berkeley.

- Duvaut, G. and J. L. Lions (1976). *Inequalities in mechanics and physics*. Springer-Verlag, New York.
- Ekeland, I., R. Temam and a. joint (1976). *Convex analysis and variational problems*. Amsterdam North-Holland Pub. Co., New York.
- El-Sayed, M. E. M., D. Marjadi and E. Sandgren (1991). "Force Method Formulations Based on Hamilton Principle." *Computers & Structures* **38**(3): 301-316.
- Fenves, G. L., W. H. Huang, A. S. Whittaker, P. W. Clark and S. A. Mahin (1998). Modeling and Characterization of Seismic Isolation Bearings. Buffalo, Multidisciplinary Center for Earthquake Engineering Research.
- Fletcher, R. (2000). *Practical methods of optimization*. Wiley, Chichester.
- Fritzen, P. and J. Wittekindt (1997). "Numerical Solution of Viscoplastic Constitutive Equations with Internal State Variables .1. Algorithms and Implementation." *Mathematical Methods in the Applied Sciences* **20**(16): 1411-1425.
- Gertz, M. E. and S. J. Wright (2001). Object-Oriented Software for Quadratic Programming, Mathematics and Computer Science Division, Argonne National Laboratory.
- Glowinski, R. and P. Le Tallec (1989). *Augmented Lagrangian and operator-splitting methods in nonlinear mechanics*. Society for Industrial and Applied Mathematics, Philadelphia.
- Golub, G. H. and C. F. Van Loan (1996). *Matrix computations*. Johns Hopkins University Press, Baltimore.
- Hall, C. A., W. C. Rheinboldt and M. L. Wenner (1991). "DEM displacement-plastic strain formulation of punch stretching." *Computers & Structures* **40**(4): 877-883.

- Han, W. and B. D. Reddy (1999). *Plasticity : mathematical theory and numerical analysis*. Springer, New York.
- Haug, E. J., D. Negrut and M. Iancu (1997). "A State-Space-Based Implicit Integration Algorithm for Differential-Algebraic Equations of Multibody Dynamics." *Mechanics of Structures & Machines* **25**(3): 311-334.
- Hiriart-Urruty, J.-B. and C. Lemaréchal (1993). *Convex analysis and minimization algorithms. I, Fundamentals*. Springer-Verlag, New York.
- Hsu, T. T. C. (1993). *Unified theory of reinforced concrete*. CRC Press, Boca Raton.
- <http://training.fema.gov/EMIWeb/nonlin.htm> NONLIN,
<http://training.fema.gov/EMIWeb/nonlin.htm>, Accessed October 19, 2002.
- Huddleston, J. V. (1979). "Nonlinear Analysis of Elastically Constrained Tie-Rods under Transverse Loads." *International Journal of Mechanical Sciences* **21**(10): 623-630.
- Hughes, T. J. R. (1987). *The finite element method : linear static and dynamic finite element analysis*. Prentice-Hall, Englewood Cliffs, N.J.
- Inaudi, J. A. and J. C. de la Llera (1993). *Dynamic analysis of nonlinear structures using state-space formulation and partitioned integration schemes*. Earthquake Engineering Research Center University of California, Berkeley.
- Isac, G. (1992). *Complementarity problems: Lecture notes in mathematics 1528*. Springer-Verlag, Berlin.
- Iura, M. and S. N. Atluri (1995). "Dynamic Analysis of Planar Flexible Beams with Finite Rotations by Using Inertial and Rotating Frames." *Computers and Structures* **55**(3): 453-462.

- Iwan, W. D. (1966). "A distributed-element model for hysteresis and its steady-state dynamic response." *Journal of Applied Mechanics* **33**(42): 893-900.
- Johnson, C. (1977). "Mixed Finite-Element Method for Plasticity Problems with Hardening." *Siam Journal on Numerical Analysis* **14**(4): 575-583.
- José, J. V. and E. J. Saletan (1998). *Classical dynamics : a contemporary approach*. New York, Cambridge England.
- Kane, C., J. E. Marsden, M. Ortiz and M. West (2000). "Variational integrators and the Newmark algorithm for conservative and dissipative mechanical systems." *International Journal for Numerical Methods in Engineering* **49**(10 Dec): 1295-1325.
- Kinderlehrer, D. and G. Stampacchia (1980). *An introduction to variational inequalities and their applications*. Academic Press, New York.
- Kunnath, S. K. and A. M. Reinhorn (1990). "Model for inelastic biaxial bending interaction of reinforced concrete beam-columns." *ACI Structural Journal* **87**(3): 284-291.
- LARSA (2002). LARSA. Long Island, New York, LARSA, Inc.
- Lo, S. H. (1992). "Geometrically nonlinear formulation of 3D finite strain beam element with large rotations." *Computers and Structures* **44**(1-2): 147-157.
- Lowes, L. and A. Altoontash (2002). Modeling the Behavior of Reinforced Concrete Beam-Column Building Joints Subjected to Earthquake Loading. Seventh U.S. National Conference on Earthquake Engineering 7NCEE, Boston.
- Lubliner, J. (1990). *Plasticity theory*. London, New York Macmillan.
- Maier, G. (1970). "A Matrix Structural Theory of Piecewise Linear Elastoplasticity with Interacting Yield Planes." *Meccanica* **5**(1): 54.

- Marsden, J. E. and M. West (2001). "Discrete mechanics and variational integrators."
Acta Numerica **10**: 357-514.
- Mazzolani, F. M. and V. Piluso (1996). *Theory and design of seismic resistant steel frames*. New York, London.
- McGuire, W., R. H. Gallagher and R. D. Ziemian (2000). *Matrix structural analysis*.
John Wiley, New York.
- Nagarajaiah, S., M. C. Constantinou and A. M. Reinhorn (1989). *Nonlinear dynamic analysis of three-dimensional base isolated structures (3D-BASIS)*. National Center for Earthquake Engineering Research, Buffalo, NY.
- Nelson, R. B. and A. Dorfmann (1995). "Parallel elastoplastic models of inelastic material behavior." *Journal of Engineering Mechanics-ASCE* **121**(10 Oct): 1089-1097.
- Neuenhofer, A. and F. C. Filippou (1997). "Evaluation of Nonlinear Frame Finite-Element Models." *Journal of Structural Engineering-ASCE* **123**(7): 958-966.
- Neuenhofer, A. and F. C. Filippou (1998). "Geometrically Nonlinear Flexibility-Based Frame Finite Element." *Journal of Structural Engineering-ASCE* **124**(6): 704-711.
- Nguyen, Q. S. (2000). *Stability and nonlinear solid mechanics*. New York, Chichester.
- Nocedal, J. and S. J. Wright (1999). *Numerical optimization*. Springer, New York.
- Panagiotopoulos, P. D. (1985). *Inequality problems in mechanics and applications : convex and nonconvex energy functions*. Birkhäuser, Boston.
- Papadopoulos, P. and J. Lu (1998). "A General Framework for the Numerical Solution of Problems in Finite Elasto-Plasticity." *Computer Methods in Applied Mechanics and Engineering* **159**(1-2): 1-18.

- Papadopoulos, P. and R. L. Taylor (1994). "On the Application of Multi-Step Integration Methods to Infinitesimal Elastoplasticity." *International Journal for Numerical Methods in Engineering* **37**(18): 3169-3184.
- Park, Y. J., A. M. Reinhorn and S. K. Kunnath (1987). IDARC: Inelastic Damage Analysis of Reinforced Concrete Frame - Shear wall Structures, State University of New York at Buffalo.
- Park, Y. J., Y. K. Wen and A. H. S. Ang (1986). "Random Vibration of Hysteretic Systems under Bi-Directional Ground Motions." *Earthquake Engineering & Structural Dynamics* **14**(4): 543-557.
- Pian, T. H. H. and K. Sumihara (1984). "Rational Approach for Assumed Stress Finite-Elements." *International Journal for Numerical Methods in Engineering* **20**(9): 1685-1695.
- Reissner, E. (1972). "On one-dimensional finite-strain beam theory: the plane problem." *Journal of Applied Mathematics and Physics (ZAMP)* **23**(5): 795-804.
- Reissner, E. (1973). "On one-dimensional large-displacement finite-strain beam theory." *Studies in Applied Mathematics* **11**(2): 87-95.
- Richard, R. M. and J. R. Blalock (1969). "Finite element analysis of inelastic structures." *AIAA Journal* **7**: 432-438.
- Romano, G. and G. Alfano (1995). Variational principles, approximations and discrete formulations in plasticity. Fourth International Conference on Computational Plasticity (COMPLAS IV), Barcelona.

- Romano, G., L. Rosati and F. M. de Sciarra (1993). "Variational theory for finite-step elasto-plastic problems." *International Journal of Solids & Structures* **30**(17): 2317-2334.
- Scheck, F. (1994). *Mechanics : from Newton's laws to deterministic chaos*. New York, Berlin.
- Schulz, M. and F. C. Filippou (2001). "Non-linear spatial Timoshenko beam element with curvature interpolation." *International Journal for Numerical Methods in Engineering* **50**(4): 761-785.
- Shaflucas, C. W. (1969). Applications of discrete calculus of variations, Masters, State University of New York at Buffalo, Buffalo.
- Shi, P. and I. Babuska (1997). "Analysis and Computation of a Cyclic Plasticity Model by Aid of Ddassl." *Computational Mechanics* **19**(5): 380-385.
- Simeonov, V. K. (1999). Three-dimensional inelastic dynamic structural analysis of frame systems, PhD Dissertation, University at Buffalo, Buffalo.
- Simeonov, V. K., M. V. Sivaselvan and A. M. Reinhorn (2000). "Nonlinear analysis of structural frame systems by the state-space approach." *Computer-Aided Civil and Infrastructure Engineering* **15**(2): 76-89.
- Simo, J. C. and S. Govindjee (1991). "Non-linear B-stability and symmetry preserving return mapping algorithms for plasticity and viscoplasticity." *International Journal for Numerical Methods in Engineering* **31**(1): 151-176.
- Simo, J. C. and T. J. R. Hughes (1998). *Computational inelasticity*. Springer, New York.

- Simo, J. C., J. G. Kennedy and R. L. Taylor (1989). "Complementary mixed finite element formulations for elastoplasticity." *Computer Methods in Applied Mechanics & Engineering* **74**(2): 177-206.
- Simo, J. C. and M. Ortiz (1985). "A Unified Approach to Finite Deformation Elastoplastic Analysis Based on the use of Hyperelastic Constitutive Equations." *Computer Methods in Applied Mechanics & Engineering* **49**(2): 221-245.
- Simo, J. C. and L. Vu-quoc (1986). "A three-dimensional finite-strain rod model. Part II: Computational aspects." *Computer Methods in Applied Mechanics and Engineering* **58**(1): 79-116.
- Sivaselvan, M. V. and A. M. Reinhorn (2000). "Hysteretic models for deteriorating inelastic structures." *Journal of Engineering Mechanics-ASCE* **126**(6): 633-640.
- Sivaselvan, M. V. and A. M. Reinhorn (2002). "Collapse Analysis: Large Inelastic Deformations Analysis of Planar Frames." *Journal of Structural Engineering-ASCE* **128**(12): (To Appear).
- Stavroulakis, G. E. (2001). "Computational nonsmooth mechanics: Variational and hemivariational inequalities." *Nonlinear Analysis-Theory Methods & Applications* **47**(8): 5113-5124.
- Stern, T. E. (1965). *Theory of nonlinear networks and systems; an introduction*. Mass. Addison-Wesley, Reading.
- Stroud, A. H. and D. Secrest (1966). *Gauss Quadrature Formulas*. Prentice-Hall, Englewood Cliffs, NJ.
- Thyagarajan, R. S. (1989). *Modeling and Analysis of Hysteretic Structural Behavior*. Pasadena, California Institute of Technology.

- Tin-Loi, F. (1997). "Complementarity and nonlinear structural analysis of skeletal structures." *Structural Engineering & Mechanics* **5**(5): 491-505.
- Trefethen, L. N. and D. Bau (1997). *Numerical linear algebra*. Society for Industrial and Applied Mathematics, Philadelphia.
- Vian, D., M. Sivaselvan, M. Bruneau and A. Reinhorn (2001). Analysis, Testing and Initial Recommendations on Collapse Limit States of Frames. Research Progress and Accomplishments (2000-2001) MCEER-01-SP01, Multidisciplinary Center for Earthquake Engineering Research, University at Buffalo.
- Washizu, K. (1982). *Variational methods in elasticity and plasticity*. New York, Oxford.
- Weaver, W. and J. M. Gere (1990). *Matrix analysis of framed structures*. Chapman & Hall, New York.
- Wen, Y. K. (1976). "Method for random vibrations of hysteretic systems." *Journal of Engineering Mechanics-ASCE* **102**(EM2): 249-263.
- Yang, Y.-B. and S.-R. Kuo (1994). *Theory and analysis of nonlinear framed structures*. Prentice Hall, New York.

APPENDIX I. REVIEW OF MATRIX STRUCTURAL ANALYSIS

This appendix establishes the notation of matrix structural analysis that is used in the other sections. Fig. AI.1 shows a frame structure subject to external *nodal loads* along with the global coordinate system and a typical element isolated. The forces at the ends of the member are given by the vector $\mathbf{P}^{e,i}$ in the global coordinates and by the vector $\bar{\mathbf{P}}^{e,i}$ in element local coordinate system as shown in Fig. AI.2. These force vectors are related by the transformation:

$$\mathbf{P}^{e,i} = \mathbf{R}^T \bar{\mathbf{P}}^{e,i} \quad (\text{AI.1})$$

where \mathbf{R} is the matrix that rotates global coordinates into local coordinates (Weaver and Gere (1990)). Define \mathbf{Q}^i as the vector of independent internal forces in the member. The end force vector is related to the independent internal forces by the equilibrium transformation:

$$\bar{\mathbf{P}}^{e,i} = \mathbf{T}_R^T \mathbf{Q}^i \quad (\text{AI.2})$$

where the transformation \mathbf{T}_R matrix is developed in other sections of this work according to the nature of the element under consideration (see for example section 4.4). Combining equations (AI.1) and (AI.2), we have:

$$\mathbf{P}^{e,i} = \mathbf{B}^{e,i} \mathbf{Q}^i \quad (\text{AI.3})$$

where $\mathbf{B}^{e,i} = \mathbf{R}^T \mathbf{T}_R^T$ is the equilibrium matrix of the element i . The cross-sectional stress-resultants along the length of the element are given by:

$$\mathcal{F}(x) = \mathbf{b}(x) \mathbf{Q}^i \quad (\text{AI.4})$$

where \mathcal{F} is the vector of cross-sectional stress-resultants, and \mathbf{b} is the Force Interpolation Matrix function. These transformations are shown in Fig. AI.2.

Let $\dot{\mathbf{u}}^{e,i}$ be the vector of element end velocities in the global coordinate system, $\dot{\mathbf{u}}^{e,i}$, the vector of element end velocities in the element coordinate system, $\dot{\mathbf{q}}^i$, the vector of element deformation rates including rotations but without rigid body displacements, and $\dot{\boldsymbol{\epsilon}}$, the vector of cross-sectional strains. Then, by the Principle of Virtual Work, corresponding to the equilibrium equations (AI.1), (AI.2), (AI.3) and (AI.4), we have the compatibility equations:

$$\dot{\mathbf{u}}^{e,i} = \mathbf{R}\dot{\mathbf{u}}^{e,i} \quad (\text{AI.5})$$

$$\dot{\mathbf{q}}^i = \mathbf{T}_R \dot{\mathbf{u}}^{e,i} \quad (\text{AI.6})$$

$$\dot{\mathbf{q}}^i = (\mathbf{B}^{e,i})^T \dot{\mathbf{u}}^{e,i} \quad (\text{AI.7})$$

$$\mathcal{F}(x) = \mathbf{b}(x)\mathbf{Q}^i \quad (\text{AI.8})$$

The transformations (AI.1)-(AI.8) are shown in the Tonti diagram, Fig. AI.3.

Let the structure have a total of N_{DOF} displacement degrees of freedom (DOF) that are either free or have specified non-zero displacements. The fixed DOF need not be considered. Let the number of elements be N_{elem} . The number of DOF of each element can be different, but are shown here as 12, corresponding to frame members, for simplicity. The incidence (or connectivity) matrix of the structure is defined as follows:

It should be noted that (AI.11) is not used in implementation, but is specified only for notational convenience in derivations. In actual implementation, an algorithm such that used for assembling the conventional Stiffness Matrix (Weaver and Gere (1990)) is used to assemble \mathbf{B} . Also, in small displacement theory, the velocities and deformation rates in the above equations can be replaced by the corresponding displacements and deformations. But the rate forms are used here since they extend to large displacements.

For a dynamic problem, the equations of motion of the structure are given by:

$$\mathbf{M}\ddot{\mathbf{u}} + \mathbf{C}\dot{\mathbf{u}} + \mathbf{B}\mathbf{F} = \mathbf{P} \quad (\text{AI.14})$$

where \mathbf{M} and \mathbf{C} are respectively the mass and damping matrices of the structure. Of the total of N_{DOF} DOF of the structure, let N_{free} be unconstrained and N_{spec} have specified non-zero displacements. Of the N_{free} unconstrained DOF, let N_{mass} have mass, N_{damp} have damping (i.e., the partition of the damping matrix associated with these DOF is positive definite), but no mass and the remaining N_{static} , neither mass nor damping (quasi-static DOF). The equations of motion can then be partitioned as follows:

$$N_{DOF} \begin{cases} N_{mass} \rightarrow \\ N_{damp} \rightarrow \\ N_{static} \rightarrow \\ N_{spec} \rightarrow \end{cases} \begin{bmatrix} \mathbf{M} & \mathbf{0} & \mathbf{0} & \mathbf{0} \\ \mathbf{0} & \mathbf{0} & \mathbf{0} & \mathbf{0} \\ \mathbf{0} & \mathbf{0} & \mathbf{0} & \mathbf{0} \\ \mathbf{0} & \mathbf{0} & \mathbf{0} & \mathbf{0} \end{bmatrix} \begin{Bmatrix} \ddot{\mathbf{u}}^1 \\ \ddot{\mathbf{u}}^2 \\ \ddot{\mathbf{u}}^3 \\ \ddot{\mathbf{u}}^4 \end{Bmatrix} + \begin{bmatrix} \mathbf{C}_{11} & \mathbf{C}_{12} & \mathbf{0} & \mathbf{0} \\ \mathbf{C}_{12}^T & \mathbf{C}_{22} & \mathbf{0} & \mathbf{0} \\ \mathbf{0} & \mathbf{0} & \mathbf{0} & \mathbf{0} \\ \mathbf{0} & \mathbf{0} & \mathbf{0} & \mathbf{0} \end{bmatrix} \begin{Bmatrix} \dot{\mathbf{u}}^1 \\ \dot{\mathbf{u}}^2 \\ \dot{\mathbf{u}}^3 \\ \dot{\mathbf{u}}^4 \end{Bmatrix} + \begin{bmatrix} \mathbf{B}_1^T \\ \mathbf{B}_2^T \\ \mathbf{B}_3^T \\ \mathbf{B}_4^T \end{bmatrix}^T \mathbf{F} = \begin{Bmatrix} \mathbf{P}^1 \\ \mathbf{P}^2 \\ \mathbf{P}^3 \\ \mathbf{P}^4 \end{Bmatrix} \quad (\text{AI.15})$$

Notice that the last $N_{static} + N_{spec}$ equations are algebraic. The N_{static} equations are constraints on the stress-resultants \mathbf{F} , arising from equilibrium of the quasi-static DOF. It will be seen that the last N_{spec} equations can be eliminated using the principle of virtual work. Further developments are presented in the respective sections as necessary.

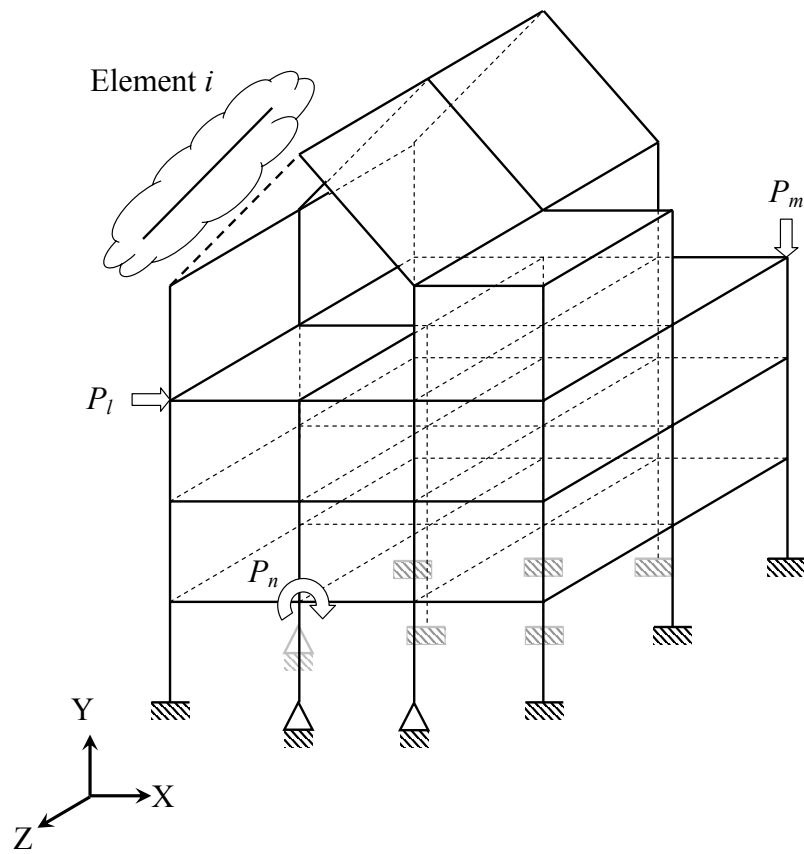


Fig. A1.1. 3D Frame Structure

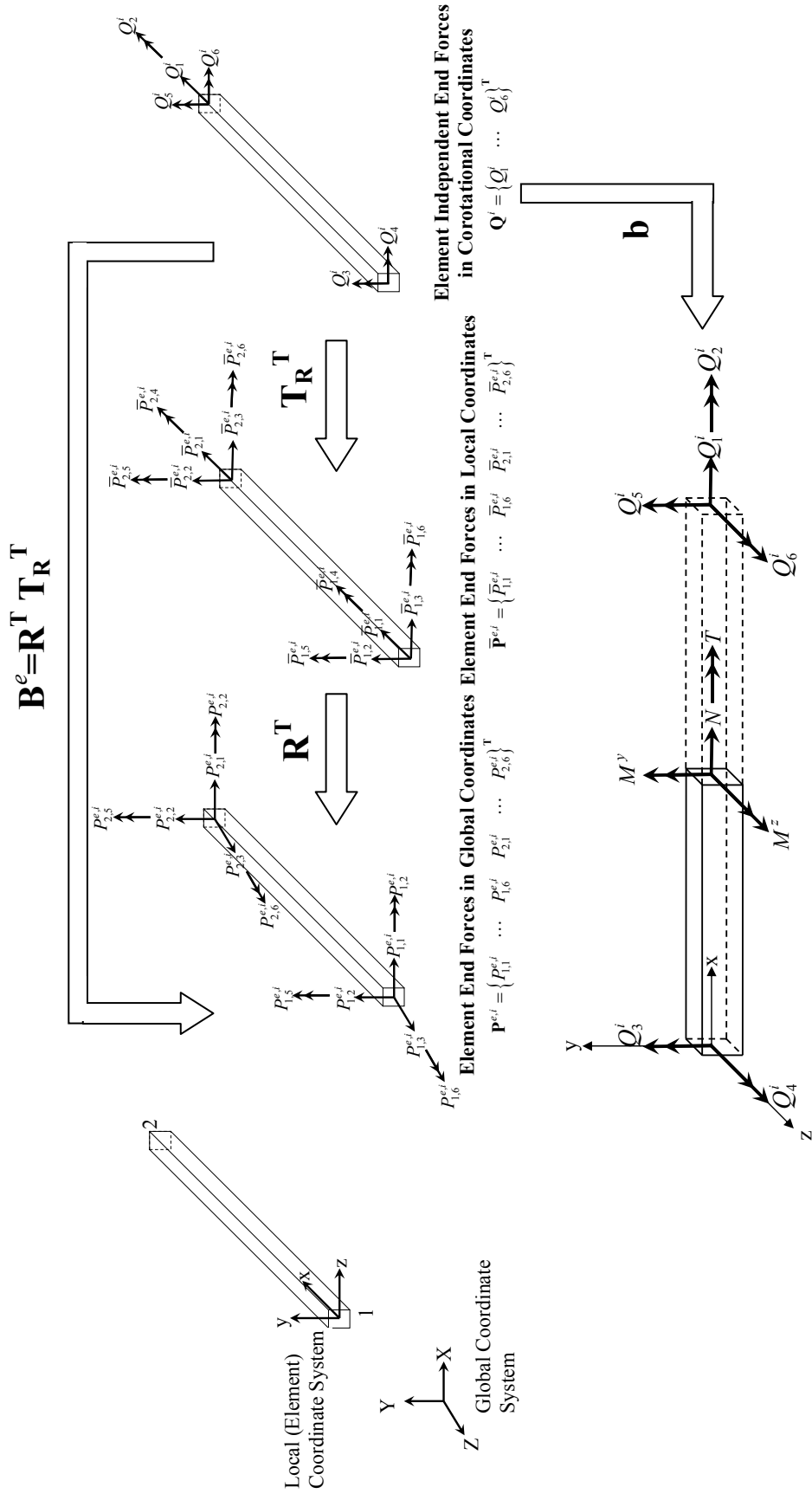


Fig. A1.2. Transformations in Typical Element i

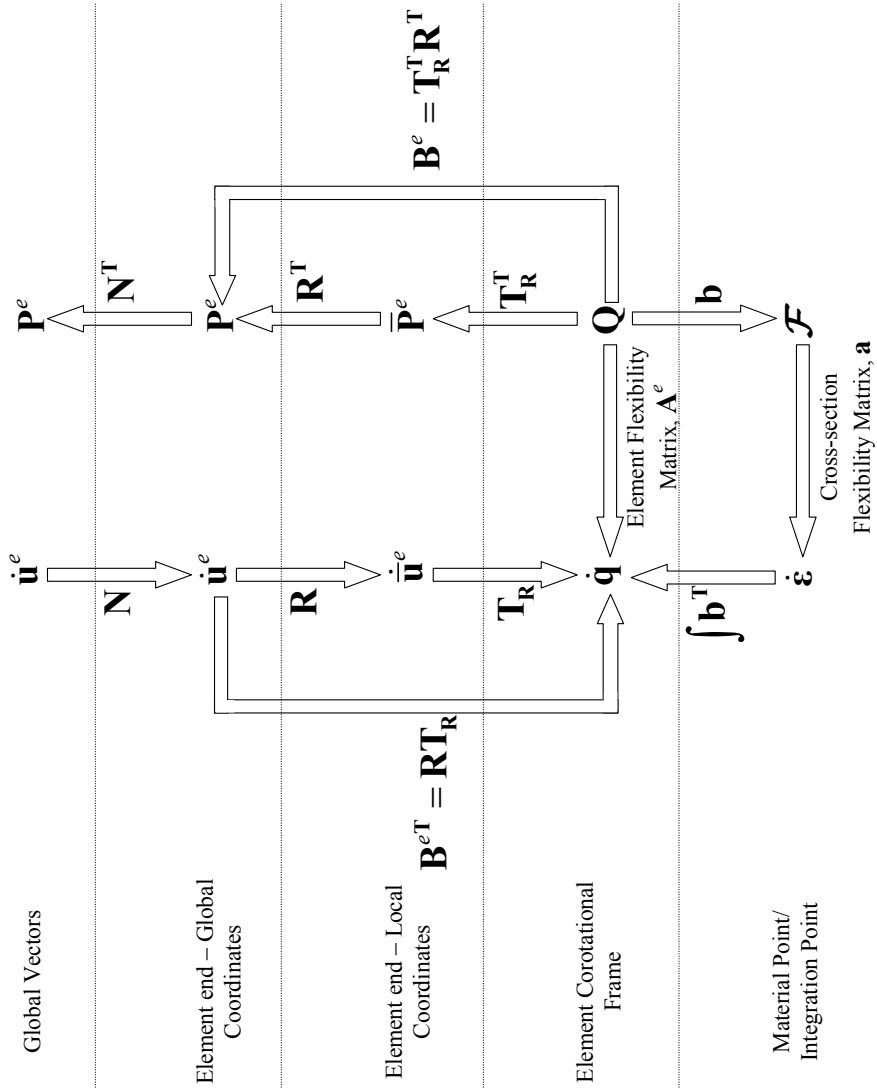


Fig. A1.3. Transformations (Tonti Diagram)

APPENDIX II. PRINCIPLE OF VIRTUAL FORCES IN RATE FORM

Starting from the rate form of the nonlinear compatibility equations (4.2)-(4.4), we set out to obtain a variational equation of the form:

$$\begin{Bmatrix} \dot{q}_1 \\ \dot{q}_2 \\ \dot{q}_3 \end{Bmatrix} = \int_0^L \mathbf{b}^T \begin{Bmatrix} \dot{\varepsilon} \\ \dot{\phi} \end{Bmatrix} dx \quad (\text{AII.1})$$

The following are the boundary conditions:

$$\dot{\theta}|_{x=0} = \dot{q}_2, \dot{\theta}|_{x=L} = \dot{q}_3 \quad (\text{AII.2})$$

$$\dot{\xi}|_{x=L} = \dot{q}_1, \xi|_{x=0} = \xi|_{x=0} = 0, \xi|_{x=L} = \xi_L \quad (\text{AII.3})$$

$$\eta|_{x=0} = \dot{\eta}|_{x=0} = \eta|_{x=L} = \dot{\eta}|_{x=L} = 0 \quad (\text{AII.4})$$

Substituting equation (4.1) in (4.3) and integrating over the length of the element, we have:

$$\int_0^L \frac{d\xi}{dx} dx = \int_0^L \dot{\varepsilon} \cos \theta dx - \int_0^L \frac{d\eta}{dx} \dot{\theta} dx \quad (\text{AII.5})$$

Integrating the second term on the right hand side of Eq. (AII.5) by parts and imposing the boundary conditions, the following relation is obtained:

$$\dot{q}_1 = \int_0^L \dot{\varepsilon} \cos \theta dx + \int_0^L \eta \frac{d\dot{\theta}}{dx} dx \quad (\text{AII.6})$$

Substituting Eq. (4.2) in Eq. (AII.6) results in:

$$\dot{q}_1 = \int_0^L [(\cos \theta + \eta\phi) \quad \eta(1 + \varepsilon)] \begin{Bmatrix} \dot{\varepsilon} \\ \dot{\phi} \end{Bmatrix} dx \quad (\text{AII.7})$$

Similarly, starting from equations (4.4) and , integration by parts and substituting Eq. (4.2) results in:

$$\dot{q}_3 = \int_0^L \left[\left(\frac{\xi \phi - \sin \theta}{\xi_L} \right) \frac{\xi}{\xi_L} (1 + \varepsilon) \right] \begin{Bmatrix} \dot{\varepsilon} \\ \dot{\phi} \end{Bmatrix} dx \quad (\text{AII.8})$$

Also, integrating equation (4.2) over the length of the element results in:

$$\dot{q}_3 - \dot{q}_2 = \int_0^L \left[\phi \quad (1 + \varepsilon) \right] \begin{Bmatrix} \dot{\varepsilon} \\ \dot{\phi} \end{Bmatrix} dx \quad (\text{AII.9})$$

The following integral relationship follows by combining equations (AII.7), (AII.8) and (AII.9):

$$\begin{Bmatrix} \dot{q}_1 \\ \dot{q}_2 \\ \dot{q}_3 \end{Bmatrix} = \int_0^L \mathbf{b}^{*T} \begin{Bmatrix} \dot{\varepsilon} \\ \dot{\phi} \end{Bmatrix} dx \quad (\text{AII.10})$$

where,

$$\mathbf{b}^* = \begin{bmatrix} (\cos \theta + \eta \phi) & \phi \left(\frac{\xi}{\xi_L} - 1 \right) - \frac{\sin \theta}{\xi_L} & \phi \left(\frac{\xi}{\xi_L} \right) - \frac{\sin \theta}{\xi_L} \\ \eta (1 + \varepsilon) & \left(\frac{\xi}{\xi_L} - 1 \right) (1 + \varepsilon) & \frac{\xi}{\xi_L} (1 + \varepsilon) \end{bmatrix} \quad (\text{AII.11})$$

Consideration of the section constitutive equations leads to a different strain measure conjugate to the bending moment, and results in the transformation of \mathbf{b}^* into the equilibrium matrix \mathbf{b} . In the presence of centerline axial strain, the plane section hypothesis yields the following for the strain of a fiber at a distance y from the centerline:

$$\varepsilon(y) = \varepsilon - (1 + \varepsilon) \phi y \quad (\text{AII.12})$$

In rate form, this gives:

$$\dot{\varepsilon}(y) = \dot{\varepsilon} - \dot{\varepsilon}\phi y - (1 + \varepsilon)\dot{\phi}y \quad (\text{AII.13})$$

Integrating the resulting stress rates over the cross section, it can be shown that the stress resultant rates are given by:

$$\begin{Bmatrix} \dot{P} \\ \dot{M} \end{Bmatrix} = \begin{bmatrix} \iint_A E' dA & -\iint_A E' y dA \\ -\iint_A E' y dA & \iint_A E' y^2 dA \end{bmatrix} \begin{bmatrix} 1 & 0 \\ \phi & (1 + \varepsilon) \end{bmatrix} \begin{Bmatrix} \dot{\varepsilon} \\ \dot{\phi} \end{Bmatrix} = \mathbf{K}' \begin{bmatrix} 1 & 0 \\ \phi & (1 + \varepsilon) \end{bmatrix} \begin{Bmatrix} \dot{\varepsilon} \\ \dot{\phi} \end{Bmatrix} \quad (\text{AII.14})$$

or

$$\begin{Bmatrix} \dot{\varepsilon} \\ \dot{\phi} \end{Bmatrix} = \begin{bmatrix} 1 & 0 \\ -\frac{\phi}{(1 + \varepsilon)} & \frac{1}{(1 + \varepsilon)} \end{bmatrix} \mathbf{f} \begin{Bmatrix} \dot{P} \\ \dot{M} \end{Bmatrix} \quad (\text{AII.15})$$

where \mathbf{K}' is the section tangent rigidity matrix and \mathbf{f} is the section flexibility matrix, $\mathbf{f} = (\mathbf{K}')^{-1}$. By introducing the strain measure $\tilde{\phi} = (1 + \varepsilon)\phi$ we see that the constitutive equations can be written as:

$$\begin{Bmatrix} \dot{\varepsilon} \\ \dot{\tilde{\phi}} \end{Bmatrix} = \mathbf{f} \begin{Bmatrix} \dot{P} \\ \dot{M} \end{Bmatrix} \quad (\text{AII.16})$$

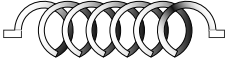
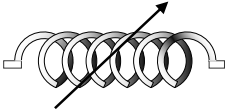
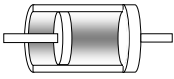
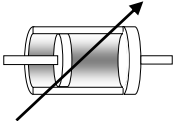

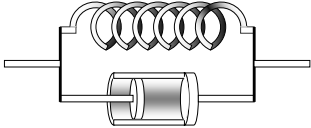
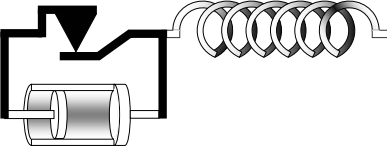

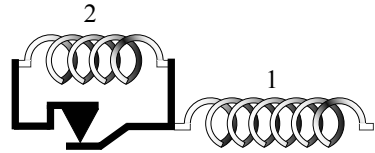
and that:

$$\mathbf{b}^{*T} \begin{bmatrix} 1 & 0 \\ -\frac{\phi}{(1 + \varepsilon)} & \frac{1}{(1 + \varepsilon)} \end{bmatrix} = \mathbf{b}^T \quad (\text{AII.17})$$

The variational Eq. (AII.10) now leads to equation (4.5).

APPENDIX III.

ONE-DIMENSIONAL RECIPROCAL COMPONENTS

Component	Schematic	Lagrangian	Dissipation
Linear-elastic spring (Stiffness = k)		$\frac{1}{2}ku^2$ or $\frac{1}{2k}j^2$	-
Nonlinear elastic spring		Strain energy or Complementary strain energy	-
Linear viscous damper (Damping constant = c)		-	$\frac{1}{2}c\dot{u}^2$ or $\frac{1}{2c}j^2$
Nonlinear viscous damper		-	$\frac{1}{n+1}c \dot{u} ^{n+1}$ or $\frac{n}{n+1}\frac{ j ^{n+1/n}}{c^{1/n}}$
Maxwell element		$\frac{1}{2k}j^2$	$\frac{1}{2c}j^2$
Kelvin element		$\frac{1}{2}ku^2$	$\frac{1}{2}c\dot{u}^2$
Viscoplastic element (Yield force = F_y)		$\frac{1}{2k}j^2$	$\frac{1}{2c}\langle j - F_y \rangle^2$
Elastic-plastic element		$\frac{1}{2k}j^2$	$U_c(j)$
Kinematic Hardening		$\frac{1}{2k_1}j_1^2 + \frac{1}{2k_2}j_2^2$	$U_c(j_1 - j_2)$

APPENDIX IV. LAGRANGIAN FORMULATION OF CONTINUA

AIV.1. Three Dimensional Continuum

In this subsection, the Lagrangian formulation of Section 5 is extended to the three dimensional continuum. The reader is referred to Belytschko et al. (2000) for a concise review of the continuum mechanics concepts used here. The notation followed here is also from this reference. Vectors and tensors are written in bold face and their Cartesian components are written in italics with subscripts.

AIV.1.1. Review of Continuum Kinematics

Consider a body occupying a region Ω of space with boundary Γ at time $t=0$. This is called the *reference configuration* of the body. The position vector of a point in the body is \mathbf{X} . In Cartesian coordinates, the vector is represented by its components X_i . The motion of the body is described by the map ϕ , so that at time t , the position vector of the point \mathbf{X} is $\mathbf{x} = \phi(\mathbf{X}, t)$. The displacement of the point \mathbf{X} is \mathbf{u} and $\mathbf{x} = \mathbf{X} + \mathbf{u}$. The deformation gradient tensor \mathbf{F} is defined as:

$$\mathbf{F} = \frac{\partial \mathbf{x}}{\partial \mathbf{X}} \quad \text{or} \quad F_{ij} = \delta_{ij} + u_{i,j} \quad (\text{AIV.1})$$

The Green-Lagrange strain tensor is defined as:

$$\mathbf{E} = \frac{1}{2}(\mathbf{F}^T \mathbf{F} - \mathbf{I}) \quad \text{or} \quad E_{ij} = \frac{1}{2}(F_{ki} F_{kj} - \delta_{ij}) \quad (\text{AIV.2})$$

where \mathbf{I} is the identity matrix and δ_{ij} is the Kronecker delta ($\delta_{ij}=1$ if $i=j$, 0 otherwise).

Using the definition of the deformation gradient, the Green-Lagrange strain tensor may be written in terms of the displacements as:

$$E_{ij} = \frac{1}{2} (u_{i,j} + u_{j,i} + u_{k,i} u_{k,j}) \quad (\text{AIV.3})$$

Using equation (AIV.3), the material time derivative of the Green-Lagrange strain tensor can be obtained as:

$$\begin{aligned} \dot{E}_{ij} &= \frac{1}{2} (\dot{u}_{i,j} + \dot{u}_{j,i} + u_{k,i} \dot{u}_{k,j} + \dot{u}_{k,i} u_{k,j}) \\ &= \frac{1}{2} (\delta_{ik} \dot{u}_{k,j} + \delta_{jk} \dot{u}_{j,i} + u_{k,i} \dot{u}_{k,j} + \dot{u}_{k,i} u_{k,j}) \\ &= \frac{1}{2} [(\delta_{ik} + u_{k,i}) \dot{u}_{k,j} + (\delta_{jk} + \dot{u}_{k,i}) \dot{u}_{j,i}] \\ &= \frac{1}{2} [(\delta_{ip} \delta_{jq} + \delta_{iq} \delta_{jp}) (\delta_{pk} + u_{k,p}) \dot{u}_{k,q}] \end{aligned} \quad (\text{AIV.4})$$

Hence we obtain the strain rate-velocity relationship:

$$\dot{E}_{ij} = B_{ijk}^* \dot{u}_k \quad (\text{AIV.5})$$

where $B_{ijk}^* = \frac{1}{2} (\delta_{ip} \delta_{jq} + \delta_{iq} \delta_{jp}) (\delta_{pk} + u_{k,p}) \frac{\partial}{\partial X_q}$ is the strain rate-velocity operator.

The stress measure that is work conjugate to the Green-Lagrange strain tensor is the second Piola-Kirchhoff stress \mathbf{S} defined by the relation:

$$\tau_i = F_{ik} S_{ij} n_j \quad (\text{AIV.6})$$

where $\boldsymbol{\tau}$ is the traction vector and \mathbf{n} is the unit normal in the reference configuration. Γ_u and Γ_τ are the portions of the boundary with prescribed displacement and prescribed traction respectively.

AIV.1.2. Continuum Plasticity

Finite deformation plasticity can be formulated in several ways. These are discussed in an excellent fashion by Simo and Ortiz (1985). Of these, the *material formulation* is adopted here. Other formulations are equally applicable using appropriate kinematic operators B_{ijk}^* . The fundamental assumption of finite deformation plasticity is the multiplicative decomposition of the deformation gradient tensor into plastic and elastic parts:

$$\mathbf{F} = \mathbf{F}^e \mathbf{F}^p \quad (\text{AIV.7})$$

where the elastic deformation \mathbf{F}^e is obtained by unloading the body to an intermediate configuration (Simo and Ortiz (1985)). The material formulation then defines the following relationships:

1. The plastic Green-Lagrange strain tensor:

$$\mathbf{E}^p = \frac{1}{2} \left(\mathbf{F}^{pT} \mathbf{F}^p - \mathbf{I} \right) \quad (\text{AIV.8})$$

2. The elastic Green-Lagrange strain tensor:

$$\mathbf{E}^e = \mathbf{E} - \mathbf{E}^p \quad (\text{AIV.9})$$

3. The elastic stress-strain relationship:

$$\mathbf{E}^e = \rho_0 \frac{\partial \psi}{\partial \mathbf{S}} \quad (\text{AIV.10})$$

where \mathbf{S} is the second Piola-Kirchhoff stress tensor and $\psi(\mathbf{S})$ is the complementary strain energy function per unit mass, assumed here to be quadratic so that

$\psi(\mathbf{S}) = \frac{1}{2} A_{ijkl} S_{ij} S_{kl}$ where A_{ijkl} is the inverse of the elasticity tensor and ρ_0 is the mass

density in the reference configuration.

4. The yield condition:

$$\Phi(\mathbf{S}, \mathbf{F}) = 0 \quad (\text{AIV.11})$$

so that the elastic domain is $C = \{\mathbf{S} \mid \Phi(\mathbf{S}, \mathbf{F}) < 0\}$.

5. The flow rule:

$$\dot{\mathbf{E}}^p \in \partial \mathbf{U}_C \quad (\text{AIV.12})$$

as in equation (2.25) of Section 2.

The Lagrangian formulation of the continuum is now presented.

AIV.1.3. Lagrangian Formulation

It is proposed that the Lagrangian and dissipation *density* functions (i.e. per unit mass) and the action integral of the continuum are given respectively by:

$$\mathcal{L} = \frac{1}{2} \dot{u}_k \dot{u}_k + \frac{1}{2} A_{ijkl} \dot{J}_{ij} \dot{J}_{kl} + \frac{1}{\rho_0} J_{ij} B_{ijk}^* \dot{u}_k \quad (\text{AIV.13})$$

$$\varphi(\mathbf{J}, \dot{\mathbf{u}}) = \mathbf{U}_C(\mathbf{J}) + \frac{1}{2} c_{ij} \dot{u}_i \dot{u}_j \quad (\text{AIV.14})$$

$$\begin{aligned} \delta \mathcal{I} = & -\delta \int_0^T \int_{\Omega} \rho_0 \mathcal{L} d\Omega dt \\ & + \int_0^T \int_{\Omega} \rho_0 \frac{\partial \varphi}{\partial \dot{u}_k} \delta u_k d\Omega dt + \int_0^T \int_{\Omega} \rho_0 \frac{\partial \varphi}{\partial \dot{J}_{ij}} \delta J_{ij} d\Omega dt \\ & - \int_0^T \int_{\Omega} \rho_0 f_k \delta u_k d\Omega dt - \int_0^T \int_{\Gamma} \tau_k \delta u_k d\Gamma dt \end{aligned} \quad (\text{AIV.15})$$

where $J_{ij} = \int_0^t S_{ij} d\tau$, the impulse of the second Piola-Kirchhoff stress tensor, S_{ij} and \mathbf{c} is the damping per unit mass. It is shown next that the governing equations of the continuum can be derived from this Lagrangian formulation as Euler-Lagrange Equations.

AIV.1.4. Derivation of Euler-Lagrange Equations

Consider the first integral of equation (AIV.15):

$$\delta \int_0^T \int_{\Omega} \rho_0 \mathcal{L} d\Omega dt = \delta \int_0^T \int_{\Omega} \left(\frac{1}{2} \rho_0 \dot{u}_k \dot{u}_k + \frac{1}{2} \rho_0 A_{ijkl} \dot{J}_{ij} \dot{J}_{kl} + J_{ij} B_{ijk}^* \dot{u}_k \right) d\Omega dt \quad (\text{AIV.16})$$

By integrating by parts in time, the first two terms of the integral on the right hand side can be written as follows:

$$\delta \int_0^T \int_{\Omega} \frac{1}{2} \rho_0 \dot{u}_k \dot{u}_k d\Omega dt = - \int_0^T \int_{\Omega} \rho_0 \ddot{u}_k \delta u_k d\Omega dt \quad (\text{AIV.17})$$

$$\delta \int_0^T \int_{\Omega} \frac{1}{2} \rho_0 A_{ijkl} \dot{J}_{ij} \dot{J}_{kl} d\Omega dt = - \int_0^T \int_{\Omega} \rho_0 A_{ijkl} \ddot{J}_{ij} \delta J_{kl} d\Omega dt \quad (\text{AIV.18})$$

Consider now the integrand of the third term:

$$J_{ij} B_{ijk}^* \dot{u}_k = \frac{1}{2} J_{ij} (\delta_{ip} \delta_{jq} + \delta_{iq} \delta_{jp}) (\delta_{pk} + u_{k,p}) \dot{u}_{k,q}$$

Now $\frac{1}{2} J_{ij} (\delta_{ip} \delta_{jq} + \delta_{iq} \delta_{jp}) = \frac{1}{2} (J_{pq} + J_{qp}) = J_{pq}$ due to the symmetry of the second Piola-

Kirchhoff stress tensor and hence of the impulse tensor \mathbf{J} . Hence:

$$J_{ij} B_{ijk}^* \dot{u}_k = J_{pq} (\delta_{pk} + u_{k,p}) \dot{u}_{k,q} = J_{ij} (\delta_{ik} + u_{k,i}) \dot{u}_{k,j} \quad (\text{AIV.19})$$

replacing the indices p and q by i and j respectively. Substituting, we have:

$$\begin{aligned}
\delta \int_0^T \int_{\Omega} J_{ij} B_{ijk}^* \dot{u}_k d\Omega dt &= \int_0^T \int_{\Omega} \delta J_{ij} (\delta_{ik} + u_{k,i}) \dot{u}_{k,j} d\Omega dt \\
&+ \int_0^T \int_{\Omega} J_{ij} \delta u_{k,i} \dot{u}_{k,j} d\Omega dt \\
&+ \int_0^T \int_{\Omega} J_{ij} (\delta_{ik} + u_{k,i}) \delta \dot{u}_{k,j} d\Omega dt
\end{aligned} \tag{AIV.20}$$

Consider the following time integral:

$$\begin{aligned}
\int_0^T J_{ij} (\delta_{ik} + u_{k,i}) \delta \dot{u}_{k,j} dt &= J_{ij} (\delta_{ik} + u_{k,i}) \delta u_{k,j} \Big|_0^T \\
&- \int_0^T \dot{J}_{ij} (\delta_{ik} + u_{k,i}) \delta u_{k,j} dt - \int_0^T J_{ij} \dot{u}_{k,i} \delta u_{k,j} dt
\end{aligned}$$

The first term on the right hand side vanishes because $\delta \mathbf{u}$ is prescribed at the beginning and end of the time interval in Hamilton's principle. Moreover, using the symmetry of \mathbf{J} , the indices, i and j in the third term can be switched to obtain:

$$\int_0^T J_{ij} (\delta_{ik} + u_{k,i}) \delta \dot{u}_{k,j} dt = - \int_0^T \dot{J}_{ij} (\delta_{ik} + u_{k,i}) \delta u_{k,j} dt - \int_0^T J_{ij} \dot{u}_{k,j} \delta u_{k,i} dt \tag{AIV.21}$$

Since $\delta_{ik} + u_{k,i} = F_{ki}$, the deformation gradient:

$$\dot{J}_{ij} (\delta_{ik} + u_{k,i}) = S_{ij} F_{ki} = S_{ji} F_{ki} = P_{jk} \tag{AIV.22}$$

where \mathbf{P} is the unsymmetric first Piola-Kirchhoff stress tensor. The second equality above follows from the symmetry of the second Piola-Kirchhoff stress tensor, \mathbf{S} . Notice also that similar to equation (AIV.19), the first integrand on the right hand side of equation (AIV.20) can be written as:

$$\delta J_{ij} (\delta_{ik} + u_{k,i}) \dot{u}_{k,j} = \delta J_{ij} B_{ijk}^* \dot{u}_k \quad (\text{AIV.23})$$

Substituting equations (AIV.21), (AIV.22) and (AIV.23) in equation (AIV.20), we have:

$$\delta \int_0^T \int_{\Omega} J_{ij} B_{ijk}^* \dot{u}_k d\Omega dt = \int_0^T \int_{\Omega} \delta J_{ij} B_{ijk}^* \dot{u}_k d\Omega dt - \int_0^T \int_{\Omega} P_{jk} \delta u_{k,j} d\Omega dt \quad (\text{AIV.24})$$

Notice that the second integral of equation (AIV.21) cancels out the second integral of equation (AIV.20) in a fashion similar to the spatially discrete case of section 5.8. Now consider the spatial integral:

$$\begin{aligned} \int_{\Omega} P_{jk} \delta u_{k,j} d\Omega &= \int_{\Omega} (P_{jk} \delta u_k)_{,j} d\Omega - \int_{\Omega} P_{jk,j} \delta u_k d\Omega \\ &= \int_{\Gamma} P_{jk} n_j \delta u_k d\Gamma - \int_{\Omega} P_{jk,j} \delta u_k d\Omega \end{aligned} \quad (\text{AIV.25})$$

where Γ is the boundary of the domain, \mathbf{n} is the unit vector normal to the boundary and the second equality follows from Gauss' theorem. Substituting equation (AIV.25) in equation (AIV.24), we have:

$$\begin{aligned} \delta \int_0^T \int_{\Omega} J_{ij} B_{ijk}^* \dot{u}_k d\Omega dt &= \int_0^T \int_{\Omega} \delta J_{ij} B_{ijk}^* \dot{u}_k d\Omega dt + \int_0^T \int_{\Omega} P_{jk,j} \delta u_k d\Omega dt \\ &\quad - \int_0^T \int_{\Gamma} P_{jk} n_j \delta u_k d\Gamma dt \end{aligned} \quad (\text{AIV.26})$$

Substituting equations (AIV.17), (AIV.18) and (AIV.26) in equation (AIV.15) and grouping terms containing δu_k and δJ_{ij} gives:

$$\begin{aligned}
& \int_0^T \int_{\Omega} \left(\rho_0 \ddot{u}_k + \rho_0 \frac{\partial \varphi}{\partial \dot{u}_k} - P_{jk,j} - \rho_0 f_k \right) \delta u_k d\Omega dt \\
& + \int_0^T \int_{\Omega} \left(\rho_0 A_{ijkl} \ddot{J}_{kl} + \rho_0 \frac{\partial \varphi}{\partial \dot{J}_{ij}} - B_{ijk}^* \dot{u}_k \right) \delta J_{ij} d\Omega dt \\
& + \int_0^T \int_{\Gamma} \left(P_{jk} n_j - \tau_k \right) \delta u_k d\Gamma dt \\
& = 0
\end{aligned} \tag{AIV.27}$$

Let Γ_u and Γ_τ be the portions of the boundary with prescribed displacement and prescribed traction respectively. Then due to the arbitrariness of δu_k everywhere but on Γ_u , and due to the arbitrariness of δJ_{ij} , we have:

$$-\rho_0 \ddot{u}_k - \rho_0 \frac{\partial \varphi}{\partial \dot{u}_k} + P_{jk,j} + \rho_0 f_k = 0 \tag{AIV.28}$$

$$\rho_0 A_{ijkl} \ddot{J}_{kl} + \rho_0 \frac{\partial \varphi}{\partial \dot{J}_{ij}} - B_{ijk}^* \dot{u}_k = 0 \tag{AIV.29}$$

$$\begin{aligned}
P_{jk} n_j &= \tau_k \quad \text{on } \Gamma_\tau \\
\delta u_k &= 0 \quad \text{on } \Gamma_u
\end{aligned} \tag{AIV.30}$$

Equation (AIV.28) is the equation of motion expressed in the reference configuration (see for example, Belytschko, Liu et al. (2000)), equation (AIV.29) is the equation of compatibility and equation (AIV.30) represents the boundary conditions. It has thus been demonstrated that the Lagrangian function, the dissipation function and the action integral of equations (AIV.13)-(AIV.15) determine the governing equations of the three dimensional continuum.

AIV.2. Large Deformation Beam Element

A Lagrangian formulation is now presented for the large deformation beam element of Section 4 in the element corotational system.

AIV.2.1. Kinematics

Consider the rate-compatibility equations (4.2), (4.3) and (4.4) of Section 4. Multiplying equation (4.3) by $\cos\theta$ and equation (4.4) by $\sin\theta$ and adding, we have:

$$\dot{\varepsilon} = \cos\theta \frac{d\dot{\xi}}{dx} + \sin\theta \frac{d\dot{\eta}}{dx} \quad (\text{AIV.31})$$

Similarly, multiplying equation (4.3) by $\sin\theta$ and equation (4.4) by $\cos\theta$ and subtracting, we have:

$$\dot{\theta} = -\frac{\sin\theta}{1+\varepsilon} \frac{d\dot{\xi}}{dx} + \frac{\cos\theta}{1+\varepsilon} \frac{d\dot{\eta}}{dx} \quad (\text{AIV.32})$$

Differentiating equation (AIV.32) further with respect to x gives:

$$\dot{\dot{\theta}} = -\frac{d}{dx} \left(\frac{\sin\theta}{1+\varepsilon} \frac{d}{dx} \right) \dot{\xi} + \frac{d}{dx} \left(\frac{\cos\theta}{1+\varepsilon} \frac{d}{dx} \right) \dot{\eta} \quad (\text{AIV.33})$$

If the displacements in the x and y directions are denoted by u and v respectively, then $\dot{u} = \dot{\xi}$ and $\dot{v} = \dot{\eta}$. Combining this with equations (AIV.31) and (AIV.33), the following compatibility relations is obtained:

$$\dot{\varepsilon} = \mathbf{B}^* \dot{\mathbf{u}} \quad (\text{AIV.34})$$

where $\varepsilon = \left\{ \varepsilon \quad \tilde{\phi} \right\}^T$, $\mathbf{u} = \{u, v\}^T$ and \mathbf{B}^* is the compatibility operator:

$$\mathbf{B}^* = \begin{bmatrix} \cos \theta \frac{d}{dx} & \sin \theta \frac{d}{dx} \\ -\frac{d}{dx} \left(\frac{\sin \theta}{1 + \varepsilon} \frac{d}{dx} \right) & \frac{d}{dx} \left(\frac{\cos \theta}{1 + \varepsilon} \frac{d}{dx} \right) \end{bmatrix} \quad (\text{AIV.35})$$

AIV.2.2. Constitutive Relations

The constitutive relations are those of multi-axial plasticity discussed in Section 2.6. We have from equation (2.33):

$$\dot{\boldsymbol{\varepsilon}} = \dot{\boldsymbol{\varepsilon}}^e + \dot{\boldsymbol{\varepsilon}}^p \quad (\text{AIV.36})$$

The stress-resultant vector, $\mathcal{F} = \{P \quad M\}^T$. The plastic strain rate is:

$$\dot{\boldsymbol{\varepsilon}}^p = \frac{\partial \varphi}{\partial \mathcal{F}} \quad (\text{AIV.37})$$

where φ , the dissipation function, is given by $\varphi = \mathbf{U}_C$, the indicator function of the elastic domain $C = \{\mathcal{F} \mid \Phi(\mathcal{F}) < 0\}$, Φ being the yield function of the cross-section of the beam. The elastic strain is given by:

$$\boldsymbol{\varepsilon}^e = \frac{\partial}{\partial \mathcal{F}} \left(\frac{1}{2} \mathcal{F}^T \mathbf{a} \mathcal{F} \right) \quad (\text{AIV.38})$$

where \mathbf{a} is the elastic flexibility matrix of the cross-section.

AIV.2.3. Lagrangian Formulation

It is proposed that the Lagrangian and dissipation *density* functions (i.e. per unit undeformed length) and the action integral of the continuum are given respectively by:

$$\mathcal{L} = \frac{1}{2} \rho_0 \dot{\mathbf{u}}^T \dot{\mathbf{u}} + \frac{1}{2} \mathbf{J}^T \mathbf{a} \mathbf{J} + \mathbf{J}^T \mathbf{B}^* \dot{\mathbf{u}} \quad (\text{AIV.39})$$

$$\varphi(\dot{\mathbf{J}}, \dot{\mathbf{u}}) = \mathbf{U}_c(\dot{\mathbf{J}}) + \frac{1}{2} \dot{\mathbf{u}}^T \mathbf{c} \dot{\mathbf{u}} \quad (\text{AIV.40})$$

$$\begin{aligned} \delta \mathcal{I} = & -\delta \int_0^T \int_0^L \mathcal{L} dx dt + \int_0^T \int_0^L \delta \mathbf{u}^T \frac{\partial \varphi}{\partial \dot{\mathbf{u}}} dx dt + \int_0^T \int_0^L \delta \mathbf{J}^T \frac{\partial \varphi}{\partial \dot{\mathbf{J}}} dx dt \\ & - \int_0^T \int_0^L \delta \mathbf{u}^T \mathbf{f} dx dt - \int_0^T \delta \mathbf{q}^T \mathbf{Q} dt \end{aligned} \quad (\text{AIV.41})$$

where $\mathbf{J} = \int_0^t \mathcal{F} d\tau$, the impulse of the stress-resultant, \mathbf{c} is the damping per unit undeformed length and \mathbf{Q} and \mathbf{q} are the element end force and displacement vectors respectively. It is shown next that the governing equations of the beam-column can be derived from this Lagrangian formulation as Euler-Lagrange Equations.

AIV.2.4. Equilibrium Matrix

Before showing that the Euler-Lagrange equations of the Lagrangian formulation, equations (AIV.39) through (AIV.41), are the equilibrium and compatibility equations of the beam-column, it is necessary to obtain the adjoint of the compatibility matrix, \mathbf{B}^* , the equilibrium matrix, \mathbf{B} . Considering the internal power, integrating by parts and using equation (AIV.32) gives:

$$\begin{aligned} \int_0^L \mathcal{F}^T \mathbf{B}^* \dot{\mathbf{u}} dx = & \int_0^L \dot{\mathbf{u}}^T \mathbf{B} \mathcal{F} dx + \left(P \cos \theta + \frac{dM}{dx} \frac{\sin \theta}{1 + \varepsilon} \right) \dot{\mathbf{u}} \Big|_0^L \\ & + \left(P \sin \theta - \frac{dM}{dx} \frac{\cos \theta}{1 + \varepsilon} \right) \dot{\mathbf{v}} \Big|_0^L + M \dot{\theta} \Big|_0^L \end{aligned} \quad (\text{AIV.42})$$

where \mathbf{B} is the equilibrium matrix:

$$\mathbf{B} = \begin{bmatrix} \sin \theta - \cos \theta \frac{d}{dx} & -\frac{d}{dx} \left(\frac{\sin \theta}{1 + \varepsilon} \frac{d}{dx} \right) \\ -\cos \theta - \sin \theta \frac{d}{dx} & \frac{d}{dx} \left(\frac{\cos \theta}{1 + \varepsilon} \frac{d}{dx} \right) \end{bmatrix} \quad (\text{AIV.43})$$

Using the boundary condition of equations (AII.2), (AII.3) and (AII.4) of Appendix II, we have:

$$\int_0^L \mathcal{F}^T \mathbf{B}^* \dot{\mathbf{u}} dx = \int_0^L \dot{\mathbf{u}}^T \mathbf{B} \mathcal{F} dx + \left(P \cos \theta + \frac{dM}{dx} \frac{\sin \theta}{1 + \varepsilon} \right) \dot{q}_1 + M(L) \dot{q}_3 - M(0) \dot{q}_2 \quad (\text{AIV.44})$$

The Euler-Lagrange equations can now be derived.

AIV.2.5. Derivation of Euler-Lagrange Equations

Consider the first integral of equation (AIV.41):

$$\delta \int_0^T \int_0^L \mathcal{L} dx dt = \delta \int_0^T \int_0^L \left(\frac{1}{2} \rho_0 \dot{\mathbf{u}}^T \dot{\mathbf{u}} + \frac{1}{2} \mathbf{J}^T \mathbf{a} \mathbf{J} + \mathbf{J}^T \mathbf{B}^* \dot{\mathbf{u}} \right) dx dt \quad (\text{AIV.45})$$

By integrating by parts in time, the first two terms of the integral on the right hand side can be written as follows:

$$\delta \int_0^T \int_0^L \frac{1}{2} \rho_0 \dot{\mathbf{u}}^T \dot{\mathbf{u}} dx dt = - \int_0^T \int_0^L \delta \mathbf{u}^T \rho_0 \ddot{\mathbf{u}} dx dt \quad (\text{AIV.46})$$

$$\delta \int_0^T \int_0^L \frac{1}{2} \mathbf{J}^T \mathbf{a} \mathbf{J} dx dt = - \int_0^T \int_0^L \delta \mathbf{J}^T \mathbf{a} \ddot{\mathbf{J}} dx dt \quad (\text{AIV.47})$$

Consider the third term:

$$\delta \int_0^T \int_0^L \mathbf{J}^T \mathbf{B}^* \dot{\mathbf{u}} dx dt = \int_0^T \int_0^L \delta \mathbf{J}^T \mathbf{B}^* \dot{\mathbf{u}} dx dt + \int_0^T \int_0^L \mathbf{J}^T \delta \mathbf{B}^* \dot{\mathbf{u}} dx dt + \int_0^T \int_0^L \mathbf{J}^T \mathbf{B}^* \delta \dot{\mathbf{u}} dx dt \quad (\text{AIV.48})$$

Integrating the third term by parts in time:

$$\int_0^T \int_0^L \mathbf{J}^T \mathbf{B}^* \delta \dot{\mathbf{u}} dx dt = \int_0^L \mathbf{J}^T \mathbf{B}^* \delta \mathbf{u} \Big|_0^T dx - \int_0^T \int_0^L \mathbf{J}^T \dot{\mathbf{B}}^* \delta \mathbf{u} dx dt - \int_0^T \int_0^L \dot{\mathbf{J}}^T \mathbf{B}^* \delta \mathbf{u} dx dt \quad (\text{AIV.49})$$

The term $\dot{\mathbf{B}}^* \delta \mathbf{u}$ is examined. We have the following terms:

$$\dot{B}_{11}^* = -\dot{\theta} \sin \theta \frac{d}{dx} = -\sin \theta \left[-\frac{\sin \theta}{1+\varepsilon} \frac{d\dot{u}}{dx} + \frac{\cos \theta}{1+\varepsilon} \frac{d\dot{v}}{dx} \right] \frac{d}{dx} \quad (\text{AIV.50})$$

$$\dot{B}_{12}^* = \dot{\theta} \cos \theta \frac{d}{dx} = \cos \theta \left[-\frac{\sin \theta}{1+\varepsilon} \frac{d\dot{u}}{dx} + \frac{\cos \theta}{1+\varepsilon} \frac{d\dot{v}}{dx} \right] \frac{d}{dx} \quad (\text{AIV.51})$$

$$\begin{aligned} \dot{B}_{21}^* &= \frac{d}{dx} \left[\left(-\frac{\cos \theta}{1+\varepsilon} \dot{\theta} + \frac{\sin \theta}{(1+\varepsilon)^2} \dot{\varepsilon} \right) \frac{d}{dx} \right] \\ &= \frac{d}{dx} \left\{ \left[-\frac{\cos \theta}{1+\varepsilon} \left(-\frac{\sin \theta}{1+\varepsilon} \frac{d\dot{u}}{dx} + \frac{\cos \theta}{1+\varepsilon} \frac{d\dot{v}}{dx} \right) + \frac{\sin \theta}{(1+\varepsilon)^2} \left(\cos \theta \frac{d\dot{u}}{dx} + \sin \theta \frac{d\dot{v}}{dx} \right) \right] \frac{d}{dx} \right\} \quad (\text{AIV.52}) \\ &= \frac{d}{dx} \left[\left(\frac{\sin 2\theta}{(1+\varepsilon)^2} \frac{d\dot{u}}{dx} - \frac{\cos 2\theta}{(1+\varepsilon)^2} \frac{d\dot{v}}{dx} \right) \frac{d}{dx} \right] \end{aligned}$$

$$\dot{B}_{22}^* = \frac{d}{dx} \left[\left(-\frac{\cos 2\theta}{(1+\varepsilon)^2} \frac{d\dot{u}}{dx} - \frac{\sin 2\theta}{(1+\varepsilon)^2} \frac{d\dot{v}}{dx} \right) \frac{d}{dx} \right] \quad (\text{AIV.53})$$

Therefore from equations (AIV.50) and (AIV.51),

$$\begin{aligned} \dot{B}_{11}^* \delta u + \dot{B}_{12}^* \delta v &= \left[-\frac{\sin \theta}{1+\varepsilon} \frac{d\dot{u}}{dx} + \frac{\cos \theta}{1+\varepsilon} \frac{d\dot{v}}{dx} \right] \left[-\sin \theta \frac{d\delta u}{dx} + \cos \theta \frac{d\delta v}{dx} \right] \\ &= \left[-\frac{\sin \theta}{1+\varepsilon} \frac{d\delta u}{dx} + \frac{\cos \theta}{1+\varepsilon} \frac{d\delta v}{dx} \right] \left[-\sin \theta \frac{d\dot{u}}{dx} + \cos \theta \frac{d\dot{v}}{dx} \right] \quad (\text{AIV.54}) \end{aligned}$$

Thus it is seen that $\dot{B}_{11}^* \delta u + \dot{B}_{12}^* \delta v = \delta B_{11}^* \dot{u} + \delta B_{12}^* \dot{v}$. Similarly from equations (AIV.52) and

(AIV.53), it can be concluded that $\dot{B}_{21}^* \delta u + \dot{B}_{22}^* \delta v = \delta B_{21}^* \dot{u} + \delta B_{22}^* \dot{v}$. Combining these two

results, we have:

$$\dot{\mathbf{B}} \delta \mathbf{u} = \delta \mathbf{B} \dot{\mathbf{u}} \quad (\text{AIV.55})$$

Substituting equations (AIV.49) and (AIV.55) in equation (AIV.48) and using the fact that $\delta \mathbf{u} = 0$ at $t = 0$ and $t = T$, we get:

$$\delta \int_0^T \int_0^L \mathbf{J}^T \mathbf{B}^* \dot{\mathbf{u}} dx dt = \int_0^T \int_0^L \delta \mathbf{J}^T \mathbf{B}^* \dot{\mathbf{u}} dx dt - \int_0^T \int_0^L \dot{\mathbf{J}}^T \mathbf{B}^* \delta \mathbf{u} dx dt \quad (\text{AIV.56})$$

Using the adjoint relationship, equation (AIV.42):

$$\int_0^L \dot{\mathbf{J}}^T \mathbf{B}^* \delta \mathbf{u} dx = \int_0^L \delta \mathbf{u}^T \mathbf{B} \dot{\mathbf{J}} dx + \left(P \cos \theta + \frac{dM}{dx} \frac{\sin \theta}{1 + \varepsilon} \right) \delta q_1 + M(L) \delta q_3 - M(0) \delta q_2 \quad (\text{AIV.57})$$

Substituting equation (AIV.57) in (AIV.56) and then equations (AIV.46), (AIV.47) and (AIV.56) in (AIV.41) and collecting the terms in $\delta \mathbf{u}$, $\delta \mathbf{J}$ and $\delta \mathbf{q}$, we have:

$$\begin{aligned} & \int_0^T \int_0^L \delta \mathbf{u}^T \left(\rho_0 \ddot{\mathbf{u}} + \frac{\partial \varphi}{\partial \dot{\mathbf{u}}} + \mathbf{B} \dot{\mathbf{J}} - \mathbf{f} \right) dx dt + \int_0^T \int_0^L \delta \mathbf{J}^T \left(\mathbf{a} \ddot{\mathbf{J}} + \frac{\partial \varphi}{\partial \dot{\mathbf{J}}} - \mathbf{B}^* \dot{\mathbf{u}} \right) dx dt \\ & - \int_0^T \left(Q_1 - P \cos \theta + \frac{dM}{dx} \frac{\sin \theta}{1 + \varepsilon} \right) \delta q_1 dt - \int_0^T (Q_2 - M(L)) \delta q_1 dt - \int_0^T (Q_3 + M(0)) \delta q_1 dt \quad (\text{AIV.58}) \\ & = 0 \end{aligned}$$

Due to the arbitrariness of the virtual displacement and impulse fields, we have the pointwise relations:

$$\rho_0 \ddot{\mathbf{u}} + \frac{\partial \varphi}{\partial \dot{\mathbf{u}}} + \mathbf{B} \dot{\mathbf{J}} - \mathbf{f} = \mathbf{0} \quad (\text{AIV.59})$$

$$\mathbf{a} \ddot{\mathbf{J}} + \frac{\partial \varphi}{\partial \dot{\mathbf{J}}} - \mathbf{B}^* \dot{\mathbf{u}} = \mathbf{0} \quad (\text{AIV.60})$$

$$\begin{aligned} Q_1 &= P \cos \theta + \frac{dM}{dx} \frac{\sin \theta}{1 + \varepsilon} \\ Q_2 &= M(L) \\ Q_3 &= -M(0) \end{aligned} \quad (\text{AIV.61})$$

Equation (AIV.59) is the equation of equilibrium of an infinitesimal segment of the beam. This can be verified (see for example, Huddleston (1979)). Equation (AIV.60) is the equation of compatibility and equations (AIV.61) are the boundary conditions.

It is recognized that the key to the proposed Lagrangian formulation being invariant under finite deformations in all three cases, the discrete case in Section 5 and the continuum and beam-column discussed in this Appendix is the symmetry of the derivative of the compatibility operator with respect to the displacement field.

Multidisciplinary Center for Earthquake Engineering Research List of Technical Reports

The Multidisciplinary Center for Earthquake Engineering Research (MCEER) publishes technical reports on a variety of subjects related to earthquake engineering written by authors funded through MCEER. These reports are available from both MCEER Publications and the National Technical Information Service (NTIS). Requests for reports should be directed to MCEER Publications, Multidisciplinary Center for Earthquake Engineering Research, State University of New York at Buffalo, Red Jacket Quadrangle, Buffalo, New York 14261. Reports can also be requested through NTIS, 5285 Port Royal Road, Springfield, Virginia 22161. NTIS accession numbers are shown in parenthesis, if available.

- NCEER-87-0001 "First-Year Program in Research, Education and Technology Transfer," 3/5/87, (PB88-134275, A04, MF-A01).
- NCEER-87-0002 "Experimental Evaluation of Instantaneous Optimal Algorithms for Structural Control," by R.C. Lin, T.T. Soong and A.M. Reinhorn, 4/20/87, (PB88-134341, A04, MF-A01).
- NCEER-87-0003 "Experimentation Using the Earthquake Simulation Facilities at University at Buffalo," by A.M. Reinhorn and R.L. Ketter, to be published.
- NCEER-87-0004 "The System Characteristics and Performance of a Shaking Table," by J.S. Hwang, K.C. Chang and G.C. Lee, 6/1/87, (PB88-134259, A03, MF-A01). This report is available only through NTIS (see address given above).
- NCEER-87-0005 "A Finite Element Formulation for Nonlinear Viscoplastic Material Using a Q Model," by O. Gyebe and G. Dasgupta, 11/2/87, (PB88-213764, A08, MF-A01).
- NCEER-87-0006 "Symbolic Manipulation Program (SMP) - Algebraic Codes for Two and Three Dimensional Finite Element Formulations," by X. Lee and G. Dasgupta, 11/9/87, (PB88-218522, A05, MF-A01).
- NCEER-87-0007 "Instantaneous Optimal Control Laws for Tall Buildings Under Seismic Excitations," by J.N. Yang, A. Akbarpour and P. Ghaemmaghami, 6/10/87, (PB88-134333, A06, MF-A01). This report is only available through NTIS (see address given above).
- NCEER-87-0008 "IDARC: Inelastic Damage Analysis of Reinforced Concrete Frame - Shear-Wall Structures," by Y.J. Park, A.M. Reinhorn and S.K. Kunnath, 7/20/87, (PB88-134325, A09, MF-A01). This report is only available through NTIS (see address given above).
- NCEER-87-0009 "Liquefaction Potential for New York State: A Preliminary Report on Sites in Manhattan and Buffalo," by M. Budhu, V. Vijayakumar, R.F. Giese and L. Baumgras, 8/31/87, (PB88-163704, A03, MF-A01). This report is available only through NTIS (see address given above).
- NCEER-87-0010 "Vertical and Torsional Vibration of Foundations in Inhomogeneous Media," by A.S. Veletsos and K.W. Dotson, 6/1/87, (PB88-134291, A03, MF-A01). This report is only available through NTIS (see address given above).
- NCEER-87-0011 "Seismic Probabilistic Risk Assessment and Seismic Margins Studies for Nuclear Power Plants," by Howard H.M. Hwang, 6/15/87, (PB88-134267, A03, MF-A01). This report is only available through NTIS (see address given above).
- NCEER-87-0012 "Parametric Studies of Frequency Response of Secondary Systems Under Ground-Acceleration Excitations," by Y. Yong and Y.K. Lin, 6/10/87, (PB88-134309, A03, MF-A01). This report is only available through NTIS (see address given above).
- NCEER-87-0013 "Frequency Response of Secondary Systems Under Seismic Excitation," by J.A. HoLung, J. Cai and Y.K. Lin, 7/31/87, (PB88-134317, A05, MF-A01). This report is only available through NTIS (see address given above).
- NCEER-87-0014 "Modelling Earthquake Ground Motions in Seismically Active Regions Using Parametric Time Series Methods," by G.W. Ellis and A.S. Cakmak, 8/25/87, (PB88-134283, A08, MF-A01). This report is only available through NTIS (see address given above).

- NCEER-87-0015 "Detection and Assessment of Seismic Structural Damage," by E. DiPasquale and A.S. Cakmak, 8/25/87, (PB88-163712, A05, MF-A01). This report is only available through NTIS (see address given above).
- NCEER-87-0016 "Pipeline Experiment at Parkfield, California," by J. Isenberg and E. Richardson, 9/15/87, (PB88-163720, A03, MF-A01). This report is available only through NTIS (see address given above).
- NCEER-87-0017 "Digital Simulation of Seismic Ground Motion," by M. Shinozuka, G. Deodatis and T. Harada, 8/31/87, (PB88-155197, A04, MF-A01). This report is available only through NTIS (see address given above).
- NCEER-87-0018 "Practical Considerations for Structural Control: System Uncertainty, System Time Delay and Truncation of Small Control Forces," J.N. Yang and A. Akbarpour, 8/10/87, (PB88-163738, A08, MF-A01). This report is only available through NTIS (see address given above).
- NCEER-87-0019 "Modal Analysis of Nonclassically Damped Structural Systems Using Canonical Transformation," by J.N. Yang, S. Sarkani and F.X. Long, 9/27/87, (PB88-187851, A04, MF-A01).
- NCEER-87-0020 "A Nonstationary Solution in Random Vibration Theory," by J.R. Red-Horse and P.D. Spanos, 11/3/87, (PB88-163746, A03, MF-A01).
- NCEER-87-0021 "Horizontal Impedances for Radially Inhomogeneous Viscoelastic Soil Layers," by A.S. Veletsos and K.W. Dotson, 10/15/87, (PB88-150859, A04, MF-A01).
- NCEER-87-0022 "Seismic Damage Assessment of Reinforced Concrete Members," by Y.S. Chung, C. Meyer and M. Shinozuka, 10/9/87, (PB88-150867, A05, MF-A01). This report is available only through NTIS (see address given above).
- NCEER-87-0023 "Active Structural Control in Civil Engineering," by T.T. Soong, 11/11/87, (PB88-187778, A03, MF-A01).
- NCEER-87-0024 "Vertical and Torsional Impedances for Radially Inhomogeneous Viscoelastic Soil Layers," by K.W. Dotson and A.S. Veletsos, 12/87, (PB88-187786, A03, MF-A01).
- NCEER-87-0025 "Proceedings from the Symposium on Seismic Hazards, Ground Motions, Soil-Liquefaction and Engineering Practice in Eastern North America," October 20-22, 1987, edited by K.H. Jacob, 12/87, (PB88-188115, A23, MF-A01). This report is available only through NTIS (see address given above).
- NCEER-87-0026 "Report on the Whittier-Narrows, California, Earthquake of October 1, 1987," by J. Pantelic and A. Reinhorn, 11/87, (PB88-187752, A03, MF-A01). This report is available only through NTIS (see address given above).
- NCEER-87-0027 "Design of a Modular Program for Transient Nonlinear Analysis of Large 3-D Building Structures," by S. Srivastav and J.F. Abel, 12/30/87, (PB88-187950, A05, MF-A01). This report is only available through NTIS (see address given above).
- NCEER-87-0028 "Second-Year Program in Research, Education and Technology Transfer," 3/8/88, (PB88-219480, A04, MF-A01).
- NCEER-88-0001 "Workshop on Seismic Computer Analysis and Design of Buildings With Interactive Graphics," by W. McGuire, J.F. Abel and C.H. Conley, 1/18/88, (PB88-187760, A03, MF-A01). This report is only available through NTIS (see address given above).
- NCEER-88-0002 "Optimal Control of Nonlinear Flexible Structures," by J.N. Yang, F.X. Long and D. Wong, 1/22/88, (PB88-213772, A06, MF-A01).
- NCEER-88-0003 "Substructuring Techniques in the Time Domain for Primary-Secondary Structural Systems," by G.D. Manolis and G. Juhn, 2/10/88, (PB88-213780, A04, MF-A01).
- NCEER-88-0004 "Iterative Seismic Analysis of Primary-Secondary Systems," by A. Singhal, L.D. Lutes and P.D. Spanos, 2/23/88, (PB88-213798, A04, MF-A01).

- NCEER-88-0005 "Stochastic Finite Element Expansion for Random Media," by P.D. Spanos and R. Ghanem, 3/14/88, (PB88-213806, A03, MF-A01).
- NCEER-88-0006 "Combining Structural Optimization and Structural Control," by F.Y. Cheng and C.P. Pantelides, 1/10/88, (PB88-213814, A05, MF-A01).
- NCEER-88-0007 "Seismic Performance Assessment of Code-Designed Structures," by H.H-M. Hwang, J-W. Jaw and H-J. Shau, 3/20/88, (PB88-219423, A04, MF-A01). This report is only available through NTIS (see address given above).
- NCEER-88-0008 "Reliability Analysis of Code-Designed Structures Under Natural Hazards," by H.H-M. Hwang, H. Ushiba and M. Shinozuka, 2/29/88, (PB88-229471, A07, MF-A01). This report is only available through NTIS (see address given above).
- NCEER-88-0009 "Seismic Fragility Analysis of Shear Wall Structures," by J-W Jaw and H.H-M. Hwang, 4/30/88, (PB89-102867, A04, MF-A01).
- NCEER-88-0010 "Base Isolation of a Multi-Story Building Under a Harmonic Ground Motion - A Comparison of Performances of Various Systems," by F-G Fan, G. Ahmadi and I.G. Tadjbakhsh, 5/18/88, (PB89-122238, A06, MF-A01). This report is only available through NTIS (see address given above).
- NCEER-88-0011 "Seismic Floor Response Spectra for a Combined System by Green's Functions," by F.M. Lavelle, L.A. Bergman and P.D. Spanos, 5/1/88, (PB89-102875, A03, MF-A01).
- NCEER-88-0012 "A New Solution Technique for Randomly Excited Hysteretic Structures," by G.Q. Cai and Y.K. Lin, 5/16/88, (PB89-102883, A03, MF-A01).
- NCEER-88-0013 "A Study of Radiation Damping and Soil-Structure Interaction Effects in the Centrifuge," by K. Weissman, supervised by J.H. Prevost, 5/24/88, (PB89-144703, A06, MF-A01).
- NCEER-88-0014 "Parameter Identification and Implementation of a Kinematic Plasticity Model for Frictional Soils," by J.H. Prevost and D.V. Griffiths, to be published.
- NCEER-88-0015 "Two- and Three- Dimensional Dynamic Finite Element Analyses of the Long Valley Dam," by D.V. Griffiths and J.H. Prevost, 6/17/88, (PB89-144711, A04, MF-A01).
- NCEER-88-0016 "Damage Assessment of Reinforced Concrete Structures in Eastern United States," by A.M. Reinhorn, M.J. Seidel, S.K. Kunnath and Y.J. Park, 6/15/88, (PB89-122220, A04, MF-A01). This report is only available through NTIS (see address given above).
- NCEER-88-0017 "Dynamic Compliance of Vertically Loaded Strip Foundations in Multilayered Viscoelastic Soils," by S. Ahmad and A.S.M. Israil, 6/17/88, (PB89-102891, A04, MF-A01).
- NCEER-88-0018 "An Experimental Study of Seismic Structural Response With Added Viscoelastic Dampers," by R.C. Lin, Z. Liang, T.T. Soong and R.H. Zhang, 6/30/88, (PB89-122212, A05, MF-A01). This report is available only through NTIS (see address given above).
- NCEER-88-0019 "Experimental Investigation of Primary - Secondary System Interaction," by G.D. Manolis, G. Juhn and A.M. Reinhorn, 5/27/88, (PB89-122204, A04, MF-A01).
- NCEER-88-0020 "A Response Spectrum Approach For Analysis of Nonclassically Damped Structures," by J.N. Yang, S. Sarkani and F.X. Long, 4/22/88, (PB89-102909, A04, MF-A01).
- NCEER-88-0021 "Seismic Interaction of Structures and Soils: Stochastic Approach," by A.S. Veletsos and A.M. Prasad, 7/21/88, (PB89-122196, A04, MF-A01). This report is only available through NTIS (see address given above).
- NCEER-88-0022 "Identification of the Serviceability Limit State and Detection of Seismic Structural Damage," by E. DiPasquale and A.S. Cakmak, 6/15/88, (PB89-122188, A05, MF-A01). This report is available only through NTIS (see address given above).

- NCEER-88-0023 "Multi-Hazard Risk Analysis: Case of a Simple Offshore Structure," by B.K. Bhartia and E.H. Vanmarcke, 7/21/88, (PB89-145213, A05, MF-A01).
- NCEER-88-0024 "Automated Seismic Design of Reinforced Concrete Buildings," by Y.S. Chung, C. Meyer and M. Shinozuka, 7/5/88, (PB89-122170, A06, MF-A01). This report is available only through NTIS (see address given above).
- NCEER-88-0025 "Experimental Study of Active Control of MDOF Structures Under Seismic Excitations," by L.L. Chung, R.C. Lin, T.T. Soong and A.M. Reinhorn, 7/10/88, (PB89-122600, A04, MF-A01).
- NCEER-88-0026 "Earthquake Simulation Tests of a Low-Rise Metal Structure," by J.S. Hwang, K.C. Chang, G.C. Lee and R.L. Ketter, 8/1/88, (PB89-102917, A04, MF-A01).
- NCEER-88-0027 "Systems Study of Urban Response and Reconstruction Due to Catastrophic Earthquakes," by F. Kozin and H.K. Zhou, 9/22/88, (PB90-162348, A04, MF-A01).
- NCEER-88-0028 "Seismic Fragility Analysis of Plane Frame Structures," by H.H-M. Hwang and Y.K. Low, 7/31/88, (PB89-131445, A06, MF-A01).
- NCEER-88-0029 "Response Analysis of Stochastic Structures," by A. Kardara, C. Bucher and M. Shinozuka, 9/22/88, (PB89-174429, A04, MF-A01).
- NCEER-88-0030 "Nonnormal Accelerations Due to Yielding in a Primary Structure," by D.C.K. Chen and L.D. Lutes, 9/19/88, (PB89-131437, A04, MF-A01).
- NCEER-88-0031 "Design Approaches for Soil-Structure Interaction," by A.S. Veletsos, A.M. Prasad and Y. Tang, 12/30/88, (PB89-174437, A03, MF-A01). This report is available only through NTIS (see address given above).
- NCEER-88-0032 "A Re-evaluation of Design Spectra for Seismic Damage Control," by C.J. Turkstra and A.G. Tallin, 11/7/88, (PB89-145221, A05, MF-A01).
- NCEER-88-0033 "The Behavior and Design of Noncontact Lap Splices Subjected to Repeated Inelastic Tensile Loading," by V.E. Sagan, P. Gergely and R.N. White, 12/8/88, (PB89-163737, A08, MF-A01).
- NCEER-88-0034 "Seismic Response of Pile Foundations," by S.M. Mamoon, P.K. Banerjee and S. Ahmad, 11/1/88, (PB89-145239, A04, MF-A01).
- NCEER-88-0035 "Modeling of R/C Building Structures With Flexible Floor Diaphragms (IDARC2)," by A.M. Reinhorn, S.K. Kunnath and N. Panahshahi, 9/7/88, (PB89-207153, A07, MF-A01).
- NCEER-88-0036 "Solution of the Dam-Reservoir Interaction Problem Using a Combination of FEM, BEM with Particular Integrals, Modal Analysis, and Substructuring," by C-S. Tsai, G.C. Lee and R.L. Ketter, 12/31/88, (PB89-207146, A04, MF-A01).
- NCEER-88-0037 "Optimal Placement of Actuators for Structural Control," by F.Y. Cheng and C.P. Pantelides, 8/15/88, (PB89-162846, A05, MF-A01).
- NCEER-88-0038 "Teflon Bearings in Aseismic Base Isolation: Experimental Studies and Mathematical Modeling," by A. Mokha, M.C. Constantinou and A.M. Reinhorn, 12/5/88, (PB89-218457, A10, MF-A01). This report is available only through NTIS (see address given above).
- NCEER-88-0039 "Seismic Behavior of Flat Slab High-Rise Buildings in the New York City Area," by P. Weidlinger and M. Ettouney, 10/15/88, (PB90-145681, A04, MF-A01).
- NCEER-88-0040 "Evaluation of the Earthquake Resistance of Existing Buildings in New York City," by P. Weidlinger and M. Ettouney, 10/15/88, to be published.
- NCEER-88-0041 "Small-Scale Modeling Techniques for Reinforced Concrete Structures Subjected to Seismic Loads," by W. Kim, A. El-Attar and R.N. White, 11/22/88, (PB89-189625, A05, MF-A01).

- NCEER-88-0042 "Modeling Strong Ground Motion from Multiple Event Earthquakes," by G.W. Ellis and A.S. Cakmak, 10/15/88, (PB89-174445, A03, MF-A01).
- NCEER-88-0043 "Nonstationary Models of Seismic Ground Acceleration," by M. Grigoriu, S.E. Ruiz and E. Rosenblueth, 7/15/88, (PB89-189617, A04, MF-A01).
- NCEER-88-0044 "SARCF User's Guide: Seismic Analysis of Reinforced Concrete Frames," by Y.S. Chung, C. Meyer and M. Shinozuka, 11/9/88, (PB89-174452, A08, MF-A01).
- NCEER-88-0045 "First Expert Panel Meeting on Disaster Research and Planning," edited by J. Pantelic and J. Stoyke, 9/15/88, (PB89-174460, A05, MF-A01).
- NCEER-88-0046 "Preliminary Studies of the Effect of Degrading Infill Walls on the Nonlinear Seismic Response of Steel Frames," by C.Z. Chrysostomou, P. Gergely and J.F. Abel, 12/19/88, (PB89-208383, A05, MF-A01).
- NCEER-88-0047 "Reinforced Concrete Frame Component Testing Facility - Design, Construction, Instrumentation and Operation," by S.P. Pessiki, C. Conley, T. Bond, P. Gergely and R.N. White, 12/16/88, (PB89-174478, A04, MF-A01).
- NCEER-89-0001 "Effects of Protective Cushion and Soil Compliancy on the Response of Equipment Within a Seismically Excited Building," by J.A. HoLung, 2/16/89, (PB89-207179, A04, MF-A01).
- NCEER-89-0002 "Statistical Evaluation of Response Modification Factors for Reinforced Concrete Structures," by H.H-M. Hwang and J-W. Jaw, 2/17/89, (PB89-207187, A05, MF-A01).
- NCEER-89-0003 "Hysteretic Columns Under Random Excitation," by G-Q. Cai and Y.K. Lin, 1/9/89, (PB89-196513, A03, MF-A01).
- NCEER-89-0004 "Experimental Study of 'Elephant Foot Bulge' Instability of Thin-Walled Metal Tanks," by Z-H. Jia and R.L. Ketter, 2/22/89, (PB89-207195, A03, MF-A01).
- NCEER-89-0005 "Experiment on Performance of Buried Pipelines Across San Andreas Fault," by J. Isenberg, E. Richardson and T.D. O'Rourke, 3/10/89, (PB89-218440, A04, MF-A01). This report is available only through NTIS (see address given above).
- NCEER-89-0006 "A Knowledge-Based Approach to Structural Design of Earthquake-Resistant Buildings," by M. Subramani, P. Gergely, C.H. Conley, J.F. Abel and A.H. Zaghaw, 1/15/89, (PB89-218465, A06, MF-A01).
- NCEER-89-0007 "Liquefaction Hazards and Their Effects on Buried Pipelines," by T.D. O'Rourke and P.A. Lane, 2/1/89, (PB89-218481, A09, MF-A01).
- NCEER-89-0008 "Fundamentals of System Identification in Structural Dynamics," by H. Imai, C-B. Yun, O. Maruyama and M. Shinozuka, 1/26/89, (PB89-207211, A04, MF-A01).
- NCEER-89-0009 "Effects of the 1985 Michoacan Earthquake on Water Systems and Other Buried Lifelines in Mexico," by A.G. Ayala and M.J. O'Rourke, 3/8/89, (PB89-207229, A06, MF-A01).
- NCEER-89-R010 "NCEER Bibliography of Earthquake Education Materials," by K.E.K. Ross, Second Revision, 9/1/89, (PB90-125352, A05, MF-A01). This report is replaced by NCEER-92-0018.
- NCEER-89-0011 "Inelastic Three-Dimensional Response Analysis of Reinforced Concrete Building Structures (IDARC-3D), Part I - Modeling," by S.K. Kunnath and A.M. Reinhorn, 4/17/89, (PB90-114612, A07, MF-A01). This report is available only through NTIS (see address given above).
- NCEER-89-0012 "Recommended Modifications to ATC-14," by C.D. Poland and J.O. Malley, 4/12/89, (PB90-108648, A15, MF-A01).
- NCEER-89-0013 "Repair and Strengthening of Beam-to-Column Connections Subjected to Earthquake Loading," by M. Corazao and A.J. Durrani, 2/28/89, (PB90-109885, A06, MF-A01).

- NCEER-89-0014 "Program EXKAL2 for Identification of Structural Dynamic Systems," by O. Maruyama, C-B. Yun, M. Hoshiya and M. Shinozuka, 5/19/89, (PB90-109877, A09, MF-A01).
- NCEER-89-0015 "Response of Frames With Bolted Semi-Rigid Connections, Part I - Experimental Study and Analytical Predictions," by P.J. DiCorso, A.M. Reinhorn, J.R. Dickerson, J.B. Radzinski and W.L. Harper, 6/1/89, to be published.
- NCEER-89-0016 "ARMA Monte Carlo Simulation in Probabilistic Structural Analysis," by P.D. Spanos and M.P. Mignolet, 7/10/89, (PB90-109893, A03, MF-A01).
- NCEER-89-P017 "Preliminary Proceedings from the Conference on Disaster Preparedness - The Place of Earthquake Education in Our Schools," Edited by K.E.K. Ross, 6/23/89, (PB90-108606, A03, MF-A01).
- NCEER-89-0017 "Proceedings from the Conference on Disaster Preparedness - The Place of Earthquake Education in Our Schools," Edited by K.E.K. Ross, 12/31/89, (PB90-207895, A012, MF-A02). This report is available only through NTIS (see address given above).
- NCEER-89-0018 "Multidimensional Models of Hysteretic Material Behavior for Vibration Analysis of Shape Memory Energy Absorbing Devices, by E.J. Graesser and F.A. Cozzarelli, 6/7/89, (PB90-164146, A04, MF-A01).
- NCEER-89-0019 "Nonlinear Dynamic Analysis of Three-Dimensional Base Isolated Structures (3D-BASIS)," by S. Nagarajaiah, A.M. Reinhorn and M.C. Constantinou, 8/3/89, (PB90-161936, A06, MF-A01). This report has been replaced by NCEER-93-0011.
- NCEER-89-0020 "Structural Control Considering Time-Rate of Control Forces and Control Rate Constraints," by F.Y. Cheng and C.P. Pantelides, 8/3/89, (PB90-120445, A04, MF-A01).
- NCEER-89-0021 "Subsurface Conditions of Memphis and Shelby County," by K.W. Ng, T-S. Chang and H-H.M. Hwang, 7/26/89, (PB90-120437, A03, MF-A01).
- NCEER-89-0022 "Seismic Wave Propagation Effects on Straight Jointed Buried Pipelines," by K. Elhadi and M.J. O'Rourke, 8/24/89, (PB90-162322, A10, MF-A02).
- NCEER-89-0023 "Workshop on Serviceability Analysis of Water Delivery Systems," edited by M. Grigoriu, 3/6/89, (PB90-127424, A03, MF-A01).
- NCEER-89-0024 "Shaking Table Study of a 1/5 Scale Steel Frame Composed of Tapered Members," by K.C. Chang, J.S. Hwang and G.C. Lee, 9/18/89, (PB90-160169, A04, MF-A01).
- NCEER-89-0025 "DYNA1D: A Computer Program for Nonlinear Seismic Site Response Analysis - Technical Documentation," by Jean H. Prevost, 9/14/89, (PB90-161944, A07, MF-A01). This report is available only through NTIS (see address given above).
- NCEER-89-0026 "1:4 Scale Model Studies of Active Tendon Systems and Active Mass Dampers for Aseismic Protection," by A.M. Reinhorn, T.T. Soong, R.C. Lin, Y.P. Yang, Y. Fukao, H. Abe and M. Nakai, 9/15/89, (PB90-173246, A10, MF-A02). This report is available only through NTIS (see address given above).
- NCEER-89-0027 "Scattering of Waves by Inclusions in a Nonhomogeneous Elastic Half Space Solved by Boundary Element Methods," by P.K. Hadley, A. Askar and A.S. Cakmak, 6/15/89, (PB90-145699, A07, MF-A01).
- NCEER-89-0028 "Statistical Evaluation of Deflection Amplification Factors for Reinforced Concrete Structures," by H.H.M. Hwang, J-W. Jaw and A.L. Ch'ng, 8/31/89, (PB90-164633, A05, MF-A01).
- NCEER-89-0029 "Bedrock Accelerations in Memphis Area Due to Large New Madrid Earthquakes," by H.H.M. Hwang, C.H.S. Chen and G. Yu, 11/7/89, (PB90-162330, A04, MF-A01).
- NCEER-89-0030 "Seismic Behavior and Response Sensitivity of Secondary Structural Systems," by Y.Q. Chen and T.T. Soong, 10/23/89, (PB90-164658, A08, MF-A01).
- NCEER-89-0031 "Random Vibration and Reliability Analysis of Primary-Secondary Structural Systems," by Y. Ibrahim, M. Grigoriu and T.T. Soong, 11/10/89, (PB90-161951, A04, MF-A01).

- NCEER-89-0032 "Proceedings from the Second U.S. - Japan Workshop on Liquefaction, Large Ground Deformation and Their Effects on Lifelines, September 26-29, 1989," Edited by T.D. O'Rourke and M. Hamada, 12/1/89, (PB90-209388, A22, MF-A03).
- NCEER-89-0033 "Deterministic Model for Seismic Damage Evaluation of Reinforced Concrete Structures," by J.M. Bracci, A.M. Reinhorn, J.B. Mander and S.K. Kunnath, 9/27/89, (PB91-108803, A06, MF-A01).
- NCEER-89-0034 "On the Relation Between Local and Global Damage Indices," by E. DiPasquale and A.S. Cakmak, 8/15/89, (PB90-173865, A05, MF-A01).
- NCEER-89-0035 "Cyclic Undrained Behavior of Nonplastic and Low Plasticity Silts," by A.J. Walker and H.E. Stewart, 7/26/89, (PB90-183518, A10, MF-A01).
- NCEER-89-0036 "Liquefaction Potential of Surficial Deposits in the City of Buffalo, New York," by M. Budhu, R. Giese and L. Baumgrass, 1/17/89, (PB90-208455, A04, MF-A01).
- NCEER-89-0037 "A Deterministic Assessment of Effects of Ground Motion Incoherence," by A.S. Veletsos and Y. Tang, 7/15/89, (PB90-164294, A03, MF-A01).
- NCEER-89-0038 "Workshop on Ground Motion Parameters for Seismic Hazard Mapping," July 17-18, 1989, edited by R.V. Whitman, 12/1/89, (PB90-173923, A04, MF-A01).
- NCEER-89-0039 "Seismic Effects on Elevated Transit Lines of the New York City Transit Authority," by C.J. Costantino, C.A. Miller and E. Heymsfield, 12/26/89, (PB90-207887, A06, MF-A01).
- NCEER-89-0040 "Centrifugal Modeling of Dynamic Soil-Structure Interaction," by K. Weissman, Supervised by J.H. Prevost, 5/10/89, (PB90-207879, A07, MF-A01).
- NCEER-89-0041 "Linearized Identification of Buildings With Cores for Seismic Vulnerability Assessment," by I-K. Ho and A.E. Aktan, 11/1/89, (PB90-251943, A07, MF-A01).
- NCEER-90-0001 "Geotechnical and Lifeline Aspects of the October 17, 1989 Loma Prieta Earthquake in San Francisco," by T.D. O'Rourke, H.E. Stewart, F.T. Blackburn and T.S. Dickerman, 1/90, (PB90-208596, A05, MF-A01).
- NCEER-90-0002 "Nonnormal Secondary Response Due to Yielding in a Primary Structure," by D.C.K. Chen and L.D. Lutes, 2/28/90, (PB90-251976, A07, MF-A01).
- NCEER-90-0003 "Earthquake Education Materials for Grades K-12," by K.E.K. Ross, 4/16/90, (PB91-251984, A05, MF-A05). This report has been replaced by NCEER-92-0018.
- NCEER-90-0004 "Catalog of Strong Motion Stations in Eastern North America," by R.W. Busby, 4/3/90, (PB90-251984, A05, MF-A01).
- NCEER-90-0005 "NCEER Strong-Motion Data Base: A User Manual for the GeoBase Release (Version 1.0 for the Sun3)," by P. Friberg and K. Jacob, 3/31/90 (PB90-258062, A04, MF-A01).
- NCEER-90-0006 "Seismic Hazard Along a Crude Oil Pipeline in the Event of an 1811-1812 Type New Madrid Earthquake," by H.H.M. Hwang and C-H.S. Chen, 4/16/90, (PB90-258054, A04, MF-A01).
- NCEER-90-0007 "Site-Specific Response Spectra for Memphis Sheahan Pumping Station," by H.H.M. Hwang and C.S. Lee, 5/15/90, (PB91-108811, A05, MF-A01).
- NCEER-90-0008 "Pilot Study on Seismic Vulnerability of Crude Oil Transmission Systems," by T. Ariman, R. Dobry, M. Grigoriu, F. Kozin, M. O'Rourke, T. O'Rourke and M. Shinozuka, 5/25/90, (PB91-108837, A06, MF-A01).
- NCEER-90-0009 "A Program to Generate Site Dependent Time Histories: EQGEN," by G.W. Ellis, M. Srinivasan and A.S. Cakmak, 1/30/90, (PB91-108829, A04, MF-A01).
- NCEER-90-0010 "Active Isolation for Seismic Protection of Operating Rooms," by M.E. Talbott, Supervised by M. Shinozuka, 6/8/9, (PB91-110205, A05, MF-A01).

- NCEER-90-0011 "Program LINEARID for Identification of Linear Structural Dynamic Systems," by C-B. Yun and M. Shinozuka, 6/25/90, (PB91-110312, A08, MF-A01).
- NCEER-90-0012 "Two-Dimensional Two-Phase Elasto-Plastic Seismic Response of Earth Dams," by A.N. Yiagos, Supervised by J.H. Prevost, 6/20/90, (PB91-110197, A13, MF-A02).
- NCEER-90-0013 "Secondary Systems in Base-Isolated Structures: Experimental Investigation, Stochastic Response and Stochastic Sensitivity," by G.D. Manolis, G. Juhn, M.C. Constantinou and A.M. Reinhorn, 7/1/90, (PB91-110320, A08, MF-A01).
- NCEER-90-0014 "Seismic Behavior of Lightly-Reinforced Concrete Column and Beam-Column Joint Details," by S.P. Pessiki, C.H. Conley, P. Gergely and R.N. White, 8/22/90, (PB91-108795, A11, MF-A02).
- NCEER-90-0015 "Two Hybrid Control Systems for Building Structures Under Strong Earthquakes," by J.N. Yang and A. Danielians, 6/29/90, (PB91-125393, A04, MF-A01).
- NCEER-90-0016 "Instantaneous Optimal Control with Acceleration and Velocity Feedback," by J.N. Yang and Z. Li, 6/29/90, (PB91-125401, A03, MF-A01).
- NCEER-90-0017 "Reconnaissance Report on the Northern Iran Earthquake of June 21, 1990," by M. Mehrain, 10/4/90, (PB91-125377, A03, MF-A01).
- NCEER-90-0018 "Evaluation of Liquefaction Potential in Memphis and Shelby County," by T.S. Chang, P.S. Tang, C.S. Lee and H. Hwang, 8/10/90, (PB91-125427, A09, MF-A01).
- NCEER-90-0019 "Experimental and Analytical Study of a Combined Sliding Disc Bearing and Helical Steel Spring Isolation System," by M.C. Constantinou, A.S. Mokha and A.M. Reinhorn, 10/4/90, (PB91-125385, A06, MF-A01). This report is available only through NTIS (see address given above).
- NCEER-90-0020 "Experimental Study and Analytical Prediction of Earthquake Response of a Sliding Isolation System with a Spherical Surface," by A.S. Mokha, M.C. Constantinou and A.M. Reinhorn, 10/11/90, (PB91-125419, A05, MF-A01).
- NCEER-90-0021 "Dynamic Interaction Factors for Floating Pile Groups," by G. Gazetas, K. Fan, A. Kaynia and E. Kausel, 9/10/90, (PB91-170381, A05, MF-A01).
- NCEER-90-0022 "Evaluation of Seismic Damage Indices for Reinforced Concrete Structures," by S. Rodriguez-Gomez and A.S. Cakmak, 9/30/90, PB91-171322, A06, MF-A01).
- NCEER-90-0023 "Study of Site Response at a Selected Memphis Site," by H. Desai, S. Ahmad, E.S. Gazetas and M.R. Oh, 10/11/90, (PB91-196857, A03, MF-A01).
- NCEER-90-0024 "A User's Guide to Strongmo: Version 1.0 of NCEER's Strong-Motion Data Access Tool for PCs and Terminals," by P.A. Friberg and C.A.T. Susch, 11/15/90, (PB91-171272, A03, MF-A01).
- NCEER-90-0025 "A Three-Dimensional Analytical Study of Spatial Variability of Seismic Ground Motions," by L-L. Hong and A.H.-S. Ang, 10/30/90, (PB91-170399, A09, MF-A01).
- NCEER-90-0026 "MUMOID User's Guide - A Program for the Identification of Modal Parameters," by S. Rodriguez-Gomez and E. DiPasquale, 9/30/90, (PB91-171298, A04, MF-A01).
- NCEER-90-0027 "SARCF-II User's Guide - Seismic Analysis of Reinforced Concrete Frames," by S. Rodriguez-Gomez, Y.S. Chung and C. Meyer, 9/30/90, (PB91-171280, A05, MF-A01).
- NCEER-90-0028 "Viscous Dampers: Testing, Modeling and Application in Vibration and Seismic Isolation," by N. Makris and M.C. Constantinou, 12/20/90 (PB91-190561, A06, MF-A01).
- NCEER-90-0029 "Soil Effects on Earthquake Ground Motions in the Memphis Area," by H. Hwang, C.S. Lee, K.W. Ng and T.S. Chang, 8/2/90, (PB91-190751, A05, MF-A01).

- NCEER-91-0001 "Proceedings from the Third Japan-U.S. Workshop on Earthquake Resistant Design of Lifeline Facilities and Countermeasures for Soil Liquefaction, December 17-19, 1990," edited by T.D. O'Rourke and M. Hamada, 2/1/91, (PB91-179259, A99, MF-A04).
- NCEER-91-0002 "Physical Space Solutions of Non-Proportionally Damped Systems," by M. Tong, Z. Liang and G.C. Lee, 1/15/91, (PB91-179242, A04, MF-A01).
- NCEER-91-0003 "Seismic Response of Single Piles and Pile Groups," by K. Fan and G. Gazetas, 1/10/91, (PB92-174994, A04, MF-A01).
- NCEER-91-0004 "Damping of Structures: Part 1 - Theory of Complex Damping," by Z. Liang and G. Lee, 10/10/91, (PB92-197235, A12, MF-A03).
- NCEER-91-0005 "3D-BASIS - Nonlinear Dynamic Analysis of Three Dimensional Base Isolated Structures: Part II," by S. Nagarajaiah, A.M. Reinhorn and M.C. Constantinou, 2/28/91, (PB91-190553, A07, MF-A01). This report has been replaced by NCEER-93-0011.
- NCEER-91-0006 "A Multidimensional Hysteretic Model for Plasticity Deforming Metals in Energy Absorbing Devices," by E.J. Graesser and F.A. Cozzarelli, 4/9/91, (PB92-108364, A04, MF-A01).
- NCEER-91-0007 "A Framework for Customizable Knowledge-Based Expert Systems with an Application to a KBES for Evaluating the Seismic Resistance of Existing Buildings," by E.G. Ibarra-Anaya and S.J. Fenves, 4/9/91, (PB91-210930, A08, MF-A01).
- NCEER-91-0008 "Nonlinear Analysis of Steel Frames with Semi-Rigid Connections Using the Capacity Spectrum Method," by G.G. Deierlein, S-H. Hsieh, Y-J. Shen and J.F. Abel, 7/2/91, (PB92-113828, A05, MF-A01).
- NCEER-91-0009 "Earthquake Education Materials for Grades K-12," by K.E.K. Ross, 4/30/91, (PB91-212142, A06, MF-A01). This report has been replaced by NCEER-92-0018.
- NCEER-91-0010 "Phase Wave Velocities and Displacement Phase Differences in a Harmonically Oscillating Pile," by N. Makris and G. Gazetas, 7/8/91, (PB92-108356, A04, MF-A01).
- NCEER-91-0011 "Dynamic Characteristics of a Full-Size Five-Story Steel Structure and a 2/5 Scale Model," by K.C. Chang, G.C. Yao, G.C. Lee, D.S. Hao and Y.C. Yeh, 7/2/91, (PB93-116648, A06, MF-A02).
- NCEER-91-0012 "Seismic Response of a 2/5 Scale Steel Structure with Added Viscoelastic Dampers," by K.C. Chang, T.T. Soong, S-T. Oh and M.L. Lai, 5/17/91, (PB92-110816, A05, MF-A01).
- NCEER-91-0013 "Earthquake Response of Retaining Walls; Full-Scale Testing and Computational Modeling," by S. Alampalli and A-W.M. Elgamal, 6/20/91, to be published.
- NCEER-91-0014 "3D-BASIS-M: Nonlinear Dynamic Analysis of Multiple Building Base Isolated Structures," by P.C. Tsopelas, S. Nagarajaiah, M.C. Constantinou and A.M. Reinhorn, 5/28/91, (PB92-113885, A09, MF-A02).
- NCEER-91-0015 "Evaluation of SEAOC Design Requirements for Sliding Isolated Structures," by D. Theodossiou and M.C. Constantinou, 6/10/91, (PB92-114602, A11, MF-A03).
- NCEER-91-0016 "Closed-Loop Modal Testing of a 27-Story Reinforced Concrete Flat Plate-Core Building," by H.R. Somaprasad, T. Toksoy, H. Yoshiyuki and A.E. Aktan, 7/15/91, (PB92-129980, A07, MF-A02).
- NCEER-91-0017 "Shake Table Test of a 1/6 Scale Two-Story Lightly Reinforced Concrete Building," by A.G. El-Attar, R.N. White and P. Gergely, 2/28/91, (PB92-222447, A06, MF-A02).
- NCEER-91-0018 "Shake Table Test of a 1/8 Scale Three-Story Lightly Reinforced Concrete Building," by A.G. El-Attar, R.N. White and P. Gergely, 2/28/91, (PB93-116630, A08, MF-A02).
- NCEER-91-0019 "Transfer Functions for Rigid Rectangular Foundations," by A.S. Veletsos, A.M. Prasad and W.H. Wu, 7/31/91, to be published.

- NCEER-91-0020 "Hybrid Control of Seismic-Excited Nonlinear and Inelastic Structural Systems," by J.N. Yang, Z. Li and A. Daniellians, 8/1/91, (PB92-143171, A06, MF-A02).
- NCEER-91-0021 "The NCEER-91 Earthquake Catalog: Improved Intensity-Based Magnitudes and Recurrence Relations for U.S. Earthquakes East of New Madrid," by L. Seeber and J.G. Armbruster, 8/28/91, (PB92-176742, A06, MF-A02).
- NCEER-91-0022 "Proceedings from the Implementation of Earthquake Planning and Education in Schools: The Need for Change - The Roles of the Changemakers," by K.E.K. Ross and F. Winslow, 7/23/91, (PB92-129998, A12, MF-A03).
- NCEER-91-0023 "A Study of Reliability-Based Criteria for Seismic Design of Reinforced Concrete Frame Buildings," by H.H.M. Hwang and H-M. Hsu, 8/10/91, (PB92-140235, A09, MF-A02).
- NCEER-91-0024 "Experimental Verification of a Number of Structural System Identification Algorithms," by R.G. Ghanem, H. Gavin and M. Shinozuka, 9/18/91, (PB92-176577, A18, MF-A04).
- NCEER-91-0025 "Probabilistic Evaluation of Liquefaction Potential," by H.H.M. Hwang and C.S. Lee," 11/25/91, (PB92-143429, A05, MF-A01).
- NCEER-91-0026 "Instantaneous Optimal Control for Linear, Nonlinear and Hysteretic Structures - Stable Controllers," by J.N. Yang and Z. Li, 11/15/91, (PB92-163807, A04, MF-A01).
- NCEER-91-0027 "Experimental and Theoretical Study of a Sliding Isolation System for Bridges," by M.C. Constantinou, A. Kartoum, A.M. Reinhorn and P. Bradford, 11/15/91, (PB92-176973, A10, MF-A03).
- NCEER-92-0001 "Case Studies of Liquefaction and Lifeline Performance During Past Earthquakes, Volume 1: Japanese Case Studies," Edited by M. Hamada and T. O'Rourke, 2/17/92, (PB92-197243, A18, MF-A04).
- NCEER-92-0002 "Case Studies of Liquefaction and Lifeline Performance During Past Earthquakes, Volume 2: United States Case Studies," Edited by T. O'Rourke and M. Hamada, 2/17/92, (PB92-197250, A20, MF-A04).
- NCEER-92-0003 "Issues in Earthquake Education," Edited by K. Ross, 2/3/92, (PB92-222389, A07, MF-A02).
- NCEER-92-0004 "Proceedings from the First U.S. - Japan Workshop on Earthquake Protective Systems for Bridges," Edited by I.G. Buckle, 2/4/92, (PB94-142239, A99, MF-A06).
- NCEER-92-0005 "Seismic Ground Motion from a Haskell-Type Source in a Multiple-Layered Half-Space," A.P. Theoharis, G. Deodatis and M. Shinozuka, 1/2/92, to be published.
- NCEER-92-0006 "Proceedings from the Site Effects Workshop," Edited by R. Whitman, 2/29/92, (PB92-197201, A04, MF-A01).
- NCEER-92-0007 "Engineering Evaluation of Permanent Ground Deformations Due to Seismically-Induced Liquefaction," by M.H. Baziar, R. Dobry and A-W.M. Elgamel, 3/24/92, (PB92-222421, A13, MF-A03).
- NCEER-92-0008 "A Procedure for the Seismic Evaluation of Buildings in the Central and Eastern United States," by C.D. Poland and J.O. Malley, 4/2/92, (PB92-222439, A20, MF-A04).
- NCEER-92-0009 "Experimental and Analytical Study of a Hybrid Isolation System Using Friction Controllable Sliding Bearings," by M.Q. Feng, S. Fujii and M. Shinozuka, 5/15/92, (PB93-150282, A06, MF-A02).
- NCEER-92-0010 "Seismic Resistance of Slab-Column Connections in Existing Non-Ductile Flat-Plate Buildings," by A.J. Durrani and Y. Du, 5/18/92, (PB93-116812, A06, MF-A02).
- NCEER-92-0011 "The Hysteretic and Dynamic Behavior of Brick Masonry Walls Upgraded by Ferrocement Coatings Under Cyclic Loading and Strong Simulated Ground Motion," by H. Lee and S.P. Prawl, 5/11/92, to be published.
- NCEER-92-0012 "Study of Wire Rope Systems for Seismic Protection of Equipment in Buildings," by G.F. Demetriades, M.C. Constantinou and A.M. Reinhorn, 5/20/92, (PB93-116655, A08, MF-A02).

- NCEER-92-0013 "Shape Memory Structural Dampers: Material Properties, Design and Seismic Testing," by P.R. Witting and F.A. Cozzarelli, 5/26/92, (PB93-116663, A05, MF-A01).
- NCEER-92-0014 "Longitudinal Permanent Ground Deformation Effects on Buried Continuous Pipelines," by M.J. O'Rourke, and C. Nordberg, 6/15/92, (PB93-116671, A08, MF-A02).
- NCEER-92-0015 "A Simulation Method for Stationary Gaussian Random Functions Based on the Sampling Theorem," by M. Grigoriu and S. Balopoulou, 6/11/92, (PB93-127496, A05, MF-A01).
- NCEER-92-0016 "Gravity-Load-Designed Reinforced Concrete Buildings: Seismic Evaluation of Existing Construction and Detailing Strategies for Improved Seismic Resistance," by G.W. Hoffmann, S.K. Kunnath, A.M. Reinhorn and J.B. Mander, 7/15/92, (PB94-142007, A08, MF-A02).
- NCEER-92-0017 "Observations on Water System and Pipeline Performance in the Limón Area of Costa Rica Due to the April 22, 1991 Earthquake," by M. O'Rourke and D. Ballantyne, 6/30/92, (PB93-126811, A06, MF-A02).
- NCEER-92-0018 "Fourth Edition of Earthquake Education Materials for Grades K-12," Edited by K.E.K. Ross, 8/10/92, (PB93-114023, A07, MF-A02).
- NCEER-92-0019 "Proceedings from the Fourth Japan-U.S. Workshop on Earthquake Resistant Design of Lifeline Facilities and Countermeasures for Soil Liquefaction," Edited by M. Hamada and T.D. O'Rourke, 8/12/92, (PB93-163939, A99, MF-E11).
- NCEER-92-0020 "Active Bracing System: A Full Scale Implementation of Active Control," by A.M. Reinhorn, T.T. Soong, R.C. Lin, M.A. Riley, Y.P. Wang, S. Aizawa and M. Higashino, 8/14/92, (PB93-127512, A06, MF-A02).
- NCEER-92-0021 "Empirical Analysis of Horizontal Ground Displacement Generated by Liquefaction-Induced Lateral Spreads," by S.F. Bartlett and T.L. Youd, 8/17/92, (PB93-188241, A06, MF-A02).
- NCEER-92-0022 "IDARC Version 3.0: Inelastic Damage Analysis of Reinforced Concrete Structures," by S.K. Kunnath, A.M. Reinhorn and R.F. Lobo, 8/31/92, (PB93-227502, A07, MF-A02).
- NCEER-92-0023 "A Semi-Empirical Analysis of Strong-Motion Peaks in Terms of Seismic Source, Propagation Path and Local Site Conditions, by M. Kamiyama, M.J. O'Rourke and R. Flores-Berrones, 9/9/92, (PB93-150266, A08, MF-A02).
- NCEER-92-0024 "Seismic Behavior of Reinforced Concrete Frame Structures with Nonductile Details, Part I: Summary of Experimental Findings of Full Scale Beam-Column Joint Tests," by A. Beres, R.N. White and P. Gergely, 9/30/92, (PB93-227783, A05, MF-A01).
- NCEER-92-0025 "Experimental Results of Repaired and Retrofitted Beam-Column Joint Tests in Lightly Reinforced Concrete Frame Buildings," by A. Beres, S. El-Borgi, R.N. White and P. Gergely, 10/29/92, (PB93-227791, A05, MF-A01).
- NCEER-92-0026 "A Generalization of Optimal Control Theory: Linear and Nonlinear Structures," by J.N. Yang, Z. Li and S. Vongchavalitkul, 11/2/92, (PB93-188621, A05, MF-A01).
- NCEER-92-0027 "Seismic Resistance of Reinforced Concrete Frame Structures Designed Only for Gravity Loads: Part I - Design and Properties of a One-Third Scale Model Structure," by J.M. Bracci, A.M. Reinhorn and J.B. Mander, 12/1/92, (PB94-104502, A08, MF-A02).
- NCEER-92-0028 "Seismic Resistance of Reinforced Concrete Frame Structures Designed Only for Gravity Loads: Part II - Experimental Performance of Subassemblages," by L.E. Aycaardi, J.B. Mander and A.M. Reinhorn, 12/1/92, (PB94-104510, A08, MF-A02).
- NCEER-92-0029 "Seismic Resistance of Reinforced Concrete Frame Structures Designed Only for Gravity Loads: Part III - Experimental Performance and Analytical Study of a Structural Model," by J.M. Bracci, A.M. Reinhorn and J.B. Mander, 12/1/92, (PB93-227528, A09, MF-A01).

- NCEER-92-0030 "Evaluation of Seismic Retrofit of Reinforced Concrete Frame Structures: Part I - Experimental Performance of Retrofitted Subassemblages," by D. Choudhuri, J.B. Mander and A.M. Reinhorn, 12/8/92, (PB93-198307, A07, MF-A02).
- NCEER-92-0031 "Evaluation of Seismic Retrofit of Reinforced Concrete Frame Structures: Part II - Experimental Performance and Analytical Study of a Retrofitted Structural Model," by J.M. Bracci, A.M. Reinhorn and J.B. Mander, 12/8/92, (PB93-198315, A09, MF-A03).
- NCEER-92-0032 "Experimental and Analytical Investigation of Seismic Response of Structures with Supplemental Fluid Viscous Dampers," by M.C. Constantinou and M.D. Symans, 12/21/92, (PB93-191435, A10, MF-A03). This report is available only through NTIS (see address given above).
- NCEER-92-0033 "Reconnaissance Report on the Cairo, Egypt Earthquake of October 12, 1992," by M. Khater, 12/23/92, (PB93-188621, A03, MF-A01).
- NCEER-92-0034 "Low-Level Dynamic Characteristics of Four Tall Flat-Plate Buildings in New York City," by H. Gavin, S. Yuan, J. Grossman, E. Pekelis and K. Jacob, 12/28/92, (PB93-188217, A07, MF-A02).
- NCEER-93-0001 "An Experimental Study on the Seismic Performance of Brick-Infilled Steel Frames With and Without Retrofit," by J.B. Mander, B. Nair, K. Wojtkowski and J. Ma, 1/29/93, (PB93-227510, A07, MF-A02).
- NCEER-93-0002 "Social Accounting for Disaster Preparedness and Recovery Planning," by S. Cole, E. Pantoja and V. Razak, 2/22/93, (PB94-142114, A12, MF-A03).
- NCEER-93-0003 "Assessment of 1991 NEHRP Provisions for Nonstructural Components and Recommended Revisions," by T.T. Soong, G. Chen, Z. Wu, R-H. Zhang and M. Grigoriu, 3/1/93, (PB93-188639, A06, MF-A02).
- NCEER-93-0004 "Evaluation of Static and Response Spectrum Analysis Procedures of SEAOC/UBC for Seismic Isolated Structures," by C.W. Winters and M.C. Constantinou, 3/23/93, (PB93-198299, A10, MF-A03).
- NCEER-93-0005 "Earthquakes in the Northeast - Are We Ignoring the Hazard? A Workshop on Earthquake Science and Safety for Educators," edited by K.E.K. Ross, 4/2/93, (PB94-103066, A09, MF-A02).
- NCEER-93-0006 "Inelastic Response of Reinforced Concrete Structures with Viscoelastic Braces," by R.F. Lobo, J.M. Bracci, K.L. Shen, A.M. Reinhorn and T.T. Soong, 4/5/93, (PB93-227486, A05, MF-A02).
- NCEER-93-0007 "Seismic Testing of Installation Methods for Computers and Data Processing Equipment," by K. Kosar, T.T. Soong, K.L. Shen, J.A. HoLung and Y.K. Lin, 4/12/93, (PB93-198299, A07, MF-A02).
- NCEER-93-0008 "Retrofit of Reinforced Concrete Frames Using Added Dampers," by A. Reinhorn, M. Constantinou and C. Li, to be published.
- NCEER-93-0009 "Seismic Behavior and Design Guidelines for Steel Frame Structures with Added Viscoelastic Dampers," by K.C. Chang, M.L. Lai, T.T. Soong, D.S. Hao and Y.C. Yeh, 5/1/93, (PB94-141959, A07, MF-A02).
- NCEER-93-0010 "Seismic Performance of Shear-Critical Reinforced Concrete Bridge Piers," by J.B. Mander, S.M. Waheed, M.T.A. Chaudhary and S.S. Chen, 5/12/93, (PB93-227494, A08, MF-A02).
- NCEER-93-0011 "3D-BASIS-TABS: Computer Program for Nonlinear Dynamic Analysis of Three Dimensional Base Isolated Structures," by S. Nagarajaiah, C. Li, A.M. Reinhorn and M.C. Constantinou, 8/2/93, (PB94-141819, A09, MF-A02).
- NCEER-93-0012 "Effects of Hydrocarbon Spills from an Oil Pipeline Break on Ground Water," by O.J. Helweg and H.H.M. Hwang, 8/3/93, (PB94-141942, A06, MF-A02).
- NCEER-93-0013 "Simplified Procedures for Seismic Design of Nonstructural Components and Assessment of Current Code Provisions," by M.P. Singh, L.E. Suarez, E.E. Matheu and G.O. Maldonado, 8/4/93, (PB94-141827, A09, MF-A02).
- NCEER-93-0014 "An Energy Approach to Seismic Analysis and Design of Secondary Systems," by G. Chen and T.T. Soong, 8/6/93, (PB94-142767, A11, MF-A03).

- NCEER-93-0015 "Proceedings from School Sites: Becoming Prepared for Earthquakes - Commemorating the Third Anniversary of the Loma Prieta Earthquake," Edited by F.E. Winslow and K.E.K. Ross, 8/16/93, (PB94-154275, A16, MF-A02).
- NCEER-93-0016 "Reconnaissance Report of Damage to Historic Monuments in Cairo, Egypt Following the October 12, 1992 Dahshur Earthquake," by D. Sykora, D. Look, G. Croci, E. Karaesmen and E. Karaesmen, 8/19/93, (PB94-142221, A08, MF-A02).
- NCEER-93-0017 "The Island of Guam Earthquake of August 8, 1993," by S.W. Swan and S.K. Harris, 9/30/93, (PB94-141843, A04, MF-A01).
- NCEER-93-0018 "Engineering Aspects of the October 12, 1992 Egyptian Earthquake," by A.W. Elgamal, M. Amer, K. Adalier and A. Abul-Fadl, 10/7/93, (PB94-141983, A05, MF-A01).
- NCEER-93-0019 "Development of an Earthquake Motion Simulator and its Application in Dynamic Centrifuge Testing," by I. Krstelj, Supervised by J.H. Prevost, 10/23/93, (PB94-181773, A-10, MF-A03).
- NCEER-93-0020 "NCEER-Taisei Corporation Research Program on Sliding Seismic Isolation Systems for Bridges: Experimental and Analytical Study of a Friction Pendulum System (FPS)," by M.C. Constantinou, P. Tsopelas, Y-S. Kim and S. Okamoto, 11/1/93, (PB94-142775, A08, MF-A02).
- NCEER-93-0021 "Finite Element Modeling of Elastomeric Seismic Isolation Bearings," by L.J. Billings, Supervised by R. Shepherd, 11/8/93, to be published.
- NCEER-93-0022 "Seismic Vulnerability of Equipment in Critical Facilities: Life-Safety and Operational Consequences," by K. Porter, G.S. Johnson, M.M. Zadeh, C. Scawthorn and S. Eder, 11/24/93, (PB94-181765, A16, MF-A03).
- NCEER-93-0023 "Hokkaido Nansei-oki, Japan Earthquake of July 12, 1993, by P.I. Yanev and C.R. Scawthorn, 12/23/93, (PB94-181500, A07, MF-A01).
- NCEER-94-0001 "An Evaluation of Seismic Serviceability of Water Supply Networks with Application to the San Francisco Auxiliary Water Supply System," by I. Markov, Supervised by M. Grigoriu and T. O'Rourke, 1/21/94, (PB94-204013, A07, MF-A02).
- NCEER-94-0002 "NCEER-Taisei Corporation Research Program on Sliding Seismic Isolation Systems for Bridges: Experimental and Analytical Study of Systems Consisting of Sliding Bearings, Rubber Restoring Force Devices and Fluid Dampers," Volumes I and II, by P. Tsopelas, S. Okamoto, M.C. Constantinou, D. Ozaki and S. Fujii, 2/4/94, (PB94-181740, A09, MF-A02 and PB94-181757, A12, MF-A03).
- NCEER-94-0003 "A Markov Model for Local and Global Damage Indices in Seismic Analysis," by S. Rahman and M. Grigoriu, 2/18/94, (PB94-206000, A12, MF-A03).
- NCEER-94-0004 "Proceedings from the NCEER Workshop on Seismic Response of Masonry Infills," edited by D.P. Abrams, 3/1/94, (PB94-180783, A07, MF-A02).
- NCEER-94-0005 "The Northridge, California Earthquake of January 17, 1994: General Reconnaissance Report," edited by J.D. Goltz, 3/11/94, (PB94-193943, A10, MF-A03).
- NCEER-94-0006 "Seismic Energy Based Fatigue Damage Analysis of Bridge Columns: Part I - Evaluation of Seismic Capacity," by G.A. Chang and J.B. Mander, 3/14/94, (PB94-219185, A11, MF-A03).
- NCEER-94-0007 "Seismic Isolation of Multi-Story Frame Structures Using Spherical Sliding Isolation Systems," by T.M. Al-Hussaini, V.A. Zayas and M.C. Constantinou, 3/17/94, (PB94-193745, A09, MF-A02).
- NCEER-94-0008 "The Northridge, California Earthquake of January 17, 1994: Performance of Highway Bridges," edited by I.G. Buckle, 3/24/94, (PB94-193851, A06, MF-A02).
- NCEER-94-0009 "Proceedings of the Third U.S.-Japan Workshop on Earthquake Protective Systems for Bridges," edited by I.G. Buckle and I. Friedland, 3/31/94, (PB94-195815, A99, MF-A06).

- NCEER-94-0010 "3D-BASIS-ME: Computer Program for Nonlinear Dynamic Analysis of Seismically Isolated Single and Multiple Structures and Liquid Storage Tanks," by P.C. Tsopelas, M.C. Constantinou and A.M. Reinhorn, 4/12/94, (PB94-204922, A09, MF-A02).
- NCEER-94-0011 "The Northridge, California Earthquake of January 17, 1994: Performance of Gas Transmission Pipelines," by T.D. O'Rourke and M.C. Palmer, 5/16/94, (PB94-204989, A05, MF-A01).
- NCEER-94-0012 "Feasibility Study of Replacement Procedures and Earthquake Performance Related to Gas Transmission Pipelines," by T.D. O'Rourke and M.C. Palmer, 5/25/94, (PB94-206638, A09, MF-A02).
- NCEER-94-0013 "Seismic Energy Based Fatigue Damage Analysis of Bridge Columns: Part II - Evaluation of Seismic Demand," by G.A. Chang and J.B. Mander, 6/1/94, (PB95-18106, A08, MF-A02).
- NCEER-94-0014 "NCEER-Taisei Corporation Research Program on Sliding Seismic Isolation Systems for Bridges: Experimental and Analytical Study of a System Consisting of Sliding Bearings and Fluid Restoring Force/Damping Devices," by P. Tsopelas and M.C. Constantinou, 6/13/94, (PB94-219144, A10, MF-A03).
- NCEER-94-0015 "Generation of Hazard-Consistent Fragility Curves for Seismic Loss Estimation Studies," by H. Hwang and J-R. Huo, 6/14/94, (PB95-181996, A09, MF-A02).
- NCEER-94-0016 "Seismic Study of Building Frames with Added Energy-Absorbing Devices," by W.S. Pong, C.S. Tsai and G.C. Lee, 6/20/94, (PB94-219136, A10, A03).
- NCEER-94-0017 "Sliding Mode Control for Seismic-Excited Linear and Nonlinear Civil Engineering Structures," by J. Yang, J. Wu, A. Agrawal and Z. Li, 6/21/94, (PB95-138483, A06, MF-A02).
- NCEER-94-0018 "3D-BASIS-TABS Version 2.0: Computer Program for Nonlinear Dynamic Analysis of Three Dimensional Base Isolated Structures," by A.M. Reinhorn, S. Nagarajaiah, M.C. Constantinou, P. Tsopelas and R. Li, 6/22/94, (PB95-182176, A08, MF-A02).
- NCEER-94-0019 "Proceedings of the International Workshop on Civil Infrastructure Systems: Application of Intelligent Systems and Advanced Materials on Bridge Systems," Edited by G.C. Lee and K.C. Chang, 7/18/94, (PB95-252474, A20, MF-A04).
- NCEER-94-0020 "Study of Seismic Isolation Systems for Computer Floors," by V. Lambrou and M.C. Constantinou, 7/19/94, (PB95-138533, A10, MF-A03).
- NCEER-94-0021 "Proceedings of the U.S.-Italian Workshop on Guidelines for Seismic Evaluation and Rehabilitation of Unreinforced Masonry Buildings," Edited by D.P. Abrams and G.M. Calvi, 7/20/94, (PB95-138749, A13, MF-A03).
- NCEER-94-0022 "NCEER-Taisei Corporation Research Program on Sliding Seismic Isolation Systems for Bridges: Experimental and Analytical Study of a System Consisting of Lubricated PTFE Sliding Bearings and Mild Steel Dampers," by P. Tsopelas and M.C. Constantinou, 7/22/94, (PB95-182184, A08, MF-A02).
- NCEER-94-0023 "Development of Reliability-Based Design Criteria for Buildings Under Seismic Load," by Y.K. Wen, H. Hwang and M. Shinozuka, 8/1/94, (PB95-211934, A08, MF-A02).
- NCEER-94-0024 "Experimental Verification of Acceleration Feedback Control Strategies for an Active Tendon System," by S.J. Dyke, B.F. Spencer, Jr., P. Quast, M.K. Sain, D.C. Kaspari, Jr. and T.T. Soong, 8/29/94, (PB95-212320, A05, MF-A01).
- NCEER-94-0025 "Seismic Retrofitting Manual for Highway Bridges," Edited by I.G. Buckle and I.F. Friedland, published by the Federal Highway Administration (PB95-212676, A15, MF-A03).
- NCEER-94-0026 "Proceedings from the Fifth U.S.-Japan Workshop on Earthquake Resistant Design of Lifeline Facilities and Countermeasures Against Soil Liquefaction," Edited by T.D. O'Rourke and M. Hamada, 11/7/94, (PB95-220802, A99, MF-E08).

- NCEER-95-0001 “Experimental and Analytical Investigation of Seismic Retrofit of Structures with Supplemental Damping: Part 1 - Fluid Viscous Damping Devices,” by A.M. Reinhorn, C. Li and M.C. Constantinou, 1/3/95, (PB95-266599, A09, MF-A02).
- NCEER-95-0002 “Experimental and Analytical Study of Low-Cycle Fatigue Behavior of Semi-Rigid Top-And-Seat Angle Connections,” by G. Pekcan, J.B. Mander and S.S. Chen, 1/5/95, (PB95-220042, A07, MF-A02).
- NCEER-95-0003 “NCEER-ATC Joint Study on Fragility of Buildings,” by T. Anagnos, C. Rojahn and A.S. Kiremidjian, 1/20/95, (PB95-220026, A06, MF-A02).
- NCEER-95-0004 “Nonlinear Control Algorithms for Peak Response Reduction,” by Z. Wu, T.T. Soong, V. Gattulli and R.C. Lin, 2/16/95, (PB95-220349, A05, MF-A01).
- NCEER-95-0005 “Pipeline Replacement Feasibility Study: A Methodology for Minimizing Seismic and Corrosion Risks to Underground Natural Gas Pipelines,” by R.T. Eguchi, H.A. Seligson and D.G. Honegger, 3/2/95, (PB95-252326, A06, MF-A02).
- NCEER-95-0006 “Evaluation of Seismic Performance of an 11-Story Frame Building During the 1994 Northridge Earthquake,” by F. Naeim, R. DiSulio, K. Benuska, A. Reinhorn and C. Li, to be published.
- NCEER-95-0007 “Prioritization of Bridges for Seismic Retrofitting,” by N. Basöz and A.S. Kiremidjian, 4/24/95, (PB95-252300, A08, MF-A02).
- NCEER-95-0008 “Method for Developing Motion Damage Relationships for Reinforced Concrete Frames,” by A. Singhal and A.S. Kiremidjian, 5/11/95, (PB95-266607, A06, MF-A02).
- NCEER-95-0009 “Experimental and Analytical Investigation of Seismic Retrofit of Structures with Supplemental Damping: Part II - Friction Devices,” by C. Li and A.M. Reinhorn, 7/6/95, (PB96-128087, A11, MF-A03).
- NCEER-95-0010 “Experimental Performance and Analytical Study of a Non-Ductile Reinforced Concrete Frame Structure Retrofitted with Elastomeric Spring Dampers,” by G. Pekcan, J.B. Mander and S.S. Chen, 7/14/95, (PB96-137161, A08, MF-A02).
- NCEER-95-0011 “Development and Experimental Study of Semi-Active Fluid Damping Devices for Seismic Protection of Structures,” by M.D. Symans and M.C. Constantinou, 8/3/95, (PB96-136940, A23, MF-A04).
- NCEER-95-0012 “Real-Time Structural Parameter Modification (RSPM): Development of Innervated Structures,” by Z. Liang, M. Tong and G.C. Lee, 4/11/95, (PB96-137153, A06, MF-A01).
- NCEER-95-0013 “Experimental and Analytical Investigation of Seismic Retrofit of Structures with Supplemental Damping: Part III - Viscous Damping Walls,” by A.M. Reinhorn and C. Li, 10/1/95, (PB96-176409, A11, MF-A03).
- NCEER-95-0014 “Seismic Fragility Analysis of Equipment and Structures in a Memphis Electric Substation,” by J-R. Huo and H.H.M. Hwang, 8/10/95, (PB96-128087, A09, MF-A02).
- NCEER-95-0015 “The Hanshin-Awaji Earthquake of January 17, 1995: Performance of Lifelines,” Edited by M. Shinozuka, 11/3/95, (PB96-176383, A15, MF-A03).
- NCEER-95-0016 “Highway Culvert Performance During Earthquakes,” by T.L. Youd and C.J. Beckman, available as NCEER-96-0015.
- NCEER-95-0017 “The Hanshin-Awaji Earthquake of January 17, 1995: Performance of Highway Bridges,” Edited by I.G. Buckle, 12/1/95, to be published.
- NCEER-95-0018 “Modeling of Masonry Infill Panels for Structural Analysis,” by A.M. Reinhorn, A. Madan, R.E. Valles, Y. Reichmann and J.B. Mander, 12/8/95, (PB97-110886, MF-A01, A06).
- NCEER-95-0019 “Optimal Polynomial Control for Linear and Nonlinear Structures,” by A.K. Agrawal and J.N. Yang, 12/11/95, (PB96-168737, A07, MF-A02).

- NCEER-95-0020 "Retrofit of Non-Ductile Reinforced Concrete Frames Using Friction Dampers," by R.S. Rao, P. Gergely and R.N. White, 12/22/95, (PB97-133508, A10, MF-A02).
- NCEER-95-0021 "Parametric Results for Seismic Response of Pile-Supported Bridge Bents," by G. Mylonakis, A. Nikolaou and G. Gazetas, 12/22/95, (PB97-100242, A12, MF-A03).
- NCEER-95-0022 "Kinematic Bending Moments in Seismically Stressed Piles," by A. Nikolaou, G. Mylonakis and G. Gazetas, 12/23/95, (PB97-113914, MF-A03, A13).
- NCEER-96-0001 "Dynamic Response of Unreinforced Masonry Buildings with Flexible Diaphragms," by A.C. Costley and D.P. Abrams, 10/10/96, (PB97-133573, MF-A03, A15).
- NCEER-96-0002 "State of the Art Review: Foundations and Retaining Structures," by I. Po Lam, to be published.
- NCEER-96-0003 "Ductility of Rectangular Reinforced Concrete Bridge Columns with Moderate Confinement," by N. Wehbe, M. Saiidi, D. Sanders and B. Douglas, 11/7/96, (PB97-133557, A06, MF-A02).
- NCEER-96-0004 "Proceedings of the Long-Span Bridge Seismic Research Workshop," edited by I.G. Buckle and I.M. Friedland, to be published.
- NCEER-96-0005 "Establish Representative Pier Types for Comprehensive Study: Eastern United States," by J. Kulicki and Z. Prucz, 5/28/96, (PB98-119217, A07, MF-A02).
- NCEER-96-0006 "Establish Representative Pier Types for Comprehensive Study: Western United States," by R. Imbsen, R.A. Schamber and T.A. Osterkamp, 5/28/96, (PB98-118607, A07, MF-A02).
- NCEER-96-0007 "Nonlinear Control Techniques for Dynamical Systems with Uncertain Parameters," by R.G. Ghanem and M.I. Bujakov, 5/27/96, (PB97-100259, A17, MF-A03).
- NCEER-96-0008 "Seismic Evaluation of a 30-Year Old Non-Ductile Highway Bridge Pier and Its Retrofit," by J.B. Mander, B. Mahmoodzadegan, S. Bhadra and S.S. Chen, 5/31/96, (PB97-110902, MF-A03, A10).
- NCEER-96-0009 "Seismic Performance of a Model Reinforced Concrete Bridge Pier Before and After Retrofit," by J.B. Mander, J.H. Kim and C.A. Ligozio, 5/31/96, (PB97-110910, MF-A02, A10).
- NCEER-96-0010 "IDARC2D Version 4.0: A Computer Program for the Inelastic Damage Analysis of Buildings," by R.E. Valles, A.M. Reinhorn, S.K. Kunnath, C. Li and A. Madan, 6/3/96, (PB97-100234, A17, MF-A03).
- NCEER-96-0011 "Estimation of the Economic Impact of Multiple Lifeline Disruption: Memphis Light, Gas and Water Division Case Study," by S.E. Chang, H.A. Seligson and R.T. Eguchi, 8/16/96, (PB97-133490, A11, MF-A03).
- NCEER-96-0012 "Proceedings from the Sixth Japan-U.S. Workshop on Earthquake Resistant Design of Lifeline Facilities and Countermeasures Against Soil Liquefaction, Edited by M. Hamada and T. O'Rourke, 9/11/96, (PB97-133581, A99, MF-A06).
- NCEER-96-0013 "Chemical Hazards, Mitigation and Preparedness in Areas of High Seismic Risk: A Methodology for Estimating the Risk of Post-Earthquake Hazardous Materials Release," by H.A. Seligson, R.T. Eguchi, K.J. Tierney and K. Richmond, 11/7/96, (PB97-133565, MF-A02, A08).
- NCEER-96-0014 "Response of Steel Bridge Bearings to Reversed Cyclic Loading," by J.B. Mander, D-K. Kim, S.S. Chen and G.J. Premus, 11/13/96, (PB97-140735, A12, MF-A03).
- NCEER-96-0015 "Highway Culvert Performance During Past Earthquakes," by T.L. Youd and C.J. Beckman, 11/25/96, (PB97-133532, A06, MF-A01).
- NCEER-97-0001 "Evaluation, Prevention and Mitigation of Pounding Effects in Building Structures," by R.E. Valles and A.M. Reinhorn, 2/20/97, (PB97-159552, A14, MF-A03).
- NCEER-97-0002 "Seismic Design Criteria for Bridges and Other Highway Structures," by C. Rojahn, R. Mayes, D.G. Anderson, J. Clark, J.H. Hom, R.V. Nutt and M.J. O'Rourke, 4/30/97, (PB97-194658, A06, MF-A03).

- NCEER-97-0003 "Proceedings of the U.S.-Italian Workshop on Seismic Evaluation and Retrofit," Edited by D.P. Abrams and G.M. Calvi, 3/19/97, (PB97-194666, A13, MF-A03).
- NCEER-97-0004 "Investigation of Seismic Response of Buildings with Linear and Nonlinear Fluid Viscous Dampers," by A.A. Seleemah and M.C. Constantinou, 5/21/97, (PB98-109002, A15, MF-A03).
- NCEER-97-0005 "Proceedings of the Workshop on Earthquake Engineering Frontiers in Transportation Facilities," edited by G.C. Lee and I.M. Friedland, 8/29/97, (PB98-128911, A25, MR-A04).
- NCEER-97-0006 "Cumulative Seismic Damage of Reinforced Concrete Bridge Piers," by S.K. Kunnath, A. El-Bahy, A. Taylor and W. Stone, 9/2/97, (PB98-108814, A11, MF-A03).
- NCEER-97-0007 "Structural Details to Accommodate Seismic Movements of Highway Bridges and Retaining Walls," by R.A. Imbsen, R.A. Schamber, E. Thorkildsen, A. Kartoum, B.T. Martin, T.N. Rosser and J.M. Kulicki, 9/3/97, (PB98-108996, A09, MF-A02).
- NCEER-97-0008 "A Method for Earthquake Motion-Damage Relationships with Application to Reinforced Concrete Frames," by A. Singhal and A.S. Kiremidjian, 9/10/97, (PB98-108988, A13, MF-A03).
- NCEER-97-0009 "Seismic Analysis and Design of Bridge Abutments Considering Sliding and Rotation," by K. Fishman and R. Richards, Jr., 9/15/97, (PB98-108897, A06, MF-A02).
- NCEER-97-0010 "Proceedings of the FHWA/NCEER Workshop on the National Representation of Seismic Ground Motion for New and Existing Highway Facilities," edited by I.M. Friedland, M.S. Power and R.L. Mayes, 9/22/97, (PB98-128903, A21, MF-A04).
- NCEER-97-0011 "Seismic Analysis for Design or Retrofit of Gravity Bridge Abutments," by K.L. Fishman, R. Richards, Jr. and R.C. Divito, 10/2/97, (PB98-128937, A08, MF-A02).
- NCEER-97-0012 "Evaluation of Simplified Methods of Analysis for Yielding Structures," by P. Tsopelas, M.C. Constantinou, C.A. Kircher and A.S. Whittaker, 10/31/97, (PB98-128929, A10, MF-A03).
- NCEER-97-0013 "Seismic Design of Bridge Columns Based on Control and Repairability of Damage," by C-T. Cheng and J.B. Mander, 12/8/97, (PB98-144249, A11, MF-A03).
- NCEER-97-0014 "Seismic Resistance of Bridge Piers Based on Damage Avoidance Design," by J.B. Mander and C-T. Cheng, 12/10/97, (PB98-144223, A09, MF-A02).
- NCEER-97-0015 "Seismic Response of Nominally Symmetric Systems with Strength Uncertainty," by S. Balopoulou and M. Grigoriu, 12/23/97, (PB98-153422, A11, MF-A03).
- NCEER-97-0016 "Evaluation of Seismic Retrofit Methods for Reinforced Concrete Bridge Columns," by T.J. Wipf, F.W. Klaiber and F.M. Russo, 12/28/97, (PB98-144215, A12, MF-A03).
- NCEER-97-0017 "Seismic Fragility of Existing Conventional Reinforced Concrete Highway Bridges," by C.L. Mullen and A.S. Cakmak, 12/30/97, (PB98-153406, A08, MF-A02).
- NCEER-97-0018 "Loss Assessment of Memphis Buildings," edited by D.P. Abrams and M. Shinozuka, 12/31/97, (PB98-144231, A13, MF-A03).
- NCEER-97-0019 "Seismic Evaluation of Frames with Infill Walls Using Quasi-static Experiments," by K.M. Mosalam, R.N. White and P. Gergely, 12/31/97, (PB98-153455, A07, MF-A02).
- NCEER-97-0020 "Seismic Evaluation of Frames with Infill Walls Using Pseudo-dynamic Experiments," by K.M. Mosalam, R.N. White and P. Gergely, 12/31/97, (PB98-153430, A07, MF-A02).
- NCEER-97-0021 "Computational Strategies for Frames with Infill Walls: Discrete and Smeared Crack Analyses and Seismic Fragility," by K.M. Mosalam, R.N. White and P. Gergely, 12/31/97, (PB98-153414, A10, MF-A02).

- NCEER-97-0022 "Proceedings of the NCEER Workshop on Evaluation of Liquefaction Resistance of Soils," edited by T.L. Youd and I.M. Idriss, 12/31/97, (PB98-155617, A15, MF-A03).
- MCEER-98-0001 "Extraction of Nonlinear Hysteretic Properties of Seismically Isolated Bridges from Quick-Release Field Tests," by Q. Chen, B.M. Douglas, E.M. Maragakis and I.G. Buckle, 5/26/98, (PB99-118838, A06, MF-A01).
- MCEER-98-0002 "Methodologies for Evaluating the Importance of Highway Bridges," by A. Thomas, S. Eshenaur and J. Kulicki, 5/29/98, (PB99-118846, A10, MF-A02).
- MCEER-98-0003 "Capacity Design of Bridge Piers and the Analysis of Overstrength," by J.B. Mander, A. Dutta and P. Goel, 6/1/98, (PB99-118853, A09, MF-A02).
- MCEER-98-0004 "Evaluation of Bridge Damage Data from the Loma Prieta and Northridge, California Earthquakes," by N. Basoz and A. Kiremidjian, 6/2/98, (PB99-118861, A15, MF-A03).
- MCEER-98-0005 "Screening Guide for Rapid Assessment of Liquefaction Hazard at Highway Bridge Sites," by T. L. Youd, 6/16/98, (PB99-118879, A06, not available on microfiche).
- MCEER-98-0006 "Structural Steel and Steel/Concrete Interface Details for Bridges," by P. Ritchie, N. Kaulh and J. Kulicki, 7/13/98, (PB99-118945, A06, MF-A01).
- MCEER-98-0007 "Capacity Design and Fatigue Analysis of Confined Concrete Columns," by A. Dutta and J.B. Mander, 7/14/98, (PB99-118960, A14, MF-A03).
- MCEER-98-0008 "Proceedings of the Workshop on Performance Criteria for Telecommunication Services Under Earthquake Conditions," edited by A.J. Schiff, 7/15/98, (PB99-118952, A08, MF-A02).
- MCEER-98-0009 "Fatigue Analysis of Unconfined Concrete Columns," by J.B. Mander, A. Dutta and J.H. Kim, 9/12/98, (PB99-123655, A10, MF-A02).
- MCEER-98-0010 "Centrifuge Modeling of Cyclic Lateral Response of Pile-Cap Systems and Seat-Type Abutments in Dry Sands," by A.D. Gadre and R. Dobry, 10/2/98, (PB99-123606, A13, MF-A03).
- MCEER-98-0011 "IDARC-BRIDGE: A Computational Platform for Seismic Damage Assessment of Bridge Structures," by A.M. Reinhorn, V. Simeonov, G. Mylonakis and Y. Reichman, 10/2/98, (PB99-162919, A15, MF-A03).
- MCEER-98-0012 "Experimental Investigation of the Dynamic Response of Two Bridges Before and After Retrofitting with Elastomeric Bearings," by D.A. Wendichansky, S.S. Chen and J.B. Mander, 10/2/98, (PB99-162927, A15, MF-A03).
- MCEER-98-0013 "Design Procedures for Hinge Restrainers and Hinge Sear Width for Multiple-Frame Bridges," by R. Des Roches and G.L. Fenves, 11/3/98, (PB99-140477, A13, MF-A03).
- MCEER-98-0014 "Response Modification Factors for Seismically Isolated Bridges," by M.C. Constantinou and J.K. Quarshie, 11/3/98, (PB99-140485, A14, MF-A03).
- MCEER-98-0015 "Proceedings of the U.S.-Italy Workshop on Seismic Protective Systems for Bridges," edited by I.M. Friedland and M.C. Constantinou, 11/3/98, (PB2000-101711, A22, MF-A04).
- MCEER-98-0016 "Appropriate Seismic Reliability for Critical Equipment Systems: Recommendations Based on Regional Analysis of Financial and Life Loss," by K. Porter, C. Scawthorn, C. Taylor and N. Blais, 11/10/98, (PB99-157265, A08, MF-A02).
- MCEER-98-0017 "Proceedings of the U.S. Japan Joint Seminar on Civil Infrastructure Systems Research," edited by M. Shinozuka and A. Rose, 11/12/98, (PB99-156713, A16, MF-A03).
- MCEER-98-0018 "Modeling of Pile Footings and Drilled Shafts for Seismic Design," by I. PoLam, M. Kapuskar and D. Chaudhuri, 12/21/98, (PB99-157257, A09, MF-A02).

- MCEER-99-0001 "Seismic Evaluation of a Masonry Infilled Reinforced Concrete Frame by Pseudodynamic Testing," by S.G. Buonopane and R.N. White, 2/16/99, (PB99-162851, A09, MF-A02).
- MCEER-99-0002 "Response History Analysis of Structures with Seismic Isolation and Energy Dissipation Systems: Verification Examples for Program SAP2000," by J. Scheller and M.C. Constantinou, 2/22/99, (PB99-162869, A08, MF-A02).
- MCEER-99-0003 "Experimental Study on the Seismic Design and Retrofit of Bridge Columns Including Axial Load Effects," by A. Dutta, T. Kokorina and J.B. Mander, 2/22/99, (PB99-162877, A09, MF-A02).
- MCEER-99-0004 "Experimental Study of Bridge Elastomeric and Other Isolation and Energy Dissipation Systems with Emphasis on Uplift Prevention and High Velocity Near-source Seismic Excitation," by A. Kasalanati and M. C. Constantinou, 2/26/99, (PB99-162885, A12, MF-A03).
- MCEER-99-0005 "Truss Modeling of Reinforced Concrete Shear-flexure Behavior," by J.H. Kim and J.B. Mander, 3/8/99, (PB99-163693, A12, MF-A03).
- MCEER-99-0006 "Experimental Investigation and Computational Modeling of Seismic Response of a 1:4 Scale Model Steel Structure with a Load Balancing Supplemental Damping System," by G. Pekcan, J.B. Mander and S.S. Chen, 4/2/99, (PB99-162893, A11, MF-A03).
- MCEER-99-0007 "Effect of Vertical Ground Motions on the Structural Response of Highway Bridges," by M.R. Button, C.J. Cronin and R.L. Mayes, 4/10/99, (PB2000-101411, A10, MF-A03).
- MCEER-99-0008 "Seismic Reliability Assessment of Critical Facilities: A Handbook, Supporting Documentation, and Model Code Provisions," by G.S. Johnson, R.E. Sheppard, M.D. Quilici, S.J. Eder and C.R. Scawthorn, 4/12/99, (PB2000-101701, A18, MF-A04).
- MCEER-99-0009 "Impact Assessment of Selected MCEER Highway Project Research on the Seismic Design of Highway Structures," by C. Rojahn, R. Mayes, D.G. Anderson, J.H. Clark, D'Appolonia Engineering, S. Gloyd and R.V. Nutt, 4/14/99, (PB99-162901, A10, MF-A02).
- MCEER-99-0010 "Site Factors and Site Categories in Seismic Codes," by R. Dobry, R. Ramos and M.S. Power, 7/19/99, (PB2000-101705, A08, MF-A02).
- MCEER-99-0011 "Restrainer Design Procedures for Multi-Span Simply-Supported Bridges," by M.J. Randall, M. Saiidi, E. Maragakis and T. Isakovic, 7/20/99, (PB2000-101702, A10, MF-A02).
- MCEER-99-0012 "Property Modification Factors for Seismic Isolation Bearings," by M.C. Constantinou, P. Tsopelas, A. Kasalanati and E. Wolff, 7/20/99, (PB2000-103387, A11, MF-A03).
- MCEER-99-0013 "Critical Seismic Issues for Existing Steel Bridges," by P. Ritchie, N. Kauh and J. Kulicki, 7/20/99, (PB2000-101697, A09, MF-A02).
- MCEER-99-0014 "Nonstructural Damage Database," by A. Kao, T.T. Soong and A. Vender, 7/24/99, (PB2000-101407, A06, MF-A01).
- MCEER-99-0015 "Guide to Remedial Measures for Liquefaction Mitigation at Existing Highway Bridge Sites," by H.G. Cooke and J. K. Mitchell, 7/26/99, (PB2000-101703, A11, MF-A03).
- MCEER-99-0016 "Proceedings of the MCEER Workshop on Ground Motion Methodologies for the Eastern United States," edited by N. Abrahamson and A. Becker, 8/11/99, (PB2000-103385, A07, MF-A02).
- MCEER-99-0017 "Quindío, Colombia Earthquake of January 25, 1999: Reconnaissance Report," by A.P. Asfura and P.J. Flores, 10/4/99, (PB2000-106893, A06, MF-A01).
- MCEER-99-0018 "Hysteretic Models for Cyclic Behavior of Deteriorating Inelastic Structures," by M.V. Sivaselvan and A.M. Reinhorn, 11/5/99, (PB2000-103386, A08, MF-A02).

- MCEER-99-0019 "Proceedings of the 7th U.S.- Japan Workshop on Earthquake Resistant Design of Lifeline Facilities and Countermeasures Against Soil Liquefaction," edited by T.D. O'Rourke, J.P. Bardet and M. Hamada, 11/19/99, (PB2000-103354, A99, MF-A06).
- MCEER-99-0020 "Development of Measurement Capability for Micro-Vibration Evaluations with Application to Chip Fabrication Facilities," by G.C. Lee, Z. Liang, J.W. Song, J.D. Shen and W.C. Liu, 12/1/99, (PB2000-105993, A08, MF-A02).
- MCEER-99-0021 "Design and Retrofit Methodology for Building Structures with Supplemental Energy Dissipating Systems," by G. Pekcan, J.B. Mander and S.S. Chen, 12/31/99, (PB2000-105994, A11, MF-A03).
- MCEER-00-0001 "The Marmara, Turkey Earthquake of August 17, 1999: Reconnaissance Report," edited by C. Scawthorn; with major contributions by M. Bruneau, R. Eguchi, T. Holzer, G. Johnson, J. Mander, J. Mitchell, W. Mitchell, A. Papageorgiou, C. Scaethorn, and G. Webb, 3/23/00, (PB2000-106200, A11, MF-A03).
- MCEER-00-0002 "Proceedings of the MCEER Workshop for Seismic Hazard Mitigation of Health Care Facilities," edited by G.C. Lee, M. Ettouney, M. Grigoriu, J. Hauer and J. Nigg, 3/29/00, (PB2000-106892, A08, MF-A02).
- MCEER-00-0003 "The Chi-Chi, Taiwan Earthquake of September 21, 1999: Reconnaissance Report," edited by G.C. Lee and C.H. Loh, with major contributions by G.C. Lee, M. Bruneau, I.G. Buckle, S.E. Chang, P.J. Flores, T.D. O'Rourke, M. Shinozuka, T.T. Soong, C-H. Loh, K-C. Chang, Z-J. Chen, J-S. Hwang, M-L. Lin, G-Y. Liu, K-C. Tsai, G.C. Yao and C-L. Yen, 4/30/00, (PB2001-100980, A10, MF-A02).
- MCEER-00-0004 "Seismic Retrofit of End-Sway Frames of Steel Deck-Truss Bridges with a Supplemental Tendon System: Experimental and Analytical Investigation," by G. Pekcan, J.B. Mander and S.S. Chen, 7/1/00, (PB2001-100982, A10, MF-A02).
- MCEER-00-0005 "Sliding Fragility of Unrestrained Equipment in Critical Facilities," by W.H. Chong and T.T. Soong, 7/5/00, (PB2001-100983, A08, MF-A02).
- MCEER-00-0006 "Seismic Response of Reinforced Concrete Bridge Pier Walls in the Weak Direction," by N. Abo-Shadi, M. Saiidi and D. Sanders, 7/17/00, (PB2001-100981, A17, MF-A03).
- MCEER-00-0007 "Low-Cycle Fatigue Behavior of Longitudinal Reinforcement in Reinforced Concrete Bridge Columns," by J. Brown and S.K. Kunnath, 7/23/00, (PB2001-104392, A08, MF-A02).
- MCEER-00-0008 "Soil Structure Interaction of Bridges for Seismic Analysis," I. PoLam and H. Law, 9/25/00, (PB2001-105397, A08, MF-A02).
- MCEER-00-0009 "Proceedings of the First MCEER Workshop on Mitigation of Earthquake Disaster by Advanced Technologies (MEDAT-1), edited by M. Shinozuka, D.J. Inman and T.D. O'Rourke, 11/10/00, (PB2001-105399, A14, MF-A03).
- MCEER-00-0010 "Development and Evaluation of Simplified Procedures for Analysis and Design of Buildings with Passive Energy Dissipation Systems," by O.M. Ramirez, M.C. Constantinou, C.A. Kircher, A.S. Whittaker, M.W. Johnson, J.D. Gomez and C. Chrysostomou, 11/16/01, (PB2001-105523, A23, MF-A04).
- MCEER-00-0011 "Dynamic Soil-Foundation-Structure Interaction Analyses of Large Caissons," by C-Y. Chang, C-M. Mok, Z-L. Wang, R. Settgast, F. Waggoner, M.A. Ketchum, H.M. Gonnermann and C-C. Chin, 12/30/00, (PB2001-104373, A07, MF-A02).
- MCEER-00-0012 "Experimental Evaluation of Seismic Performance of Bridge Restrainers," by A.G. Vlassis, E.M. Maragakis and M. Saiid Saiidi, 12/30/00, (PB2001-104354, A09, MF-A02).
- MCEER-00-0013 "Effect of Spatial Variation of Ground Motion on Highway Structures," by M. Shinozuka, V. Saxena and G. Deodatis, 12/31/00, (PB2001-108755, A13, MF-A03).
- MCEER-00-0014 "A Risk-Based Methodology for Assessing the Seismic Performance of Highway Systems," by S.D. Werner, C.E. Taylor, J.E. Moore, II, J.S. Walton and S. Cho, 12/31/00, (PB2001-108756, A14, MF-A03).

- MCEER-01-0001 "Experimental Investigation of P-Delta Effects to Collapse During Earthquakes," by D. Vian and M. Bruneau, 6/25/01, (PB2002-100534, A17, MF-A03).
- MCEER-01-0002 "Proceedings of the Second MCEER Workshop on Mitigation of Earthquake Disaster by Advanced Technologies (MEDAT-2)," edited by M. Bruneau and D.J. Inman, 7/23/01, (PB2002-100434, A16, MF-A03).
- MCEER-01-0003 "Sensitivity Analysis of Dynamic Systems Subjected to Seismic Loads," by C. Roth and M. Grigoriu, 9/18/01, (PB2003-100884, A12, MF-A03).
- MCEER-01-0004 "Overcoming Obstacles to Implementing Earthquake Hazard Mitigation Policies: Stage 1 Report," by D.J. Alesch and W.J. Petak, 12/17/01, (PB2002-107949, A07, MF-A02).
- MCEER-01-0005 "Updating Real-Time Earthquake Loss Estimates: Methods, Problems and Insights," by C.E. Taylor, S.E. Chang and R.T. Eguchi, 12/17/01, (PB2002-107948, A05, MF-A01).
- MCEER-01-0006 "Experimental Investigation and Retrofit of Steel Pile Foundations and Pile Bents Under Cyclic Lateral Loadings," by A. Shama, J. Mander, B. Blabac and S. Chen, 12/31/01, (PB2002-107950, A13, MF-A03).
- MCEER-02-0001 "Assessment of Performance of Bolu Viaduct in the 1999 Duzce Earthquake in Turkey" by P.C. Roussis, M.C. Constantinou, M. Erdik, E. Durukal and M. Dicleli, 5/8/02, (PB2003-100883, A08, MF-A02).
- MCEER-02-0002 "Seismic Behavior of Rail Counterweight Systems of Elevators in Buildings," by M.P. Singh, Rildova and L.E. Suarez, 5/27/02. (PB2003-100882, A11, MF-A03).
- MCEER-02-0003 "Development of Analysis and Design Procedures for Spread Footings," by G. Mylonakis, G. Gazetas, S. Nikolaou and A. Chauncey, 10/02/02, (PB2004-101636, A13, MF-A03, CD-A13).
- MCEER-02-0004 "Bare-Earth Algorithms for Use with SAR and LIDAR Digital Elevation Models," by C.K. Huyck, R.T. Eguchi and B. Houshmand, 10/16/02, (PB2004-101637, A07, CD-A07).
- MCEER-02-0005 "Review of Energy Dissipation of Compression Members in Concentrically Braced Frames," by K.Lee and M. Bruneau, 10/18/02, (PB2004-101638, A10, CD-A10).
- MCEER-03-0001 "Experimental Investigation of Light-Gauge Steel Plate Shear Walls for the Seismic Retrofit of Buildings" by J. Berman and M. Bruneau, 5/2/03, (PB2004-101622, A10, MF-A03, CD-A10).
- MCEER-03-0002 "Statistical Analysis of Fragility Curves," by M. Shinozuka, M.Q. Feng, H. Kim, T. Uzawa and T. Ueda, 6/16/03, (PB2004-101849, A09, CD-A09).
- MCEER-03-0003 "Proceedings of the Eighth U.S.-Japan Workshop on Earthquake Resistant Design of Lifeline Facilities and Countermeasures Against Liquefaction," edited by M. Hamada, J.P. Bardet and T.D. O'Rourke, 6/30/03, (PB2004-104386, A99, CD-A99).
- MCEER-03-0004 "Proceedings of the PRC-US Workshop on Seismic Analysis and Design of Special Bridges," edited by L.C. Fan and G.C. Lee, 7/15/03, (PB2004-104387, A14, CD-A14).
- MCEER-03-0005 "Urban Disaster Recovery: A Framework and Simulation Model," by S.B. Miles and S.E. Chang, 7/25/03, (PB2004-104388, A07, CD-A07).
- MCEER-03-0006 "Behavior of Underground Piping Joints Due to Static and Dynamic Loading," by R.D. Meis, M. Maragakis and R. Siddharthan, 11/17/03.
- MCEER-03-0007 "Seismic Vulnerability of Timber Bridges and Timber Substructures," by A.A. Shama, J.B. Mander, I.M. Friedland and D.R. Allicock, 12/15/03.
- MCEER-04-0001 "Experimental Study of Seismic Isolation Systems with Emphasis on Secondary System Response and Verification of Accuracy of Dynamic Response History Analysis Methods," by E. Wolff and M. Constantinou, 1/16/04.

- MCEER-04-0002 “Tension, Compression and Cyclic Testing of Engineered Cementitious Composite Materials,” by K. Kesner and S.L. Billington, 3/1/04.
- MCEER-04-0003 “Cyclic Testing of Braces Laterally Restrained by Steel Studs to Enhance Performance During Earthquakes,” by O.C. Celik, J.W. Berman and M. Bruneau, 3/16/04.
- MCEER-04-0004 “Methodologies for Post Earthquake Building Damage Detection Using SAR and Optical Remote Sensing: Application to the August 17, 1999 Marmara, Turkey Earthquake,” by C.K. Huyck, B.J. Adams, S. Cho, R.T. Eguchi, B. Mansouri and B. Houshmand, 6/15/04.
- MCEER-04-0005 “Nonlinear Structural Analysis Towards Collapse Simulation: A Dynamical Systems Approach,” by M.V. Sivaselvan and A.M. Reinhorn, 6/16/04.



MULTIDISCIPLINARY CENTER FOR EARTHQUAKE ENGINEERING RESEARCH

A National Center of Excellence in Advanced Technology Applications

University at Buffalo, State University of New York

Red Jacket Quadrangle ■ Buffalo, New York 14261

Phone: (716) 645-3391 ■ Fax: (716) 645-3399

E-mail: mceer@mceermail.buffalo.edu ■ WWW Site <http://mceer.buffalo.edu>



University at Buffalo *The State University of New York*

ISSN 1520-295X